

---

# The Electron

---

*Riccardo Fantoni*



May 15, 2025

# Preface

The electron is the main actor of this assay, a mysterious character and at the same time omnipresent in our daily life. At the same time elementary and complex. We will initially follow a top-down causation [1] to introduce it from symmetry principles and then a bottom-up causation to introduce various systems made of it.

It is an elementary particle and as such is described by a vector, a wave function, of a finite dimensional irreducible unitary representation of its group of symmetries (the Galileo group in the non-relativistic case and the Poincare' group in the relativistic case, extended to the parity transformation). The invariants of the group are the mass and the spin and the electron has spin 1/2. The spin-statistics theorem states that, as a consequence of Lorentz invariance and of locality, half integer spin particles must obey to Fermi statistics and integer spin particles must obey to Bose statistics. So many electrons must obey to the Pauli exclusion principle

Its role in a ionic crystal in the Feynman polaron problem, in atomic structure in the Mendeleev periodic system, and in the redox chemical bond is discussed as few electron systems examples.

The assay continues with the properties of a many electron system, the Jellium. Its ground state and finite temperature state are discussed from a (computational) theoretical point of view. Some phenomenology is also presented in the very end.

The assay then gives a description of the equation of state and structure of a white dwarf a stellar core remnant composed mostly of electron-degenerate matter which has a white hot color temperature and reddens as it cools down.

The assay is then concluded with a description of the renormalization group theory for phase transitions in statistical physics.

Of course the assay has no pretensions of completeness of any kind since the argument is so vast that one could devote to it a whole encyclopedia. Nonetheless the few arguments that are touched are rigorous and go somewhat in depth. It could certainly be an interesting reading for the graduate student but in some of its parts (especially Chapters 2,3, and 6) could become a valid instrument for researchers from the high- to the low-energy physics communities.

The project of the assay has been made possible by my rather fortunate encounters of many of the few 'maestri' in the field of relativistic quantum mechanics like prof. Adriano Di Giacomo from the physics department of the University of Pisa, Italy and prof. Robert Leigh from the department of physics of the University of Illinois at Urbana/Champaign among others, in the field of the electron gas like my first master advisor prof. Mario Pio Tosi from the Scuola Normale Superiore di Pisa, Italy, my second master advisor prof. David Matthew Ceperley from the National Center for Supercomputing Applications of the University of Illinois at Urbana/Champaign, and prof. Bernard Jancovici from the laboratory for theoretical physics of the University of Paris Sud at Orsay, France among others, and in the field of cosmology, gravitation, and compact objects in the Universe like my graduate courses prof. Stuart Shapiro from the University of Illinois at Urbana/Champaign among others.

I must mention the fact that the third chapter of the assay is the result of my first Ph.D.

studies while working in the group of prof. David Matthew Ceperley on the Path Integral Monte Carlo (PIMC) method. The form that is presented here is the original version written on 1998 in preparation of my Ph.D. thesis which describes the results obtained with my own PIMC code. My advisor did not consider it sufficiently interesting to be worth a publication. As a matter of fact I would discover only in 2001 after I had to come back to Trieste in 2000 to give birth to my daughter that a certain Dr. Carlo Pierleoni from l' Aquila had just published exactly the same results in a three author Phys. Rev. Lett. collaboration.

The assay is organized in 8 chapters. In the first introductory chapter we describe the physical constants and properties of the isolated electron and give some historical background. In chapter two we show how the electron as an elementary particle can be described as a vector of a finite dimensional irreducible unitary representation of its group of symmetries and how relativistic quantum mechanics can explain the spin-statistics theorem. In the following chapters we start studying the interaction of the electron with the environment. We will always see the electron as the protagonist of the interaction. So in the third chapter we present the Feynman polaron problem that sees one electron interacting with a crystal of ions. In chapter four we study the role of few electrons in the periodic system of the elements of Mendeleev. In the fifth chapter we see how few electrons determine the RedOx chemical bond between elements. In chapter six we study many electrons in the thermodynamic limit. This quantum plasma is called the Jellium. In the seventh chapter we study a white dwarf, a compact object of the universe that has consumed all its nuclear fuel and support itself against gravity by the pressure of the residual cold electron plasma. In the last chapter eight we describe the properties of phase transition in statistical physics and how the renormalization group explains how it is irrelevant the nature of the liquid studied being it Jellium or other.

*PREFACE*

---

*To my Grandmother*

*nonna Ione*

*To my Parents*

*my father and my mother a couple for  
56 years, to their patience, never los-  
ing hope, and extraordinary acumen*



# Contents

Preface	i
1 Introduction	1
Appendices	
Appendix A Particle Data Group	15
2 The particle	23
2.1 Definition of Invariance . . . . .	23
2.1.1 Conventions . . . . .	24
2.2 Invariance in quantum mechanics . . . . .	24
2.3 Invariance and time evolution . . . . .	27
2.4 Galilean relativity . . . . .	27
2.4.1 Spatial translations . . . . .	27
2.4.2 Rotations . . . . .	28
2.4.3 Galilean transformations . . . . .	28
2.4.4 Galileo group . . . . .	29
2.4.5 Parity invariance . . . . .	30
2.4.6 Time reversal . . . . .	31
2.5 Einstein Relativity . . . . .	34
2.5.1 The irreducible unitary representation of the Poincaré group . . . . .	38
2.5.2 Wave functions in coordinate space . . . . .	49
2.6 The relativistic wave equations . . . . .	50
2.6.1 Particles of spin 0 . . . . .	50
2.6.2 Particles of spin 1/2 . . . . .	53
2.6.3 Particles of spin 1 . . . . .	63
2.7 The second quantization . . . . .	65
2.7.1 Fock space . . . . .	65
2.7.2 Field operators . . . . .	68
2.7.3 Transformation properties of the field operators . . . . .	69
2.7.4 Locality and spin-statistics theorem . . . . .	71
Appendices	
Appendix B Commutators	79
Appendix C The Levi-Civita symbol	81

---

<b>Appendix D Angular momentum</b>	<b>83</b>
<b>Appendix E SU(2)</b>	<b>85</b>
<b>Appendix F Velocity transformations</b>	<b>87</b>
<b>3 The Polaron</b>	<b>89</b>
3.1 Introduction . . . . .	89
3.2 The model . . . . .	90
3.3 The observables . . . . .	91
3.4 Discrete path integral expressions . . . . .	92
3.5 Sampling the path . . . . .	93
3.6 Choice of $T_k$ and $\pi_k$ . . . . .	95
3.7 Correlated sampling . . . . .	96
3.8 Numerical Results . . . . .	98
3.9 Conclusions . . . . .	102
<b>Appendices</b>	
<b>Appendix G Estimating errors</b>	<b>107</b>
<b>4 Mendeleev Periodic System</b>	<b>109</b>
4.1 Electron states in the atom . . . . .	109
4.2 Periodic Table . . . . .	111
<b>5 RedOx Chemical Reactions</b>	<b>115</b>
5.1 Mathematical discovery in 1D . . . . .	116
5.2 Mathematical discovery in 2D . . . . .	117
<b>6 The Electron Gas</b>	<b>119</b>
6.1 The model . . . . .	120
6.1.1 Lindhard theory of static screening in Jellium ground state . . . . .	121
6.1.2 Ewald sums . . . . .	123
6.2 Jellium in its ground state . . . . .	123
6.2.1 Monte Carlo simulation (Diffusion) . . . . .	124
6.2.2 Expectation values in DMC . . . . .	125
6.2.3 Trial wave-function . . . . .	127
6.2.4 The radial distribution function . . . . .	130
6.2.5 Results for the radial distribution function and structure factor . . . . .	132
6.2.6 Results for the internal energy . . . . .	132
6.3 Jellium at finite temperature . . . . .	132
6.3.1 Monte Carlo simulation (Path Integral) . . . . .	136
6.3.2 Results for the radial distribution function and structure factor . . . . .	142
6.3.3 Results for the internal energy . . . . .	142
6.3.4 Phase diagram . . . . .	146
6.4 Some physical realizations and phenomenology . . . . .	147
6.4.1 Molten halides and some alloys of metallic elements . . . . .	149
6.4.2 Structure of trivalent-metal halides . . . . .	150
6.4.3 Chemical short-range order in liquid alloys . . . . .	152
6.4.4 Liquid metals . . . . .	153

---

**Appendices**

<b>Appendix H Ideal gas energy and exchange energy as a function of polarization</b>	<b>157</b>
<b>Appendix I Jastrow, backflow, and three-body</b>	<b>159</b>
<b>Appendix J The Random-Phase-Approximation</b>	<b>161</b>
<b>Appendix K Analytic expressions for the non-interacting fermions ground state</b>	<b>163</b>
K.1 Radial distribution function . . . . .	163
K.2 Static structure factor . . . . .	163
K.3 Internal energy . . . . .	164
<b>Appendix L Radial distribution functions sum rules for the electron gas ground state</b>	<b>167</b>
L.1 Cusp conditions . . . . .	167
L.2 The Random-Phase-Approximation (RPA) . . . . .	167
<b>Appendix M The primitive action</b>	<b>169</b>
<b>Appendix N The pair-product action</b>	<b>171</b>
<b>Appendix O Linear-Response-Theory</b>	<b>173</b>
O.1 Fluctuation-dissipation theorem . . . . .	174
O.2 Kramers-Kronig relations . . . . .	175
O.3 The dielectric function . . . . .	176
<b>7 The White Dwarf</b>	<b>179</b>
7.1 Introduction . . . . .	179
7.2 The thermodynamics of the ideal quantum gas . . . . .	180
7.2.1 Relativistic effects at high density in a gas of fermions . . . . .	183
7.2.2 The onset of quantum statistics . . . . .	184
7.2.3 The Chandrasekhar limit . . . . .	186
7.3 The structure of the ideal quantum gas . . . . .	188
7.4 Conclusions . . . . .	190
<b>Appendices</b>	
<b>Appendix P The adiabatic equation of state for a relativistic ideal electron gas at finite temperature</b>	<b>195</b>
<b>8 The Renormalization Group</b>	<b>197</b>
8.1 Notation . . . . .	197
8.2 The origin of RG . . . . .	198
8.3 The decay of correlation functions . . . . .	199
8.4 The challenges posed by critical phenomena . . . . .	201
8.5 The critical exponents . . . . .	204
8.5.1 The classical exponent values . . . . .	204
8.5.2 The Ising exponent values . . . . .	205
8.5.3 Exponent relations . . . . .	205
8.6 The Gaussian model and the upper critical dimension . . . . .	206

---

*CONTENTS*

---

8.7 The task of RG . . . . .	206
8.8 The basis and formulation . . . . .	208
<b>List of Figures</b>	<b>215</b>
<b>Bibliography</b>	<b>219</b>
<b>Index</b>	<b>237</b>

# Chapter 1

## Introduction

Composition:	Elementary particle [2]
Statistics:	Fermionic [3]
Family:	Lepton [3]
Generation:	First [3]
Interactions:	Weak, electromagnetic, gravity [3]
Symbol:	$e^-$ , $\beta^-$ [3]
Antiparticle:	Positron [3]
Theorized:	Richard Laming (1838–1851), [4] G. Johnstone Stoney (1874) and others.
Discovered:	J. J. Thomson (1897) [5]
Mass ( $m$ ):	$9.1093837139(28) \times 10^{-31}$ kg [3] $5.485799090441(97) \times 10^{-4}$ Da $[1822.888486209(53)]^{-1}$ Da $0.51099895069(16)$ MeV/c <sup>2</sup> [3]
Mean lifetime:	$> 6.6 \times 10^{28}$ years [6] (stable)
Electric charge:	$-1 e$ [3] $-1.602176634 \times 10^{-19}$ C [3]
Magnetic moment:	$-9.2847646917(29) \times 10^{-24}$ J/T [3] $-1.00115965218128(18) \mu_B$ [3]
Spin:	$\frac{1}{2} \hbar$ [3]
Weak isospin:	LH: $-\frac{1}{2}$ , RH: 0 [3]
Weak hypercharge:	LH: -1, RH: -2 [3]

The **electron**  $e^-$  is a subatomic particle with a negative one elementary electric charge  $e$ . Electrons belong to the first generation of the lepton particle family, and are generally thought to be elementary particles because they have no known components or substructure [2]. The electron's mass,  $m$ , is approximately  $\frac{1}{1836}$  that of the proton. Quantum mechanical properties of the electron include an intrinsic angular momentum (spin) of a half-integer value, expressed in units of the reduced Planck constant,  $\hbar$ . Being fermions, no two electrons can occupy the same quantum state, per the Pauli exclusion principle. Like all elementary particles, electrons exhibit properties of both particles and waves: They can collide with other particles and can

be diffracted like light. The wave properties of electrons are easier to observe with experiments than those of other particles like neutrons and protons because electrons have a lower mass and hence a longer de Broglie wavelength for a given energy. In Chapter 2 we will present the proof of the Pauli exclusion principle by first principles. We will introduce an elementary particle as a vector of a unitary irreducible representation of the group of the symmetries in our universe and prove the spin-statistics theorem which states that, as a consequence of Lorentz invariance and of locality, half integer spin particles must obey to Fermi statistics and integer spin particles must obey to Bose statistics.

Electrons play an essential role in numerous physical phenomena, such as electricity, magnetism, chemistry, and thermal conductivity; they also participate in gravitational, electromagnetic, and weak interactions. Since an electron has charge, it has a surrounding electric field; if that electron is moving relative to an observer, the observer will observe it to generate a magnetic field. Electromagnetic fields produced from other sources will affect the motion of an electron according to the Lorentz force law. Electrons radiate or absorb energy in the form of photons when they are accelerated [7].

Laboratory instruments are capable of trapping individual electrons as well as electron plasma by the use of electromagnetic fields. Special telescopes can detect electron plasma in outer space. Electrons are involved in many applications, such as tribology or frictional charging, electrolysis, electrochemistry, battery technologies, electronics, welding, cathode-ray tubes, photoelectricity, photovoltaic solar panels, electron microscopes, radiation therapy, lasers, gaseous ionization detectors, and particle accelerators.

Interactions involving electrons with other subatomic particles are of interest in fields such as chemistry and nuclear physics. The Coulomb force interaction between the positive protons within atomic nuclei and the negative electrons without allows the composition of the two known as atoms. Ionization or differences in the proportions of negative electrons versus positive nuclei changes the binding energy of an atomic system. The exchange or sharing of the electrons between two or more atoms is the main cause of chemical bonding [8]. This will be briefly presented in Chapter 5.

Electrons participate in nuclear reactions, such as nucleosynthesis in stars, where they are known as  $\beta^-$  particles. Electrons can be created through beta decay of radioactive isotopes and in high-energy collisions, for instance, when cosmic rays enter the atmosphere. The antiparticle of the electron is called the positron; it is identical to the electron, except that it carries electrical charge of the opposite sign (See for example Section 2.6). When an electron collides with a positron, both particles can be annihilated, producing gamma ray photons.

The ancient Greeks noticed that amber attracted small objects when rubbed with fur. Along with lightning, this phenomenon is one of humanity's earliest recorded experiences with electricity. In his 1600 treatise *De Magnete*, the English scientist William Gilbert coined the Neo-Latin term *electrica*, to refer to those substances with property similar to that of amber which attract small objects after being rubbed. Both electric and electricity are derived from the Latin *electrum* (also the root of the alloy of the same name), which came from the Greek word for amber, *ηλεκτρον* (*élektron*).

In 1838, British natural philosopher Richard Laming first hypothesized the concept of an indivisible quantity of electric charge to explain the chemical properties of atoms [4]. Irish physicist George Johnstone Stoney named this charge "electron" in 1891, and J. J. Thomson and his team of British physicists (John S. Townsend and H. A. Wilson) identified it as a particle in 1897 during the cathode-ray tube experiment [5]. J. J. Thomson would subsequently in 1899 give estimates for the electron charge and mass as well:  $e \sim 6.8 \times 10^{-10}$  esu and  $m \sim 3 \times 10^{-26}$  g.

The electron's charge was more carefully measured by the American physicists Robert Millikan [9] and Harvey Fletcher in their oil-drop experiment of 1909, the results of which were

---

## 1. INTRODUCTION

---

published in 1911. This experiment used an electric field to prevent a charged droplet of oil from falling as a result of gravity. This device could measure the electric charge from as few as 1-150 ions with an error margin of less than 0.3%. Comparable experiments had been done earlier by Abram Ioffe, who independently obtained the same result as Millikan using charged microparticles of metals, then published his results in 1913. However, oil drops were more stable than water drops because of their slower evaporation rate, and thus more suited to precise experimentation over longer periods of time. The experiment of Millikan took place in the Ryerson Physical Laboratory at the University of Chicago. Millikan received the Nobel Prize in Physics in 1923.

In particle physics, the electroweak interaction or electroweak force is the unified description of two of the fundamental interactions of nature: electromagnetism (electromagnetic interaction) and the weak interaction. Although these two forces appear very different at everyday low energies, the theory models them as two different aspects of the same force. Above the unification energy, on the order of 246 GeV,<sup>1</sup> they would merge into a single force. Thus, if the temperature is high enough — approximately 1015 K — then the electromagnetic force and weak force merge into a combined electroweak force [10, 11, 12]. In this standard model of electroweak interaction one initially supposes massless leptons. In 1964 Peter Higgs proposed the *Higgs mechanism* [13]. The Higgs field is a scalar field with two neutral and two electrically charged components that form a complex doublet of the weak isospin SU(2) symmetry. Its “Sombrero potential” leads it to take a nonzero value everywhere (including otherwise empty space), which breaks the weak isospin symmetry of the electroweak interaction and, via the Higgs mechanism, gives a rest mass to leptons, among which figures the electron, and the  $W^\pm$ ,  $Z^0$  gauge bosons through a rotation by the Weinberg angle. After a 40-year search, a subatomic particle with the expected properties was discovered in 2012 by the ATLAS and CMS experiments at the Large Hadron Collider (LHC) at CERN near Geneva, Switzerland. Even if these scalar particles are plagued by triviality issues from a rigorous mathematical point of view [14, 15, 16, 17, 18, 19, 20, 21, 22, 23, 24].

Fermions with negative chirality<sup>2</sup> (also called “left-handed” fermions) have a weak isospin  $T = \frac{1}{2}$  and can be grouped into doublets with  $T_3 = \pm\frac{1}{2}$  that behave the same way under the weak interaction. By convention, electrically charged fermions are assigned  $T_3$  with the same sign as their electric charge. In all cases, the corresponding anti-fermion has reversed chirality (“right-handed” anti-fermion) and reversed sign  $T_3$ . Fermions with  $T = T_3 = 0$  form singlets that do not undergo charged weak interactions. Particles with  $T_3 = 0$  do not interact with  $W^\pm$  gauge bosons; however, they do all interact with the  $Z^0$  gauge boson. The weak isospin conservation law relates to the conservation of  $T_3$ ; weak interactions conserve  $T_3$ . It is also conserved by the electromagnetic and strong interactions. However, interaction with the Higgs field does not conserve  $T_3$ , as directly seen in propagating fermions, which mix their helicities by the mass terms that result from their Higgs couplings. Since the Higgs field vacuum expectation value is nonzero, particles interact with this field all the time, even in vacuum. Interaction with the Higgs field changes particles’ weak isospin. Only a specific combination of electric charge is conserved. The electric charge,  $Q = T_3 + \frac{1}{2}Y_W$ , where  $Y_W$  is the weak hypercharge. In 1961 Sheldon Glashow proposed this relation by analogy to the Gell-Mann-Nishijima formula for charge to isospin [25].

Have you ever asked yourselves how can we be certain that the Sun is a giant nuclear candle? If Galileo Galilei was here he would ask: “where are the proofs?” The proofs can be found in the Gran Sasso Laboratory where we measure the flux of solar neutrinos. Every second, on every centimeter square of the Earth, arrive something like sixty billions neutrinos. Night and

---

<sup>1</sup>The particular number 246 GeV is taken to be the vacuum expectation value  $v = (G_F \sqrt{2})^{-1/2}$  of the Higgs field (where  $G_F$  is the Fermi coupling constant).

<sup>2</sup>The chirality and intrinsic helicity are two characteristic properties of massive and massless particles respectively. This will be used in Section 2.5.1.

Day. In fact, Earth is transparent to these mysterious particles that goes through anything without ever stopping. If our eyes could see the neutrinos, the night would not exist! And what do these neutrinos tell us? Performing the exact calculations, we discover that their flux corresponds exactly to that predicted for a perfectly regulated nuclear candle. But who controls this “fire”? The answer lies in the extraordinary discovery of Fermi first and Salam, Weinberg, and Glashow later: The weak charge, that Enrico Fermi identified as a new force of Nature. This is the “security valve” which allows the production of the Sun “fuel”: the neutrinos. Even if the Sun is made almost exclusively by protons and electrons, the Fermi force allows the necessary transformation for fusion to happen. Without this perfect regulation, the Sun would not be our “neverending” source of light and life.

We live in an electrically neutral environment; everything around us is electrically neutral; but our lives are moved by electrical unbalances, like the synapses in the neurons in our brain, or the nervous terminations moving our muscles. Already Luigi Galvani (Bologna, 9 September 1737 - Bologna, 4 December 1798) discovered biological electricity (with his theory on the electrical fluid in frogs) and some of its applications like the electrochemical cell, the galvanometer, or the galvanization. Alessandro Volta (Como, 18 February 1745 - Como, 5 March 1827) in the same period invented the first electrical generator, the “pila” in 1799. Our heart, our respiration, the chlorophyll photosynthesis <sup>3</sup> of our sisters the plants, the biological rhythms are ruled by electrical unbalances. These are local unbalances since a global unbalance would result in a thermodynamic instability. After all the simplest mathematical model of an electron gas requires a uniform neutralizing background of positive charge which confines harmonically the electrons which would otherwise run away to infinity. This is commonly called **Jellium**.

If we introduce a charge in an electron gas if the charge is negative it will create a hole around itself and it will soon be screened by the other charges far around it and neutrality is restored. If we introduce two like negative charges in an electron gas when they are close together the other charges will be unable to screen simultaneously both external charges so that in the two holes created around them there will be a region between them with a net positive charge (the one of the background) with a net resulting attraction between the two like negative charges.

If the external charge is positive it will also be screened far away but it may undergo *clustering* with the other charges. We will then have atom or molecule formation.

The **atom** of Democrito (Abdera, between 470 and 457 b.C. - between 360 and 350 b.C.) is itself neutral. It is the main actor in chemistry. It hasn't been easy to reach its modern mathematical model. First John Dalton (Eaglesfield, 5 or 6 September 1766 - Manchester, 27 July 1844) in 1803 described an atom as a heavy central particle surrounded by an atmosphere of caloric, the supposed substance of heat at the time. The size of the atom was determined by the diameter of the caloric atmosphere. He provided a method of calculating relative atomic weights for the chemical elements, which provides the means for the assignment of molecular formulas for all chemical substances. Later Sir Joseph John Thomson (Manchester, 18 December 1856 - Cambridge, 30 August 1940) believed that the corpuscles, the “electrons”, emerged from the atoms of the trace gas inside his cathode-ray tubes. He thus concluded that atoms were divisible, and that the corpuscles were their building blocks. In 1904, he suggested a model of the atom, hypothesizing that it was a sphere of positive matter within which electrostatic forces determined the positioning of the corpuscles. To explain the overall neutral charge of the atom, he proposed that the corpuscles were distributed in a uniform sea of positive charge. In this “plum pudding model”, the electrons were seen as embedded in the positive charge like raisins in a plum pudding (although in Thomson's model they were not stationary, but orbiting rapidly). Later Ernest Rutherford, 1st Baron Rutherford of Nelson (Brightwater, 30 August

---

<sup>3</sup>Certainly related to the photoelectric effect discovered by Albert Einstein (Ulma, 14 March 1879 – Princeton, 18 April 1955).

## 1. INTRODUCTION

---

1871 - Cambridge, 19 October 1937) in 1911 performed the Geiger–Marsden experiment, which demonstrated the nuclear nature of atoms by measuring the deflection of alpha particles passing through a thin gold foil. He was inspired to ask Geiger and Marsden in this experiment to look for alpha particles with very high deflection angles, which was not expected according to any theory of matter at that time. Such deflection angles, although rare, were found. Reflecting on these results in one of his last lectures, Rutherford was quoted as saying: “It was quite the most incredible event that has ever happened to me in my life. It was almost as incredible as if you fired a 15-inch shell at a piece of tissue paper and it came back and hit you.” It was Rutherford’s interpretation of this data that led him to propose the “nucleus”, a very small, charged region containing much of the atom’s mass. In 1912, Rutherford was joined by Niels Henrik David Bohr (Copenhagen, 7 October 1885 - Copenhagen, 18 November 1962) who postulated that electrons moved in specific orbits about the compact nucleus. Bohr adapted Rutherford’s nuclear structure to be consistent with Max Planck’s quantum hypothesis. The resulting Rutherford–Bohr model was the basis for quantum mechanical atomic physics of Heisenberg which remains valid today. In Chapter 4 we present the properties of the periodic system of the elements as can be predicted by quantum physics. And in Chapter 5 we present the relevance of the electron in a **chemical bond** between elements.

Stripping one or more electrons from an atom one gets an “**ion**” which is therefore positively charged. If we introduce an electron in a crystal of positive ions we call it a **polaron** which will be presented in Chapter 3.

Charles-Augustin de Coulomb (Angoulême, 14 June 1736 - Paris, 23 August 1806) discovered the mathematical law of interaction between two charges of electrical charge  $q_1$  and  $q_2$  separated by a distance  $r$ . *Coulomb force* (in Gauss units)

$$\vec{F}_{12} = r \frac{q_1 q_2}{r^3}, \quad (1.1)$$

gives rise to an *electric field* around charge one  $\vec{E}(r) = \vec{F}_{12}/q_2$ . The electric field is generated by an electric potential  $\vec{E}(r) = -\vec{\nabla}\varphi(r)$  with  $\varphi(r) = q/r$ , the Coulomb potential. The Coulomb potential satisfies to the equation of Baron Simón Denis Poisson (Pithiviers, 21 June 1781 - Paris, 25 April 1840)<sup>4</sup>

$$\vec{\nabla}^2 \varphi(r) = -4\pi q \delta^3(r), \quad (1.4)$$

where  $\delta^3$  is a Dirac delta function in 3 dimensions. Poisson equation is the equation of Pierre-Simon, Marquis de Laplace (Beaumont-en-Auge, 23 March 1749 - Paris, 5 March 1827) with a source term due to the charge  $q$ . Later Johann Carl Friedrich Gauss (Braunschweig, 30 April 1777 - Gottinga, 23 February 1855) discovered that

$$4\pi q = - \int_{\Omega} \vec{\nabla}^2 \varphi(r) dr = - \int_{\partial\Omega} \mathbf{n} \cdot \vec{\nabla} \varphi(r) dS = \int_{\partial\Omega} \mathbf{n} \cdot \vec{E}(r) dS = \Phi_E, \quad (1.5)$$

---

<sup>4</sup>For charges living in  $n$ -dimensions we have

$$\varphi(r) = q \begin{cases} 1/r & n = 3 \\ -\ln(r/\ell) & n = 2 \\ -r & n = 1 \end{cases}, \quad (1.2)$$

where  $\ell$  is a length. And the Poisson equation becomes

$$\vec{\nabla}^2 \varphi(r) = -q \delta^n(r) \begin{cases} 4\pi & n = 3 \\ 2\pi & n = 2 \\ 2 & n = 1 \end{cases}, \quad (1.3)$$

where  $\delta^n$  is a Dirac delta function in  $n$  dimensions.

---

which states the important mathematical result that the flux  $\Phi_E$  of the electric field through any closed surface containing charge  $q$  is fixed. In Eq. (1.5)  $dr$  is the infinitesimal volume integral,  $ndS$  is the infinitesimal surface element with  $n$  its outward normal versor,  $\Omega$  is the volume region considered in the volume integral, and  $\partial\Omega$  is its bounding surface.

The representation of the electron as a pointwise particle poses the problem of an infinite self-energy diverging as  $1/r$ . On the other side the electrostatic energy for assembling a system on  $N$  point charges of charge  $q_i$  is that required to bring them close together from infinity

$$E = \frac{1}{2} \sum_{i \neq j=1}^N \frac{q_i q_j}{|\mathbf{r}_i - \mathbf{r}_j|}, \quad (1.6)$$

But again a divergence problem arises as soon as one introduces a charge density  $\rho(\mathbf{r})$  to rewrite this energy with a continuous expression

$$E = \frac{1}{2} \int d\mathbf{r} \int d\mathbf{r}' \frac{\rho(\mathbf{r})\rho(\mathbf{r}')}{|\mathbf{r} - \mathbf{r}'|}, \quad (1.7)$$

where one readily recognize a divergence for a linear, planar, or spatial charge density. Also in these cases is necessary to deal with infinities.

An electron moving in an electric field  $\vec{E} = -\vec{\nabla}\varphi$  and a magnetic field  $\vec{B} = \vec{\nabla} \times \vec{A}$ , where  $\vec{A}$  is the vector potential, is subject to the Lorentz force which in Gaussian units reads  $\vec{F} = q(\vec{E} + \frac{\vec{v}}{c} \times \vec{B})$  where  $q = -e$  is the electron charge,  $\vec{v}$  is the speed of the electron, and  $c$  is the speed of light. In order to reach to this result from the Hamilton equations of motion it is necessary to start with a classical Hamiltonian  $H = \frac{1}{2m} (\vec{p} - \frac{q}{c} \vec{A})^2 + q\varphi$ . This amounts to the following transformation recipe  $\vec{p} \rightarrow \vec{p} - \frac{q}{c} \vec{A}$ . If we start from a quantum Hamiltonian  $\hat{H} = \frac{1}{2m} \hat{p}^2 = \frac{1}{2m} (\hat{\sigma} \cdot \hat{p})(\hat{\sigma} \cdot \hat{p})$ , where  $\hat{\sigma} = (\sigma_1, \sigma_2, \sigma_3)$  and  $\sigma_i$  are the Pauli matrices described in Appendix E such that  $(\hat{\sigma} \cdot \hat{A})(\hat{\sigma} \cdot \hat{B}) = \hat{A} \cdot \hat{B} + i\hat{\sigma} \cdot (\hat{A} \times \hat{B})$  for any two operators  $\hat{A}$  and  $\hat{B}$ . After applying the transformation recipe required by classical electrodynamics we find

$$\hat{H} = \frac{1}{2m} \left( \hat{p} - \frac{q}{c} \vec{A} \right)^2 - \frac{q\hbar}{2mc} \hat{\sigma} \cdot \vec{B} + q\varphi, \quad (1.8)$$

where we have used  $\hat{p} \times \vec{A} = -i\hbar(\vec{\nabla} \times \vec{A}) - \vec{A} \times \hat{p}$ . The spin magnetic moment turns out to have a g-factor  $g = 2$ . This derivation from the nonrelativistic Schrödinger-Pauli theory is due to R. P. Feynman and is alternative to the one obtained by P. A. M. Dirac from the nonrelativistic limit of his equation. More generally a particle of spin  $s$  has an “intrinsic” magnetic moment  $\mu$ . The corresponding quantum mechanical operator is proportional to the spin operator  $\hat{s}$  (for example  $\hat{s} = \hat{\sigma}\hbar/2$  for particles of spin  $s = 1/2$ ) and can therefore be written as  $\hat{\mu} = \mu\hat{s}/s$ . This contributes a term  $-\hat{\mu} \cdot \vec{B}$  to the Hamiltonian. The intrinsic magnetic moment of the electron is consequently  $-\mu_B$  where  $\mu_B = e\hbar/2mc \approx 0.927 \times 10^{-20}$  erg/gauss. This quantity is called the *Bohr magneton*. A charged, spin  $s = 1/2$ , particle that does not possess any internal structure has a spin magnetic moment  $\hat{\mu} = gq\hat{s}/2mc$ . The full relativistic quantum electrodynamics (QED) theory predicts a correction to the spin magnetic moment that is called *anomalous magnetic moment* and denoted with  $a = (g - 2)/2$ . For the electron, the correction of first order in the fine-structure constant  $\alpha = e^2/hc$  is  $a_e = \alpha/2\pi \approx 0.001\,161\,4$ . This result was first found by Julian Schwinger in 1948 [26] and is engraved on his tombstone. As of 2016, the coefficients of the QED formula for the anomalous magnetic moment of the electron are known analytically up to  $\alpha^3$  and have been calculated up to order  $\alpha^5$   $a_e = 0.001\,159\,652\,181\,643(764)$ . The QED prediction agrees with the experimentally measured value to more than 10 significant figures, making the

## 1. INTRODUCTION

---

magnetic moment of the electron one of the most accurately verified predictions in the history of physics. The current experimental value and uncertainty is:  $a_e = 0.001\ 159\ 652\ 180\ 59(13)$ . This required measuring  $g$  to an accuracy of around 1 part in 10 trillion.

From the first discoveries of electrostatics soon enough James Clerk Maxwell (Edinburgh, 13 June 1831 – Cambridge, 5 November 1879) wrote his equations for electrodynamics. The most synthetic way to write these important equations describing electromagnetism is through the geometric language of the differential forms (here we use Gauss units and set additionally the speed of light  $c = 1$ )

$$d \cdot F = 0, \quad (1.9)$$

$$d \star F = 4\pi \star J. \quad (1.10)$$

Here  $d$  stands for an exterior derivative [27],  $\star$  is the Hodge star that stands for the dual,  $F = dA$  is the **Faraday** two form that subtend the electromagnetic asymmetric tensor  $F_{\mu\nu}$  containing the electric and magnetic fields,  $A = (\varphi, \vec{A})$  is the electromagnetic 4-potential one form where  $\varphi$  is the electric scalar potential for the electric field  $\vec{E} = -\vec{\nabla}\varphi - \partial\vec{A}/\partial t$  and  $\vec{A}$  the magnetic vector potential for the magnetic field  $\vec{B} = \vec{\nabla} \times \vec{A}$ ,  $\star F$  is **Maxwell** two form dual to Faraday, and  $\star J$  is the **charge** three form with  $J = (\rho, \vec{J})$  the 4-current density one form with  $\rho$  the electric charge density and  $\vec{J}$  the electric current density. So that the total charge  $Q$  inside a three dimensional hypersurface region  $S$  is  $Q = \int_S \star J$ . Also from  $dd \star F = 0$  follows  $d \star J = 0$  which is the law of conservation of charge. Eq. (1.9) summarizes Faraday's law and the non-existence of magnetic monopoles and it is a consequence of the general result that  $dd = 0$ . Eq. (1.10) summarizes Ampere's law with Maxwell's correction to take into account of the displacement current and Gauss's law.

The Maxwell equations are invariant under the gauge transformation  $\vec{A} \rightarrow \vec{A} + \vec{\nabla}\psi$  and  $\varphi \rightarrow \varphi - \partial\psi/\partial t$  with the gauge function  $\psi(t, r)$  any scalar. Which means that electromagnetism has  $U(1)$  gauge freedom.

Now, start with the scalar  $\varphi$ . Its gradient  $d\varphi$  is a one form. Take its dual to get the three form  $\star d\varphi$ . Take its exterior derivative to get the four form  $d \star d\varphi$ . Take its dual, to get the scalar  $-\star d \star d\varphi \equiv \square\varphi = -(\partial^2\varphi/\partial t^2) + \vec{\nabla}^2\varphi$ . This is the Jean-Baptiste le Rond d'Alembert (16 November 1717 - 29 October 1783) wave operator.

Start with the one form  $A$ . Get the two form  $dA$ . Take its dual to get the two form  $\star dA$ . Take its exterior derivative to get the three form  $d \star dA$ . Take its dual, to get the one form  $4\pi J = \star d \star dA$ . This is the wave equation for the electromagnetic 4-potential. And from here follow the electromagnetic waves. For example for the zero component in vacuum in absence of charges one finds  $\square\varphi = 0$  whose solution with forward and backward propagation along the direction  $k$  is of the form  $\varphi(t, r) = f(\mathbf{k} \cdot \mathbf{r} - \omega t) + g(\mathbf{k} \cdot \mathbf{r} + \omega t)$ , where  $\omega = 2\pi/T$  is the angular frequency of the wave of period  $T$ ,  $\mathbf{k} = 2\pi/\lambda$  is the wave vector for a wavelength  $\lambda$ , the speed of the wave is  $\omega/k = \lambda/T = 1$ , and  $f, g$  are arbitrary functions. Alternatively one may think of a spherical wave solution of the following kind,  $\varphi_{s.w.}(t, r) \propto \exp[i(\pm kr - \omega t)]/r$ .

In flat spacetime, express the coordinates of one electron as a function of his proper time as  $a^\mu(\tau)$ . The density-current 4-vector for this electron is then

$$J^\mu(x) = e \int \delta^4[x - a(\tau)] \dot{a}^\mu d\tau, \quad (1.11)$$

where  $x \equiv (t, \mathbf{r})$  and as usual we denote with the dot a partial time derivative. This density-current drives the electromagnetic field,  $F$ . Then Maxwell equation (1.10) becomes  $F_{\mu,\nu}^\nu = 4\pi J_\mu$  where as usual the comma stands for a partial derivative. Or  $A^\nu,_\nu - \eta^{\nu\alpha} A_{\mu,\alpha\nu} = 4\pi J_\mu$  where

$\eta_{\mu\nu}$  is the metric of the Lorentz coordinate system of the flat spacetime. Make use of the gauge freedom to set Lorentz gauge,  $A^{\nu}{}_{,\nu} = 0$ , to get

$$\square A_\mu = -4\pi J_\mu. \quad (1.12)$$

This can be solved through the Green's function method rewriting  $A^\mu(x) = e \int G[x - a(\tau)] \dot{a}^\mu d\tau$  with the Green's function satisfying the following wave equation

$$\square G = -4\pi \delta^4(x). \quad (1.13)$$

The causal solution of this equation is given in terms of the retarded potential

$$A_\mu(t, \mathbf{r}) = \int \frac{J_\mu(t_{\text{retarded}}, \mathbf{r}')}{|\mathbf{r} - \mathbf{r}'|} d\mathbf{r}', \quad (1.14)$$

$$t_{\text{retarded}} = t - |\mathbf{r} - \mathbf{r}'|, \quad (1.15)$$

where remember that we chose the speed of light  $c = 1$ .

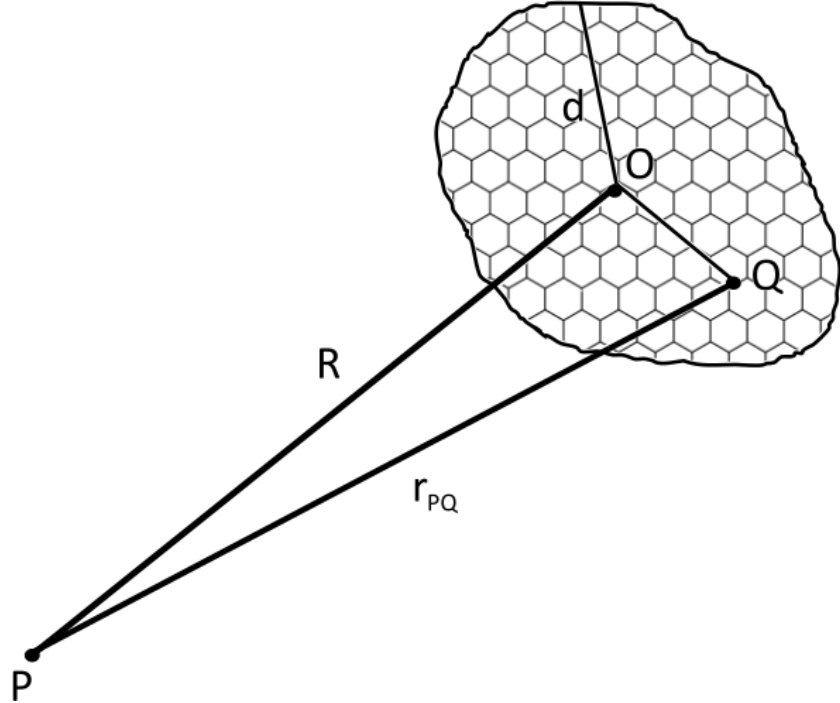


Figure 1.1: Radiation zone of a current system. The shaded area is where are the currents. The origin of the coordinate system  $O$  is chosen inside this region.  $Q$  is any point of the currents.  $P$  is where we measure the electromagnetic field radiated out.  $d$  is the linear extension of the current system.

With reference to Fig. 1.1 we briefly discuss the radiation electromagnetic field of a current system [7] consisting of a single pointwise electron  $\vec{J} = \rho \vec{v}$  with  $\vec{I} = \int \vec{J} d\mathbf{r} = e \vec{v}$ , where  $\vec{v}$  is the electron velocity. The radiation zone is characterized by the points  $P$  shown in the figure such that  $R \gg d$  and  $R \gg \lambda$  with  $\lambda$  the wavelength of the radiation. Nothing at all is presupposed

## 1. INTRODUCTION

---

about the ratio  $d/\lambda$ . If a point  $O$  within the current system is chosen as the origin of coordinates as is shown in the figure, then  $r_{PQ} \approx R - \mathbf{n} \cdot \mathbf{r}_Q$  where  $\overline{OP} = R$ ,  $\mathbf{r}_Q$  is the position vector of a source point  $Q$ , and  $\mathbf{n}$  is a versor in the  $P$  direction. Considering the spherical wave solution to Eq. (1.12) we can replace  $r_{PQ}$  with  $R$  in the denominator but not in the exponent, so that

$$(A_\mu)_P = \frac{e^{i(kR-\omega t)}}{R} \int d\mathbf{r}_Q (J_\mu)_Q e^{-ik(\mathbf{n} \cdot \mathbf{r}_Q)}. \quad (1.16)$$

In the transition to the fields intensities  $\mathbf{F} = d\mathbf{A}$  we note that  $\partial R / \partial \mathbf{r}_P = \mathbf{n}$ . Moreover we note that

$$\frac{\partial}{\partial \mathbf{r}_P} \frac{e^{ikR}}{R} = e^{ikR} \frac{\partial}{\partial \mathbf{r}_P} \frac{1}{R} + \frac{1}{R} \frac{\partial}{\partial \mathbf{r}_P} e^{ikR}, \quad (1.17)$$

but since the gradient in the first term gives rise to an additional factor  $1/R$  and the one in the second term gives rise to a multiplication by  $k$  we can neglect the first term altogether in the radiation zone where  $kR \gg 1$ . So  $\vec{B} = \vec{\nabla}_P \times \vec{A} \approx ik\mathbf{n} \times \vec{A}$ ,  $\vec{\nabla}_P \vec{A} \approx ik\mathbf{n} \cdot \vec{A}$ , and thanks to the Lorentz gauge condition  $\varphi \approx \mathbf{n} \cdot \vec{A}$ . So  $\vec{E} \approx ik[\vec{A} - \mathbf{n}(\mathbf{n} \cdot \vec{A})] = ik\vec{A}_\perp$ .

If we now also require that  $\lambda \gg d$  (or  $kd \ll 1$ ), a condition frequently satisfied for antennas, the exponential function  $e^{-ik(\mathbf{n} \cdot \mathbf{r}_Q)}$  can be expanded in a power series. This correspond to a decomposition of the radiation into multipoles. In the first approximation one sets  $e^{-ik(\mathbf{n} \cdot \mathbf{r}_Q)} \approx 1$  so that we do not have to worry about retardation due to the position of the emitter within the current system. The Poynting vector in this dipole radiation approximation is then given by

$$\vec{S} = \frac{\vec{E} \times \vec{B}}{4\pi} = \frac{E^2}{4\pi} \mathbf{n}, \quad (1.18)$$

$$\vec{E} = ik \frac{e^{i(kR-\omega t)}}{R} \vec{I}_\perp, \quad (1.19)$$

where for the case of a linear oscillation parallel to the  $z$  axis  $I_\perp = I \sin \theta$ . The energy radiated per second is obtained by integrating the Poynting vector over the surface of a sphere containing the oscillating electron

$$\int \vec{S} \cdot \mathbf{n} dS = \frac{2}{3} \left( \frac{d\vec{I}}{dt} \right)_{\text{retarded}}^2, \quad (1.20)$$

where  $dS = R^2 d\Omega$  and  $\Omega$  the solid angle and we used the fact that  $\omega/k = 1$  to reconstruct the time derivative.

Nikola Tesla (Smiljan, 10 July 1856 - New York, 7 January 1943) invented machines to transmit electricity without wires through alternating currents, electromagnetic induction generated by a varying in time magnetic field according to Eq. (1.9), and Maxwell displacement current generated by a varying in time electric field according to Eq. (1.10).

Very similar to the wave equation of d'Alembert is the Erwin Rudolf Josef Alexander Schrödinger (Vienna, 12 August 1887 - Vienna, 4 January 1961) equation for the wavefunction  $\varphi$  of a free particle of mass  $m = 1/2$ . This reads  $i\hbar(\partial\varphi/\partial t) + \hbar^2 \vec{\nabla}^2 \varphi = 0$ . The only difference with the d'Alembert equation is that it is of order one in time. And from here follows the wave-particle duality of quantum mechanics. For example for an eigenstate of eigenenergy  $E$  one may find a plane wave propagating along the direction of versor  $\mathbf{n}$  given by  $\varphi_{p.w.}(t, \mathbf{r}) \propto \exp[(\pm i\sqrt{E}\mathbf{n} \cdot \mathbf{r} - iEt)/\hbar]$  or otherwise a spherical wave [28]  $\varphi_{s.w.}(t, \mathbf{r}) \propto \exp[(\pm i\sqrt{E}\mathbf{r} - iEt)/\hbar]/r$ . The speed of this wave is  $\sqrt{E}$ .

One of the pillar thought experiments of quantum physics is the double slit experiment where a beam of electrons that impinges on a double slit may either produce an interference pattern on a screen posed behind the two slits as if the electron were waves or just a two bands pattern in correspondence of the two slits as if they were particles.

Clearly energy eigenstate of Schrödinger equation will have a well defined energy  $E$  and zero energy standard deviation  $\Delta E$ . The eigenstate probability distribution,  $|\varphi(t, \mathbf{r})|^2$ , will be steady state carrying no information on the dynamics of the electrons. In other words if  $\Delta E = 0$  then Heisenberg uncertainty principle,  $\Delta E \Delta t \geq \hbar/2$  tells us that the time standard deviation must diverge. In this case the electrons will behave like waves and produce an interference pattern in the two slit experiment.

Otherwise it is possible to create an electron “time wave-packet” by summing together several different energies eigenstates in a Fourier series in  $E$  so to have a finite non-zero standard deviation in energy. And as a consequence a finite standard deviation on time. This will allow to gather some dynamical information on the electrons beam.

But we can at the same time sum together several different momenta eigenstates in a Fourier series in  $p$  to create a “spacetime wave-packet” which according to the Heisenberg uncertainty principle  $\Delta q \cdot \Delta p \geq 3\hbar/2$  will also have a finite position standard deviation. Here we denote with  $\mathbf{q} \equiv \mathbf{r}$ . This will allow the observer to predict the “classical” trajectory of the electron spacetime wave-packet. In this case, playing with the slit width and  $\Delta q$  we can observe the particle behavior of the electrons with the disappearance of the interference pattern in the two slit experiment.

Something similar can be done with the Coherent State (CS) of John Rider Klauder (Reading, January 24, 1932 – New York, October 24, 2024) [29, 30, 31, 32, 33]<sup>5</sup>

$$\varphi(\mathbf{q}; \mathbf{Q}, \mathbf{P}) = \langle \mathbf{q} | e^{-i\mathbf{Q}\hat{\mathbf{p}}/\hbar} e^{i\mathbf{P}\hat{\mathbf{q}}/\hbar} | 0 \rangle, \quad (1.21)$$

where  $\hat{\mathbf{q}}, \hat{\mathbf{p}}$  are the position and momentum operators in position representation respectively and  $\varphi_0(\mathbf{q}) = \langle \mathbf{q} | 0 \rangle$  is a fiducial wavefunction such that  $\langle 0 | \hat{\mathbf{q}} | 0 \rangle = \langle 0 | \hat{\mathbf{p}} | 0 \rangle = 0$ . The time evolution of this wavefunction according to the quantum Hamiltonian  $\hat{H}(\hat{\mathbf{q}}, \hat{\mathbf{p}})$  is then given by  $\varphi(t, \mathbf{q}; \mathbf{Q}, \mathbf{P}) = e^{-i\hat{H}t/\hbar} \varphi(\mathbf{q}; \mathbf{Q}, \mathbf{P}) \approx \varphi(\mathbf{q}; \mathbf{Q}(t), \mathbf{P}(t))$  where  $\mathbf{Q}(t)$  and  $\mathbf{P}(t)$  follow Hamilton’s equations of motion according to the corresponding classical Hamiltonian  $H(\mathbf{Q}, \mathbf{P})$ , i.e. the one that has the functional form of the quantum mechanical Hamiltonian with explicit c-number substitution. Unfortunately this extremely useful time evolution property that holds exactly for the Harmonic Oscillator (HO) case,<sup>6</sup> is lost for a more general potential energy  $V(\hat{\mathbf{q}})$  (see section 2B of Ref. [30]), for which it is in any case still possible to expand on a local minimum and approximate it there with a quadratic potential. If Klauder dynamical property would remain exact and valid for a generic potential it could be possible to perform a “quantum molecular dynamics” simulation on an electron liquid. We are thinking at a computer experiment that could be used to study the statistical properties of a many electrons system in thermodynamic equilibrium at a given temperature  $T$ . Unfortunately for the time being this has never been done and the only quantum simulation method available is the path integral Monte Carlo [34]. Molecular dynamics being only available in the non-quantum regime.

The computer experiment with some of its most recent realization to study the Jellium will be presented in Chapter 6. Variational and diffusion Monte Carlo methods are able to study the ground state properties of Jellium. Path integral Monte Carlo methods are able to determine the finite non-zero temperature properties. The properties of interest are the structure, the pressure, the internal energy, and various other thermodynamic quantities, the superconducting fraction.

<sup>5</sup>They were called ‘continuous representation’ by the inventor J. R. Klauder and later renamed CS by J. P. Gazeau who first used them.

<sup>6</sup>It holds exactly also for a general linear or quadratic Hamiltonian.

## 1. INTRODUCTION

---

Unfortunately the Monte Carlo method is exact only for boson (and boltzmann) fluids. For fermion fluids, the yet unsolved “sign problem” requires the formulation of some approximation in the numerical calculation. So that even computationally we are still unable to extract exact statistical mechanical properties for fermions. Another limitation of the path integral Monte Carlo is that, whereas it is able to describe the molecules formation from the constituent atomic species, it is unable to describe the atom formation from the constituent electrons and nuclei, unless for an highly diluted system. This is due to the fact that since the mass of an electron is three orders of magnitude smaller than the one of the nucleous the degeneracy temperature of the electons is three orders of magnitude bigger than the one of the nuclei, at a given density. Therefore it is very unlikely that an electron, with a world-line with many particle exchanges, will bind to a nucleous, which has a world-line with many less particle exchanges.

The computer experiment allows also to study the cumbersome problem of the fluid phases coexistence. Of interest here are the phase transitions of the electron gas. From a mathematical point of view a phase transition appears as a non analyticity of the thermodynamic quantities of a many body system in the thermodynamic limit. The most complete theory for phase transitions in statistical physics is the **Renormalization Group** which predicts universal behaviors for the liquid in a neighborhood of a phase transition being it Jellium or something else. This will be presented briefly in Chapter 8.

Of particular interest for our everyday life is the *solid state* [35, 36, 37]. We live in a world made of surfaces between different phases but the solid is all around us, the soil, the walls of our houses, our same selves. Electrons play a fundamental role in solids, in crystals, in glasses. First of all it is possible to make a distinction between solids that conduct electrons, the *metals*, and solids that do not, the *insulators*. This way to classify a solid on the base of its ability to conduct electrons has been refined and needed revision over the years as technological advances allowed the observation and later reproduction of some important emerging physical phenomena related to electrons conduction. Such as the discovery of *semiconductors* and *superconductors*. Probably the first physical theories of electron conduction are the the Drude Theory of Metals <sup>7</sup> and the Sommerfeld Theory of Metals. Later theories dealt with the failure of the free electron model. Another way to classify a solid is through their crystal lattices characteristics in real and reciprocal space. As be determined by X-ray diffraction.

Electrons in a solid may be either tightly bound to the atoms forming the crystal or stripped from these atoms to form a gas around them. There are specific theories describing the electron energy levels in a periodic potential, the ones for the electrons in the gas, that form *bands*, and the ones for the bound electrons, that form *orbitals*, and their deformations. Usually the electrons in a solid should be described by a quantum theory, but the semiclassical limit may grasp already some general characteristic properties of their dynamics. Of course surface effect may play a role both as *finite size corrections* to the thermodynamic limit of the electron gas and for the chemical physics nature of the surface. Another important issue to take into account is the fact that since the mass of an electron is three orders of magnitude smaller than the one of the nucleus the degeneracy temperature of the electrons is three orders of magnitude bigger than the one of the nuclei, at a given density. Therefore it may be possible, to a first level of accuracy, to give a non-quantum description of the nuclei. In this respect a classical theory of a harmonic crystal may become a first meaningful approximation. Of course for a more faithful and complete description we should worry of a quantum theory of a harmonic crystal able to measure the *phonons* dispersion relations and other properties. Another important correction to this description would be to take care of anharmonic effects in crystals. Each of the four

---

<sup>7</sup>At room temperature the mean square velocities of the electrons in Drude theory are of the order of  $10^5 \text{ m/s}$ . The electrical current in a wire is instead quasi instantaneous because it is the result of a disturbance that propagates from one electron to another and is much faster than the drift velocity of electrons in the metal.

characteristic solids: insulators, semiconductors, metals, and superconductors, will have its own peculiarities in their theoretical descriptions.

In Chapter 7 we study the thermodynamic properties of a **white dwarf**, [38] a star that has consumed all her nuclear energy ending in a plasma made of a core with iron nuclei and an halo made of an electron liquid that is cooling down, supporting itself against gravity by the pressure of the cold electrons. These are found in the lower-left corner of the Hertzsprung–Russell diagram below the main sequence that contains our sun.

# Appendices



## **Appendix A**

# **Particle Data Group**

We include here the particle listing for the electron from the Particle Data Group [3] followed by an illustrative key.

**e**

$$J = \frac{1}{2}$$

## e MASS (atomic mass units u)

The primary determination of an electron's mass comes from measuring the ratio of the mass to that of a nucleus, so that the result is obtained in u (atomic mass units). The conversion factor to MeV is more uncertain than the mass of the electron in u; indeed, the recent improvements in the mass determination are not evident when the result is given in MeV. In this datablock we give the result in u, and in the following datablock in MeV.

VALUE ( $10^{-6}$ u)	DOCUMENT ID	TECN	COMMENT
<b>548.579909065±0.000000016</b>	TIESINGA	21	RVUE 2018 CODATA value
• • • We do not use the following data for averages, fits, limits, etc. • • •			
548.579909070±0.000000016	MOHR	16	RVUE 2014 CODATA value
548.57990946 ± 0.00000022	MOHR	12	RVUE 2010 CODATA value
548.57990943 ± 0.00000023	MOHR	08	RVUE 2006 CODATA value
548.57990945 ± 0.00000024	MOHR	05	RVUE 2002 CODATA value
548.5799092 ± 0.0000004	<sup>1</sup> BEIER	02	CNTR Penning trap
548.5799110 ± 0.0000012	MOHR	99	RVUE 1998 CODATA value
548.5799111 ± 0.0000012	<sup>2</sup> FARNHAM	95	CNTR Penning trap
548.579903 ± 0.000013	COHEN	87	RVUE 1986 CODATA value

<sup>1</sup> BEIER 02 compares Larmor frequency of the electron bound in a  $^{12}\text{C}^{5+}$  ion with the cyclotron frequency of a single trapped  $^{12}\text{C}^{5+}$  ion.

<sup>2</sup> FARNHAM 95 compares cyclotron frequency of trapped electrons with that of a single trapped  $^{12}\text{C}^{6+}$  ion.

## e MASS

The mass is known more precisely in u (atomic mass units) than in MeV.

The conversion is:  $1 \text{ u} = 931.494\ 102\ 42(28) \text{ MeV}/c^2$  (2018 CODATA value, TIESINGA 21). The conversion error dominates the uncertainty of the masses given below.

VALUE (MeV)	DOCUMENT ID	TECN	COMMENT
<b>0.51099895000±0.00000000015</b>	TIESINGA	21	RVUE 2018 CODATA value
• • • We do not use the following data for averages, fits, limits, etc. • • •			
0.5109989461 ± 0.0000000031	MOHR	16	RVUE 2014 CODATA value
0.510998928 ± 0.000000011	MOHR	12	RVUE 2010 CODATA value
0.510998910 ± 0.000000013	MOHR	08	RVUE 2006 CODATA value
0.510998918 ± 0.000000044	MOHR	05	RVUE 2002 CODATA value
0.510998901 ± 0.000000020	<sup>1,2</sup> BEIER	02	CNTR Penning trap
0.510998902 ± 0.000000021	MOHR	99	RVUE 1998 CODATA value
0.510998903 ± 0.000000020	<sup>1,3</sup> FARNHAM	95	CNTR Penning trap
0.510998895 ± 0.000000024	<sup>1</sup> COHEN	87	RVUE 1986 CODATA value
0.5110034 ± 0.0000014	COHEN	73	RVUE 1973 CODATA value

<sup>1</sup> Converted to MeV using the 1998 CODATA value of the conversion constant,  $931.494013 \pm 0.000037$  MeV/u.

<sup>2</sup> BEIER 02 compares Larmor frequency of the electron bound in a  $^{12}\text{C}^{5+}$  ion with the cyclotron frequency of a single trapped  $^{12}\text{C}^{5+}$  ion.

<sup>3</sup> FARNHAM 95 compares cyclotron frequency of trapped electrons with that of a single trapped  $^{12}\text{C}^{6+}$  ion.

### $(m_{e^+} - m_{e^-}) / m_{\text{average}}$

A test of *CPT* invariance.

VALUE	CL%	DOCUMENT ID	TECN	COMMENT
$<8 \times 10^{-9}$	90	<sup>1</sup> FEE	93	CNTR Positronium spectroscopy
<b>• • •</b> We do not use the following data for averages, fits, limits, etc. <b>• • •</b>				
$<4 \times 10^{-23}$	90	<sup>2</sup> DOLGOV	14	From photon mass limit
$<4 \times 10^{-8}$	90	CHU	84	CNTR Positronium spectroscopy

<sup>1</sup> FEE 93 value is obtained under the assumption that the positronium Rydberg constant is exactly half the hydrogen one.

<sup>2</sup> DOLGOV 14 result is obtained under the assumption that any mass difference between electron and positron would lead to a non-zero photon mass. The PDG 12 limit of  $1 \times 10^{-18}$  eV on the photon mass is in turn used to derive the value quoted here.

### $|q_{e^+} + q_{e^-}|/e$

A test of *CPT* invariance. See also similar tests involving the proton.

VALUE	DOCUMENT ID	TECN	COMMENT
$<4 \times 10^{-8}$	<sup>1</sup> HUGHES	92	RVUE
<b>• • •</b> We do not use the following data for averages, fits, limits, etc. <b>• • •</b>			
$<2 \times 10^{-18}$	<sup>2</sup> SCHAEFER	95	THEO Vacuum polarization
$<1 \times 10^{-18}$	<sup>3</sup> MUELLER	92	THEO Vacuum polarization

<sup>1</sup> HUGHES 92 uses recent measurements of Rydberg-energy and cyclotron-frequency ratios.

<sup>2</sup> SCHAEFER 95 removes model dependency of MUELLER 92.

<sup>3</sup> MUELLER 92 argues that an inequality of the charge magnitudes would, through higher-order vacuum polarization, contribute to the net charge of atoms.

## e MAGNETIC MOMENT ANOMALY

### $\mu_e/\mu_B - 1 = (g-2)/2$

VALUE (units $10^{-6}$ )	DOCUMENT ID	TECN	CHG	COMMENT
<b>1159.65218062 ± 0.00000012 OUR AVERAGE</b>				
1159.65218059 ± 0.00000013	<sup>1</sup> FAN	23	MRS	Single electron
1159.65218073 ± 0.00000028	HANNEKE	08	MRS	Single electron
1159.6521884 ± 0.0000043	VANDYCK	87	MRS	— Single electron
<b>• • •</b> We do not use the following data for averages, fits, limits, etc. <b>• • •</b>				
1159.65218128 ± 0.00000018	TIESINGA	21	RVUE	2018 CODATA value
1159.65218091 ± 0.00000026	MOHR	16	RVUE	2014 CODATA value
1159.65218076 ± 0.00000027	MOHR	12	RVUE	2010 CODATA value
1159.65218111 ± 0.00000074	<sup>2</sup> MOHR	08	RVUE	2006 CODATA value

1159.65218085 ± 0.00000076	<sup>3</sup> ODOM	06	MRS	–	Single electron
1159.6521859 ± 0.0000038	MOHR	05	RVUE		2002 CODATA value
1159.6521869 ± 0.0000041	MOHR	99	RVUE		1998 CODATA value
1159.652193 ± 0.000010	COHEN	87	RVUE		1986 CODATA value
1159.6521879 ± 0.0000043	<sup>4</sup> VANDYCK	87	MRS	+	Single positron

<sup>1</sup> FAN 23 report the most accurate measurement of the electron magnetic moment. A one-electron quantum cyclotron is used. We do not propagate at the moment this measurement to the fine structure and other physical constants. When discrepancies in the independent determinations of alpha are resolved, the new measurement uncertainty of 0.13 ppt is available for precise tests for BSM physics.

<sup>2</sup> MOHR 08 average is dominated by ODOM 06.

<sup>3</sup> Superseded by HANNEKE 08 per private communication with Gerald Gabrielse.

<sup>4</sup> This VANDYCK 87 result is for a positron. We do not take it into account for the average to avoid the assumption of CPT invariance.

### ( $g_{e^+} - g_{e^-}$ ) / $g_{\text{average}}$

A test of *CPT* invariance.

VALUE (units $10^{-12}$ )	CL%	DOCUMENT ID	TECN	COMMENT
– 0.5 ± 2.1		<sup>1</sup> VANDYCK 87	MRS	Penning trap
• • • We do not use the following data for averages, fits, limits, etc. • • •				
< 12	95	<sup>2</sup> VASSERMAN 87	CNTR	Assumes $m_{e^+} = m_{e^-}$
22 ± 64		SCHWINBERG 81	MRS	Penning trap

<sup>1</sup> VANDYCK 87 measured  $(g_-/g_+) - 1$  and we converted it.

<sup>2</sup> VASSERMAN 87 measured  $(g_+ - g_-)/(g-2)$ . We multiplied by  $(g-2)/g = 1.2 \times 10^{-3}$ .

### e ELECTRIC DIPOLE MOMENT (d)

A nonzero value is forbidden by both *T* invariance and *P* invariance.

VALUE ( $10^{-28}$ ecm)	CL%	DOCUMENT ID	TECN	COMMENT
< 0.041	90	<sup>1</sup> ROUSSY	23	ESR electrons in intramolecular electric field
• • • We do not use the following data for averages, fits, limits, etc. • • •				
< 0.11	90	<sup>2</sup> ANDREEV	18	CNTR ThO molecules
< 1.3	90	<sup>3</sup> CAIRNCROSS	17	ESR $^{180}\text{Hf}^{19}\text{F}$ molecules
– 5570 ± 7980 ± 120		KIM	15	CNTR $\text{Gd}_3\text{Ga}_5\text{O}_{12}$ molecules
< 0.87	90	<sup>4</sup> BARON	14	CNTR ThO molecules
< 6050	90	<sup>5</sup> ECKEL	12	CNTR $\text{Eu}_{0.5}\text{Ba}_{0.5}\text{TiO}_3$ molecules
< 10.5	90	<sup>6</sup> HUDSON	11	NMR YbF molecules
6.9 ± 7.4		REGAN	02	MRS $^{205}\text{Tl}$ beams
18 ± 12 ± 10		<sup>7</sup> COMMINS	94	MRS $^{205}\text{Tl}$ beams
– 27 ± 83		<sup>7</sup> ABDULLAH	90	MRS $^{205}\text{Tl}$ beams
– 1400 ± 2400		CHO	89	NMR TIF molecules
– 150 ± 550 ± 150		MURTHY	89	Cs, no <i>B</i> field

– 5000	$\pm 11000$	LAMOREAUX	87	NMR	$^{199}\text{Hg}$
19000	$\pm 34000$	SANDARS	75	MRS	Thallium
7000	$\pm 22000$	PLAYER	70	MRS	Xenon
< 30000	90	WEISSKOPF	68	MRS	Cesium

<sup>1</sup> ROUSSY 23 gives a measurement corresponding to this limit as  $(-1.3 \pm 2.0 \pm 0.6) \times 10^{-30} \text{ ecm}$ .

<sup>2</sup> ANDREEV 18 gives a measurement corresponding to this limit as  $(4.3 \pm 3.1 \pm 2.6) \times 10^{-30} \text{ ecm}$ .

<sup>3</sup> CAIRNCROSS 17 gives a measurement corresponding to this limit as  $(0.09 \pm 0.77 \pm 0.17) \times 10^{-28} \text{ ecm}$ .

<sup>4</sup> BARON 14 gives a measurement corresponding to this limit as  $(-0.21 \pm 0.37 \pm 0.25) \times 10^{-28} \text{ ecm}$ .

<sup>5</sup> ECKEL 12 gives a measurement corresponding to this limit as  $(-1.07 \pm 3.06 \pm 1.74) \times 10^{-25} \text{ ecm}$ .

<sup>6</sup> HUDSON 11 gives a measurement corresponding to this limit as  $(-2.4 \pm 5.7 \pm 1.5) \times 10^{-28} \text{ ecm}$ .

<sup>7</sup> ABDULLAH 90, COMMINS 94, and REGAN 02 use the relativistic enhancement of a valence electron's electric dipole moment in a high-Z atom.

## $e^-$ MEAN LIFE / BRANCHING FRACTION

A test of charge conservation. See the “Note on Testing Charge Conservation and the Pauli Exclusion Principle” following this section in our 1992 edition (Physical Review **D45** S1 (1992), p. VI.10).

Most of these experiments are one of three kinds: Attempts to observe (a) the 255.5 keV gamma ray produced in  $e^- \rightarrow \nu_e \gamma$ , (b) the (K) shell x ray produced when an electron decays without additional energy deposit, e.g.,  $e^- \rightarrow \nu_e \bar{\nu}_e \nu_e$  (“disappearance” experiments), and (c) nuclear de-excitation gamma rays after the electron disappears from an atomic shell and the nucleus is left in an excited state. The last can include both weak boson and photon mediating processes. We use the best  $e^- \rightarrow \nu_e \gamma$  limit for the Summary Tables.

Note that we use the mean life rather than the half life, which is often reported.

## $e \rightarrow \nu_e \gamma$ and astrophysical limits

VALUE (yr)	CL%	DOCUMENT ID	TECN	COMMENT
$>6.6 \times 10^{28}$	90	AGOSTINI	15B	$e^- \rightarrow \nu \gamma$
<b>• • •</b> We do not use the following data for averages, fits, limits, etc. <b>• • •</b>				
$>1.22 \times 10^{26}$	68	<sup>1</sup> Klapdor-Kleingrothaus et al. 07	CNTR	$e^- \rightarrow \nu \gamma$
$>4.6 \times 10^{26}$	90	BACK	02	BORX $e^- \rightarrow \nu \gamma$
$>3.4 \times 10^{26}$	68	BELLI	00B	DAMA $e^- \rightarrow \nu \gamma$ , liquid Xe
$>3.7 \times 10^{25}$	68	AHARONOV	95B	CNTR $e^- \rightarrow \nu \gamma$
$>2.35 \times 10^{25}$	68	BALYSH	93	CNTR $e^- \rightarrow \nu \gamma$ , $^{76}\text{Ge}$ detector
$>1.5 \times 10^{25}$	68	AVIGNONE	86	CNTR $e^- \rightarrow \nu \gamma$
$>1 \times 10^{39}$	2	ORITO	85	ASTR Astrophysical argument
$>3 \times 10^{23}$	68	BELLOTTI	83B	CNTR $e^- \rightarrow \nu \gamma$

<sup>1</sup> The authors of A. Derbin et al, arXiv:0704.2047v1 argue that this limit is overestimated by at least a factor of 5.

<sup>2</sup> ORITO 85 assumes that electromagnetic forces extend out to large enough distances and that the age of our galaxy is  $10^{10}$  years.

## Disappearance and nuclear-de-excitation experiments

VALUE (yr)	CL%	DOCUMENT ID	TECN	COMMENT
$>6.4 \times 10^{24}$	68	<sup>1</sup> BELLI	99B	DAMA De-excitation of $^{129}\text{Xe}$
<b>• • • We do not use the following data for averages, fits, limits, etc. • • •</b>				
$>1.2 \times 10^{24}$	90	ABGRALL	17	HPGE Ge K-shell disappearance
$>4.2 \times 10^{24}$	68	BELLI	99	DAMA Iodine L-shell disappearance
$>2.4 \times 10^{23}$	90	<sup>2</sup> BELLI	99D	DAMA De-excitation of $^{127}\text{I}$ (in NaI)
$>4.3 \times 10^{23}$	68	AHARONOV	95B	CNTR Ge K-shell disappearance
$>2.7 \times 10^{23}$	68	REUSSER	91	CNTR Ge K-shell disappearance
$>2 \times 10^{22}$	68	BELLOTTI	83B	CNTR Ge K-shell disappearance

<sup>1</sup> BELLI 99B limit on charge nonconserving  $e^-$  capture involving excitation of the 236.1 keV nuclear state of  $^{129}\text{Xe}$ ; the 90% CL limit is  $3.7 \times 10^{24}$  yr. Less stringent limits for other states are also given.

<sup>2</sup> BELLI 99D limit on charge nonconserving  $e^-$  capture involving excitation of the 57.6 keV nuclear state of  $^{127}\text{I}$ . Less stringent limits for the other states and for the state of  $^{23}\text{Na}$  are also given.

## LIMITS ON LEPTON-FLAVOR VIOLATION IN PRODUCTION

Forbidden by lepton family number conservation.

This section was added for the 2008 edition of this *Review* and is not complete. For a list of further measurements see references in the papers listed below.

### $\sigma(e^+ e^- \rightarrow e^\pm \tau^\mp) / \sigma(e^+ e^- \rightarrow \mu^+ \mu^-)$

VALUE	CL%	DOCUMENT ID	TECN	COMMENT
$<8.9 \times 10^{-6}$	95	AUBERT	07P	BABR $e^+ e^-$ at $E_{\text{cm}} = 10.58$ GeV
<b>• • • We do not use the following data for averages, fits, limits, etc. • • •</b>				
$<1.8 \times 10^{-3}$	95	GOMEZ-CAD...	91	MRK2 $e^+ e^-$ at $E_{\text{cm}} = 29$ GeV

### $\sigma(e^+ e^- \rightarrow \mu^\pm \tau^\mp) / \sigma(e^+ e^- \rightarrow \mu^+ \mu^-)$

VALUE	CL%	DOCUMENT ID	TECN	COMMENT
$<4.0 \times 10^{-6}$	95	AUBERT	07P	BABR $e^+ e^-$ at $E_{\text{cm}} = 10.58$ GeV
<b>• • • We do not use the following data for averages, fits, limits, etc. • • •</b>				
$<6.1 \times 10^{-3}$	95	GOMEZ-CAD...	91	MRK2 $e^+ e^-$ at $E_{\text{cm}} = 29$ GeV

## e REFERENCES

FAN	23	PRL 130 071801	X. Fan <i>et al.</i>	(HARV, NWES)
ROUSSY	23	SCI 381 46	T.S. Roussy <i>et al.</i>	(COLO)
TIESINGA	21	RMP 93 025010	E. Tiesinga <i>et al.</i>	(NIST)
ANDREEV	18	NAT 562 355	V. Andreev <i>et al.</i>	(ACME Collab.)
ABGRALL	17	PRL 118 161801	N. Abgrall <i>et al.</i>	(MAJORANA Collab.)
CAIRNCROSS	17	PRL 119 153001	W.B. Cairncross <i>et al.</i>	(NIST, COLO)
MOHR	16	RMP 88 035009	P.J. Mohr, D.B. Newell, B.N. Taylor	(NIST)
AGOSTINI	15B	PRL 115 231802	M. Agostini <i>et al.</i>	(Borexino Collab.)
KIM	15	PR D91 102004	Y.J. Kim <i>et al.</i>	(IND, YALE, LANL)
BARON	14	SCI 343 269	J. Baron <i>et al.</i>	(ACME Collab.)
DOLGOV	14	PL B732 244	A.D. Dolgov, V.A. Novikov	
ECKEL	12	PRL 109 193003	S. Eckel, A.O. Sushkov, S.K. Lamoreaux	(YALE)
MOHR	12	RMP 84 1527	P.J. Mohr, B.N. Taylor, D.B. Newell	(NIST)
PDG	12	PR D86 010001	J. Beringer <i>et al.</i>	(PDG Collab.)
HUDSON	11	NAT 473 493	J.J. Hudson <i>et al.</i>	(LOIC)

HANNEKE	08	PRL 100 120801	D. Hanneke, S. Fogwell, G. Gabrielse	(HARV)
MOHR	08	RMP 80 633	P.J. Mohr, B.N. Taylor, D.B. Newell	(NIST)
AUBERT	07P	PR D75 031103	B. Aubert <i>et al.</i>	(BABAR Collab.)
KLAPDOR-K...	07	PL B644 109	H.V. Klapdor-Kleingrothaus, I.V. Krivosheina, I.V. Titkova	(HARV)
ODOM	06	PRL 97 030801	B. Odom <i>et al.</i>	(HARV)
MOHR	05	RMP 77 1	P.J. Mohr, B.N. Taylor	(NIST)
BACK	02	PL B525 29	H.O. Back <i>et al.</i>	(Borexino/SASSO Collab.)
BEIER	02	PRL 88 011603	T. Beier <i>et al.</i>	
REGAN	02	PRL 88 071805	B.C. Regan <i>et al.</i>	
BELLI	00B	PR D61 117301	P. Belli <i>et al.</i>	(DAMA Collab.)
BELLI	99	PL B460 236	P. Belli <i>et al.</i>	(DAMA Collab.)
BELLI	99B	PL B465 315	P. Belli <i>et al.</i>	(DAMA Collab.)
BELLI	99D	PR C60 065501	P. Belli <i>et al.</i>	(DAMA Collab.)
MOHR	99	JPCRD 28 1713	P.J. Mohr, B.N. Taylor	(NIST)
Also		RMP 72 351	P.J. Mohr, B.N. Taylor	(NIST)
AHARONOV	95B	PR D52 3785	Y. Aharonov <i>et al.</i>	(SCUC, PNL, ZARA+)
Also		PL B353 168	Y. Aharonov <i>et al.</i>	(SCUC, PNL, ZARA+)
FARNHAM	95	PRL 75 3598	D.L. Farnham, R.S. van Dyck, P.B. Schwinberg	(WASH)
SCHAEEFER	95	PR A51 838	A. Schaefer, J. Reinhardt	(FRAN)
COMMINS	94	PR A50 2960	E.D. Commins <i>et al.</i>	
BALYSH	93	PL B298 278	A. Balysh <i>et al.</i>	(KIAE, MPIK, SASSO)
FEE	93	PR A48 192	M.S. Fee <i>et al.</i>	
HUGHES	92	PRL 69 578	R.J. Hughes, B.I. Deutch	(LANL, AARH)
MUELLER	92	PRL 69 3432	B. Muller, M.H. Thoma	(DUKE)
PDG	92	PR D45 S1	K. Hikasa <i>et al.</i>	(KEK, LBL, BOST+)
GOMEZ-CAD...	91	PRL 66 1007	J.J. Gomez-Cadenas <i>et al.</i>	(SLAC MARK-2 Collab.)
REUSSER	91	PL B255 143	D. Reusser <i>et al.</i>	(NEUC, CIT, PSI)
ABDULLAH	90	PRL 65 2347	K. Abdullah <i>et al.</i>	(LBL, UCB)
CHO	89	PRL 63 2559	D. Cho, K. Sangster, E.A. Hinds	(YALE)
MURTHY	89	PL 63 965	S.A. Murthy <i>et al.</i>	(AMHT)
COHEN	87	RMP 59 1121	E.R. Cohen, B.N. Taylor	(RISC, NBS)
LAMOREAUX	87	PRL 59 2275	S.K. Lamoreaux <i>et al.</i>	(WASH)
VANDYCK	87	PRL 59 26	R.S. van Dyck, P.B. Schwinberg, H.G. Dehmelt	(WASH)
VASSERMAN	87	PL B198 302	I.B. Vasserman <i>et al.</i>	(NOVO)
Also		PL B187 172	I.B. Vasserman <i>et al.</i>	(NOVO)
AVIGNONE	86	PR D34 97	F.T. Avignone <i>et al.</i>	(PNL, SCUC)
ORITO	85	PRL 54 2457	S. Orito, M. Yoshimura	(TOKY, KEK)
CHU	84	PRL 52 1689	S. Chu, A.P. Mills, J.L. Hall	(BELL, NBS, COLO)
BELLOTTI	83B	PL 124B 435	E. Bellotti <i>et al.</i>	(MILA)
SCHWINBERG	81	PRL 47 1679	P.B. Schwinberg, R.S. van Dyck, H.G. Dehmelt	(WASH)
SANDARS	75	PR A11 473	P.G.H. Sandars, D.M. Sternheimer	(OXF, BNL)
COHEN	73	JPCRD 2 664	E.R. Cohen, B.N. Taylor	(RISC, NBS)
PLAYER	70	JP B3 1620	M.A. Player, P.G.H. Sandars	(OXF)
WEISSKOPF	68	PRL 21 1645	M.C. Weisskopf <i>et al.</i>	(BRAN)

## Illustrative Key to the Particle Listings

Name of particle. "Old" name used before 1986 renaming scheme also given if different. See the section "Naming Scheme for Hadrons" for details.

**$a_0(1200)$**

$I^G(J^{PC}) = 1^-(0^{++})$

Particle quantum numbers (where known).

OMMITTED FROM SUMMARY TABLE

Evidence not compelling, may be a kinematic effect.

Indicates particle omitted from Particle Physics Summary Table, implying particle's existence is not confirmed.

Quantity tabulated below.

Top line gives our best value (and error) of quantity tabulated here, based on weighted average of measurements used. Could also be from fit, best limit, estimate, or other evaluation. See next page for details.

Footnote number linking measurement to text of footnote.

**$a_0(1200)$  MASS**

VALUE (MeV)	EVTS	DOCUMENT ID	TECN	CHG	COMMENT
<b>1206 ± 7 OUR AVERAGE</b>					
1210 ± 8 ± 9	3000	FENNER 87	MMS	—	3.5 $\pi^- p$
1198 ± 10		PIERCE 83	ASPK	+	2.1 $K^- p$
1216 ± 11 ± 9	1500	MERRILL 81	HBC	0	3.2 $K^- p$
• • • We do not use the following data for averages, fits, limits, etc. • • •					
1192 ± 16	200	LYNCH 81	HBC	±	2.7 $\pi^- p$

General comments on particle.

Number of events above background.

Measured value used in averages, fits, limits, etc.

Error in measured value (often statistical only; followed by systematic if separately known; the two are combined in quadrature for averaging and fitting.)

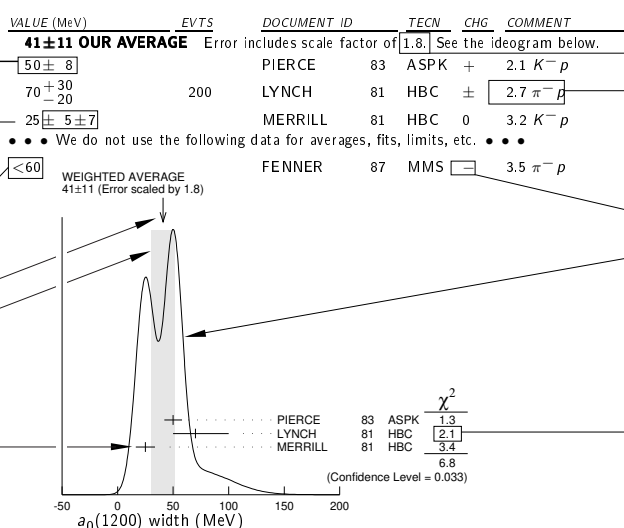
Measured value *not* used in averages, fits, limits, etc. See the Introductory Text for explanations.

Arrow points to weighted average.

Shaded pattern extends  $\pm 1\sigma$  (scaled by "scale factor" S) from weighted average.

Value and error for each experiment.

**$a_0(1200)$  WIDTH**



Scale factor > 1 indicates possibly inconsistent data.

Reaction producing particle, or general comments.

"Change bar" indicates result added or changed since previous edition.

Charge(s) of particle(s) detected.

Ideogram to display possibly inconsistent data. Curve is sum of Gaussians, one for each experiment (area of Gaussian = 1/error; width of Gaussian =  $\pm$ error). See Introductory Text for discussion.

Contribution of experiment to  $\chi^2$  (if no entry present, experiment not used in calculating  $\chi^2$  or scale factor because of very large error).

Partial decay mode (labeled by  $\Gamma_i$ ).

Mode	Fraction ( $\Gamma_i/\Gamma$ )	Scale factor/ Confidence level
$\Gamma_1 3\pi$	(65.2 ± 1.3) %	S=1.7
$\Gamma_2 K\bar{K}$	(34.8 ± 1.3) %	S=1.7
$\Gamma_3 \eta\pi^\pm$	< 5 $\times 10^{-4}$	CL=95%

Our best value for branching fraction as determined from data averaging, fitting, evaluating, limit selection, etc. This list is basically a compact summary of results in the Branching Ratio section below.

Branching ratio.

Our best value (and error) of quantity tabulated, as determined from constrained fit (using *all significant* measured branching ratios for this particle).

Weighted average of measurements of this ratio only.

Footnote (referring to LYNCH 81).

**$a_0(1200)$  BRANCHING RATIOS**

VALUE	DOCUMENT ID	TECN	CHG	COMMENT
<b>0.652 ± 0.013 OUR FIT</b>				Error includes scale factor of 1.7.
<b>0.643 ± 0.010 OUR AVERAGE</b>				
0.64 ± 0.01	PIERCE 83	ASPK	+	2.1 $K^- p$
0.74 ± 0.06	MERRILL 81	HBC	0	3.2 $K^- p$
• • • We do not use the following data for averages, fits, limits, etc. • • •				
0.48 ± 0.15	LYNCH 81	HBC	±	2.7 $\pi^- p$

Branching ratio in terms of partial decay mode(s)  $\Gamma_i$  above.

Confidence level for measured upper limit.

References, ordered inversely by year, then author.

"Document id" used on data entries above.

Journal, report, preprint, etc. (See abbreviations on next page.)

**$\Gamma(3\pi)/\Gamma_{\text{total}}$**

$\Gamma_1/\Gamma$

VALUE	DOCUMENT ID	TECN	CHG	COMMENT
<b>0.348 ± 0.013 OUR FIT</b>				Error includes scale factor of 1.7.
<b>0.345 ± 0.010 OUR AVERAGE</b>				
0.345 ± 0.005	PIERCE 83	ASPK	+	2.1 $K^- p$

**$\Gamma(K\bar{K})/\Gamma_{\text{total}}$**

$\Gamma_2/\Gamma$

VALUE	DOCUMENT ID	TECN	CHG	COMMENT
<b>0.348 ± 0.013 OUR FIT</b>				Error includes scale factor of 1.7.
<b>0.345 ± 0.010 OUR AVERAGE</b>				

**$\Gamma(\eta\pi^\pm)/\Gamma_{\text{total}}$**

$\Gamma_3/\Gamma$

VALUE	DOCUMENT ID	TECN	CHG	COMMENT
<b>0.535 ± 0.030 OUR FIT</b>				Error includes scale factor of 1.7.
<b>0.50 ± 0.03</b>	MERRILL 81	HBC	0	3.2 $K^- p$

**$\Gamma(\eta\pi^\pm)/\Gamma_{\text{total}}$**

$0.71\Gamma_3/\Gamma$

VALUE (units $10^{-4}$ )	CL%	DOCUMENT ID	TECN	CHG	COMMENT
< 3.5	95	PIERCE 83	ASPK	+	2.1 $K^- p$

**$a_0(1200)$  REFERENCES**

FENNER 87	PRL 55 14	H. Fenner et al.	(SLAC) (FNAL) (JPF)
PIERCE 83	PL 123B 230	J.H. Pierce	
LYNCH 81	PR D24 610	G.R. Lynch et al.	(CLEO Collab.)
MERRILL 81	PRL 47 143	D.W. Merrill et al.	(SACL, CERN)

Partial list of author(s) in addition to first author.

Quantum number determinations in this reference.

Institution(s) of author(s). (See abbreviations on next page.)

# Chapter 2

## The particle

In Relativistic Quantum Theory [39] we describe a pointwise, structureless, elementary, free particle through a finite dimensional irreducible unitary representation of its group of symmetries (the Galileo group in the non-relativistic case and the Poincaré group in the relativistic case, extended to the parity transformation). The invariants of the group are the mass and the spin. The wave functions of the particles are in bijective correspondence with the vectors of such representations, and the scalar product for such vectors is expressible in terms of wave functions. We determine the wave equation satisfied by the particles. In the relativistic case, the locality requirement, forces the introduction of “negative energy” solutions. It is an experimental fact that the number of particles may change in physical processes. Then, there exist transitions between states with different number of particles. We will present a formalism that allows to describe systems of many free particles, used in any many-body theory, relativistic or not, and known as Fock method. It allows to describe many particles states with the correct statistics and to introduce operators that change the number of particles (creation and annihilation operators). We will introduce the free field operators, and we will interpret in terms of field operators the negative energy solutions of the equations of free motion. We will denote as “antiparticles” the negative energy particles with a non-hermitian field operator. We construct the representation of the group on the many free particles states. And we prove the spin-statistics theorem which states that, as a consequence of Lorentz invariance and of locality, half integer spin particles must obey to *Fermi statistics* and integer spin particles must obey to *Bose statistics*.

This chapter is extracted from the “Theoretical Physics” course given by Prof. Adriano di Giacomo at the physics department of the University of Pisa in 1993.

### 2.1 Definition of Invariance

A reference frame is defined by a set of operative rules to measure physical quantities.

The same physical phenomenon can be observed from two different reference frames. In order for the two reference frames to be defined, the transformation between the quantities measured in the two frames must be known.

In a given reference frame a phenomenon obeys certain physical laws. A physical law is a relationship which poses conditions on the quantities measured at a given instant.

The frames are said to be equivalent respect to a class of phenomena if:

- a) Any physical situation realizable in one can also be realizable in the other.
- b) The time evolution laws are the same in the two frames.

The equivalence between frames produced by the invariance is an equivalence relationship in the mathematical sense: Given  $R, R', R''$  three frames;  $R$  is equivalent to  $R$ , if  $R$  is equivalent to  $R'$  then  $R'$  is equivalent to  $R$ ; if  $R$  is equivalent to  $R'$  and  $R'$  is equivalent to  $R''$  then  $R$  is equivalent to  $R''$ .

The transformation laws between quantities in equivalent frames form a group:

- a) The identity transformation exists: The one between any frame and itself.
- b) Given any transformation, an inverse transformation exists which is itself an equivalence relationship respect to the class of phenomena in exam.
- c) The product of two equivalence relationships, defined as the application in succession and ordered of two transformations, is still an equivalence relationship.

The equivalence of a class of frames relative to a set of phenomena is called *invariance* of such phenomena relative to the group of transformations between the frames.

### 2.1.1 Conventions

Through the note we will conform to the following conventions:

#### Units

We will always use relativistic units with  $\hbar = 1, c = 1$ . In these units, we have for the elementary charge  $e^2/4\pi = 1/137$ .

#### Fourier transform

The tridimensional Fourier transform is

$$f(\mathbf{p}) = \int f(\mathbf{q}) e^{-i\mathbf{q} \cdot \mathbf{p}} d\mathbf{q}, \quad (2.1)$$

$$f(\mathbf{q}) = \int f(\mathbf{p}) e^{i\mathbf{q} \cdot \mathbf{p}} \frac{d\mathbf{p}}{(2\pi)^3}, \quad (2.2)$$

and analogously for the four-dimensional case.

#### Operators

We will not introduce a different symbol for the operators on the Hilbert space and their eigenvalues. The reader should understand the difference from the context of the various equations introduced.

## 2.2 Invariance in quantum mechanics

In quantum mechanics the invariance respect to a change of reference frame is defined as follows:

- a) The possible states in the two frames are the vectors of a same Hilbert space. The observables are the same. The transformation law is a mapping of the Hilbert space onto itself.
  - b) Starting from the same initial state the time evolution is the same in the two frames.
-

The invariance transformations are a group. So an invariance transformation is a realization of the group on an Hilbert space.

Let  $|a\rangle$  be a state, in a certain frame, defined by the simultaneous measure of a complete set of commuting observables. Any vector of the form  $x_a|a\rangle$  where  $x_a$  is an arbitrary phase factor, is an eigenstate of the same observables with the same eigenvalues. So it represents the same physical state. The phase is not observable. A measurement on  $|a\rangle$  means to observe the probability that  $|a\rangle$  contains a state  $|b\rangle$  defined by the measure instruments. What one measures is

$$P_{ab} = |\langle b|a\rangle|^2, \quad (2.3)$$

where the phases  $x_a$  and  $x_b$  cancel. A vector of the Hilbert space modulo a phase is called a “ray” of the Hilbert space and will be denoted  $|\{a\}\rangle$ .

**Wigner theorem:** Given a bijective transformation between rays in a Hilbert space  $|\{s\}\rangle \rightarrow |\{s'\}\rangle$  such that

$$|\langle \{s'_2\} | \{s'_1\} \rangle|^2 = |\langle \{s_2\} | \{s_1\} \rangle|^2 \quad \forall |\{s_1\}\rangle, |\{s_2\}\rangle \quad (2.4)$$

it is always possible to choose the phases in such a way that the transformation is realized on the Hilbert space vectors as a unitary or antiunitary transformation.

**Proof:**

1. Let  $|e_n\rangle$  be an orthonormal complete base of the Hilbert space and let  $|\{e_n\}\rangle$  be the correspondent rays. The transformed rays are orthonormal

$$\langle e_i | e_j \rangle = \delta_{ij} \implies |\langle \{e'_i\} | \{e'_j\} \rangle|^2 = \delta_{ij} \quad (2.5)$$

Let us choose in an arbitrary way a set of phases on the rays  $|\{e'_i\}\rangle$ , i.e. a set of vectors  $|e'_i\rangle$  that represent the states. Then

$$\langle e'_i | e'_j \rangle = \delta_{ij}, \quad (2.6)$$

The set of vectors so obtained is also a complete base of the Hilbert space. In fact, if there exists a vector  $|v'\rangle$  such that  $\langle v'|v'\rangle \neq 0$  and  $\langle v'|e'_n\rangle = 0 \quad \forall n$ , then, by hypothesis, there would exist a vector  $|v\rangle$  such that  $\langle v|v\rangle \neq 0$  and  $\langle v|e_n\rangle = 0 \quad \forall n$ , against the hypothesis of completeness of the base  $|e_n\rangle$ .

2. Let  $|F_k\rangle = |e_1\rangle + |e_k\rangle$ . The generic representative of the transformed ray  $|\{F'_k\}\rangle$  will be

$$|F'_k\rangle = x_k(|e'_1\rangle + y_k|e'_k\rangle), \quad (2.7)$$

with  $x_k$  and  $y_k$  phases factors. In fact

$$|\langle F_k | e_n \rangle| = \delta_{n1} + \delta_{nk} \implies |\langle F'_k | e'_n \rangle| = \delta_{n1} + \delta_{nk}. \quad (2.8)$$

Next I can define the following  $S$  transformation

$$|Se_1\rangle = |e'_1\rangle \quad |Se_k\rangle = y_k|e'_k\rangle \quad (2.9)$$

$$|SF_k\rangle = \frac{1}{x_k}|F'_k\rangle = |e'_1\rangle + y_k|e'_k\rangle. \quad (2.10)$$

With this choice

$$|SF_k\rangle = |Se_1\rangle + |Se_k\rangle. \quad (2.11)$$

In other words we realized the transformation  $S$  as a linear transformation on vectors of kind  $|F_k\rangle$ . Let us next extend this construction to all vectors of the Hilbert space.

3. Consider a generic vector

$$|v\rangle = \sum_n a_n |e_n\rangle. \quad (2.12)$$

Let us assume, without loss of generality,  $a_1$  real. The correspondent ray  $|\{v\}\rangle$  will be transformed into a ray  $|\{v'\}\rangle$  with the following generic representative

$$|v'\rangle = \sum_n a'_n |e'_n\rangle, \quad (2.13)$$

and since by hypothesis

$$|\langle v|e_n\rangle|^2 = |\langle v'|e'_n\rangle|^2, \quad (2.14)$$

we have

$$|a'_n| = |a_n|. \quad (2.15)$$

We define

$$|Se_1\rangle = |e'_1\rangle, \quad (2.16)$$

$$|Se_n\rangle = y_n |e'_n\rangle \quad \forall n \neq 1, \quad (2.17)$$

with  $y_n$  some phase factors, so that for any vector belonging to the transformed ray  $|\{v'\}\rangle$

$$|v'\rangle = x \left\{ a_1 |Se_1\rangle + \sum_{n=2}^{\infty} \frac{a'_n}{y_n} |Se_n\rangle \right\}, \quad (2.18)$$

with  $x$  a phase factor. We then define

$$|Sv\rangle = \frac{1}{x} |v'\rangle. \quad (2.19)$$

By hypothesis it must be

$$|\langle F_k|v\rangle|^2 = |a_1 + a_k|^2 = |\langle SF_k|Sv\rangle|^2 = \left| a_1 + \frac{a'_k}{y_k} \right|^2. \quad (2.20)$$

Since we also have  $|a_k| = |a'_k|$  we require

$$\mathbf{Re}(a_1 a_k) = \mathbf{Re} \left( a_1 \frac{a'_k}{y_k} \right). \quad (2.21)$$

Then there are only two possibilities:

- i.  $a_k = a'_k/y_k$
- ii.  $a_k = (a'_k/y_k)^*$

or

- i.  $|Sv\rangle = S(\sum_n a_n |e_n\rangle) = \sum_n a_n |Se_n\rangle$
- ii.  $|Sv\rangle = S(\sum_n a_n |e_n\rangle) = \sum_n a_n^* |Se_n\rangle$

In the first case the operator  $S$  is linear, in the second is antilinear. We also have

- i.  $\langle Sv_1|Sv_2\rangle = \langle v_1|v_2\rangle \quad \forall |v_1\rangle, |v_2\rangle$
- ii.  $\langle Sv_1|Sv_2\rangle = \langle v_2|v_1\rangle \quad \forall |v_1\rangle, |v_2\rangle$

In the first case  $S$  is unitary, in the second it is antiunitary.

## 2.3 Invariance and time evolution

The requirement b) for invariance tells us that the evolution of the transformed must coincide with the transformation of the evolved

$$U(t, t')S(t')|\psi\rangle = S(t)U(t, t')|\psi\rangle, \quad (2.22)$$

where  $U(t, t')$  is the time evolution operator. Since  $|\psi\rangle$  is arbitrary we must have

$$S^\dagger(t)U(t, t')S(t') = U(t, t'). \quad (2.23)$$

If the Hamiltonian  $H$  is independent of time

$$U(t, t') = e^{-iH(t-t')}, \quad (2.24)$$

and we require

$$S(t) = e^{-iH(t-t')}S(t')e^{iH(t-t')}. \quad (2.25)$$

## 2.4 Galilean relativity

We require invariance under translations, rotations, and velocity transformations for pointwise non relativistic particles.

### 2.4.1 Spatial translations

Let us consider a reference frame  $R'$  translated by  $\mathbf{a}$  relative to the frame  $R$ . If the spatial translations are a symmetry of the system it must exist a unitary transformation  $U(\mathbf{a})$  which relates the dynamical variables  $\mathbf{q}'$  and  $\mathbf{p}'$  in  $R'$  to the variables  $\mathbf{q}$  and  $\mathbf{p}$  in  $R$ . The transformation law must be

$$\mathbf{q}' = \mathbf{q} - \mathbf{a}, \quad (2.26)$$

$$\mathbf{p}' = \mathbf{p}. \quad (2.27)$$

It is easy to see that the unitary operator exists and is

$$U(\mathbf{a}) = e^{i\mathbf{a} \cdot \mathbf{p}}. \quad (2.28)$$

Since the transformation is unitary the commutation relations do not change

$$[q'_i, p'_j] = [q_i, p_j] = i\delta_{ij}, \quad (2.29)$$

$$[q'_i, q'_j] = [q_i, q_j] = 0, \quad (2.30)$$

$$[p'_i, p'_j] = [p_i, p_j] = 0, \quad (2.31)$$

where  $\mathbf{q} = U(\mathbf{a})^\dagger \mathbf{q} U(\mathbf{a})$  and  $\mathbf{p} = U(\mathbf{a})^\dagger \mathbf{p} U(\mathbf{a})$ . Moreover from Hadamard lemma (B.11) follows immediately that Eqs. (2.26)-(2.27) are satisfied.

The invariance of the time evolution between two frames  $R$  and  $R'$  imposes

$$U^\dagger(\mathbf{a}, t)e^{-iH(t-t')}U(\mathbf{a}, t') = e^{-iH(t-t')}, \quad (2.32)$$

which means

$$[\mathbf{p}, H] = 0. \quad (2.33)$$

In other words, the momentum is a constant of motion. We can also write

$$\frac{\partial H}{\partial \mathbf{q}} = 0. \quad (2.34)$$

### 2.4.2 Rotations

A rotation is defined by a versor  $\hat{n}$  which indicates the axis of rotation and an angle  $\theta$ . We define  $\boldsymbol{\theta} = \theta \hat{n}$ . The angles are taken as positive for anti-clockwise rotations. Let us consider a frame  $R'$  rotated by  $\boldsymbol{\theta}$  relative to frame  $R$ . The component of a vector  $v$  will change according to

$$v'_i = R(\boldsymbol{\theta})_{ij} v_j, \quad (2.35)$$

where  $R(\boldsymbol{\theta})$  is the rotation matrix. For infinitesimal transformations

$$\delta v = v' - v \approx -\boldsymbol{\theta} \wedge v. \quad (2.36)$$

If the quantum system is invariant under rotations it must be possible to construct a unitary transformation on the Hilbert space which realizes the transformation and commutes with the time evolution. Let us then consider the angular momentum

$$\mathbf{J} = \mathbf{q} \wedge \mathbf{p}. \quad (2.37)$$

It is easy to verify that for  $v = q$  or  $v = p$  we have

$$[\boldsymbol{\theta} \cdot \mathbf{J}, v] = -i\boldsymbol{\theta} \wedge v. \quad (2.38)$$

Then the transformation we are looking for is

$$U(\boldsymbol{\theta}) = e^{i\boldsymbol{\theta} \cdot \mathbf{J}}, \quad (2.39)$$

as can be readily verified for infinitesimal transformations

$$v' = U^\dagger(\boldsymbol{\theta})vU(\boldsymbol{\theta}) \approx v - i[\boldsymbol{\theta} \cdot \mathbf{J}, v] = v - \boldsymbol{\theta} \wedge v. \quad (2.40)$$

The transformation commutes with the time evolution if

$$[\mathbf{J}, H] = 0 \quad (2.41)$$

which means that  $H$  must be a scalar and the angular momentum a constant of motion. Since the transformation is unitary it preserves the commutation relations.

If the particle has a spin the generator of the rotations is the total angular momentum

$$\mathbf{J} = \mathbf{q} \wedge \mathbf{p} + \mathbf{s}. \quad (2.42)$$

### 2.4.3 Galilean transformations

If we go from a frame  $R$  to a frame  $R'$  moving relative to  $R$  with a constant speed  $v$  we must have

$$q' = q - tv, \quad (2.43)$$

$$p' = p - mv. \quad (2.44)$$

It is easy to verify that these laws of transformation are induced by the unitary operator

$$U(t, v) = e^{i(p t - q m) \cdot v}, \quad (2.45)$$

so that

$$U^\dagger(t, v)qU(t, v) = q - tv, \quad (2.46)$$

$$U^\dagger(t, v)pU(t, v) = p - mv. \quad (2.47)$$

If the Galilean transformation has to be an invariance we must also require

$$U(t, \mathbf{v}) = e^{-iH(t-t')} U(t', \mathbf{v}) e^{iH(t-t')}, \quad (2.48)$$

or

$$t\mathbf{p} - m\mathbf{q} = e^{-iH(t-t')} (t'\mathbf{p} - m\mathbf{q}) e^{iH(t-t')}. \quad (2.49)$$

If the system is invariant under translations  $[\mathbf{p}, H] = 0$ , so

$$(t - t')\mathbf{p} = m\mathbf{q} - m e^{-iH(t-t')} \mathbf{q} e^{iH(t-t')}. \quad (2.50)$$

For infinitesimal time differences we get

$$\frac{\mathbf{p}}{m} = i[H, \mathbf{q}] = \frac{\partial H}{\partial \mathbf{p}}. \quad (2.51)$$

So

$$H = \frac{\mathbf{p}^2}{2m}. \quad (2.52)$$

#### 2.4.4 Galileo group

We analyzed the symmetries under translations, rotations, and Galileo transformations for a non relativistic system. The corresponding unitary transformations are

$$U(\mathbf{a}) = e^{i\mathbf{a} \cdot \mathbf{p}}, \quad (2.53)$$

$$U(\boldsymbol{\theta}) = e^{i\boldsymbol{\theta} \cdot \mathbf{J}}, \quad (2.54)$$

$$U(\mathbf{v}) = e^{-i\mathbf{v} \cdot \mathbf{K}} \quad \mathbf{K} = m\mathbf{q} - t\mathbf{p} \quad (2.55)$$

The group corresponding to the set of these transformations is called “Galileo group” and the corresponding invariance “galilean invariance”.

From the canonical commutation relationships, the following algebra for the group generators, follows

$$[p_\mu, p_\nu] = 0 \quad P_0 = H \quad (2.56)$$

$$[\mathbf{J}, H] = 0 \quad [J_i, p_j] = i\epsilon_{ijk}p_k \quad (2.57)$$

$$[J_i, J_j] = i\epsilon_{ijk}J_k \quad [J_i, K_j] = i\epsilon_{ijk}K_k \quad (2.58)$$

$$[K_i, K_j] = 0 \quad [K_i, p_j] = im\delta_{ij} \quad [K_i, H] = ip_i \quad (2.59)$$

In the Hilbert space of the physical system is then defined an unitary representation of the group that transforms the spec into itself.

If this representation is reducible it is possible to write the Hilbert space as a direct sum of one or more orthogonal Hilbert spaces each one transforming in itself. The generators are written as sum of the generators acting in each subspace and generators acting on different irreducible subspaces commute. The states in each subspace evolve with their Hamiltonian each in states belonging to the same subspace.

A physical system can then be written as a sum of irreducible representations of the Galileo group.

The simplest case is a particle without internal structure. In this case the only internal variable is the spin which commutes with the orbital variables. A complete set of state is

$$|\mathbf{p}\rangle|s, s_z\rangle. \quad (2.60)$$

Assuming the usual metric

$$\langle \mathbf{p}' | \mathbf{p} \rangle = (2\pi)^3 \delta^3(\mathbf{p} - \mathbf{p}'), \quad (2.61)$$

$$\langle s'_z | s_z \rangle = \delta_{s'_z s_z} \quad (2.62)$$

these states constitute an irreducible representation of the Galileo group if the states  $|s_z\rangle$  are an irreducible representation of internal rotations. Let us show this explicitly:

$$p|\mathbf{p}\rangle = p|\mathbf{p}\rangle, \quad (2.63)$$

$$\begin{aligned} p e^{i\theta \cdot \mathbf{J}} |\mathbf{p}\rangle &= e^{i\theta \cdot \mathbf{J}} e^{-i\theta \cdot \mathbf{J}} p e^{i\theta \cdot \mathbf{J}} |\mathbf{p}\rangle \\ &= R(\theta) p e^{i\theta \cdot \mathbf{J}} |\mathbf{p}\rangle, \end{aligned} \quad (2.64)$$

where  $p$  on the right hand side denotes the momentum operator acting on the eigenstate  $|\mathbf{p}\rangle$  and on the left denotes the eigenvalue. The eigenvalues of the rotated state is the rotated momentum. In the same way:

$$\begin{aligned} p e^{-iv \cdot \mathbf{K}} |\mathbf{p}\rangle &= e^{-iv \cdot \mathbf{K}} e^{iv \cdot \mathbf{K}} p e^{-iv \cdot \mathbf{K}} |\mathbf{p}\rangle \\ &= (\mathbf{p} - mv) e^{-iv \cdot \mathbf{K}} |\mathbf{p}\rangle, \end{aligned} \quad (2.65)$$

so

$$e^{i\theta \cdot \mathbf{J}} |\mathbf{p}\rangle = |R(\theta)\mathbf{p}\rangle, \quad (2.66)$$

$$e^{-iv \cdot \mathbf{K}} |\mathbf{p}\rangle = |\mathbf{p} - mv\rangle, \quad (2.67)$$

and we see that starting from any vector  $|\mathbf{p}\rangle$  it is possible to reach any other vector  $|\mathbf{p}'\rangle$  through successive applications of rotations or of Galileo transformations. The internal degrees of freedom only transform by rotations independently.

So a pointwise free particle is described by an irreducible unitary representation of the Galileo group.

#### 2.4.5 Parity invariance

The parity transformation is defined by

$$\mathbf{p} \rightarrow -\mathbf{p} \quad \mathbf{q} \rightarrow -\mathbf{q} \quad s \rightarrow s \quad (2.68)$$

This is a canonical transformation since it does not change the commutation relations. The transformation operator is

$$U_P = e^{i\frac{\pi}{2}(\mathbf{p}+i\mathbf{q}) \cdot (\mathbf{p}-i\mathbf{q})}. \quad (2.69)$$

The parity transformation has square 1

$$U_P = U_P^{-1} = U_P^\dagger. \quad (2.70)$$

If the parity transformation is an invariance we must have

$$U_P^{-1} H U_P = H \quad (2.71)$$

or

$$[U_P, H] = 0. \quad (2.72)$$

Let us now prove Eq. (2.69) in the one-dimensional case

$$U_P = e^{i\frac{\pi}{2}(p^2 + q^2 - 1)}. \quad (2.73)$$

Apart from a phase this operator coincides with the time evolution operator of a harmonic oscillator of mass 1 and  $\omega = 1$  from time  $t = 0$  to time  $t = \pi$ . The Heisenberg equations for

$$q(t) = e^{iHt}q(0)e^{-iHt}, \quad (2.74)$$

$$p(t) = e^{iHt}p(0)e^{-iHt}, \quad (2.75)$$

are

$$\dot{q} = i[H, q], \quad (2.76)$$

$$\dot{p} = i[H, p], \quad (2.77)$$

with  $H = (p^2 + q^2)/2$ . They have solution

$$q(t) = q \cos t + p \sin t, \quad (2.78)$$

$$p(t) = p \cos t - q \sin t. \quad (2.79)$$

It follows for  $t = \pi$

$$q(\pi) = U_P^\dagger q U_P = -q, \quad (2.80)$$

$$p(\pi) = U_P^\dagger p U_P = -p, \quad (2.81)$$

which is what we wanted.

#### 2.4.6 Time reversal

The time reversal acts as follows

$$q \rightarrow q \quad p \rightarrow -p \quad s \rightarrow -s \quad t \rightarrow -t \quad (2.82)$$

This transformation cannot be realized by a unitary operator because in such case the commutation relations would be preserved. Instead we want, in one dimension,

$$[q, p] = i \rightarrow [q, -p] = -i \quad (2.83)$$

If the transformation is antiunitary this is possible:

$$[q', p'] = U_T^\dagger [q, p] U_T = U_T^\dagger i U_T = -i. \quad (2.84)$$

An antilinear operator is defined by

$$T|s_1\rangle = |Ts_1\rangle \quad T|s_2\rangle = |Ts_2\rangle \quad (2.85)$$

$$T(a|s_1\rangle + b|s_2\rangle) = a^*T|s_1\rangle + b^*T|s_2\rangle. \quad (2.86)$$

For a linear operator  $O$

$$\langle a|Ob\rangle = \langle O^\dagger a|b\rangle = \langle b|O^\dagger a\rangle^*, \quad (2.87)$$

and the operator is Hermitian if

$$\langle a|Ob\rangle = \langle Oa|b\rangle. \quad (2.88)$$

For an antilinear operator  $T$

$$\langle a|Tb\rangle = \langle b|T^\dagger a\rangle, \quad (2.89)$$

which is antilinear in  $|a\rangle$  and in  $|b\rangle$ . An antilinear operator is antiunitary if

$$TT^\dagger = T^\dagger T = 1, \quad (2.90)$$

or

$$\langle a|T^\dagger Tb\rangle = \langle Tb|Ta\rangle = \langle a|b\rangle. \quad (2.91)$$

The transformed of  $O$  under  $T$

$$O' = T^\dagger OT, \quad (2.92)$$

is still linear and

$$\langle b|T^\dagger OTa\rangle = \langle OTa|Tb\rangle = \langle Ta|O^\dagger Tb\rangle. \quad (2.93)$$

In particular for  $O = i$  we find

$$T^\dagger iT = TiT^\dagger = -i. \quad (2.94)$$

The time reversal is realizable with an antiunitary operator:

$$T^\dagger qT = q \quad T^\dagger pT = -p \quad T^\dagger sT = -s \quad (2.95)$$

Moreover, in order to have invariance, we must require

$$T^\dagger HT = H. \quad (2.96)$$

If  $O$  is an observable

$$\langle b|OTa\rangle = \langle b|TT^\dagger OTa\rangle = \langle T^\dagger OTa|T^\dagger b\rangle. \quad (2.97)$$

So if  $T^\dagger OT = \pm O$  we have

$$\langle b|OTa\rangle = \pm \langle Oa|T^\dagger b\rangle. \quad (2.98)$$

For eigenstates of  $O$ ,  $O|a\rangle = O_a|a\rangle$ , we have

$$\langle b|OTa\rangle = \pm O_a \langle a|T^\dagger b\rangle = \pm O_a \langle b|Ta\rangle, \quad (2.99)$$

which means that  $|Ta\rangle$  is an eigenstate of  $O$  with the transformed eigenvalue.

So for a state  $|a\rangle = |p, s_z\rangle$  we have

$$|Ta\rangle = | -p, -s_z\rangle, \quad (2.100)$$

modulo a phase.

For a spinless particle with canonical variables  $\mathbf{q}$  and  $\mathbf{p}$  the time reversal is realized through

$$\langle \mathbf{q} | T\mathbf{a} \rangle = \psi_{T\mathbf{a}}(\mathbf{q}) = \psi_a^*(\mathbf{q}) = \langle \mathbf{q} | \mathbf{a} \rangle^*, \quad (2.101)$$

on wave functions in coordinate representation. In fact we have

$$\langle \mathbf{a} | T^\dagger \mathbf{p} T \mathbf{b} \rangle = \langle \mathbf{p} T \mathbf{b} | T \mathbf{a} \rangle = \int \psi_b(\mathbf{q}) (-i\nabla) \psi_a^*(\mathbf{q}) d\mathbf{q} = - \int \psi_a^*(\mathbf{q}) (-i\nabla) \psi_b(\mathbf{q}) d\mathbf{q} = - \langle \mathbf{a} | \mathbf{p} \mathbf{b} \rangle \quad (2.102)$$

where we used an integration by parts. Analogously we verify

$$\langle \mathbf{a} | T^\dagger \mathbf{q} T \mathbf{b} \rangle = \langle \mathbf{q} T \mathbf{b} | T \mathbf{a} \rangle = \langle \mathbf{a} | \mathbf{q} \mathbf{b} \rangle. \quad (2.103)$$

The Hamiltonian is an Hermitian function of  $\mathbf{q}$  and  $\mathbf{p}$ . In the coordinate representation,  $\mathbf{q}$  is a real variable and  $\mathbf{p} = -i\nabla$ . The transformation  $\mathbf{p} \rightarrow -\mathbf{p}$  is equivalent to a complex conjugation. We will have invariance under  $T$  if  $H(\mathbf{q}, \mathbf{p}) = H(\mathbf{q}, -\mathbf{p})$  or if  $H$  is real. A Hamiltonian of the form

$$H = \frac{\mathbf{p}^2}{2m} + V(\mathbf{q}), \quad (2.104)$$

is invariant under  $T$ .

If the particle has spin, it is described by  $2s+1$  functions of  $\mathbf{q}$

$$\psi(\mathbf{q}) = \begin{pmatrix} \psi_1(\mathbf{q}) \\ \vdots \\ \psi_{2s+1}(\mathbf{q}) \end{pmatrix}. \quad (2.105)$$

The spin is represented by three matrices  $\boldsymbol{\Sigma} = (\Sigma_1, \Sigma_2, \Sigma_3)$  independent from  $\mathbf{q}$ . We now take

$$\psi_{T\mathbf{a}}(\mathbf{q}) = U\psi_a^*(\mathbf{q}), \quad (2.106)$$

with  $U$  an unitary matrix independent from  $\mathbf{q}$  and acting on spin space. To have the correct spin transformations we must have

$$\langle \mathbf{a} | T^\dagger s T \mathbf{b} \rangle = \langle s T \mathbf{b} | T \mathbf{a} \rangle = - \langle \mathbf{a} | s \mathbf{b} \rangle, \quad (2.107)$$

or

$$- \int \psi_a^\dagger \boldsymbol{\Sigma} \psi_b = \int \psi_b^{\text{Tr}} U^\dagger \boldsymbol{\Sigma} U \psi_a^*, \quad (2.108)$$

which means

$$U^{\text{Tr}} \boldsymbol{\Sigma}^{\text{Tr}} U^\dagger{}^{\text{Tr}} = -\boldsymbol{\Sigma}, \quad (2.109)$$

and taking the complex conjugate, since  $\boldsymbol{\Sigma}^\dagger = \boldsymbol{\Sigma}$ , we find

$$U^\dagger \boldsymbol{\Sigma} U = -\boldsymbol{\Sigma}^*. \quad (2.110)$$

With the usual choice of phases in the angular momentum representation  $\Sigma_1$  and  $\Sigma_3$  are real matrices and  $\Sigma_2$  is pure imaginary.

For example for spin 1/2 particles

$$\Sigma_3 = \frac{1}{2} \begin{pmatrix} 1 & 0 \\ 0 & -1 \end{pmatrix} \quad \Sigma_1 = \frac{1}{2} \begin{pmatrix} 0 & 1 \\ 1 & 0 \end{pmatrix} \quad \Sigma_2 = \frac{1}{2} \begin{pmatrix} 0 & i \\ -i & 0 \end{pmatrix} \quad (2.111)$$

Then apart from an unessential phase we find

$$U = e^{i\pi\Sigma_2}, \quad (2.112)$$

a rotation of  $\pi$  around the 2 axis, which changes sign to  $\Sigma_1$  and  $\Sigma_3$ . In conclusions we have

$$\psi_{T\mathbf{a}} = e^{i\pi\Sigma_2} \psi_a^*. \quad (2.113)$$

## 2.5 Einstein Relativity

The invariance under the Galileo group is valid in the limit of small velocities. But, actually, physics is invariant under Lorentz transformations in addition to spatial translations. This invariance is known as Einstein relativity.

The Lorentz group is defined as the group of linear transformations which leaves invariant the quadratic form

$$ds^2 = dt^2 - dx^2. \quad (2.114)$$

Let  $dx = (dx^0, dx^1, dx^2, dx^3) = (dt, dx)$  we can write

$$ds^2 = g_{\mu\nu} dx^\mu dx^\nu, \quad (2.115)$$

where Einstein summation convention is used with

$$g_{\mu\nu} = g^{\mu\nu} = \begin{pmatrix} 1 & 0 & 0 & 0 \\ 0 & -1 & 0 & 0 \\ 0 & 0 & -1 & 0 \\ 0 & 0 & 0 & -1 \end{pmatrix} \quad g^{\mu\nu} g_{\nu\alpha} = \delta_\alpha^\mu \quad (2.116)$$

The Lorentz transformations are defined as the linear transformations

$$dx'^\mu = \Lambda_\nu^\mu dx^\nu, \quad (2.117)$$

such that

$$g_{\mu\nu} dx'^\mu dx'^\nu = g_{\mu\nu} \Lambda_\alpha^\mu \Lambda_\beta^\nu dx^\alpha dx^\beta. \quad (2.118)$$

Due to the arbitrariness of  $dx^\mu$  we have

$$g_{\mu\nu} = g_{\alpha\beta} \Lambda_\mu^\alpha \Lambda_\nu^\beta, \quad (2.119)$$

or

$$g = \mathbf{\Lambda}^{\text{Tr}} g \mathbf{\Lambda}, \quad (2.120)$$

which defines the Lorentz group. Taking the 00 component in Eq. (2.119)

$$1 = g_{\alpha\beta} \Lambda_0^\alpha \Lambda_0^\beta = (\Lambda_0^0)^2 - \sum_i (\Lambda_0^i)^2, \quad (2.121)$$

or

$$(\Lambda_0^0)^2 \geq 1, \quad (2.122)$$

or

$$\Lambda_0^0 \geq 1 \quad \text{or} \quad \Lambda_0^0 \leq -1. \quad (2.123)$$

Taking the determinant in Eq. (2.119) follows

$$(\det \mathbf{\Lambda})^2 = 1, \quad (2.124)$$

or

$$\det \Lambda = \pm 1. \quad (2.125)$$

The transformations obtained continuously from the identity have  $\Lambda^0_0 \geq 1$  and  $\det \Lambda = 1$  and constitute the *proper* Lorentz group. The transformations with  $\Lambda^0_0 \geq 1$  and  $\det \Lambda = -1$  can be written as the product of the parity  $P : x \rightarrow -x$  times a proper transformation. The ones with  $\Lambda^0_0 \leq -1$  and  $\det \Lambda = 1$  as a product of the time reversal  $T : x^0 \rightarrow -x^0$  times the proper transformations. The ones with  $\Lambda^0_0 \leq 1$  and  $\det \Lambda = -1$  as  $PT$  times a proper transformation.

An infinitesimal proper transformation

$$\Lambda^\mu_{\mu'} = \delta^\mu_{\mu'} + \Omega^\mu_{\mu'}, \quad (2.126)$$

must satisfy Eq. (2.119). So

$$g_{\mu'\nu'} = g_{\mu'\nu'} + \Omega^\mu_{\mu'} g_{\mu\nu'} + \Omega^\nu_{\nu'} g_{\nu\mu'} + \mathcal{O}(\Omega^2). \quad (2.127)$$

Let

$$\Omega_{\mu\nu} = g_{\mu\alpha} \Omega^\alpha_\nu, \quad (2.128)$$

then we must have

$$\Omega_{\mu\nu} = -\Omega_{\nu\mu}. \quad (2.129)$$

The group has 6 parameters as the number of components of an antisymmetric  $4 \times 4$  matrix. The most general  $4 \times 4$  antisymmetric matrix can be written as

$$\Omega_{\mu\nu} = \frac{1}{2} \sum_{\rho\sigma} \omega_{(\rho\sigma)} M_{\mu\nu}^{(\rho\sigma)}, \quad (2.130)$$

$$M_{\mu\nu}^{(\rho\sigma)} = \delta^\rho_\mu \delta^\sigma_\nu - \delta^\rho_\nu \delta^\sigma_\mu = -M_{\mu\nu}^{(\sigma\rho)}. \quad (2.131)$$

We write

$$\left( M^{(\rho\sigma)} \right)^\mu_\nu = g^{\mu\alpha} M_{\alpha\nu}^{(\rho\sigma)}, \quad (2.132)$$

so

$$\Omega^\mu_\nu = g^{\mu\alpha} \Omega_{\alpha\nu} = g^{\mu\alpha} \frac{1}{2} \omega_{(\rho\sigma)} M_{\mu\nu}^{(\rho\sigma)} = \frac{1}{2} \omega_{(\rho\sigma)} \left( M^{(\rho\sigma)} \right)^\mu_\nu. \quad (2.133)$$

The matrices  $M^{(\mu\nu)}$  satisfy the following algebra

$$[M^{(\alpha\beta)}, M^{(\mu\nu)}] = - \left( g^{\alpha\mu} M^{(\beta\nu)} + g^{\beta\nu} M^{(\alpha\mu)} - g^{\beta\mu} M^{(\alpha\nu)} - g^{\alpha\nu} M^{(\beta\mu)} \right). \quad (2.134)$$

We can then introduce

$$J^{(\mu\nu)} \equiv -i M^{(\mu\nu)}, \quad (2.135)$$

and

$$J^i = -\frac{1}{2} \epsilon_{0ijk} J^{(jk)}, \quad (2.136)$$

$$K^i = J^{(0i)}, \quad (2.137)$$

where  $\epsilon_{\mu_0\mu_1\mu_2\mu_3}$  is the Levi-Civita symbol with  $\epsilon_{0123} = 1$ <sup>1</sup>. Then Eq. (2.134) is rewritten as

$$[J^i, J^j] = i\epsilon_{ijk}J^k, \quad (2.141)$$

$$[J^i, K^j] = i\epsilon_{ijk}K^k, \quad (2.142)$$

$$[K^i, K^j] = -i\epsilon_{ijk}J^k. \quad (2.143)$$

The generators  $J^i$  are the rotations generators, which constitute a subgroup of the Lorentz transformations. The  $K^i$  are the generators of the velocity ( $v$ ) transformations and are vectors, as follows from their commutation relations with the  $J^i$ . The infinitesimal transformations are then

$$\Lambda = 1 + i(\boldsymbol{\theta} \cdot \mathbf{J} - \boldsymbol{\alpha} \cdot \mathbf{K}). \quad (2.144)$$

The finite ones are

$$\Lambda = e^{\frac{i}{2}\sum_{\alpha\beta} J^{(\alpha\beta)}\omega_{(\alpha\beta)}} = e^{i(\boldsymbol{\theta} \cdot \mathbf{J} - \boldsymbol{\alpha} \cdot \mathbf{K})} \quad \mathbf{v} = (\tanh \alpha_1, \tanh \alpha_2, \tanh \alpha_3), \quad (2.145)$$

where  $\boldsymbol{\theta}$  is the rotation angle vector and  $\boldsymbol{\alpha}$  is the rapidity vector.

Under the Lorentz group the generators of the translations  $p_\mu$  must transform as four-vectors

$$[J^{(\mu\nu)}, p^\alpha] = i(g^{\mu\alpha}p^\nu - g^{\alpha\nu}p^\mu), \quad (2.146)$$

or

$$[J, p^0] = -\delta p^0 = -J p^0 = 0, \quad (2.147)$$

which expresses the conservation of angular momentum, and

$$[J^i, p^j] = -\delta p^j = -J^i p^j = i\epsilon_{ijk}p^k, \quad (2.148)$$

which tells us that  $p$  is a vector. On the momenta the generators of the velocity transformations act as follows

$$[K^i, p^0] = -\delta p^0 = -K^i p^0 = ig^{00}p^i, \quad (2.149)$$

$$[K^i, p^j] = -\delta p^j = -K^i p^j = -ig^{ij}p^0. \quad (2.150)$$

The invariance under translations is written as

$$[p^\mu, p^\nu] = 0. \quad (2.151)$$

The commutation relations between the generators are then

$$[p^\mu, p^\nu] = 0, \quad (2.152)$$

$$[J^{(\mu\nu)}, p^\alpha] = i(g^{\mu\alpha}p^\nu - g^{\alpha\nu}p^\mu), \quad (2.153)$$

$$[J^{(\alpha\beta)}, J^{(\mu\nu)}] = i(g^{\alpha\mu}J^{(\beta\nu)} + g^{\beta\nu}J^{(\alpha\mu)} - g^{\beta\mu}J^{(\alpha\nu)} - g^{\alpha\nu}J^{(\beta\mu)}). \quad (2.154)$$

---

<sup>1</sup>For any antisymmetric tensor  $F^{\mu\nu}$  it is possible to use a decomposition of the following kind:  $F^{\mu\nu} = (\mathbf{P}, \mathbf{A})$  with

$$A^1 = -F^{23} \quad A^2 = -F^{31} \quad A^3 = -F^{12} \quad (2.138)$$

$$P^1 = F^{01} \quad P^2 = F^{02} \quad P^3 = F^{03} \quad (2.139)$$

For the product of two tensors of this kind we have

$$\frac{1}{2}F_{\mu\nu}^{(1)}F^{(2)\mu\nu} = \mathbf{A}^{(1)} \cdot \mathbf{A}^{(2)} - \mathbf{P}^{(1)} \cdot \mathbf{P}^{(2)}. \quad (2.140)$$

They define the Lie algebra of a 10 parameters group known as the Poincaré group.

The Poincaré group is defined by the transformation laws

$$(\Lambda, a) : x \rightarrow x' = \Lambda x - a, \quad (2.155)$$

where  $a$  is a translation and  $\Lambda$  is a Lorentz transformation. We immediately find the multiplication properties of the group as

$$(\Lambda_1, a)(\Lambda_2, b) = (\Lambda_1 \Lambda_2, -\Lambda_1 b - a), \quad (2.156)$$

from which immediately follows that the translations are an abelian invariant subgroup. In fact applying repetitively Eq. (2.156) we find that the transformed by similitude of a translation  $(1, a)$ ,

$$(\Lambda, c)(1, a)(\Lambda^{-1}, -c) = (1, \Lambda(c - a) - c), \quad (2.157)$$

is still a translation.

By Wigner theorem the states of a physical system are the basis of a unitary representation of the Poincaré group. An elementary system will be described by an irreducible representation of the Poincaré group.

We note that

$$J_{\pm} = \frac{J \pm iK}{2}, \quad (2.158)$$

obey the following commutation relations

$$[J_+^i, J_+^j] = i\epsilon_{ijk}J_+^k, \quad (2.159)$$

$$[J_-^i, J_-^j] = i\epsilon_{ijk}J_-^k, \quad (2.160)$$

$$[J_+^i, J_-^j] = 0. \quad (2.161)$$

So the generators of  $J_+$  and  $J_-$  obey to the algebra  $SU(2) \otimes SU(2)$ . Let us show now that an irreducible representation of the Poincaré group, i.e. an elementary particle, is determined by the mass and the spin.

An irreducible representation is characterized by the value of the *invariants*, i.e. of the operators built with the generators of the group that commute with all the group generators. We then define

$$\Gamma_{\mu} = \frac{1}{2}\epsilon_{\mu\alpha\beta\sigma}J^{(\alpha\beta)}p^{\sigma}, \quad (2.162)$$

$$\Gamma_{\mu}p^{\mu} = 0, \quad (2.163)$$

$$g^{\mu} = J^{(\mu\nu)}p_{\nu}, \quad (2.164)$$

$$g^{\mu}p_{\mu} = 0. \quad (2.165)$$

One can prove [40, 41, 42, 43, 44]<sup>2</sup> that

$$p^2 J^{(\mu\nu)} = g^{\mu}p^{\nu} - g^{\nu}p^{\mu} - \epsilon^{\sigma\mu\nu\lambda}\Gamma_{\sigma}p_{\lambda}. \quad (2.167)$$

---

<sup>2</sup>One can use the identity

$$\epsilon^{\sigma\mu\nu\lambda}\epsilon_{\sigma\alpha\beta\rho} = \det \begin{pmatrix} \delta_{\alpha}^{\mu} & \delta_{\beta}^{\mu} & \delta_{\rho}^{\mu} \\ \delta_{\alpha}^{\nu} & \delta_{\beta}^{\nu} & \delta_{\rho}^{\nu} \\ \delta_{\alpha}^{\lambda} & \delta_{\beta}^{\lambda} & \delta_{\rho}^{\lambda} \end{pmatrix}, \quad (2.166)$$

and the definition of  $\Gamma_{\sigma}$  to calculate the product  $\epsilon^{\sigma\mu\nu\lambda}\Gamma_{\sigma}p_{\lambda}$ .

This tells us that  $J^{(\mu\nu)}$  can be expressed in terms of  $p_\mu, \Gamma_\mu$ , and  $g_\mu$  if  $p^2 = p_\mu p^\mu \neq 0$ .

Moreover we have

$$[\Gamma_\mu, \Gamma_\nu] = i\epsilon_{\rho\mu\nu\lambda}\Gamma^\rho p^\lambda, \quad (2.168)$$

$$[g_\mu, \Gamma_\sigma] = -i\Gamma_\mu p_\sigma, \quad (2.169)$$

$$[g_\mu, p_\nu] = i(g_{\mu\nu}p^2 - p_\mu p_\nu), \quad (2.170)$$

$$[g_\mu, g_\nu] = -i(g^\mu p^\nu - g^\nu p^\mu - \epsilon^{\sigma\mu\nu\lambda}\Gamma_\sigma p_\lambda) \quad (2.171)$$

$$[p_\mu, \Gamma_\sigma] = 0. \quad (2.172)$$

An invariant should be constructed with the vectors  $p_\mu, \Gamma_\mu$ , and  $g_\mu$ . Recalling that  $g_\mu p^\mu = 0$  and  $\Gamma_\mu p^\mu = 0$  the only independent invariants under the Lorentz group are

$$p^2, \Gamma^2, g^2, \Gamma_\mu g^\mu. \quad (2.173)$$

But  $g^2$  and  $\Gamma_\mu g^\mu$  do not commute with translations. Then the representation is determined by  $p^2, \Gamma^2$ , and by the sign of  $p^0$ , which is also invariant under the proper Lorentz group and commutes with translations, if  $p^2 \geq 0$ .

The physical interpretation of the two invariants is obvious:

- i. For the invariant  $p^2$  we have 4 cases

$$p^2 > 0, \quad (2.174)$$

$$p^2 = 0 \quad p \neq 0, \quad (2.175)$$

$$p^2 = 0 \quad p = 0, \quad (2.176)$$

$$p^2 < 0. \quad (2.177)$$

Since  $p^2 = m^2$  we will be interested only in the first two cases. In these two cases, for the representations of the proper group ( $\Lambda_0^0 \geq 0$  and  $\det \Lambda = 1$ ) we will have another invariant, namely the sign of  $p^0$ .

- ii. The invariant  $\Gamma^2$  can be calculated in the reference frame where  $p = 0$ . In such a frame

$$\Gamma = (\Gamma^0, \Gamma^1, \Gamma^2, \Gamma^3) = (\Gamma^0, \mathbf{\Gamma}) = (0, m\mathbf{J}) \quad \Gamma^2 = -m^2 J(J+1). \quad (2.178)$$

The modulus of  $\mathbf{J}$  in the rest frame is by definition the particle spin, so  $\Gamma^2 = -m^2 s(s+1)$

Then the representation is determined by the mass  $m$  and by the spin  $s$ , exactly as in the nonrelativistic happens for the Galileo group.

### 2.5.1 The irreducible unitary representation of the Poincaré group

We want now to explicitly construct the irreducible unitary representations of the Poincaré group.

#### Massive particles

We can build a base of the Hilbert space which diagonalizes simultaneously the components  $p_\mu$  of the four-momentum, which commute among themselves, and other observables which we will denote by now with  $\sigma$ . The vector of the base will have the form  $|\mathbf{p}, \sigma\rangle$  with

$$p_i |\mathbf{p}, \sigma\rangle = p_i |\mathbf{p}, \sigma\rangle \quad p_0 |\mathbf{p}, \sigma\rangle = \text{sgn}(p_0) p_0 |\mathbf{p}, \sigma\rangle, \quad (2.179)$$

with  $p_0 = p^0 = \sqrt{\mathbf{p}^2 + m^2}$  and  $\mathbf{p} = (p^1, p^2, p^3) = (-p_1, -p_2, -p_3)$ . We will call  $U(\Lambda)$  the unitary operators which represents the generic Lorentz transformation  $\Lambda$ . We will have

$$U(\Lambda)|\mathbf{p}, \sigma\rangle = \sum_{\sigma'} \mathcal{R}(\Lambda, \mathbf{p})_{\sigma\sigma'} |\Lambda\mathbf{p}, \sigma'\rangle. \quad (2.180)$$

In fact, using the group algebra we have

$$U^\dagger(\Lambda)p_\mu U(\Lambda) = \Lambda^\nu_\mu p_\nu, \quad (2.181)$$

then

$$\begin{aligned} p_\mu U(\Lambda)|\mathbf{p}, \sigma\rangle &= U(\Lambda)U^\dagger(\Lambda)p_\mu U(\Lambda)|\mathbf{p}, \sigma\rangle \\ &= \Lambda^\nu_\mu p_\nu U(\Lambda)|\mathbf{p}, \sigma\rangle. \end{aligned} \quad (2.182)$$

So  $U(\Lambda)|\mathbf{p}, \sigma\rangle$  belongs to the eigenvalue  $(\Lambda\mathbf{p})_\mu$  of the four-momentum. And this proves Eq. (2.180). The Lorentz invariant measure, for momentum  $\mathbf{p} = (p^0, p^1, p^2, p^3) = (p^0, \mathbf{p})$ , is

$$d\Omega_{\mathbf{p}} = \frac{d^4 p}{(2\pi)^3} \delta(\sqrt{\mathbf{p}^2} - m)\theta(p_0) = \frac{d^3 \mathbf{p}}{(2\pi)^3 2p_0}. \quad (2.183)$$

One can easily verify that with the invariant normalization

$$\langle \mathbf{p}', \sigma' | \mathbf{p}, \sigma \rangle = (2\pi)^3 2p_0 \delta(\mathbf{p} - \mathbf{p}') \delta_{\sigma\sigma'}, \quad (2.184)$$

the matrix  $\mathcal{R}(\Lambda, \mathbf{p})_{\sigma\sigma'}$  in Eq. (2.180) is unitary due to the unitarity of  $U(\Lambda)$ .

The operator  $\Gamma_\mu$  commutes with all the components of  $p_\mu$ . Then when applied to the state  $|\mathbf{p}, \sigma\rangle$  it can only mix it with states of the same  $\mathbf{p}$ .

Let us start by considering the case  $\mathbf{p}^2 = m^2 > 0$  with  $\mathbf{p} = \mathbf{0}$ ,  $|\mathbf{0}, \sigma\rangle$ , for which

$$\mathbf{p}|\mathbf{0}, \sigma\rangle = \mathbf{0} \quad p_0|\mathbf{0}, \sigma\rangle = \text{sgn}(p_0)m|\mathbf{0}, \sigma\rangle. \quad (2.185)$$

On this subspace  $\Gamma_\mu = \frac{1}{2}\epsilon_{\mu\alpha\beta\gamma} J^{(\alpha\beta)} p^\gamma$  can be easily calculated

$$\Gamma_0 = 0 \quad \mathbf{\Gamma} = m\mathbf{J} = ms. \quad (2.186)$$

The angular momentum of the rest frame is called spin by definition. The dimension of the subspace is  $2s + 1$ .

For the variable  $\sigma$  we can take the eigenvalue of one of the spin component, i.e.  $s_3$ .

If  $U(\Lambda_p)$  is a Lorentz transformation which brings the momentum from  $\mathbf{0}$  to a certain value  $\mathbf{p}$ , since  $\Gamma^\mu$  is a four-vector, we will have

$$U^\dagger(\Lambda_p)\Gamma^\mu U(\Lambda_p) = (\Lambda_p)^\mu_\nu \Gamma^\nu. \quad (2.187)$$

If we call  $\bar{\Gamma}_{\sigma'\sigma}^\mu$  the representative of the  $\Gamma^\mu$  on the subspace  $|\mathbf{0}, \sigma\rangle$  we will have

$$\begin{aligned} \Gamma^\mu U(\Lambda_p)|\mathbf{0}, \sigma\rangle &= U(\Lambda_p)U^\dagger(\Lambda_p)\Gamma^\mu U(\Lambda_p)|\mathbf{0}, \sigma\rangle \\ &= U(\Lambda_p)(\Lambda_p)^\mu_\nu \Gamma^\nu |\mathbf{0}, \sigma\rangle \\ &= (\Lambda_p)^\mu_\nu \bar{\Gamma}_{\sigma'\sigma}^\nu U(\Lambda_p)|\mathbf{0}, \sigma\rangle. \end{aligned} \quad (2.188)$$

Then  $(\Lambda_p)^\mu_\nu \bar{\Gamma}_{\sigma'\sigma}^\nu$  is the representative of  $\Gamma^\mu$  on the subspace  $|\mathbf{p}, \sigma\rangle$ , in the representation in which the base vectors are  $|\mathbf{p}, \sigma\rangle = U(\Lambda_p)|\mathbf{0}, \sigma\rangle$ .

The Lorentz transformation  $U(\Lambda_p)$  which brings the momentum from  $\mathbf{0}$  to  $p$  is not univocally defined: it is indetermined on the right by a transformation of the small group<sup>3</sup> of the initial momentum  $\mathbf{0}$  and on the left by a transformation of the small group of the final momentum  $p$ .

For each choice of these transformations we will have a choice of the base vectors  $U(\Lambda_p)|\mathbf{0}, \sigma\rangle$  and of the representative of  $\Gamma^\mu$ . We will adopt, in the following, a standard choice for  $U(\Lambda_p)$ . Namely a simple velocity transformation  $e^{-i\alpha \cdot K}$  in the  $p$  direction, which sends the momentum from  $\mathbf{0}$  to  $p$ . The base vectors are then

$$|p, \sigma\rangle = U(\Lambda_p)|\mathbf{0}, \sigma\rangle = e^{-i\alpha \cdot K}|\mathbf{0}, \sigma\rangle, \quad (2.189)$$

and

$$\Gamma^\mu(p) = (\Lambda_p)^\mu_\nu \Gamma^\nu(\mathbf{0}) = \left( p \cdot s, ms + \frac{(p \cdot s)p}{p^0 + m} \right). \quad (2.190)$$

This can be proved as follows. We can write for a general velocity transformation

$$\Lambda_p = \begin{pmatrix} \gamma & -\gamma \beta^{\text{Tr}} \\ -\gamma \beta & \mathbf{1} + (\gamma - 1)\beta \beta^{\text{Tr}}/\beta^2 \end{pmatrix} \quad \gamma = \frac{1}{\sqrt{1 - \beta^2}}, \quad (2.191)$$

with

$$-\gamma \beta = \frac{p}{m} \implies \gamma = \frac{p_0}{m} \quad \text{and} \quad (\gamma - 1)/\beta^2 = \frac{p_0^2}{m(p_0 + m)} \quad (2.192)$$

The transformation we are looking for is then

$$(\Lambda_p)^\mu_\nu = \delta^\mu_\nu - \frac{1}{p_0 + m} \left[ m \delta^\mu_0 \delta^0_\nu + \delta^\mu_0 p_\nu + \frac{p^\mu p_\nu}{m} - \delta^0_\nu p^\mu \left( 1 + 2 \frac{p_0}{m} \right) \right], \quad (2.193)$$

from which we immediately find Eq. (2.190).

To complete the construction of the representation we could now look for the representative of  $g_\mu$  defined in (2.164), using the commutation relations (2.168)-(2.172), and construct the representative of the generic  $J^{(\mu\nu)}$  using Eq. (2.167). Alternatively we may proceed as follows:

- a) Let us first consider the rotations. If  $\Lambda$  is a rotation  $R_\theta$

$$U(R_\theta)|p, \sigma\rangle = U(R_\theta)U(\Lambda_p)U^\dagger(R_\theta)U(R_\theta)|\mathbf{0}, \sigma\rangle. \quad (2.194)$$

We know that

$$U(\Lambda_p) = e^{-i\alpha \cdot K}, \quad (2.195)$$

and since

$$U^\dagger(R_\theta)KU(R_\theta) = R_\theta K, \quad (2.196)$$

we have

$$U(R_\theta)U(\Lambda_p)U^\dagger(R_\theta) = e^{-i(R_\theta \alpha) \cdot K}, \quad (2.197)$$

and

$$U(R_\theta)|p, \sigma\rangle = \left( e^{i\theta \cdot s} \right)_{\sigma' \sigma} |R_\theta p, \sigma'\rangle. \quad (2.198)$$

---

<sup>3</sup>The small group of  $p$  is the subgroup of the transformations which leaves  $p$  unchanged.

b) For a Lorentz transformation sending  $\mathbf{p}$  into  $\mathbf{p}'$

$$U(\Lambda)|\mathbf{p}, \sigma\rangle = U(\Lambda_{\mathbf{p}'})U^\dagger(\Lambda_{\mathbf{p}'})U(\Lambda)U(\Lambda_{\mathbf{p}})|\mathbf{0}, \sigma\rangle. \quad (2.199)$$

The matrix  $U^\dagger(\Lambda_{\mathbf{p}'})U(\Lambda)U(\Lambda_{\mathbf{p}})$  belongs to the small group of  $\mathbf{p} = \mathbf{0}$ , i.e. it is a rotation  $R(\Lambda, \mathbf{p})$  in the subspace  $|\mathbf{0}, \sigma\rangle$ . To determine it we just need to calculate

$$\Lambda_{\mathbf{p}'}^{-1}\Lambda\Lambda_{\mathbf{p}}, \quad (2.200)$$

using the formula (2.193) and the explicit one (2.191). If we call  $\mathcal{R}(\Lambda, \mathbf{p})_{\sigma'\sigma}$  the representative of such a rotation in the space  $|\mathbf{0}, \sigma\rangle$  we will have

$$U(\Lambda)|\mathbf{p}, \sigma\rangle = \mathcal{R}(\Lambda, \mathbf{p})_{\sigma'\sigma}|\Lambda\mathbf{p}, \sigma\rangle. \quad (2.201)$$

Explicitly, if  $\Lambda$  is a velocity transformation with velocity  $\beta$  in the direction  $\hat{\mathbf{n}}$ , we find

$$\begin{aligned} (\Lambda_{\mathbf{p}'}^{-1}\Lambda\Lambda_{\mathbf{p}}, )^{\mu}_{\nu} &= \begin{pmatrix} \bar{\mathcal{R}}_0^0 & \bar{\mathcal{R}}_0^j \\ \bar{\mathcal{R}}_i^0 & \bar{\mathcal{R}}_i^j \end{pmatrix} = \begin{pmatrix} \frac{p'_0}{m} & -\frac{p'_j}{m} \\ -\frac{p'_i}{m} & \delta_{ik} + \frac{p'_i p'_k}{m(p'_0 + m)} \end{pmatrix} \times \\ &\quad \begin{pmatrix} \gamma & -\gamma\beta n_l \\ -\gamma\beta n_k & \delta_{kl} + (\gamma - 1)n_k n_l \end{pmatrix} \begin{pmatrix} \frac{p_0}{m} & \frac{p_j}{m} \\ \frac{p_l}{m} & \delta_{lj} + \frac{m p_l p_j}{m(p_0 + m)} \end{pmatrix}. \end{aligned} \quad (2.202)$$

To first order in  $\beta$

$$p'_0 = \gamma p_0 - \gamma\beta\hat{\mathbf{n}} \cdot \mathbf{p} = p_0 - \boldsymbol{\beta} \cdot \mathbf{p} + \mathcal{O}(\beta^2), \quad (2.203)$$

$$\mathbf{p}' = -\gamma\beta\hat{\mathbf{n}}p_0 + \mathbf{p} + (\gamma - 1)\hat{\mathbf{n}}(\hat{\mathbf{n}} \cdot \mathbf{p}) = \mathbf{p} - \boldsymbol{\beta}p_0 + \mathcal{O}(\beta^2), \quad (2.204)$$

and

$$\bar{\mathcal{R}}_i^j = \delta_i^j + \frac{\beta}{p_0 + m}(n^i p_j - p^i n_j) + \mathcal{O}(\beta^2). \quad (2.205)$$

Recalling that in the vector representation  $(J^i)_{jk} = i\epsilon_{jik}$  and using  $\epsilon_{ijk}\epsilon_{ilm} = \delta_{jl}\delta_{km} - \delta_{jm}\delta_{kl}$  we finally find

$$\mathcal{R} \approx 1 - i \frac{\boldsymbol{\beta} \wedge \mathbf{p}}{p_0 + m} \cdot \mathbf{J}. \quad (2.206)$$

The finite transformation  $\mathcal{R}(\Lambda, \mathbf{p})$  is then of the following form

$$\mathcal{R}(\Lambda, \mathbf{p}) = e^{-i \frac{\boldsymbol{\beta} \wedge \mathbf{p}}{p_0 + m} \cdot \mathbf{J}}. \quad (2.207)$$

This rotation is called the Wigner rotation.

The transformations on the wave functions can be determined from the one on the states. The generic  $|\phi\rangle$  is written as

$$|\phi\rangle = \int d\Omega_{\mathbf{p}} \varphi_{\sigma}(\mathbf{p}) |\mathbf{p}, \sigma\rangle, \quad (2.208)$$

and the scalar product

$$\langle \phi' | \phi \rangle = \int d\Omega_{\mathbf{p}} \varphi'^*(\mathbf{p}) \varphi(\mathbf{p}). \quad (2.209)$$

Under a transformation  $U(\Lambda, a)$

$$|\Lambda\phi\rangle = U(\Lambda, a)|\phi\rangle = \int d\Omega_{\mathbf{p}} e^{-ipa} \varphi_\sigma(\mathbf{p}) \mathcal{R}(\Lambda, \mathbf{p})_{\sigma'\sigma} |\Lambda\mathbf{p}, \sigma'\rangle. \quad (2.210)$$

Changing variables from  $\mathbf{p}$  to  $\Lambda^{-1}\mathbf{p}$  and using the fact that the measure is invariant we find

$$|\Lambda\phi\rangle = \int d\Omega_{\mathbf{p}} e^{-i(\Lambda^{-1}\mathbf{p})a} \mathcal{R}_{\sigma'\sigma} \varphi_\sigma(\Lambda^{-1}\mathbf{p}) |\mathbf{p}, \sigma'\rangle, \quad (2.211)$$

or

$$(\Lambda\varphi)_\sigma(\mathbf{p}) = \mathcal{R}_{\sigma\sigma'} \varphi_{\sigma'}(\Lambda^{-1}\mathbf{p}). \quad (2.212)$$

The matrix  $\mathcal{R}$  is given by Eq. (2.198) for the rotations and by Eq. (2.202) for the velocity transformations and is unitary respect to the metric  $\langle \phi' | \phi \rangle$ .

For an infinitesimal transformation Eq. (2.212) gives the form of the generators:

- a) For an infinitesimal rotation of an angle  $\boldsymbol{\theta}$

$$\Lambda^{-1}\mathbf{p} \approx \mathbf{p} + \boldsymbol{\theta} \wedge \mathbf{p} \quad \mathcal{R} \approx 1 + i\boldsymbol{\theta} \cdot \mathbf{s}, \quad (2.213)$$

so

$$\delta\varphi_\sigma \equiv (\Lambda\varphi_\sigma) - \varphi_\sigma \approx i\boldsymbol{\theta} \cdot \mathbf{s}_{\sigma\sigma'} \varphi_{\sigma'} + (\boldsymbol{\theta} \wedge \mathbf{p}) \frac{\partial}{\partial \mathbf{p}} \varphi_\sigma. \quad (2.214)$$

The generator is defined by  $\delta\varphi = i(\boldsymbol{\theta} \cdot \mathbf{J})\varphi$  so

$$\mathbf{J} = \mathbf{s} - ip \wedge \frac{\partial}{\partial \mathbf{p}}. \quad (2.215)$$

- b) For a velocity transformation

$$\Lambda^{-1}\mathbf{p} \approx \mathbf{p} + \beta p_0 \quad \mathcal{R} \approx 1 - i \frac{\boldsymbol{\beta} \wedge \mathbf{p}}{p_0 + m} \cdot \mathbf{s}, \quad (2.216)$$

so

$$\delta\varphi_\sigma \approx -i(\boldsymbol{\beta} \cdot \mathbf{K})\varphi_\sigma = -i \frac{\boldsymbol{\beta} \wedge \mathbf{p}}{p_0 + m} \cdot \mathbf{s}_{\sigma\sigma'} \varphi_{\sigma'} + \boldsymbol{\beta} \cdot p_0 \frac{\partial}{\partial \mathbf{p}} \varphi_\sigma, \quad (2.217)$$

or

$$\mathbf{K} = \frac{\mathbf{p} \wedge \mathbf{s}}{p_0 + m} + ip_0 \frac{\partial}{\partial \mathbf{p}}. \quad (2.218)$$

One can verify that the generators  $\mathbf{J}$  and  $\mathbf{K}$  satisfy the algebra of the group. This completes the construction of the representation of the group on the Hilbert space of the multiplets of functions  $\varphi(\mathbf{p})$  with the metric of Eq. (2.209).

### The Helicity

We just saw that states can be taken as simultaneous eigenstates of  $p^2$  and  $\Gamma^2$  and accordingly labeled as  $|m, s, \dots\rangle$ , with

$$p^2|m, s, \dots\rangle = m^2|m, s, \dots\rangle, \quad (2.219)$$

$$\Gamma^2|m, s, \dots\rangle = -ms(s+1)|m, s, \dots\rangle. \quad (2.220)$$

What are the additional quantum numbers we can use to label the states? They must be eigenvalues of operators which commute with each other. So we are free to consider states of definite four-momentum  $p_\mu$ . Since the mass is already fixed, it is only necessary to specify in addition the three-momentum  $p$ , the energy being determined by  $p^0 = \sqrt{m^2 + p^2}$ . We cannot simultaneously give definite value for the third component of the angular momentum operator  $J^3$  because  $J$  and  $p$  do not commute. However there is an angular momentum operator which commutes with  $p$ , namely the *helicity*. This operator is the component of the spin along the direction of the momentum,  $J \cdot p / |p|$ , and its eigenvalues are labeled  $a$ . Thus the complete specification of the momentum eigenstates of a massive particle is  $|m, s; p, a\rangle$  with

$$p_\mu|m, s; p, a\rangle = p_\mu|m, s; p, a\rangle, \quad (2.221)$$

$$\frac{\mathbf{J} \cdot \mathbf{p}}{|p|}|m, s; p, a\rangle = a|m, s; p, a\rangle. \quad (2.222)$$

### Massless particles

Let us consider the base  $|p, \sigma\rangle$ . For  $p^2 = 0$  it does not exist a rest frame. We will take as the standard state the state with

$$p^\mu = (\bar{p}, 0, 0, \bar{p}), \quad (2.223)$$

with  $\bar{p}$  chosen arbitrarily. We will call  $|\bar{p}, \sigma\rangle$  the corresponding subspace. We will assume  $\text{sgn}(p^0) = 1$ . The discussion for  $\text{sgn}(p^0) = -1$  is analogous.

On the states  $|\bar{p}, \sigma\rangle$ ,  $\Gamma^\mu$  acts mixing them, since it commutes with  $p^\mu$ . The condition  $\Gamma^\mu p_\mu = 0$  gives

$$\bar{p}(\Gamma^0 - \Gamma^3) = 0. \quad (2.224)$$

We will define

$$\Gamma^0 = \bar{p}\tilde{\Gamma} \quad \Gamma^\pm = \Gamma^1 \pm \Gamma^2. \quad (2.225)$$

The the commutation rule

$$[\Gamma_\mu, \Gamma_\nu] = i\epsilon_{\mu\nu\rho\lambda}\Gamma^\rho p^\lambda, \quad (2.226)$$

gives

$$[\Gamma^\pm, \tilde{\Gamma}] = \mp\Gamma^\pm, \quad (2.227)$$

$$[\Gamma^+, \Gamma^-] = 0, \quad (2.228)$$

$$[\Gamma^2, \tilde{\Gamma}] = 0, \quad (2.229)$$

$$[\Gamma^2, \Gamma^\pm] = 0. \quad (2.230)$$

Moreover

$$\Gamma^2 = \Gamma^+ \Gamma^-, \quad (2.231)$$

since  $\Gamma_0^2 - \Gamma_3^2 = 0$ .

In a unitary representation  $\Gamma^+ = (\Gamma^-)^\dagger$ . If we diagonalize  $\tilde{\Gamma}$ ,

$$\tilde{\Gamma}|\bar{p}, a\rangle = a|\bar{p}, a\rangle, \quad (2.232)$$

from Eq. (2.227) the operators  $\Gamma^+$  and  $\Gamma^-$  are the operators of higher and lower of  $a$  respectively. Their representative is then

$$(\Gamma^+)_m n = b_n \delta_{m,n+1}, \quad (2.233)$$

$$(\Gamma^-)_m n = b_m^* \delta_{n,m+1}. \quad (2.234)$$

$$(2.235)$$

Then Eq. (2.231) imposes  $\Gamma^2 = |b_n|^2 = \alpha^2$ , independent from  $n$ . If  $\alpha \neq 0$  the  $\Gamma^\mu$  representation is infinite dimensional. In order to have a finite number of states of fixed spin and momentum it must be  $\alpha = 0$ . This implies  $\Gamma^+ = \Gamma^- = 0$  and, by Eq. (2.231),  $\Gamma^2 = 0$ . So we can say that

$$\Gamma^\mu = \tilde{\Gamma} p^\mu. \quad (2.236)$$

The physical significance of  $\tilde{\Gamma}$  can be obtained from the definition (2.162) of  $\Gamma^\mu$

$$\tilde{\Gamma} = \frac{\mathbf{J} \cdot \mathbf{p}}{|\mathbf{p}|}. \quad (2.237)$$

$\tilde{\Gamma}$  is the projection of the spin on the direction of motion, i.e. the helicity.

From Eq. (2.236) follows that  $\tilde{\Gamma}$  is an invariant. For a massless particle the helicity is a Poincaré invariant. The representation is one dimensional. The helicity is a pseudoscalar: A representation with a fixed helicity defines a system which is not invariant under parity because the transformed state has opposite helicity and is not a possible state. The invariance under parity requires the direct sum of the representations with opposite helicity. The photon exists in the two states of helicity  $\pm 1$ .

We will define the generic state  $|p\rangle$  with  $|p| = |\bar{p}|$  through a rotation starting from the state  $|\bar{p}\rangle$ . The rotation sending  $\bar{p}$  into  $p$  is undetermined on the right for a rotation around the direction of  $\bar{p}$  and on the left for a rotation around the direction of  $p$ . We will choose  $|p\rangle$  adopting a standard convention for the Euler angles that define it, i.e.

$$R_p = R_z(\varphi) R_y(\theta) R_z(-\varphi), \quad (2.238)$$

where  $\theta$  and  $\varphi$  are the polar angles of  $p$ . This convention is equivalent to define  $R_p$  as a rotation of  $\theta$  around  $\mathbf{n}_3 \wedge \hat{\mathbf{p}}$ , with  $\mathbf{n}_3$  the versor along the 3 axis and  $\hat{\mathbf{p}} = \mathbf{p}/|\mathbf{p}|$ .

With this convention

$$|p\rangle = U(R_p)|\bar{p}\rangle. \quad (2.239)$$

It is easy to verify that  $|p\rangle$  has the same helicity,  $a$ , of  $|\bar{p}\rangle$ . In fact

$$\frac{\mathbf{J} \cdot \mathbf{p}}{|\mathbf{p}|}|p\rangle = U(R_p)U^{-1}(R_p)\frac{\mathbf{J} \cdot \mathbf{p}}{|\mathbf{p}|}U(R_p)|\bar{p}\rangle = U(R_p)\frac{\mathbf{J} \cdot \mathbf{p}}{|\mathbf{p}|}|\bar{p}\rangle = a|\bar{p}\rangle = a|p\rangle. \quad (2.240)$$

We will define the state  $|\bar{p}'\rangle$  with  $\bar{p}'_\mu$  of the form (2.223) and  $\bar{p}' \neq \bar{p}$  through the transformation

$$|\bar{p}'\rangle = U(\Lambda_{\bar{p}'})|\bar{p}\rangle, \quad (2.241)$$

where  $U(\Lambda_{\bar{p}'})$  is a pure velocity transformation along the 3 axis which sends  $\bar{p}$  into  $\bar{p}'$  without rotations around  $\bar{p}$  or  $\bar{p}'$ . The rotated states of  $|\bar{p}'\rangle$  will be defined with the convention (2.239).

Once fixed the base in this way let us now construct the representation. If  $U(\Lambda)$  is the representative of the generic Lorentz transformation sending  $\mathbf{p}$  into  $\mathbf{p}'$

$$U(\Lambda)|\mathbf{p}\rangle = U(\Lambda)U(R_p)|\bar{p}\rangle = U(R_{\mathbf{p}'})U^\dagger(R_{\mathbf{p}'})U(\Lambda)U(R_p)U^\dagger(\Lambda_{\bar{p}'})U(\Lambda_{\bar{p}'})|\bar{p}'\rangle. \quad (2.242)$$

It is easy to see that

$$\mathcal{U} = R_{\mathbf{p}'}^{-1}\Lambda R_p\Lambda_{\bar{p}'}, \quad (2.243)$$

is a transformation that leaves  $\bar{p}'_\mu$  unchanged, i.e. an element of the small group of  $\bar{p}'_\mu$ . The algebra of such a group is formed by the generators  $\epsilon_{\mu\nu\rho\sigma}J^{(\nu\rho)}\bar{p}'^\sigma$ , i.e.  $\mathbf{J} \cdot \bar{p}'/|\bar{p}'|, \Gamma^+, \Gamma^-$ . Now  $\Gamma^+$  and  $\Gamma^-$  are identically zero in the representation under exam, thus  $\mathcal{U}$  is a rotation around the 3 axis of a well defined angle  $\bar{\varphi}$ .

A rotation of an angle  $\bar{\varphi}$  around the 3 axis is represented by

$$R_3(\bar{\varphi})|\bar{p}'\rangle = e^{ia\bar{\varphi}}|\bar{p}'\rangle, \quad (2.244)$$

where  $a$  is the helicity. Then Eq. (2.242) becomes

$$U(\Lambda)|\mathbf{p}\rangle = e^{ia\bar{\varphi}}|\Lambda\mathbf{p}\rangle. \quad (2.245)$$

If  $\Lambda$  is an infinitesimal rotation of parameter  $\delta\boldsymbol{\theta}$  we find

$$\begin{aligned} 1 + i\bar{\varphi}J_3 &\approx e^{i\theta\mathbf{J}\cdot(\mathbf{n}_3 \wedge \hat{\mathbf{p}})}(1 + i\delta\boldsymbol{\theta}\cdot\mathbf{J})e^{-i\theta\mathbf{J}\cdot(\mathbf{n}_3 \wedge \hat{\mathbf{p}}')} \\ &\approx 1 + i\delta\boldsymbol{\theta}\cdot\mathbf{J} - \theta[\mathbf{J}\cdot(\mathbf{n}_3 \wedge \hat{\mathbf{p}}), \delta\boldsymbol{\theta}\cdot\mathbf{J}] \\ &\approx 1 + i\delta\boldsymbol{\theta}\cdot\mathbf{J} - i\theta[(\mathbf{J}\cdot\hat{\mathbf{p}})\delta\theta_3 - J_3(\hat{\mathbf{p}}\cdot\delta\boldsymbol{\theta})], \end{aligned} \quad (2.246)$$

where in the first equality we used the fact that  $\Lambda_{\bar{p}'} = 1$ , in the second the fact that for infinitesimal rotations we may choose  $\mathbf{p}' \approx \mathbf{p}$  in the second exponential, and in the third the use of the infinitesimal rotations. We then find

$$\bar{\varphi} = \delta\theta_3(1 - \hat{p}_3\theta) + \delta\boldsymbol{\theta}\cdot\hat{\mathbf{p}}\theta, \quad (2.247)$$

and choosing  $\theta = |\mathbf{p}|/(|\mathbf{p}| + p_3)$

$$\bar{\varphi} = \delta\boldsymbol{\theta}\cdot\frac{\mathbf{p} + |\mathbf{p}|\mathbf{n}_3}{|\mathbf{p}| + p_3}. \quad (2.248)$$

Analogously if  $\Lambda$  is an infinitesimal Lorentz transformation of parameter  $\delta\boldsymbol{\beta}$  we find

$$\bar{\varphi} = \frac{\delta\beta_1 p_2 - \delta\beta_2 p_1}{|\mathbf{p}| + p_3}. \quad (2.249)$$

The generic state of the particle is written as

$$|\Phi\rangle = \int d\Omega_{\mathbf{p}} \Phi(\mathbf{p})|\mathbf{p}\rangle, \quad (2.250)$$

with the scalar product

$$\langle \Phi' | \Phi \rangle = \int d\Omega_p \Phi'^*(p) \Phi(p). \quad (2.251)$$

For a generic Lorentz transformation

$$U(\Lambda) |\Phi\rangle = \int d\Omega_p \Phi(p) e^{ia\bar{\varphi}(\Lambda, p)} |\Lambda p\rangle = \int d\Omega_p \Phi(\Lambda^{-1}p) e^{ia\bar{\varphi}(\Lambda, \Lambda^{-1}p)} |p\rangle. \quad (2.252)$$

The generators on the space of the  $\Phi(p)$  functions are

$$J = -ip \wedge \frac{\partial}{\partial p} + s, \quad (2.253)$$

$$K = ip^0 \frac{\partial}{\partial p} + \chi, \quad (2.254)$$

with

$$s_1 = a \frac{p_1}{|p| + p_3} \quad s_2 = a \frac{p_2}{|p| + p_3} \quad s_3 = a, \quad (2.255)$$

$$\chi_1 = a \frac{p_2}{|p| + p_3} \quad \chi_2 = -a \frac{p_1}{|p| + p_3} \quad \chi_3 = 0. \quad (2.256)$$

This generators obey the commutation relations of the algebra (2.141)-(2.143) and are hermitian with the metric (2.251).

This completes the construction of the group representation on the Hilbert space of functions  $\Phi(p)$  for a zero mass particle.

### The Wigner rotation

We here want to calculate explicitly the Wigner rotation for a finite Lorentz transformation, for a massive particle. The velocity transformation is written as

$$U(\Lambda) = e^{-iK \cdot y}, \quad (2.257)$$

with

$$K = ip_0 \frac{\partial}{\partial p} + \frac{p \wedge s}{p_0 + m}. \quad (2.258)$$

For zero spin

$$e^{y \cdot p_0 \frac{\partial}{\partial p}} \varphi(p) = \varphi(\Lambda^{-1}p). \quad (2.259)$$

For non-zero spin

$$U(\Lambda) \varphi(p) = e^{y \cdot p_0 \frac{\partial}{\partial p} - iy \cdot \frac{p \wedge s}{p_0 + m}} \varphi(p), \quad (2.260)$$

where  $\varphi$  has  $2s + 1$  components. The operator  $U(\Lambda)$  is the exponential of two operators which do not commute.

In general given two operators  $A$  and  $B$  one has

$$e^{A+B} = e^A \sum_{n=0}^{\infty} \int_0^1 dx_1 \cdots dx_n T(B(x_1) \cdots B(x_n)), \quad (2.261)$$

where  $B(x) = e^{-xA}Be^{xA}$  and  $T$  is the usual time ordered product

$$T(B(x_1) \cdots B(x_n)) = \frac{1}{n!} \sum_{\substack{\text{permutations} \\ \text{of } \{i_k\}}} \theta(x_{i_1} - x_{i_2}) \cdots \theta(x_{i_{n-1}} - x_n) B(x_1) \cdots B(x_n). \quad (2.262)$$

If  $A$  and  $B$  commute  $B(x) = B$  and Eq. (2.261) gives  $e^{A+B} = e^A e^B$ . Eq. (2.261) can be proved observing that  $U(\lambda) = e^{\lambda(A+B)}$  obeys the equation

$$\frac{d}{d\lambda} U(\lambda) = (A + B)U(\lambda) \quad U(0) = 1. \quad (2.263)$$

Let

$$W(\lambda) = e^{\lambda A} \sum_{n=0}^{\infty} \int_0^{\lambda} dx_1 \cdots dx_n T(B(x_1) \cdots B(x_n)). \quad (2.264)$$

One easily verifies that

$$\frac{d}{d\lambda} W(\lambda) = (A + B)W(\lambda) \quad (2.265)$$

with  $W(0) = 1$ . Then we must have  $U(\lambda) = W(\lambda)$  and for  $\lambda = 1$  Eq. (2.261) is recovered.

Let now

$$A = \mathbf{y} \cdot \mathbf{p}_0 \frac{\partial}{\partial \mathbf{p}} \quad B = -i\mathbf{y} \cdot \frac{\mathbf{p} \wedge \mathbf{s}}{\mathbf{p}_0 + m}. \quad (2.266)$$

We will have

$$B(x) = e^{-x\mathbf{y} \cdot \mathbf{p}_0 \frac{\partial}{\partial \mathbf{p}}} B(\mathbf{p}) e^{x\mathbf{y} \cdot \mathbf{p}_0 \frac{\partial}{\partial \mathbf{p}}} = B(\Lambda_{-x}^{-1} \mathbf{p}), \quad (2.267)$$

where  $\Lambda_x$  is the Lorentz transformation with parameter  $x\mathbf{y}$ . In the numerator of  $B$ , due to the vector products, only enters the component of  $\mathbf{p}$  orthogonal to  $\mathbf{y}$  and this is invariant under the transformation. So

$$B(x) = -i\mathbf{y} \cdot \frac{\mathbf{p} \wedge \mathbf{s}}{\Lambda_{-x}^{-1} \mathbf{p}_0 + m}. \quad (2.268)$$

The  $B(x)$  all commute with themselves and

$$\int_0^1 dx_1 \cdots dx_n T(B(x_1) \cdots B(x_n)) = \frac{1}{n!} \left[ \int_0^1 B(x) dx \right]^n, \quad (2.269)$$

and

$$U(\Lambda) = e^{\mathbf{y} \cdot \mathbf{p}_0 \frac{\partial}{\partial \mathbf{p}}} e^{\int_0^1 b(x) dx}, \quad (2.270)$$

Moreover

$$U(\Lambda)\varphi(\mathbf{p}) = e^{-i\mathbf{y} \cdot \int_0^1 dx \frac{\mathbf{p} \wedge \mathbf{s}}{\Lambda_{1-x}^{-1} \mathbf{p}_0 + m}} \varphi(\Lambda^{-1} \mathbf{p}), \quad (2.271)$$

Then the Wigner rotation is

$$e^{i\mathbf{s} \cdot (\mathbf{p} \wedge \mathbf{y}) \int_0^1 \frac{dx}{\Lambda_{1-x}^{-1} \mathbf{p}_0 + m}}. \quad (2.272)$$

The integral can easily be evaluated if we parametrize  $p_\mu$  in the form  $p_\perp$ ,  $p_0 = m_t \cosh y_0$ ,  $p_\parallel = m_t \sinh y_0$ , and  $m_t = \sqrt{m^2 + p_\perp^2}$ . Using this parametrization we find

$$\begin{aligned} \int_0^1 \frac{dx}{\Lambda_{1-x}^{-1} p_0 + m} &= \int_0^1 \frac{dx}{m_t \cosh[y_0 + y(1-x)] + m} \\ &= \frac{1}{y} \int_0^y \frac{dz}{m_t \cosh(y_0 + z) + m} \\ &= \frac{1}{yp_\perp} \varphi, \\ \varphi &= \arcsin \left[ \frac{m_t + m \cosh(y_0 + z)}{m + m_t \cosh(y_0 + z)} \right]_{z=0}^{z=y}, \end{aligned} \quad (2.273)$$

is the angle of the Wigner rotation.

### Discrete transformations

We want now to discuss the discrete transformations, specifically the spatial inversion and the time reversal.

The spatial inversion  $\Pi$  sends

$$\mathbf{p} \rightarrow -\mathbf{p} \quad \mathbf{J} \rightarrow \mathbf{J} \quad \mathbf{K} \rightarrow -\mathbf{K}. \quad (2.274)$$

We immediately find a representation

$$\Pi|\mathbf{p}\rangle = \eta|-\mathbf{p}\rangle, \quad (2.275)$$

and on the wave functions

$$\varphi_a(\mathbf{p}) \rightarrow -\eta\varphi_a(-\mathbf{p}), \quad (2.276)$$

where  $\eta$  is a phase factor which must be  $\pm 1$  since  $\Pi^2 = 1$ . It is easy to show that the transformation (2.276) is unitary

$$\begin{aligned} \langle \Pi a' | \Pi a \rangle &= \int d\Omega_p \varphi_a'^\dagger(-\mathbf{p}) \varphi_a(-\mathbf{p}) \\ &= \int d\Omega_p \varphi_a'^\dagger(\mathbf{p}) \varphi_a(\mathbf{p}) = \langle a' | a \rangle, \end{aligned} \quad (2.277)$$

Moreover  $\langle \Pi a' | p \Pi a \rangle = -\langle a' | p a \rangle$  or

$$\Pi^\dagger p \Pi = -p, \quad (2.278)$$

and

$$\Pi^\dagger J \Pi = J, \quad (2.279)$$

$$\Pi^\dagger K \Pi = -K, \quad (2.280)$$

since we assumed  $\eta$  independent of  $\mathbf{p}$ .

A representation of the time reversal  $T$  is in terms of the antiunitary operator

$$\varphi(\mathbf{p}) \rightarrow \eta_T C \varphi^*(-\mathbf{p}), \quad (2.281)$$

where the unitary matrix  $C$  is defined in Section 2.4.6 and  $\eta_T$  is a phase independent of  $p$ . So that

$$\begin{aligned}\langle a' | T^\dagger p T a \rangle &= \langle T a | p T a' \rangle = \int d\Omega_p \varphi_a^{\text{Tr}}(-p) p \varphi_{a'}^*(-p) \\ &= - \int d\Omega_p \varphi_{a'}^\dagger(p) p \varphi_a(p) = -\langle a' | p a \rangle\end{aligned}\quad (2.282)$$

or

$$T^\dagger p T = -p, \quad (2.283)$$

Similarly

$$\begin{aligned}\langle a' | T^\dagger J T a \rangle &= \langle T a | J T a' \rangle = \int d\Omega_p \varphi_a^{\text{Tr}}(-p) C^* \left( -ip \wedge \frac{\partial}{\partial p} + s \right) C^{\text{Tr}} \varphi_{a'}^*(-p) \\ &= \int d\Omega_p \varphi_{a'}^\dagger(-p) \left( ip \wedge \frac{\partial}{\partial p} - s \right) \varphi_a(-p),\end{aligned}\quad (2.284)$$

where we integrated by parts and used  $C s^{\text{Tr}} C^\dagger = C s^* C^\dagger = -s$  (see Eq. (2.110)). So  $\langle T a | J T a' \rangle = -\langle a' | J a \rangle$  or

$$T^\dagger J T = -J. \quad (2.285)$$

Similarly

$$T^\dagger K T = K. \quad (2.286)$$

### 2.5.2 Wave functions in coordinate space

In relativistic mechanics the coordinates,  $x = (x^0, x^1, x^2, x^3) = (t, \mathbf{x})$ , play a privileged role. The constant speed of light principle, together with the relativity principle, implies that a signal cannot propagate at a speed greater than  $c$ . This implies, for example, that the regions with  $x^2 < 0$  are causally disconnected from the events at  $x = (0, \mathbf{0})$ . This statement is simple in coordinate space but it does not have an equally explicit expression in other representations.

It is then convenient to associate to a state a wave function  $\psi(x)$  which describes the state point by point in space-time. For the description to be effectively linked to the point event it is necessary that  $\psi(x)$  transforms *locally*.

For a Lorentz transformations  $\Lambda$  this means

$$\psi(x) \xrightarrow{\Lambda} \psi'(x) = S(\Lambda)\psi(\Lambda^{-1}x), \quad (2.287)$$

or

$$\psi'(\Lambda x) = S(\Lambda)\psi(x), \quad (2.288)$$

where  $S(\Lambda)$  does not depend on the point and it is a representation of the Lorentz group.

For a translation,  $a$ , we require

$$\psi(x) \xrightarrow{a} \psi'(x) = \psi(x + a). \quad (2.289)$$

Introducing

$$p_\mu \psi(x) = i \frac{\partial}{\partial x^\mu} \psi(x), \quad (2.290)$$

the momentum eigenstate  $\psi_p(x)$  can be written as follows

$$\psi_p(x) = e^{-ipx}\psi_p(0), \quad (2.291)$$

where in the exponent we use the simplified notation  $px \equiv p_\mu x^\mu$ .

If the time evolution is local we will need that  $\psi(x)$  obeys to a partial differential equation with derivatives of *finite order*. In what follows we will try to build local wave functions for spin 0, 1/2, 1 particles. Of course the states of these particles are defined by the unitary irreducible representations of the Poincaré group. Our wave functions will have to be in bijective correspondence with the vectors of such representations, and the scalar product for such vectors will have to be expressible in terms of wave functions. Relative to this metric of the Hilbert space the symmetry transformations on the  $\psi(x)$  will have to be unitary. We will verify that the representations of the Lorentz group  $S(\Lambda)$  will necessarily be finite dimensional.

We conclude observing that

$$\psi'(0) = S(\Lambda)\psi(0), \quad (2.292)$$

in fact  $\Lambda$  is the small group of point  $x = 0$ . If we call  $U(\Lambda)$  the unitary operator which represents the Lorentz transformation  $\Lambda$  we will have

$$U(\Lambda)\psi(x) = U(\Lambda)e^{-ipx}\psi(0) = U(\Lambda)e^{-ipx}U^{-1}(\Lambda)U(\Lambda)\psi(0), \quad (2.293)$$

but

$$U(\Lambda)e^{-ipx}U^{-1}(\Lambda) = e^{-i(\Lambda p)x} = e^{-ip(\Lambda^{-1}x)}, \quad (2.294)$$

and, since  $U(\Lambda)\psi(0) = S(\Lambda)\psi(0)$ ,

$$U(\Lambda)\psi(x) = e^{-ip(\Lambda^{-1}x)}S(\Lambda)\psi(0) = S(\Lambda)\psi(\Lambda^{-1}x). \quad (2.295)$$

## 2.6 The relativistic wave equations

In Section 2.5 we introduced the Poincaré group and showed that a structureless particle is described by a unitary irreducible representation of this group identified by the mass and by the spin. We will now find the relativistic wave equations of free motion for these particles.

### 2.6.1 Particles of spin 0

For a spin 0 particle any given state  $|s\rangle$  can be represented as

$$|s\rangle = \int d\Omega_p \varphi_s(p)|p\rangle, \quad (2.296)$$

$\varphi_s(p) = \langle p|s\rangle$  is the wave function in the representation were the momenta are diagonal. The wave function associated to the state  $|p\rangle$ ,  $\psi_p(x)$ , must have the form (2.291). By the superposition principle

$$\langle x|s\rangle = \psi_s(x) = \int d\Omega_p \varphi_s(p)e^{-ipx}\psi_p(0). \quad (2.297)$$

To determine  $\psi_p(0)$  let us consider the effect of a Lorentz transformation

$$|s\rangle \xrightarrow{\Lambda} \int d\Omega_p \varphi_s(p)|\Lambda p\rangle = \int d\Omega_p \varphi_s(\Lambda^{-1}p)|p\rangle, \quad (2.298)$$

and on the wave function

$$\psi_s(x) \xrightarrow{\Lambda} \int d\Omega_p \varphi_s(\Lambda^{-1}p) e^{-ipx} \psi_p(0) = \int d\Omega_p \varphi_s(p) e^{-ip(\Lambda^{-1}x)} \psi_{\Lambda p}(0). \quad (2.299)$$

This transformation is certainly local if  $\psi_{\Lambda p}(0) = \psi_p(0)$ . This means that  $\psi_p(0)$  must be an invariant constructed with  $p_\mu$ . Since  $p^2 = m^2$ , such an invariant must be a constant, that can be chosen equal to 1.

So

$$\psi_s(x) = \int d\Omega_p \varphi_s(p) e^{-ipx}. \quad (2.300)$$

Under translation

$$\psi_s(x) \xrightarrow{a} \psi'(x) = \psi_s(x + a). \quad (2.301)$$

Under Lorentz transformation

$$\psi_s(x) \xrightarrow{\Lambda} \psi'(x) = \psi_s(\Lambda^{-1}x). \quad (2.302)$$

The function  $\psi_s(x)$  in Eq. (2.300) transforms locally and the requirement  $p^2 = m^2$  implies that it obeys the Klein-Gordon equation

$$(\square + m^2)\psi_s(x) = 0, \quad (2.303)$$

where

$$\square = \frac{\partial^2}{\partial t^2} - \sum_{i=1}^3 \frac{\partial^2}{\partial x_i^2}, \quad (2.304)$$

is the d' Alambert operator. Eq. (2.303) is invariant under transformations of the Poincaré group.

Not all solutions of Eq. (2.303) are of kind (2.300). Eq. (2.303) admits also solutions with negative energy. As a matter of fact the wave function of Eq. (2.300) obeys to the following equation

$$\left( i \frac{\partial}{\partial x^0} - \sqrt{m^2 - \nabla^2} \right) \psi_s(x) = 0, \quad (2.305)$$

which is non-local. The requirement for a local equation imposes to have negative energy solutions as well.

The general solution of Eq. (2.303) can be easily obtained working in Fourier space

$$\psi_s(x) = \int \frac{d^4 p}{(2\pi)^4} e^{-ipx} \tilde{\psi}_s(p). \quad (2.306)$$

Then Eq. (2.303) becomes

$$(p^2 - m^2) \tilde{\psi}_s(p) = 0, \quad (2.307)$$

or

$$\tilde{\psi}_s(p) = \varphi_s(p) 2\pi \delta(p^2 - m^2). \quad (2.308)$$

Integrating over  $p_0$  in Eq. (2.306)

$$\psi_s(x) = \int \frac{d^3 p}{(2\pi)^3 2p_0} [\varphi_s(\mathbf{p}, p_0) e^{-ipx} + \varphi_s(\mathbf{p}, -p_0) e^{ip_0 x^0 + i\mathbf{p} \cdot \mathbf{r}}]. \quad (2.309)$$

We then define

$$\varphi_s(\mathbf{p}, p_0) = \varphi_s^+(\mathbf{p}), \quad (2.310)$$

$$\varphi_s(\mathbf{p}, -p_0) = \varphi_s^-(\mathbf{p}), \quad (2.311)$$

so that

$$\psi_s(x) = \int d\Omega_{\mathbf{p}} [\varphi_s^+(\mathbf{p}) e^{-ipx} + \varphi_s^-(\mathbf{p}) e^{ipx}]. \quad (2.312)$$

A natural scalar product can be introduced as follows. Given two solutions of the Klein-Gordon equation (2.303),  $\psi_a(x)$  and  $\psi_b(x)$ , the quantity

$$J_\mu^{(a,b)}(x) = i\psi_a^* \overset{\leftrightarrow}{\partial}_\mu \psi_b = i[\psi_a^* \partial_\mu \psi_b - (\partial_\mu \psi_a^*) \psi_b], \quad (2.313)$$

where  $\partial_\mu \equiv \partial/\partial x^\mu$ , is conserved, i.e.

$$\partial^\mu J_\mu^{(a,b)}(x) = 0. \quad (2.314)$$

Then, due to Gauss theorem, if the  $\psi$  go to zero sufficiently rapidly at spatial infinity, the integral extended to an hypersurface of spatial kind extended to infinity,

$$\int d\sigma^\mu J_\mu^{(a,b)}(x), \quad (2.315)$$

is independent from the surface ( $d\sigma^\mu$  is the oriented normal). It can be calculated on a surface  $x^0 = \text{constant}$

$$\int d\sigma^\mu J_\mu^{(a,b)}(x) = \int dx J_0^{(a,b)}(t, x). \quad (2.316)$$

We will define the scalar product  $\langle a|b \rangle$  through

$$\begin{aligned} \langle a|b \rangle &= \int d\sigma^\mu J_\mu^{(a,b)}(x) \\ &= \int d\Omega_{\mathbf{p}} [\varphi_a^{+*}(\mathbf{p}) \varphi_b^+(\mathbf{p}) - \varphi_a^{-*}(\mathbf{p}) \varphi_b^-(\mathbf{p})]. \end{aligned} \quad (2.317)$$

The generators of the group in this representation are

$$\begin{aligned} p_\mu &= i \frac{\partial}{\partial x^\mu}, \\ J^{(\mu\nu)} &= -i \left( x^\mu \frac{\partial}{\partial x^\nu} - x^\nu \frac{\partial}{\partial x^\mu} \right), \end{aligned} \quad (2.318)$$

which are hermitians under the metric of Eq. (2.317).

The Eq. (2.305) satisfied by these wave functions is non-local. In order to have a local equation, like (2.303), it is necessary to put together positive and negative energy solutions. Actually, the Klein-Gordon Eq. (2.303) is second order in the temporal derivative, while, once the Hamiltonian is known, the evolution equation should be of the first order.

### 2.6.2 Particles of spin 1/2

The irreducible representations of the Poincaré group corresponding to particles of mass  $m$  and spin 1/2 are in correspondence with vectors  $|r, p\rangle$ , where  $r$  is the eigenvalue of one component of the spin in the rest frame.

Any state  $|a\rangle$  of the Hilbert space generated like so is of the following form

$$|a\rangle = \int d\Omega_p \sum_{r=1}^2 \varphi_a(r, p) |r, p\rangle. \quad (2.319)$$

The infinitesimal transformations of the Lorentz group are

$$\varphi_a(r, p) \rightarrow \varphi_{\Lambda a}(r, p) = \left[ 1 + i\boldsymbol{\theta} \cdot \left( \frac{1}{i} \mathbf{p} \wedge \frac{\partial}{\partial \mathbf{p}} + \mathbf{s} \right) - i\boldsymbol{\alpha} \cdot \left( ip_0 \frac{\partial}{\partial \mathbf{p}} + \frac{\mathbf{p} \wedge \mathbf{s}}{p_0 + m} \right) \right]_{rr'} \varphi_a(r', p) \quad (2.320)$$

We will now construct local wave functions for these states. The locality under translations fixes the form of the wave functions corresponding to eigenstates of momentum

$$\psi_{r,p}(x) = \psi_{r,p}(0) e^{-ipx}. \quad (2.321)$$

We will call  $\psi_{r,p}(0) \equiv u(r, p)$ . Due to the superposition principle we will have

$$\psi_a(x) = \int d\Omega_p \sum_{r=1}^2 \varphi_a(r, p) u(r, p) e^{-ipx}. \quad (2.322)$$

To find an explicit form for the local wave functions we will adopt the following strategy. We will assume specific properties of local transformations for  $\psi_a(x)$ . We will write an equation explicitly covariant under the Poincaré group transformations and will later prove that the solutions of this equation give a unitary representation of the Poincaré group. And will express the scalar product between states in terms of these wave functions.

Locality under group transformations requires

$$\psi_a(x) \xrightarrow{\Lambda} \psi_{\Lambda a}(x) = S(\Lambda) \psi_a(\Lambda^{-1}x), \quad (2.323)$$

where  $S(\Lambda)$  is a finite dimensional representation of the Lorentz group. The Lorentz group is locally isomorphic to  $SU(2) \otimes SU(2)$ . Hence the finite dimensional representations are fixed by two numbers  $(n_+, n_-)$  which determine the representations of the two groups  $SU(2)$  with generators

$$\mathbf{J}_+ = \frac{\mathbf{J} + i\mathbf{K}}{2}, \quad (2.324)$$

$$\mathbf{J}_- = \frac{\mathbf{J} - i\mathbf{K}}{2}. \quad (2.325)$$

We will heuristically construct the  $\psi$  with representations of dimension 2.

There exist two inequivalent representations of dimension 2. The  $(\frac{1}{2}, 0)$  and the  $(0, \frac{1}{2})$ . In the two representations the group generators, defined by the infinitesimal transformations

$$\boldsymbol{\Lambda} \approx 1 + i\boldsymbol{\theta} \cdot \mathbf{J} - i\boldsymbol{\alpha} \cdot \mathbf{K}, \quad (2.326)$$

are given by

$$(\frac{1}{2}, 0) : \quad \begin{cases} \mathbf{J} = \frac{\boldsymbol{\sigma}}{2} \\ \mathbf{K} = -i\frac{\boldsymbol{\sigma}}{2} \end{cases}, \quad (2.327)$$

$$(0, \frac{1}{2}) : \quad \begin{cases} \mathbf{J} = \frac{\boldsymbol{\sigma}}{2} \\ \mathbf{K} = i\frac{\boldsymbol{\sigma}}{2} \end{cases}. \quad (2.328)$$

The corresponding finite transformations are

$$S_{(\frac{1}{2},0)}(\Lambda) = e^{i\theta \cdot \frac{\sigma}{2} - \alpha \cdot \frac{\sigma}{2}}, \quad (2.329)$$

$$S_{(0,\frac{1}{2})}(\Lambda) = e^{i\theta \cdot \frac{\sigma}{2} + \alpha \cdot \frac{\sigma}{2}}, \quad (2.330)$$

with

$$S_{(0,\frac{1}{2})}(\Lambda) = S_{(\frac{1}{2},0)}^\dagger(\Lambda)^{-1}. \quad (2.331)$$

We will call  $\xi$  the spinors which transform according to  $(\frac{1}{2}, 0)$  and  $\eta$  the ones transforming according to  $(0, \frac{1}{2})$ .

Since  $J$  is an axial vector, whereas  $K$  is a polar vector, we have under parity

$$(\frac{1}{2}, 0) \xleftrightarrow{P} (0, \frac{1}{2}). \quad (2.332)$$

Then in order to construct a representation invariant under parity we need to consider a reducible representation of the Lorentz group for  $S(\Lambda)$ , namely

$$(\frac{1}{2}, 0) \oplus (0, \frac{1}{2}). \quad (2.333)$$

The vectorial space for this representation is composed by spinors of 4 components of the form

$$\begin{pmatrix} \xi \\ \eta \end{pmatrix}. \quad (2.334)$$

In such representation, the generators of the Lorentz group are

$$J = \begin{pmatrix} \frac{\sigma}{2} & 0 \\ 0 & \frac{\sigma}{2} \end{pmatrix}, \quad (2.335)$$

$$K = \begin{pmatrix} -i\frac{\sigma}{2} & 0 \\ 0 & i\frac{\sigma}{2} \end{pmatrix}. \quad (2.336)$$

Using the following identities for the Pauli matrices

$$[\theta \cdot \sigma, \sigma] = -2i\theta \wedge \sigma, \quad (2.337)$$

$$\{\alpha \cdot \sigma, \sigma\} = 2\alpha, \quad (2.338)$$

where  $[\dots]$  stands for the commutator and  $\{\dots\}$  for the anticommutator, we easily find that

$$\begin{aligned} S_{(\frac{1}{2},0)}(\Lambda)(p_0 + p \cdot \sigma)S_{(\frac{1}{2},0)}^\dagger(\Lambda) &= p_0 + p \cdot \sigma + i[\theta \cdot \frac{\sigma}{2}, p_0 + p \cdot \sigma] - \{\alpha \cdot \frac{\sigma}{2}, p_0 + p \cdot \sigma\} + \dots \\ &= p_0 + p \cdot \sigma + \frac{i}{2}[\theta \cdot \sigma, p \cdot \sigma] - \alpha \cdot \sigma p_0 - \frac{1}{2}\{\alpha \cdot \sigma, p \cdot \sigma\} + \dots \\ &= (p_0 - \alpha \cdot p + \dots) + \sigma \cdot (p - \theta \wedge p - \alpha p_0 + \dots) \\ &= p'_0 + \sigma \cdot p', \end{aligned} \quad (2.339)$$

where in the vector representation we used

$$(iJ_i)_{jk} = \epsilon_{ijk}, \quad (2.340)$$

$$(iK_i)_{j0} = (iK_i)_{0j} = \delta_{ij}, \quad (2.341)$$

and  $p'$  is the Lorentz transformed of  $p$

$$p'_\mu = \Lambda^\nu_\mu p_\nu. \quad (2.342)$$

Then an equation of the form

$$(p^0 + \mathbf{p} \cdot \boldsymbol{\sigma})\eta = c\xi, \quad (2.343)$$

where  $c$  is a scalar, is covariant under Lorentz transformations. In fact, calling  $S = S_{(\frac{1}{2}, 0)}(\Lambda)$ , we have

$$S(p^0 + \mathbf{p} \cdot \boldsymbol{\sigma})\eta = cS\xi, \quad (2.344)$$

or

$$S(p^0 + \mathbf{p} \cdot \boldsymbol{\sigma})S^\dagger S^{\dagger -1}\eta = cS\xi'. \quad (2.345)$$

Due to Eq. (2.331)  $S^{\dagger -1}\eta = \eta'$  and using Eq. (2.339)

$$(p^{0'} + \mathbf{p}' \cdot \boldsymbol{\sigma})\eta' = \xi', \quad (2.346)$$

so the equation has the same form in all reference frames. Analogously we show that  $(p^0 - \mathbf{p} \cdot \boldsymbol{\sigma})\xi$  transforms as  $(0, \frac{1}{2})$ . The most general system of first order covariant equations has then the following form

$$(p^0 + \mathbf{p} \cdot \boldsymbol{\sigma})\eta = c\xi, \quad (2.347)$$

$$(p^0 - \mathbf{p} \cdot \boldsymbol{\sigma})\xi = c'\eta, \quad (2.348)$$

and invariance under parity imposes  $c = c'$ . Multiplying the first equation by  $(p^0 - \mathbf{p} \cdot \boldsymbol{\sigma})$  and using the second equation we find

$$p^{0^2} - \mathbf{p}^2 = c^2. \quad (2.349)$$

Then if we want to describe a particle we must identify  $c$  with the mass  $m$ . In terms of bispinors we have

$$\begin{pmatrix} 0 & p^0 + \mathbf{p} \cdot \boldsymbol{\sigma} \\ p^0 - \mathbf{p} \cdot \boldsymbol{\sigma} & 0 \end{pmatrix} \begin{pmatrix} \xi \\ \eta \end{pmatrix} = m \begin{pmatrix} \xi \\ \eta \end{pmatrix}. \quad (2.350)$$

We give a more symmetric form to this equation by introducing the  $4 \times 4$  matrices

$$\gamma^0 = \begin{pmatrix} 0 & 1 \\ 1 & 0 \end{pmatrix}, \quad \boldsymbol{\gamma} = \begin{pmatrix} 0 & -\boldsymbol{\sigma} \\ \boldsymbol{\sigma} & 0 \end{pmatrix}, \quad (2.351)$$

and the bispinor  $\psi = \begin{pmatrix} \xi \\ \eta \end{pmatrix}$ . We will also introduce

$$\gamma^5 = \begin{pmatrix} 1 & 0 \\ 0 & -1 \end{pmatrix} = i\gamma^0\gamma^1\gamma^2\gamma^3 = -\frac{i}{4!}\epsilon_{\mu\nu\sigma\tau}\gamma^\mu\gamma^\nu\gamma^\sigma\gamma^\tau. \quad (2.352)$$

We then find

$$(\gamma^0 p^0 - \boldsymbol{\gamma} \cdot \mathbf{p})\psi = m\psi, \quad (2.353)$$

or

$$\gamma^\mu p_\mu \psi = m\psi. \quad (2.354)$$

Introducing the notation  $\not{p} = \gamma^\mu p_\mu$  we have

$$(\not{p} - m)\psi = 0. \quad (2.355)$$

This equation is known as the Dirac equation.

Applying the Lorentz transformation  $S(\Lambda)$  in the representation  $(\frac{1}{2}, 0) \oplus (0, \frac{1}{2})$  to the Dirac equation

$$S(\Lambda)\gamma^\mu p_\mu S^{-1}(\Lambda)S(\Lambda)\psi = mS(\Lambda)\psi. \quad (2.356)$$

Since the bispinor transforms under  $S(\Lambda)$  the covariance imposes

$$S(\Lambda)\gamma^\mu S^{-1}(\Lambda) = \Lambda^\mu_\nu \gamma^\nu, \quad (2.357)$$

which means that  $\gamma^\mu$  transform as a four-vector.

In coordinate representation

$$(i\not{\partial} - m)\psi = 0, \quad (2.358)$$

and by construction the solutions of this equation transform locally under Lorentz transformations. Of course in order to know whether they represent the states of a spin 1/2 particle of mass  $m$  we must verify that they are in bijective correspondence with the states defined in terms of the representations of the Poincaré group, and that a transformation on the states corresponds to a transformation on the wave functions.

We have

$$\{\gamma^\mu, \gamma^\nu\} = 2g^{\mu\nu}, \quad (2.359)$$

we can define the covariant component of the gamma matrices

$$\gamma_\mu = g_{\mu\nu}\gamma^\nu, \quad (2.360)$$

and we find

$$\{\gamma_\mu, \gamma_\nu\} = 2g_{\mu\nu}. \quad (2.361)$$

Also

$$\{\gamma^\mu, \gamma^5\} = 0, \quad (2.362)$$

and

$$\gamma^{0\dagger} = \gamma^0 \quad \gamma^{i\dagger} = -\gamma^i, \quad (2.363)$$

or

$$\gamma^{\mu\dagger} = \gamma^0 \gamma^\mu \gamma^0. \quad (2.364)$$

Using the matrices  $\gamma^\mu$  it is possible to write in a compact form the Lorentz transformations in the representation  $(\frac{1}{2}, 0) \oplus (0, \frac{1}{2})$ . Consider the matrices

$$\sigma_{\mu\nu} = \frac{1}{2i}[\gamma_\mu, \gamma_\nu]. \quad (2.365)$$

Under the transformation  $S(\Lambda)\sigma_{\mu\nu}S^{-1}(\Lambda)$  they transform as an antisymmetric tensor of rank 2. One can verify that

$$K^i = \frac{1}{2}\sigma^{oi} \quad J^i = \frac{1}{2}\epsilon^{oijk}\sigma_{jk} \quad i, j, k = 1, 2, 3. \quad (2.366)$$

The tensor  $\sigma_{\mu\nu}$  represents the generators of the Lorentz group and we can write

$$S(\Lambda) = e^{\frac{i}{4}\omega^{\mu\nu}\sigma_{\mu\nu}}. \quad (2.367)$$

Moreover  $\sigma_{\mu\nu}/2$  satisfies the algebra (2.154).

The matrix  $\gamma^0$  has the role of exchanging the representations  $(\frac{1}{2}, 0)$  and  $(0, \frac{1}{2})$ , so it coincides with the parity operator up to a phase,

$$\psi_a(x) \xrightarrow{P} \psi_{Pa}(x) = \eta_P \gamma^0 \psi_a(x^0, -x). \quad (2.368)$$

From the anticommutation rules (2.359) follows

$$\gamma^0 \gamma^i \gamma^0 = -\gamma^i \quad i = 1, 2, 3 \quad \gamma^0 \gamma^0 \gamma^0 = \gamma^0. \quad (2.369)$$

It is interesting to consider the set of the 16 matrices

$$1, \gamma^5, \gamma^\mu, \gamma^5 \gamma^\mu, \sigma^{\mu\nu}. \quad (2.370)$$

From the definition follow that the properties of Lorentz transformation of the matrices (2.370) are

1	scalar
$\gamma^5$	pseudoscalar
$\gamma^\mu$	vector
$\gamma^5 \gamma^\mu$	pseudovector
$\sigma^{\mu\nu}$	antisymmetric tensor

(2.371)

These 16 matrices are linearly independent (in fact they transform differently under Lorentz transformations) so they constitute a complete basis for the  $4 \times 4$  matrices, i.e. any  $4 \times 4$  matrix can be written in the form

$$\sum_{a=1}^{16} c_a \Gamma^a, \quad (2.372)$$

where  $\{\Gamma^a\}$  is the set of 16 matrices (2.370).

Note that if  $\psi$  and  $\psi'$  are two bispinors,  $\psi'^\dagger \psi$  is not a scalar density. In fact

$$\psi'^\dagger(x) \psi(x) \xrightarrow{(a, \Lambda)} \psi'^\dagger(\Lambda^{-1}x + a) S^\dagger(\Lambda) S(\Lambda) \psi(\Lambda^{-1}x + a), \quad (2.373)$$

and  $S^\dagger S \neq 1$ . The representation  $S(\Lambda)$  is not unitary as follows from its definition (2.327)-(2.328) and as should be expected since the Lorentz group is not compact. But we have

$$S^\dagger(\Lambda) \gamma^0 = \gamma^0 S^{-1}(\Lambda). \quad (2.374)$$

Then, upon defining  $\bar{\psi}' = \psi^\dagger \gamma^0$ ,  $\bar{\psi}' \psi$  is a scalar density

$$\begin{aligned} \bar{\psi}'(x) \psi(x) &\xrightarrow{(a, \Lambda)} \bar{\psi}'^\dagger(\Lambda^{-1}x + a) S^\dagger(\Lambda) \gamma^0 S(\Lambda) \psi(\Lambda^{-1}x + a) \\ &= \bar{\psi}'(\Lambda^{-1}x + a) \psi(\Lambda^{-1}x + a). \end{aligned} \quad (2.375)$$

Let us finally mention the following formulas,

$$\text{Tr}\{\gamma^{\mu_1}\gamma^{\mu_2} \cdot \gamma^{\mu_{2n+1}}\} = 0, \quad (2.376)$$

$$\text{Tr}\{\gamma^\mu\gamma^\nu\} = 4g^{\mu\nu}, \quad (2.377)$$

$$\text{Tr}\{\gamma^\mu\gamma^\nu\gamma^\rho\gamma^\sigma\} = 4\{g^{\mu\nu}g^{\rho\sigma} - g^{\mu\rho}g^{\nu\sigma} + g^{\mu\sigma}g^{\nu\rho}\}, \quad (2.378)$$

$$\text{Tr}\{\gamma^5\gamma^\mu\gamma^\nu\gamma^\rho\gamma^\sigma\} = -4i\epsilon^{\mu\nu\rho\sigma}, \quad (2.379)$$

$$\gamma_\mu A\gamma^\mu = -2A, \quad (2.380)$$

$$\gamma_\mu A\bar{B}\gamma^\mu = 4AB, \quad (2.381)$$

$$\gamma_\mu A\bar{B}\bar{C}\gamma^\mu = -2\bar{C}BA. \quad (2.382)$$

### Dirac equation solutions: momentum eigenstates

Multiplying Eq. (2.355) by  $\gamma^0$  we find

$$p^0\psi = (\boldsymbol{\alpha} \cdot \mathbf{p} + \gamma^0 m)\psi, \quad (2.383)$$

where  $\boldsymbol{\alpha} = \gamma^0\boldsymbol{\gamma}$ . Now we do a change of representation where we diagonalize  $\gamma^0$

$$\psi \rightarrow U\psi \quad \gamma^\mu \rightarrow U\gamma^\mu U^{-1} \quad U = \frac{1}{\sqrt{2}} \begin{pmatrix} 1 & 1 \\ 1 & -1 \end{pmatrix} = U^{-1}, \quad (2.384)$$

explicitly

$$U \begin{pmatrix} \xi \\ \eta \end{pmatrix} = \begin{pmatrix} \frac{\xi + \eta}{\sqrt{2}} \\ \frac{\xi - \eta}{\sqrt{2}} \end{pmatrix} \equiv \begin{pmatrix} \varphi \\ \chi \end{pmatrix}. \quad (2.385)$$

After this transformation the algebra of the  $\gamma$  matrices remains the same. The  $\gamma$  matrices are rewritten as follows

$$\gamma^0 = \begin{pmatrix} 1 & 0 \\ 0 & -1 \end{pmatrix} \quad \boldsymbol{\gamma} = \begin{pmatrix} 0 & \boldsymbol{\sigma} \\ -\boldsymbol{\sigma} & 0 \end{pmatrix} \quad \gamma^5 = \begin{pmatrix} 0 & 1 \\ 1 & 0 \end{pmatrix}. \quad (2.386)$$

Since  $\gamma^0$  is diagonal in the non-relativistic limit the states in this representation have definite parity. This is known as *Pauli representation*. The one of Eq. (2.351) as *spinorial or Kramers representation*.

Let us now find the solution with definite momentum and positive energy in the form

$$\psi_p(x) = e^{-ipx}u(r, \mathbf{p}), \quad (2.387)$$

suggested by translational invariance.

In the Pauli representation we find then

$$p^0 u_1 - \boldsymbol{\sigma} \cdot \mathbf{p} u_2 = mu_1, \quad (2.388)$$

$$-p^0 u_2 + \boldsymbol{\sigma} \cdot \mathbf{p} u_1 = mu_2, \quad (2.389)$$

where  $p^0 = \sqrt{\mathbf{p}^2 + m^2}$  and  $u = \begin{pmatrix} u_1 \\ u_2 \end{pmatrix}$ .

These equations admit two independent solutions labeled by two Pauli spinors (bidimensional)  $w_1$  and  $w_2$  orthonormal

$$u(r, p) = c \begin{pmatrix} w_r \\ \frac{\boldsymbol{\sigma} \cdot \mathbf{p}}{p^0 + m} w_r \end{pmatrix} \quad w_r^\dagger w_s = \delta_{rs}. \quad (2.390)$$

Since we know that  $\bar{u}u$  must be invariant, we find

$$\begin{aligned} \bar{u}u &= u^\dagger \gamma^0 u = w^\dagger w_r c^2 \left( 1 - \frac{\boldsymbol{\sigma}^\dagger \cdot \mathbf{p} \boldsymbol{\sigma} \cdot \mathbf{p}}{(p^0 + m)^2} \right) \\ &= c^2 \left( 1 - \frac{\mathbf{p}^2}{(p^0 + m)^2} \right) \\ &= c^2 \frac{2m}{p^0 + m} = \text{invariant.} \end{aligned} \quad (2.391)$$

We then choose conveniently  $c = \sqrt{p^0 + m}$  so that

$$u(r, p) = \begin{pmatrix} \sqrt{p^0 + m} w_r \\ \frac{\boldsymbol{\sigma} \cdot \mathbf{p}}{\sqrt{p^0 + m}} w_r \end{pmatrix}, \quad (2.392)$$

$$\bar{u}(r, p)u(s, p) = 2m\delta_{rs}. \quad (2.393)$$

As a standard base for the spinors  $w_r$  we can take the eigenstates of  $\sigma_z$

$$w_1 = \begin{pmatrix} 1 \\ 0 \end{pmatrix} \quad w_2 = \begin{pmatrix} 0 \\ 1 \end{pmatrix}. \quad (2.394)$$

As in the scalar case the Dirac equation admits also negative energy solutions. These will be of the following kind

$$\tilde{\psi}(x) = e^{ip^0 t + i\mathbf{p} \cdot \mathbf{x}} \tilde{u}(r, p), \quad (2.395)$$

Proceeding as in the previous case we find

$$\tilde{u}(r, p) = \begin{pmatrix} -\frac{\boldsymbol{\sigma} \cdot \mathbf{p}}{\sqrt{p^0 + m}} \tilde{w}_r \\ \frac{\sqrt{p^0 + m}}{\sqrt{p^0 + m}} \tilde{w}_r \end{pmatrix}. \quad (2.396)$$

Calling  $v(r, p) = \tilde{u}(r, -p)$  we find

$$v(r, p) = \begin{pmatrix} \frac{\boldsymbol{\sigma} \cdot \mathbf{p}}{\sqrt{p^0 + m}} \tilde{w}_r \\ \frac{\sqrt{p^0 + m}}{\sqrt{p^0 + m}} \tilde{w}_r \end{pmatrix}, \quad (2.397)$$

$$\bar{v}(r, p)v(s, p) = -2m\delta_{rs}. \quad (2.398)$$

The spinors  $u$  and  $v$  satisfy the following algebraic equations

$$(\not{p} - m)u(r, p) = 0, \quad (2.399)$$

$$(\not{p} + m)v(r, p) = 0, \quad (2.400)$$

and constitute a complete set of spinors for the description of the momentum eigenstates. The four solutions found form a set of independent vectors, orthogonal respect to the  $\gamma^0$  metric

$$\bar{u}(r, \mathbf{p})u(s, \mathbf{p}) = 2m\delta_{rs}, \quad (2.401)$$

$$\bar{v}(r, \mathbf{p})v(s, \mathbf{p}) = -2m\delta_{rs}, \quad (2.402)$$

$$\bar{u}(r, \mathbf{p})v(s, \mathbf{p}) = \bar{v}(r, \mathbf{p})u(s, \mathbf{p}) = 0. \quad (2.403)$$

Due to the completeness of the set we also have

$$\sum_{r=1}^2 u(r, \mathbf{p})\bar{u}(r, \mathbf{p}) = \not{p} + m, \quad (2.404)$$

$$\sum_{r=1}^2 v(r, \mathbf{p})\bar{v}(r, \mathbf{p}) = \not{p} - m. \quad (2.405)$$

### Transformation properties and connection with the Poincaré group representations

We will now explicitly study the effect of the Lorentz transformation  $S(\Lambda)$  on the solutions we just found. We will find that they realize a representation of the Poincaré group for a spin 1/2 particle.

A Lorentz transformation sends solutions with momentum  $p$  to solutions with momentum  $p' = \Lambda p$ . In fact, using the covariance property of the  $\gamma$  matrices we find

$$S(\Lambda)(\not{p} - m)u(r, \mathbf{p}) = (\not{p}' - m)S(\Lambda)u(r, \mathbf{p}) = 0. \quad (2.406)$$

In the Pauli representation we find for a rotation  $R(\boldsymbol{\theta})$

$$J = \begin{pmatrix} \boldsymbol{\sigma} & 0 \\ \frac{1}{2} & \boldsymbol{\sigma} \\ 0 & \frac{1}{2} \end{pmatrix} \quad S(R(\boldsymbol{\theta})) = \begin{pmatrix} e^{i\boldsymbol{\theta}\cdot\frac{\boldsymbol{\sigma}}{2}} & 0 \\ 0 & e^{i\boldsymbol{\theta}\cdot\frac{\boldsymbol{\sigma}}{2}} \end{pmatrix}, \quad (2.407)$$

so

$$S(R(\boldsymbol{\theta}))u(r, \mathbf{p}) = \begin{pmatrix} \sqrt{p^0 + m}e^{i\boldsymbol{\theta}\cdot\frac{\boldsymbol{\sigma}}{2}}w_r \\ \frac{(R^{-1}(\boldsymbol{\theta})\boldsymbol{\sigma}) \cdot \mathbf{p}}{\sqrt{p^0 + m}}e^{i\boldsymbol{\theta}\cdot\frac{\boldsymbol{\sigma}}{2}}w_r \\ \sqrt{p^0 + m} \end{pmatrix} = \begin{pmatrix} \sqrt{p^0 + m}e^{i\boldsymbol{\theta}\cdot\frac{\boldsymbol{\sigma}}{2}}w_r \\ \frac{\boldsymbol{\sigma} \cdot (R(\boldsymbol{\theta})\mathbf{p})}{\sqrt{p^0 + m}}e^{i\boldsymbol{\theta}\cdot\frac{\boldsymbol{\sigma}}{2}}w_r \\ \sqrt{p^0 + m} \end{pmatrix}, \quad (2.408)$$

and

$$e^{i\boldsymbol{\theta}\cdot\frac{\boldsymbol{\sigma}}{2}}w_r = \sum_{r'} \mathcal{R}(\boldsymbol{\theta})_{r'r} w_{r'} \quad \mathcal{R}(\boldsymbol{\theta})_{r'r} = \left( e^{i\boldsymbol{\theta}\cdot\frac{\boldsymbol{\sigma}}{2}} \right)_{r'r} \quad S(R(\boldsymbol{\theta}))u(r, \mathbf{p}) = \sum_{r'} \mathcal{R}(\boldsymbol{\theta})_{r'r} u(r', R\mathbf{p}). \quad (2.409)$$

A transformation of rapidity  $\boldsymbol{\alpha}$  is given by

$$S(\Lambda_{\boldsymbol{\alpha}}) = \begin{pmatrix} e^{-\boldsymbol{\alpha}\cdot\frac{\boldsymbol{\sigma}}{2}} & 0 \\ 0 & e^{\boldsymbol{\alpha}\cdot\frac{\boldsymbol{\sigma}}{2}} \end{pmatrix} = \begin{pmatrix} \cosh \frac{\alpha}{2} - \hat{\boldsymbol{\alpha}} \cdot \boldsymbol{\sigma} \sinh \frac{\alpha}{2} & 0 \\ 0 & \cosh \frac{\alpha}{2} + \hat{\boldsymbol{\alpha}} \cdot \boldsymbol{\sigma} \sinh \frac{\alpha}{2} \end{pmatrix}, \quad (2.410)$$

and in the Pauli representation

$$US(\Lambda_{\boldsymbol{\alpha}})U^{-1} = \begin{pmatrix} \cosh \frac{\alpha}{2} & -\hat{\boldsymbol{\alpha}} \cdot \boldsymbol{\sigma} \sinh \frac{\alpha}{2} \\ -\hat{\boldsymbol{\alpha}} \cdot \boldsymbol{\sigma} \sinh \frac{\alpha}{2} & \cosh \frac{\alpha}{2} \end{pmatrix}. \quad (2.411)$$

We then find explicitly

$$\begin{pmatrix} \cosh \frac{\alpha}{2} & -\hat{\boldsymbol{\alpha}} \cdot \boldsymbol{\sigma} \sinh \frac{\alpha}{2} \\ -\hat{\boldsymbol{\alpha}} \cdot \boldsymbol{\sigma} \sinh \frac{\alpha}{2} & \cosh \frac{\alpha}{2} \end{pmatrix} \begin{pmatrix} \sqrt{p^0 + m} w_r \\ \frac{\boldsymbol{\sigma} \cdot \mathbf{p}}{\sqrt{p^0 + m}} w_r \end{pmatrix} = \begin{pmatrix} \sqrt{p'^0 + m} e^{-i\varphi \boldsymbol{\sigma} \cdot \hat{\boldsymbol{\alpha}} \wedge \hat{\mathbf{p}}} w_r \\ \frac{\boldsymbol{\sigma} \cdot \mathbf{p}'}{\sqrt{p'^0 + m}} e^{-i\varphi \boldsymbol{\sigma} \cdot \hat{\boldsymbol{\alpha}} \wedge \hat{\mathbf{p}}} w_r \end{pmatrix}, \quad (2.412)$$

where

$$\tan \varphi = \frac{|\mathbf{p}| \sinh \frac{\alpha}{2}}{(p^0 + m) \cosh \frac{\alpha}{2} - p_{||} \sinh \frac{\alpha}{2}}. \quad (2.413)$$

Here we used Eqs. (E.23) and (E.24) and  $p_{||} = \hat{\boldsymbol{\alpha}} \cdot \mathbf{p}$ . The matrix  $\mathcal{R} = e^{-i\varphi \boldsymbol{\sigma} \cdot \hat{\boldsymbol{\alpha}} \wedge \hat{\mathbf{p}}}$  is a rotation of an angle  $-2\varphi \hat{\boldsymbol{\alpha}} \wedge \hat{\mathbf{p}}$  which acts on the components of the spinor  $w$ . Explicitly

$$S(\Lambda_{\boldsymbol{\alpha}})u(r, \mathbf{p}) = \sum_{r'} \mathcal{R}(\Lambda_{\boldsymbol{\alpha}}, \mathbf{p})_{r'r} u(r', \Lambda_{\boldsymbol{\alpha}} \mathbf{p}). \quad (2.414)$$

For an infinitesimal transformation ( $\alpha \ll 1$ )

$$\varphi \approx \frac{\alpha}{2} \frac{|\mathbf{p}|}{p^0 + m}, \quad (2.415)$$

$$\mathcal{R} \approx 1 - i \frac{\boldsymbol{\sigma}}{2} \cdot \frac{\boldsymbol{\alpha} \wedge \mathbf{p}}{p^0 + m} = 1 + i s \cdot \frac{\mathbf{p} \wedge \boldsymbol{\alpha}}{p^0 + m}. \quad (2.416)$$

So in general we find

$$S(\Lambda)u(r, \mathbf{p}) = \sum_{r'} \mathcal{R}(\Lambda, \mathbf{p})_{r'r} u(r', \Lambda \mathbf{p}), \quad (2.417)$$

where  $\mathcal{R}$  is the Wigner rotation associated to the transformation  $\Lambda$ . And an identical formula holds for  $v(r, \mathbf{p})$ .

Let us now consider any solution of the Dirac equation

$$\psi(x) = \sum_{r=1}^2 \int d\Omega_{\mathbf{p}} [\varphi_r^+(\mathbf{p})u(r, \mathbf{p})e^{-ipx} + \varphi_r^-(\mathbf{p})v(r, \mathbf{p})e^{ipx}]. \quad (2.418)$$

By construction the Poincaré group is realized in a local way on the space of these solutions

$$T_a : \psi(x) \xrightarrow{a} \psi'(x) = \psi(x + a), \quad (2.419)$$

$$\Lambda : \psi(x) \xrightarrow{\Lambda} \psi'(x) = \psi(\Lambda^{-1}x). \quad (2.420)$$

For infinitesimal transformations, recalling that  $(\Lambda^{-1}x)^{\mu} \approx x^{\mu} - \omega_{\nu}^{\mu} x^{\nu}$ , we have

$$\psi(x) \xrightarrow{a} (1 + a^{\mu} \partial_{\mu})\psi(x), \quad (2.421)$$

$$\psi(x) \xrightarrow{\Lambda} (1 + \frac{i}{2} \omega^{\mu\nu} \sigma_{\mu\nu} - \omega^{\mu\nu} x_{\nu} \partial_{\mu})\psi(x). \quad (2.422)$$

And the generators are

$$p_{\mu} = i\partial_{\mu}, \quad (2.423)$$

$$J_{(\mu\nu)} = \sigma_{\mu\nu} + \frac{1}{i}(x_{\mu} \partial_{\nu} - x_{\nu} \partial_{\mu}). \quad (2.424)$$

For the translations we find

$$\varphi_r^+(\mathbf{p}) \xrightarrow{a} e^{-ipa} \varphi_r^+(\mathbf{p}), \quad (2.425)$$

$$\varphi_r^-(\mathbf{p}) \xrightarrow{a} e^{ipa} \varphi_r^-(\mathbf{p}), \quad (2.426)$$

which are the usual transformations laws, in the momentum representation, for the eigenstates of the momenta  $\mathbf{p}$  and  $-\mathbf{p}$  respectively.

For Lorentz transformations we find

$$\begin{aligned} \psi(x) &\xrightarrow{\Lambda} \sum_{r,r'=1}^2 \int d\Omega_{\mathbf{p}} \left[ \varphi_r^+(\mathbf{p}) \mathcal{R}(\Lambda, \mathbf{p})_{r'r} u(r', \Lambda \mathbf{p}) e^{-ip(\Lambda^{-1}x)} + \right. \\ &\quad \left. \varphi_r^-(\mathbf{p}) \mathcal{R}(\Lambda, \mathbf{p})_{r'r} v(r', \Lambda \mathbf{p}) e^{ip(\Lambda^{-1}x)} \right] \\ &= \sum_{r,r'=1}^2 \int d\Omega_{\mathbf{p}} \left[ \varphi_r^+(\Lambda^{-1}\mathbf{p}) \mathcal{R}(\Lambda, \Lambda^{-1}\mathbf{p})_{r'r} u(r', \mathbf{p}) e^{-ipx} + \right. \\ &\quad \left. \varphi_r^-(\Lambda^{-1}\mathbf{p}) \mathcal{R}(\Lambda, \Lambda^{-1}\mathbf{p})_{r'r} v(r', \mathbf{p}) e^{ipx} \right]. \end{aligned} \quad (2.427)$$

So the law of transformation on the functions  $\varphi^\pm$  is

$$\varphi_r^+(\mathbf{p}) \xrightarrow{\Lambda} \sum_{r'} \mathcal{R}(\Lambda, \Lambda^{-1}\mathbf{p})_{rr'} \varphi_r^+(\Lambda^{-1}\mathbf{p}), \quad (2.428)$$

$$\varphi_r^-(\mathbf{p}) \xrightarrow{\Lambda} \sum_{r'} \mathcal{R}(\Lambda, \Lambda^{-1}\mathbf{p})_{rr'} \varphi_r^-(\Lambda^{-1}\mathbf{p}). \quad (2.429)$$

This law of transformation is identical with the one constructed in Section 2.5.1. The generators can be found recalling that for rotations and velocity infinitesimal transformations we have

$$\mathcal{R}(\boldsymbol{\theta}) \approx 1 + i \frac{\boldsymbol{\sigma}}{2} \cdot \boldsymbol{\theta}, \quad (2.430)$$

$$\mathcal{R}(\boldsymbol{\alpha}) \approx 1 - i \frac{\boldsymbol{\sigma}}{2} \cdot \frac{\boldsymbol{\alpha} \wedge \mathbf{p}}{p^0 + m}. \quad (2.431)$$

The result is

$$\mathbf{J} = \frac{\boldsymbol{\sigma}}{2} - ip \wedge \frac{\partial}{\partial \mathbf{p}}, \quad (2.432)$$

$$\mathbf{K} = \frac{1}{2} \frac{\mathbf{p} \wedge \boldsymbol{\sigma}}{p^0 + m} + ip^0 \frac{\partial}{\partial \mathbf{p}}, \quad (2.433)$$

which coincides with the expressions (2.215) and (2.218).

Let us now write the scalar product in terms of the  $\psi(x)$ . Let  $\psi_a$  and  $\psi_b$  be two solutions of the Dirac equation. Then the quantity

$$J_{(a,b)}^\mu(x) = \bar{\psi}_b(x) \gamma^\mu \psi_a(x), \quad (2.434)$$

is conserved

$$\partial_\mu J_{(a,b)}^\mu(x) = 0, \quad (2.435)$$

as can easily be proved from the Dirac equation and recalling that  $\gamma^0 \gamma^0 = 1$  and  $\gamma^0 \gamma^\mu \gamma^0 = \gamma^{\mu\dagger}$ .  $J_{(a,b)}^\mu$  transforms as a four-vector under Lorentz transformations

$$\begin{aligned} J_{(a,b)}^\mu(x) &\xrightarrow{\Lambda} \bar{\psi}_b(\Lambda^{-1}x) S^{-1}(\Lambda) \gamma^\mu S(\Lambda) \psi_a(\Lambda^{-1}x) \\ &= (\Lambda^{-1})^\mu_\nu \bar{\psi}_b(\Lambda^{-1}x) \gamma^\nu \psi_a(\Lambda^{-1}x), \end{aligned} \quad (2.436)$$

where we used Eq. (2.357) and (2.374). The conservation law is thus covariant. Applying Gauss theorem as in the scalar case, the integral extended to any space-like surface with normal  $d\sigma^\mu$ ,

$$\int d\sigma_\mu J_{(a,b)}^\mu(x), \quad (2.437)$$

is independent from the chosen surface. Choosing a surface  $x^0 = \text{constant}$ , it is independent from  $x^0$ . We thus define

$$\langle a|b\rangle = \int dx \bar{\psi}_b(x, t)\gamma^0\psi_a(x, t) = \int dx \bar{\psi}_b(x, 0)\gamma^0\psi_a(x, 0). \quad (2.438)$$

Respect to this scalar product, since it is Lorentz invariant and clearly translational invariant, the transformations of Eqs. (2.421)-(2.422) are realized as unitary operators. It can be easily shown that their generators (2.423)-(2.424) are hermitian respect to this scalar product.

Using the equations

$$u^\dagger(r, p)u(s, p) = v^\dagger(r, p)v(s, p) = 2p^0\delta_{rs}, \quad (2.439)$$

$$u^\dagger(r, p)v(s, -p) = 0, \quad (2.440)$$

we obtain

$$\langle a|b\rangle = \int d\Omega_p \left[ \varphi_b^{+*}(p)\varphi_a^+(p) + \varphi_b^{-*}(p)\varphi_a^-(p) \right]. \quad (2.441)$$

So the scalar product coincides, in the two subspaces relative to positive and negative energies, with the scalar product originally introduced for the representation of the Poincaré group.

We have then realized, in a local way, a unitary irreducible representation of the Poincaré group, extended to the parity transformations, for particles of mass  $m$  and spin 1/2.

### 2.6.3 Particles of spin 1

The most simple Lorentz transformation which contains spin 1 is the  $(\frac{1}{2}, \frac{1}{2})$  representation, i.e the one of four-vectors. For this representation  $|s_z|$  can assume the values 0 and 1.

A local wave function  $W^\mu(x)$  transforms according to the law

$$W^\mu(x) \xrightarrow{\Lambda} \Lambda^\mu_\nu W^\nu(\Lambda^{-1}x). \quad (2.442)$$

For the state with definite momentum

$$W_p^\mu(x) = e^{-ipx}\varepsilon^\mu(r, p), \quad (2.443)$$

For the spin to be 1, in the rest frame the four-vector  $\varepsilon^\mu(p)$  must have only spatial components. This means

$$\varepsilon^\mu(r, p)p_\mu = 0. \quad (2.444)$$

Then in addition to the Klein-Gordon equation

$$(\square + m^2)W^\mu(x) = 0, \quad (2.445)$$

$W^\mu(x)$  must satisfy the constraint (2.444) which in coordinate representation translates into

$$\partial_\mu W^\mu(x) = 0. \quad (2.446)$$

The Eqs. (2.445) and (2.446) are equivalent to the system

$$G_{\mu\nu}(x) = \partial_\mu W_\nu(x) - \partial_\nu W_\mu(x), \quad (2.447)$$

$$\partial_\mu G^{\mu\nu}(x) - m^2 W^\nu(x) = 0. \quad (2.448)$$

In fact applying  $\partial_\nu$  to the second equation and using the antisymmetry of  $G_{\mu\nu}$  we find

$$m^2 \partial_\mu W^\mu(x) = 0, \quad (2.449)$$

which coincides with Eq. (2.446) when  $m \neq 0$ . On the other hand if  $\partial_\mu W^\mu(x) = 0$  the Eq. (2.448) coincides with (2.445).

The Eqs. (2.447) and (2.448) has both positive and negative energy solutions. The general solution is of the form

$$W^\mu(x) = \sum_{r=1}^3 \int d\Omega_p [W(r, p)\varepsilon^\mu(r, p)e^{-ipx} + \tilde{W}(r, p)\varepsilon^{\mu*}(r, p)e^{ipx}], \quad (2.450)$$

where  $\varepsilon_\mu(r, p)$  are independent vectors that obey to Eq. (2.444).

By construction such solution is an irreducible representation of the Poincaré group.

We can define a scalar product, exactly in the same way we did for the spin 0 case,

$$\langle a|b\rangle = -i \int d\sigma^\nu W_{a\mu}^*(x) \overset{\leftrightarrow}{\partial}_\nu W_b^\mu(x) \quad (2.451)$$

$$= - \int d\Omega_p W_{a\mu}^*(p) W_b^\mu(p), \quad (2.452)$$

where

$$W_{a\mu}(p) = \sum_{r=1}^3 W_a(r, p)\varepsilon_\mu(r, p). \quad (2.453)$$

Note that

$$\sum_{r=1}^3 \varepsilon_\mu(r, p)\varepsilon_\nu^*(r, p) = -g_{\mu\nu} + \frac{p_\mu p_\nu}{m^2}, \quad (2.454)$$

represents the density matrix for unpolarized states. The proof is straightforward in the rest frame. The covariance fixes the form in other frames.

Let us give, for completeness, an explicit representation of the base  $\varepsilon^\mu(r, p)$ . In the rest frame we can choose any three spatial orthonormal vectors. Let them be  $\boldsymbol{\varepsilon}(r, \mathbf{0})$ . For particles with momentum  $p$  we can define, according to Eq. (2.287),

$$\varepsilon^\mu(r, p) = S(\Lambda_p)\varepsilon(r, \mathbf{0}) = (\Lambda_p)^\mu_\nu \varepsilon^\nu(r, \mathbf{0}), \quad (2.455)$$

where we used the fact that  $\varepsilon^\mu$  transform as a four-vector. Using then the explicit expression (2.193) we have

$$\varepsilon^0(r, p) = \frac{p \cdot \boldsymbol{\varepsilon}(r, \mathbf{0})}{m}, \quad (2.456)$$

$$\boldsymbol{\varepsilon}(r, p) = \boldsymbol{\varepsilon}(r, \mathbf{0}) + p \frac{p \cdot \boldsymbol{\varepsilon}(r, \mathbf{0})}{m(p^0 + m)}. \quad (2.457)$$

The canonical base is the one where  $\varepsilon^i(r, \mathbf{0}) = \delta_{ir}$ . Choosing instead as a base the eigenstates of  $s_z$  we have

$$\boldsymbol{\varepsilon}(+1, \mathbf{0}) = -\frac{i}{\sqrt{2}}(e_x + ie_y), \quad (2.458)$$

$$\boldsymbol{\varepsilon}(0, \mathbf{0}) = ie_z, \quad (2.459)$$

$$\boldsymbol{\varepsilon}(-1, \mathbf{0}) = \frac{i}{\sqrt{2}}(e_x - ie_y), \quad (2.460)$$

where  $e_x, e_y, e_z$  are the versors of the axes.

In the vectorial case the Wigner matrix  $\mathcal{R}$  is defined by

$$\mathcal{R}(\Lambda)_{r'r}\varepsilon^\mu(r', \mathbf{p}) = \Lambda^\mu_\nu\varepsilon^\nu(r, \Lambda^{-1}\mathbf{p}). \quad (2.461)$$

## 2.7 The second quantization

It is an experimental fact that the number of particles may change in physical processes: An hydrogen atom in the state  $2P$  is composed by an electron and a proton and decays into an atom in its fundamental state plus a photon, an electron which pass through the Coulomb field of nucleus is accelerated and emit photons (Bremsstrahlung), when a positron annihilates with an electron their mass is converted in energy in the form of two photons, in the scattering between two high energy protons many pions are produced, .... Then, exist transitions between states with different number of particles. In Section 2.7.1 we will present a formalism that allows to describe systems of many free particles, used in any many-body theory, relativistic or not, and known as Fock method. It allows to describe many particles states with the correct statistics and to introduce operators that change the number of particles (creation and annihilation operators).

In Section 2.7.2 we will introduce the free field operators, and we will interpret in terms of field operators the negative energy solutions of the equations of free motion.

The relativistic equations of motion can be rederived in the Lagrangian formalism and it can be shown that the Fock second quantization is equivalent to the canonical quantization of a system of an infinite number of degrees of freedom.

The Lagrangian formalism is indispensable to write theories of non-free particles: In interaction.

### 2.7.1 Fock space

Let us consider an orthonormal complete base  $|i\rangle$  for the single particle states. For example the base  $|r, \mathbf{p}\rangle$  of the positive energy states for relativistic particles introduced in Section 2.6.

If the particles are bosons, in the state  $|i\rangle$  can coexist an arbitrary number  $n_i$  of free particles.

If the particles are fermions, in the state  $|i\rangle$  can exist at most one particle.

In both cases, assigning the occupation numbers  $\{n_i\}$  in the various states  $|i\rangle$  determines completely the state of the system, since the state must be symmetric for the bosons and completely antisymmetric for the fermions.

#### Bosons

For any state  $|i\rangle$  the observable number of particles in such state,  $n_i$ , has integer eigenvalues:  $1, 2, 3, \dots$

His spectrum is the one of an harmonic oscillator. As for the harmonic oscillator is possible to define a rising (creation) operator  $b_i^\dagger$  and a lowering (annihilation) operator  $b_i$  of the eigenvalue of  $n_i$ . The commutation properties are

$$[b_i, b_i^\dagger] = 1 \quad [b_i, b_i] = [b_i^\dagger, b_i^\dagger] = 0, \quad (2.462)$$

We then define  $n_i = b_i^\dagger b_i$  with

$$[n_i, b_i] = -b_i \quad [n_i, b_i^\dagger] = b_i^\dagger. \quad (2.463)$$

The lower state  $|0_i\rangle$  corresponds to zero particles in the state  $|i\rangle$  and  $b_i|0_i\rangle = 0$  with  $\langle 0_i|0_i\rangle = 1$ . The normalized state with  $n_i$  particles is then

$$\frac{(b_i^\dagger)^{n_i}}{\sqrt{n_i!}} |0_i\rangle = |n_i\rangle. \quad (2.464)$$

A state identified by the set of occupation numbers  $\{n_i\}$  in the different states  $|i\rangle$  can be written as

$$|n_{i_1}, \dots, n_{i_k}, \dots\rangle = \prod_{i_1} \frac{(b_{i_1}^\dagger)^{n_{i_1}}}{\sqrt{n_{i_1}!}} |0\rangle \quad (2.465)$$

where  $|0\rangle = \prod_i |0_i\rangle$  is the vacuum. It is automatically symmetric under particle exchange if

$$[b_i, b_k] = [b_i^\dagger, b_k^\dagger] = 0. \quad (2.466)$$

The “harmonic oscillators” correspondent to different modes are independent and we must also have

$$[b_i, b_k^\dagger] = \delta_{ik}. \quad (2.467)$$

The total number of particles is

$$N = \sum_i n_i = \sum_i b_i^\dagger b_i, \quad (2.468)$$

Moreover  $\langle 0|0\rangle = 1$ .

### Fermions

For the fermions the occupation number can be 0 or 1 and the state must be completely antisymmetric under particle exchange. This can be realized by associating to each single particle state an harmonic anti-oscillator, requiring anticommutation between operators relative to different modes

$$[b_i, b_k]_+ = [b_i^\dagger, b_k^\dagger]_+ = 0 \quad [b_i, b_k^\dagger]_+ = \delta_{ik}, \quad (2.469)$$

$$n_i = b_i^\dagger b_i \quad N = \sum_i n_i \quad b_i|0_i\rangle = 0, \quad (2.470)$$

$$[n_i, b_k] = -b_i \delta_{ik} \quad [n_i, b_k^\dagger] = b_i^\dagger \delta_{ik}. \quad (2.471)$$

The subscript + indicates the anticommutator. The possible states in the mode  $|i\rangle$  are  $|0_i\rangle$  and  $b_i^\dagger|0_i\rangle = |1_i\rangle$ .  $b_i^{\dagger 2}|0_i\rangle = 0$  because the operator  $b_i^\dagger$  anticommutes with itself. Moreover

$$b_i b_i^\dagger |0_i\rangle = (-b_i b_i^\dagger + 1) |0_i\rangle = |0_i\rangle. \quad (2.472)$$

### Observations

Given an operator  $O$  written in terms of creation and annihilation operators we will denote with  $:O:$  the normal ordered operator for bosons or the antinormal ordered operator for fermions. For bosons it is obtained from  $O$  displacing all creation operators to the left and all annihilation operators to the right and for fermions is is obtained from  $O$  displacing all creation operators to the left and all annihilation operators to the right times  $(-1)^n$ , with  $n$  the number of needed exchanges of a creation and an annihilation operator. For example for bosons  $:bb^\dagger: = b^\dagger b = bb^\dagger - 1$ . Normal ordering is not linear. For example  $:bb^\dagger: = :1 + b^\dagger b: = :1: + :b^\dagger b: = 1 + b^\dagger b \neq b^\dagger b$ . For fermions  $:bb^\dagger: = -b^\dagger b = bb^\dagger - 1$ . In particular we will always have  $\langle 0| :O: 0 \rangle = 0$  on the vacuum. We usually refer to the normal order as the Wick order.

The (anti)commutation relations are invariant under unitary changes of base. Let  $V$  be a unitary transformation from the base  $|1_i\rangle$  for the single particle states to the base  $|1_\alpha\rangle$

$$|1_\alpha\rangle = \sum_i V_{\alpha i} |1_i\rangle \quad |1_i\rangle = \sum_i V_{i\alpha}^\dagger |1_\alpha\rangle, \quad (2.473)$$

with  $VV^\dagger = V^\dagger V = 1$ . If  $|1_i\rangle = b_i^\dagger |0\rangle$  then  $|1_\alpha\rangle = \sum_i V_{\alpha i} b_i^\dagger |0\rangle$ . Defining

$$b_\alpha^\dagger = \sum_i V_{\alpha i} b_i^\dagger \quad b_\alpha = \sum_i V_{i\alpha}^* b_i, \quad (2.474)$$

we have

$$[b_\alpha, b_\beta]_\pm = [b_\alpha^\dagger, b_\beta^\dagger]_\pm = 0, \quad (2.475)$$

$$[b_\alpha, b_\beta^\dagger]_\pm = \sum_{ij} V_{\alpha i}^* V_{\beta j} [b_i, b_j^\dagger]_\pm = \sum_i V_{\alpha i}^* V_{\beta i} = (VV^\dagger)_{\beta\alpha} = \delta_{\alpha\beta}. \quad (2.476)$$

The vacuum remains unchanged.

If the index  $i$  that label the states is continuous, as for the momentum  $p$  in the base  $|r, p\rangle$  for free particles, the (anti)commutation rules must be modified replacing the  $\delta_{ik}$  in the Eqs. (2.467) and (2.469) the diagonal element of the identity matrix in the chosen representation. For the states  $|r, p\rangle$

$$[b(r, p), b(r', p')]_\pm = [b^\dagger(r, p), b^\dagger(r', p')]_\pm = 0, \quad (2.477)$$

$$[b(r, p), b^\dagger(r', p')]_\pm = \delta_{rr'} (2\pi)^3 2p^0 \delta(p - p'), \quad (2.478)$$

where  $\pm$  denotes the commutator or anticommutator. This choice give the correct states normalization. In fact

$$\langle r, p | r', p' \rangle = \langle 0 | b(r, p) b^\dagger(r', p') | 0 \rangle = \langle 0 | [b(r, p), b^\dagger(r', p')]_\pm | 0 \rangle = \delta_{rr'} (2\pi)^3 2p^0 \delta(p - p'). \quad (2.479)$$

The density of occupation number is  $b^\dagger(r, p)b(r, p)$  and the total number of particles is

$$N = \int d\Omega_p \sum_r b^\dagger(r, p) b(r, p). \quad (2.480)$$

The commutation rules for  $N$  are

$$[N, b(r, p)] = -b(r, p) \quad [N, b^\dagger(r, p)] = b^\dagger(r, p). \quad (2.481)$$

### 2.7.2 Field operators

Let

$$|s\rangle = \int d\Omega_p \sum_r \varphi_s(r, p) |r, p\rangle, \quad (2.482)$$

be any single particle state. It can be written as

$$|s\rangle = \int d\Omega_p \sum_r \varphi_s(r, p) b^\dagger(r, p) |0\rangle, \quad (2.483)$$

with

$$\langle r', p' | s \rangle = \langle 0 | b(r', p') s \rangle = \int d\Omega_p \sum_r \varphi_s(r, p) \langle 0 | b(r', p') b^\dagger(r, p) | 0 \rangle, \quad (2.484)$$

but

$$\langle 0 | b(r', p') b^\dagger(r, p) | 0 \rangle = \delta_{rr'} (2\pi)^3 2p^0 \delta(p - p'), \quad (2.485)$$

and so

$$\langle 0 | b(r', p') s \rangle = \varphi_s(r', p'). \quad (2.486)$$

The operator  $b(r, p)$  extracts from a state the component with momentum  $p$ . We can construct an operator which acts in the same way on the  $x$  space. For a particle of any spin let us consider the positive energy solutions and build the following operator

$$\varphi_+(x) = \int d\Omega_p \sum_r b(r, p) u(r, p) e^{-ipx}. \quad (2.487)$$

The operator  $\varphi_+(x)$  has the same number of components of the function  $u(r, p)$ : 1 for spin 0, 4 for spin 1/2 and 1. In any case from Eq. (2.487) follows

$$\langle 0 | \varphi_+(x) s \rangle = \int d\Omega_p \sum_r \varphi_s(r, p) u(r, p) e^{-ipx} = \varphi_s(x), \quad (2.488)$$

where  $\varphi_s(x)$  is the wave function of the state  $|s\rangle$ .

The operator  $\varphi_+(x)$  defined in Eq. (2.487) is called field operator or better the positive energy component of the field operator. The subscript + indicates that it contains only positive energies.

The operator  $\varphi_+(x)$  is a linear superposition of solutions  $u(r, p) e^{-ipx}$  with positive energy of the wave equation, so it is a solution with positive energy of the wave equation.

Let us give the explicit formulas for the field operator

$$\text{spin 0 } \varphi_+(x) = \int d\Omega_p b(p) e^{-ipx}, \quad (2.489)$$

$$\text{spin } \frac{1}{2} \psi_+(x) = \int d\Omega_p \sum_{r=1}^2 u(r, p) b(r, p) e^{-ipx}, \quad (2.490)$$

$$\text{spin 1 } W_+^\mu(x) = \int d\Omega_p \sum_{r=1}^3 \varepsilon^\mu(r, p) b(r, p) e^{-ipx}. \quad (2.491)$$

It is possible to invert these formulas using the expressions for the scalar products defined in the various cases (2.317), (2.438), and (2.451)

$$\text{spin 0} \quad b(\mathbf{p}) = i \int d\sigma^\mu e^{ipx} \overleftrightarrow{\partial}_\mu \varphi_+(x) = i \int dx e^{ipx} \overleftrightarrow{\partial}_0 \varphi_+(x), \quad (2.492)$$

$$\text{spin } \frac{1}{2} \quad b(r, \mathbf{p}) = \int dx u^\dagger(r, \mathbf{p}) e^{ipx} \psi_+(x), \quad (2.493)$$

$$\text{spin 1} \quad b(r, \mathbf{p}) = -i \int dx \varepsilon_\mu^*(r, \mathbf{p}) e^{ipx} \overleftrightarrow{\partial}_0 W_+^\mu(x). \quad (2.494)$$

All observables can be expressed in terms of  $b^\dagger(r, \mathbf{p})$  and  $b(r, \mathbf{p})$ . Then they can be expressed in terms of the fields and of their first derivatives for spin 0 and 1 particles, and in terms of the fields for spin 1/2 particles.

### 2.7.3 Transformation properties of the field operators

The invariance under a symmetry group implies the existence of a unitary representation of the group which send the Hilbert space into itself.

For a free particle the symmetry group is the Poincaré group and the representation is irreducible. We want now construct the representation of the group on the many free particles states.

Let  $U(\Lambda, a) = T_a U(\Lambda)$  be a transformation of the group with Lorentz matrix  $\Lambda$  and translation parameter  $a^\mu$ . On the single particle states we know that

$$U(\Lambda, a)|r, \mathbf{p}\rangle = e^{-i(\Lambda p)a} \mathcal{R}(\Lambda, \mathbf{p})_{r'r}|r', \Lambda \mathbf{p}\rangle, \quad (2.495)$$

where  $\mathcal{R}$  is a unitary matrix which represents the Wigner rotation. To construct the representation of the group in the Fock space we assume that the vacuum is invariant

$$U(\Lambda, a)|0\rangle = |0\rangle, \quad (2.496)$$

and we set

$$U(\Lambda, a)b^\dagger(r, \mathbf{p})U^\dagger(\Lambda, a) = e^{-i(\Lambda p)a} \mathcal{R}(\Lambda, \mathbf{p})_{r'r} b^\dagger(r', \Lambda \mathbf{p}). \quad (2.497)$$

This representation realizes the (2.495) and transforms independently the many particles states. For the annihilation operator we will then have

$$U(\Lambda, a)b(r, \mathbf{p})U^\dagger(\Lambda, a) = e^{i(\Lambda p)a} \mathcal{R}(\Lambda, \mathbf{p})_{rr'}^* b(r', \Lambda \mathbf{p}). \quad (2.498)$$

We define the transformed of  $b(r, \mathbf{p})$  as follows <sup>4</sup>

$$b(r, \mathbf{p}) \rightarrow U^\dagger(\Lambda, a)b(r, \mathbf{p})U(\Lambda, a). \quad (2.500)$$

From Eq. (2.498), recalling that

$$U^{-1}(\Lambda, a) = U(\Lambda^{-1}, -\Lambda^{-1}a), \quad (2.501)$$

---

<sup>4</sup>Note that here we must define the transformed operator using the inverse transformation respect to the one that applies to regular observables for which the measure in the two reference frames must coincide. In fact

$$\varphi_s(r, \mathbf{p}) = \langle 0|bs \rangle \rightarrow \langle 0|U^\dagger bUs \rangle \equiv \langle 0|b's \rangle, \quad (2.499)$$

where  $b'$  is the transformed operator and in the last equation we used the fact that  $U|0\rangle = |0\rangle$  and  $U|s\rangle = |s'\rangle$ .

we find

$$U^\dagger(\Lambda, a)b(r, p)U(\Lambda, a) = e^{-ipa}\mathcal{R}(\Lambda, \Lambda^{-1}p)_{rr'}b(r', \Lambda^{-1}p), \quad (2.502)$$

$$U^\dagger(\Lambda, a)b^\dagger(r, p)U(\Lambda, a) = e^{ipa}\mathcal{R}(\Lambda, \Lambda^{-1}p)_{rr'}^*b(r', \Lambda^{-1}p). \quad (2.503)$$

$$(2.504)$$

To derive Eq. (2.502) we used

$$\mathcal{R}(\Lambda^{-1}, p)_{rr'}^* = \mathcal{R}(\Lambda^{-1}, p)_{rr'}^\dagger, \quad (2.505)$$

and

$$\mathcal{R}(\Lambda^{-1}, p)_{rr'}^\dagger = \mathcal{R}(\Lambda, \Lambda^{-1}p)_{rr'}. \quad (2.506)$$

Eq. (2.506) can be derived observing that  $\mathcal{R}$  is unitary, that

$$|r, p\rangle = U(\Lambda)U^\dagger(\Lambda)|r, p\rangle = U(\Lambda)\mathcal{R}(\Lambda^{-1}, p)_{rr'}|r', \Lambda^{-1}p\rangle \quad (2.507)$$

$$= \mathcal{R}(\Lambda, \Lambda^{-1}p)_{rr'}\mathcal{R}(\Lambda^{-1}, p)_{rr'}|r'', p\rangle, \quad (2.508)$$

and that  $|r, p\rangle$  is a complete base at fixed  $p$ . Since the transformation (2.502) is unitary in Fock space it leaves unchanged the commutation relations.

The generators of the unitary transformation  $U(\Lambda, a)$  can be explicitly constructed as hermitian operators on Fock space. For infinitesimal transformations

$$U(\Lambda, a) \approx 1 - ip_\mu a^\mu + i\boldsymbol{\theta} \cdot \mathbf{J} - i\boldsymbol{\alpha} \cdot \mathbf{K}. \quad (2.509)$$

We recall that for infinitesimal rotations

$$\mathcal{R}(\Lambda)_{rr'} \approx \delta_{rr'} + i\boldsymbol{\theta} \cdot \mathbf{s}_{rr'}, \quad (2.510)$$

$$b(r, \Lambda^{-1}p) \approx b(r, p + \boldsymbol{\theta} \wedge p) \approx b(r, p) + \boldsymbol{\theta} \cdot \left( p \wedge \frac{\partial}{\partial p} \right) b(r, p), \quad (2.511)$$

and for infinitesimal velocity transformations

$$\mathcal{R}(\Lambda)_{rr'} \approx \delta_{rr'} - i\frac{\boldsymbol{\alpha} \wedge p}{p^0 + m} \cdot \mathbf{s}_{rr'}, \quad (2.512)$$

$$b(r, \Lambda^{-1}p) \approx b(r, p + \boldsymbol{\alpha} p^0) \approx b(r, p) + \boldsymbol{\alpha} \cdot p^0 \frac{\partial}{\partial p} b(r, p). \quad (2.513)$$

Using Eqs. (2.502) and (2.509) we derive the commutation relations for the generators

$$[p_\mu, b(r, p)] = -p_\mu b(r, p), \quad (2.514)$$

$$[\mathbf{J}, b(r, p)] = -\left( s - ip \wedge \frac{\partial}{\partial p} \right)_{rr'} b(r', p), \quad (2.515)$$

$$[\mathbf{K}, b(r, p)] = -\left( \frac{\mathbf{p} \wedge \mathbf{s}}{p^0 + m} + ip^0 \frac{\partial}{\partial p} \right)_{rr'} b(r', p). \quad (2.516)$$

Taking the hermitian conjugate and recalling that the  $s$  matrices are hermitian we find

$$[p_\mu, b^\dagger(r, p)] = p_\mu b^\dagger(r, p), \quad (2.517)$$

$$[\mathbf{J}, b^\dagger(r, p)] = \left( s + ip \wedge \frac{\partial}{\partial p} \right)_{r'r} b^\dagger(r', p), \quad (2.518)$$

$$[\mathbf{K}, b^\dagger(r, p)] = \left( \frac{\mathbf{p} \wedge \mathbf{s}}{p^0 + m} - ip^0 \frac{\partial}{\partial p} \right)_{r'r} b^\dagger(r', p). \quad (2.519)$$

It is possible to give an explicit representation for the operators  $p_\mu$ ,  $J$ , and  $K$  in terms of the operators  $b$  and  $b^\dagger$

$$p_\mu = \int d\Omega_p \sum_r b^\dagger(r, p) p_\mu b(r, p), \quad (2.520)$$

$$J = \int d\Omega_p \sum_r b^\dagger(r, p) \left( s - ip \wedge \frac{\partial}{\partial p} \right)_{rr'} b(r, p), \quad (2.521)$$

$$K = \int d\Omega_p \sum_r b^\dagger(r, p) \left( \frac{p \wedge s}{p^0 + m} + ip^0 \frac{\partial}{\partial p} \right)_{rr'} b(r, p), \quad (2.522)$$

so that these operators satisfy the commutation rules (2.514)-(2.516).

Let us now treat the transformation properties of the field operator. The Eq. (2.502) induces the following transformation

$$U^\dagger(\Lambda, a)\varphi_+(x)U(\Lambda, a) = \int d\Omega_p e^{-ipx} \sum_r u(r, p) e^{-ipa} \mathcal{R}(\Lambda, \Lambda^{-1}p)_{rr'} b(r', \Lambda^{-1}p). \quad (2.523)$$

Changing variables  $p \rightarrow \Lambda p$  and using Eq. (2.417) we find

$$\varphi'_+(x) \equiv U^\dagger(\Lambda, a)\varphi_+(x)U(\Lambda, a) = S(\Lambda)\varphi_+(\Lambda^{-1}x + \Lambda^{-1}a), \quad (2.524)$$

which is the correct transformation law for a local operator<sup>5</sup>. Indicating with  $x'$  the transformed event we can also write

$$\varphi'_+(x') = U^\dagger\varphi_+(x')U = S(\Lambda)\varphi_+(x). \quad (2.525)$$

This equation allows to write down immediately the action of the generators of the Poincaré group on the field operators. Denoting with  $J_{(\mu\nu)}$  and  $p_\mu$  the generators in the Fock space

$$U(T_a) = e^{-ia^\mu p_\mu} \quad U(\Lambda) = e^{\frac{i}{2}\omega^{\mu\nu} J_{(\mu\nu)}}, \quad (2.526)$$

and with  $\sigma_{\mu\nu}$  the generator of the group in the representation under which  $\varphi$  transforms, i.e. the generator of the  $S(\Lambda)$  matrix, from Eq. (2.524) follows

$$[p_\mu, \varphi_+(x)] = -i\partial_\mu \varphi_+(x), \quad (2.527)$$

$$[J_{(\mu\nu)}, \varphi_+(x)] = -[\sigma_{\mu\nu} - i(x_\mu \partial_\nu - x_\nu \partial_\mu)] \varphi_+(x), \quad (2.528)$$

as follows from Eqs. (2.423) and (2.424).

#### 2.7.4 Locality and spin-statistics theorem

In constructing the relativistic theory it is necessary to deal with local operators commuting at spacelike distances. In fact, since a signal can not propagate at speeds higher than that of light, measures occurred at spatial distances must not influence each other. As observed in Section 2.7.2 all observables can be written in terms of fields and their first derivatives. If the (anti)commutators between these quantities are zero for spacelike distances it will be possible to construct a theory that satisfies causality.

---

<sup>5</sup>We recall that  $(\Lambda, a)^{-1}x = (T_a\Lambda)^{-1}x = \Lambda^{-1}T_{-a}x = \Lambda^{-1}x + \Lambda^{-1}a$ .

From the commutators between the operators  $b(r, p)$  and  $b^\dagger(r, p)$  we can easily calculate the commutators between the fields and their derivatives. Let us consider first the scalar field

$$[\varphi_+(x), \varphi_+(y)] = 0, \quad (2.529)$$

$$[\varphi_+(x), \varphi_+^\dagger(y)] = F_+(x - y), \quad (2.530)$$

$$[\varphi_+(x), \partial_0 \varphi_+^\dagger(y)] = \frac{\partial}{\partial y^0} F_+(x - y), \quad (2.531)$$

where Eq. (2.531) follows from Eq. (2.530).

The function  $F_+$  is invariant under translations and under Lorentz transformations. It is in fact a c-number, i.e. as an operator in the Fock space it is proportional to the identity, because such is  $[b(r, p), b^\dagger(r, p)]$ . From Eq. (2.530) follows that

$$U^\dagger(\Lambda, a)[\varphi_+(x), \varphi_+^\dagger(x)]U(\Lambda, a) = F_+(x - y)U^\dagger(\Lambda, a)U(\Lambda, a) = F_+(x - y). \quad (2.532)$$

But the first member is also equal to

$$[\varphi_+(\Lambda^{-1}(x + a)), \varphi_+^\dagger(\Lambda^{-1}(x + a))] = F_+(\Lambda^{-1}(x - y)), \quad (2.533)$$

and this proves the invariance of  $F_+$  under the Poincaré group.

Explicitly we have

$$F_+(x - y) = \int d\Omega_p e^{-ip(x-y)}. \quad (2.534)$$

If  $x$  and  $y$  are at spacelike distances it is always possible to bring them to be simultaneous ( $x^0 = y^0$ ) through a Lorentz transformation. To study the behavior of  $F_+$  at spacelike distances it is sufficient to study it at equal times ( $x^0 = y^0$ ). We then have

$$F_+(0, x - y) = \int d\Omega_p e^{ip \cdot (x-y)}, \quad (2.535)$$

$$\left. \frac{\partial}{\partial y^0} F_+(x^0 - y^0, x - y) \right|_{y^0=x^0} = \frac{i}{2} \int \frac{dp}{(2\pi)^3} e^{ip \cdot (x-y)} = \frac{i}{2} \delta(x - y). \quad (2.536)$$

The integral in Eq. (2.535) can be easily calculated in terms of Bessel functions

$$F_+(0, x - y) = \frac{m}{(2\pi)^2 |x - y|} K_0(m|x - y|). \quad (2.537)$$

$F_+$  is different from zero at spacelike distances of the order of the Compton wavelength of the particle ( $\ell = h/mc$ ). So a theory constructed in terms of just the  $\varphi_+$  is non local.

But we remember that next to the positive energy solutions exist the “negative energy” solutions of the Klein-Gordon equation. In the Fock space context a dependence of the kind  $e^{ipx}$  is associated to a creation operator, rather than to a destruction operator as in the expansion for  $\varphi_+$ . While considering the negative energy solutions is then natural to introduce a “negative frequency” field

$$\varphi_-(x) = \int d\Omega_p e^{ipx} d^\dagger(p). \quad (2.538)$$

The operators  $d^\dagger(p)$  and  $d(p)$  are operator independent from  $b^\dagger(p)$  and  $b(p)$ , i.e. they describe a different particle, and so they commute with them.

Let us now construct the field

$$\varphi(x) = \varphi_+(x) + \varphi_-(x), \quad (2.539)$$

or

$$\varphi(x) = \int d\Omega_p [d(p)e^{-ipx} + d^\dagger(p)e^{ipx}], \quad (2.540)$$

$$\varphi^\dagger(x) = \int d\Omega_p [d^\dagger(p)e^{ipx} + d(p)e^{-ipx}]. \quad (2.541)$$

$$(2.542)$$

The commutators now becomes

$$[\varphi(x), \varphi(y)] = [\varphi^\dagger(x), \varphi^\dagger(y)] = 0, \quad (2.543)$$

$$[\varphi(x), \varphi^\dagger(y)] = F_+(x-y) - F_+(y-x), \quad (2.544)$$

$$[\varphi(x), \partial_0 \varphi^\dagger(y)] = \frac{\partial}{\partial y^0} [F_+(x-y) - F_+(y-x)]. \quad (2.545)$$

At equal times, at spacelike distances, we have

$$[\varphi(x^0, x), \varphi^\dagger(x^0, y)] = 0, \quad (2.546)$$

$$[\varphi(x^0, x), \partial_0 \varphi^\dagger(x^0, y)] = i\delta(x-y). \quad (2.547)$$

The theory is now *local*.

We note that the minus sign in the Eqs. (2.544) and (2.545) depends by the choice of commutation relation: The locality in Eqs. (2.546) and (2.547) would have been destroyed if we would have chosen the Fermi statistics. This is a manifestation of the so called *spin-statistics theorem*.

We note that since  $\varphi(x)$  is a superposition of solutions of the Klein-Gordon equation it itself satisfies to such equation

$$(\square + m^2)\varphi(x) = 0. \quad (2.548)$$

Note that since  $b(p) \neq d(p)$  the scalar field is not hermitian. This is also called a *charged* scalar field. The hermitian field is called *neutral*. The particle described by the creation operator  $d^\dagger$  is called *antiparticle*.

Let us now treat the spin 1/2 case. For the Dirac field,

$$\psi_+(x) = \int d\Omega_p \sum_r u(r, p)b(r, p)e^{-ipx}, \quad (2.549)$$

we have

$$\begin{aligned} [\psi_+^\alpha(x), \psi_+^\beta(y)]_+ &= \int d\Omega_p \sum_r u^\alpha(r, p)u^\beta(r, p)e^{-ip(x-y)} \\ &= \int d\Omega_p [(\not{p} + m)\gamma^0]^{\alpha\beta} e^{-ip(x-y)}, \end{aligned} \quad (2.550)$$

where we used the anticommutation relations for the  $b, b^\dagger$  and we used the Eq. (2.404) for the projector on the positive energies states.

Omitting the indexes  $\alpha, \beta$  and using the anticommutation rules of the  $\gamma$  matrices we can then write

$$[\psi_+(x), \psi_+^\dagger(y)]_+ = \left( i \frac{\partial}{\partial x^0} + m\gamma^0 + i\gamma^0 \boldsymbol{\gamma} \cdot \boldsymbol{\nabla} \right) F_+(x - y), \quad (2.551)$$

where  $F_+$  is again given by Eq. (2.535). At equal times

$$[\psi_+(x^0, x), \psi_+^\dagger(x^0, y)]_+ = \frac{i}{2} \delta(\mathbf{x} - \mathbf{y}) + (m\gamma^0 + i\gamma^0 \boldsymbol{\gamma} \cdot \boldsymbol{\nabla}) F_+(\mathbf{x} - \mathbf{y}), \quad (2.552)$$

which is non-local.

In analogy to what we did in the scalar case we introduce

$$\psi_-(x) = \int d\Omega_{\mathbf{p}} \sum_r v(r, \mathbf{p}) b^\dagger(r, \mathbf{p}) e^{ipx}, \quad (2.553)$$

where  $d^\dagger$  is the creation operator for a new particle

$$[d(r, \mathbf{p}), d^\dagger(r', \mathbf{p}')]_+ = \delta_{rr'} 2p^0 (2\pi)^3 \delta(\mathbf{p} - \mathbf{p}'), \quad (2.554)$$

$$[d, d]_+ = [d^\dagger, d^\dagger]_+ = [b, d]_+ = [b, d^\dagger]_+ = [b^\dagger, d]_+ = [b^\dagger, d^\dagger]_+ 0, \quad (2.555)$$

and

$$\psi(x) = \psi_+(x) + \psi_-(x) = \int d\Omega_{\mathbf{p}} \sum_r [u(r, \mathbf{p}) b(r, \mathbf{p}) e^{-ipx} + v(r, \mathbf{p}) d^\dagger(r, \mathbf{p}) e^{ipx}], \quad (2.556)$$

$$\psi^\dagger(x) = \int d\Omega_{\mathbf{p}} \sum_r [u^\dagger(r, \mathbf{p}) b^\dagger(r, \mathbf{p}) e^{ipx} + v^\dagger(r, \mathbf{p}) d(r, \mathbf{p}) e^{-ipx}]. \quad (2.557)$$

Then

$$[\psi(x), \psi(y)]_+ = [\psi^\dagger(x), \psi^\dagger(y)]_+ = 0, \quad (2.558)$$

$$\begin{aligned} [\psi(x), \psi^\dagger(y)]_+ &= \int d\Omega_{\mathbf{p}} \left[ (\not{p} + m) \gamma^0 e^{-ip(x-y)} + (\not{p} - m) \gamma^0 e^{ip(x-y)} \right] \\ &= \int d\Omega_{\mathbf{p}} \left[ \left( i\gamma^\mu \frac{\partial}{\partial x^\mu} + m \right) \gamma^0 e^{-ip(x-y)} + \left( i\gamma^\mu \frac{\partial}{\partial y^\mu} - m \right) \gamma^0 e^{ip(x-y)} \right] \\ &= \left( i\gamma^\mu \frac{\partial}{\partial x^\mu} + m \right) \gamma^0 [F_+(x - y) - F_+(y - x)]. \end{aligned} \quad (2.559)$$

At equal times, using  $\gamma^0 \gamma^0 = 1$ , we find

$$[\psi(x^0, x), \psi^\dagger(x^0, y)]_+ = i\delta(\mathbf{x} - \mathbf{y}), \quad (2.560)$$

which is again local. Again we must notice that in order to have Eq. (2.560) in a local form it was essential to choose the anticommutators. The commutator would have brought a minus sign for the  $vv^\dagger$  term in Eq. (2.559) and to a non-local result. This is a manifestation of the spin-statistic theorem.

Since  $\psi$  is a linear superposition of Dirac equation solutions, it itself is a solution of the Dirac equation

$$(i\not{\partial} - m)\psi(x) = 0. \quad (2.561)$$

Let us conclude with the case of a massive vectorial field. The analysis is identical to the scalar case. For a vectorial field we define

$$W_\mu(x) = \int d\Omega_p \sum_{r=1}^3 [\varepsilon_\mu(r, p)b(r, p)e^{-ipx} + \varepsilon_\mu^*(r, p)d^\dagger(r, p)e^{ipx}], \quad (2.562)$$

$$W_\mu^\dagger(x) = \int d\Omega_p \sum_{r=1}^3 [\varepsilon_\mu^*(r, p)b^\dagger(r, p)e^{ipx} + \varepsilon_\mu(r, p)d(r, p)e^{-ipx}]. \quad (2.563)$$

The commutation rules can be easily derived recalling Eq. (2.454)

$$[W_\mu(x), W_\nu^\dagger(y)] = - \left( g_{\mu\nu} + \frac{1}{m^2} \frac{\partial}{\partial x^\mu} \frac{\partial}{\partial x^\nu} \right) [F_+(x-y) - F_+(y-x)], \quad (2.564)$$

$$[W_\mu(x^0, x), W_\nu^\dagger(x^0, y)] = - \frac{i}{2m^2} [g_{\mu 0} \partial_\nu + g_{0\nu} \partial_\mu] \delta(x-y), \quad (2.565)$$

$$[W_\mu(x^0, x), \partial_0 W_\nu^\dagger(x^0, y)] = - \left( g_{\mu\nu} + \frac{\partial_\mu \partial_\nu}{m^2} \right) i \delta(x-y). \quad (2.566)$$

Also in this case the use of the Bose statistics has been essential for the locality of (2.565). Again this is a manifestation of the spin-statistics theorem.

The vectorial field  $W_\mu$  will satisfy to the following system of equations

$$(\square + m^2) W^\mu(x) = 0, \quad (2.567)$$

$$\partial_\mu W^\mu = 0 \quad (2.568)$$

The spin-statistics theorem states that, as a consequence of Lorentz invariance and of locality, half integer spin particles must obey to Fermi statistics and integer spin particles must obey to Bose statistics.

As we saw in the various cases, the introduction of the negative energy solutions does not interfere with the Lorentz structure of the fields. Since the commutation rules of the operators  $b$  and  $d$  are identical we can write the action of the group on the whole Fock space generated by  $b^\dagger$  and  $d^\dagger$ . In particular the generators are given by

$$p_\mu = \int d\Omega_p \sum_r [b^\dagger(r, p)p_\mu b(r, p) + d^\dagger(r, p)p_\mu d(r, p)], \quad (2.569)$$

$$\begin{aligned} J &= \int d\Omega_p \sum_r \left[ b^\dagger(r, p) \left( s - ip \wedge \frac{\partial}{\partial p} \right)_{rr'} b(r, p) + \right. \\ &\quad \left. d^\dagger(r, p) \left( s - ip \wedge \frac{\partial}{\partial p} \right)_{rr'} d(r, p) \right], \end{aligned} \quad (2.570)$$

$$\begin{aligned} K &= \int d\Omega_p \sum_r \left[ b^\dagger(r, p) \left( \frac{\mathbf{p} \wedge s}{p^0 + m} + ip^0 \frac{\partial}{\partial p} \right)_{rr'} b(r, p) + \right. \\ &\quad \left. d^\dagger(r, p) \left( \frac{\mathbf{p} \wedge s}{p^0 + m} + ip^0 \frac{\partial}{\partial p} \right)_{rr'} d(r, p) \right], \end{aligned} \quad (2.571)$$

as can be inferred by Eqs. (2.520)-(2.522).

On the field operators Eqs. (2.527) and (2.528) now give

$$[p_\mu, \varphi(x)] = -i\partial_\mu \varphi(x), \quad (2.572)$$

$$[J_{(\mu\nu)}, \varphi(x)] = -[\sigma_{\mu\nu} - i(x_\mu \partial_\nu - x_\nu \partial_\mu)] \varphi(x), \quad (2.573)$$

From the point of view of the Poincaré group it is evident from the construction and from the generators (2.569)-(2.571) that the antiparticle states are identical to the particle ones: they describe a system of free particles of mass  $m$ .

# Appendices



## Appendix B

# Commutators

The commutator of two operators  $A$  and  $B$  is defined as

$$[A, B] = AB - BA. \quad (\text{B.1})$$

The commutator satisfies to the following Lie algebra relations

$$[A, A] = 0, \quad (\text{B.2})$$

$$[A, B] = -[B, A], \quad (\text{B.3})$$

$$[A, [B, C]] + [B, [C, A]] + [C, [A, B]] = 0, \quad (\text{B.4})$$

where the third one is known as the Jacobi identity.

For three operators  $A, B$ , and  $C$  we also have

$$[A, B + C] = [A, B] + [A, C], \quad (\text{B.5})$$

$$[A, BC] = B[A, C] + [A, B]C. \quad (\text{B.6})$$

If  $[A, B] = \alpha \in \mathbb{C}$  then

$$[A, B^2] = B[A, B] + [A, B]B = 2\alpha B, \quad (\text{B.7})$$

$$[A, B^3] = B[A, B^2] + [A, B]B^2 = 3\alpha B^2, \quad (\text{B.8})$$

$$\dots \\ [A, B^n] = n\alpha B^{n-1}. \quad (\text{B.9})$$

Then, given a smooth function  $f$ , using its Taylor series expansion, we readily obtain

$$[A, f(B)] = \alpha \frac{df(B)}{dB}. \quad (\text{B.10})$$

In general we can prove the following lemma:

**Hadamard lemma:** Given any two operators  $A$  and  $B$  we have

$$e^A B e^{-A} = B + [A, B] + \frac{1}{2!}[A, [A, B]] + \frac{1}{3!}[A, [A, [A, B]]] + \dots \quad (\text{B.11})$$

**Proof:** Consider the function  $f(s) = e^{sA} B e^{-sA}$ . We want  $f(1)$ . Taylor expand  $f(s)$  around  $s = 0$

$$f(s) = f(0) + sf'(0) + \frac{1}{2!}s^2f''(0) + \frac{1}{3!}s^3f'''(0) + \dots, \quad (\text{B.12})$$

but it is easy to see that

$$f'(s) = e^{sA} ABe^{-sA} - e^{sA} B A e^{-sA} = e^{sA} [A, B] e^{-sA}, \quad (\text{B.13})$$

$$f''(s) = e^{sA} [A, [A, B]] e^{-sA}, \quad (\text{B.14})$$

$$f'''(s) = e^{sA} [A, [A, [A, B]]] e^{-sA}, \quad (\text{B.15})$$

and so on.

Another important result is the Baker–Campbell–Hausdorff formula:

**Baker–Campbell–Hausdorff formula:** Given any two operators  $A$  and  $B$  we have

$$\ln(e^A e^B) = A + B + \frac{1}{2}[A, B] + \frac{1}{12}([A, [A, B]] + [B, [B, A]]) - \frac{1}{24}[B, [A, [A, B]]] + \dots \quad (\text{B.16})$$

**Proof:** Consider

$$\frac{1}{1-x} = 1 + x + x^2 + x^3 + \dots \quad (\text{B.17})$$

or

$$\frac{1}{1+x} = 1 - x + x^2 - x^3 + \dots \quad (\text{B.18})$$

integrate respect to  $x$

$$\ln(1+x) = x - \frac{1}{2}x^2 + \frac{1}{3}x^3 - \frac{1}{4}x^4 + \dots \quad (\text{B.19})$$

or

$$\ln(x) = (x-1) - \frac{1}{2}(x-1)^2 + \frac{1}{3}(x-1)^3 - \frac{1}{4}(x-1)^4 + \dots \quad (\text{B.20})$$

Now

$$\begin{aligned} \ln(e^A e^B) &= \sum_{k=1} \frac{(-1)^{k-1}}{k} \left( \sum_{m,n=0} \frac{A^m B^n}{m!n!} - 1 \right)^k \\ &= \left( A + B + AB + \frac{A^2 + B^2}{2} \dots \right) - \frac{1}{2} (A^2 + B^2 + AB + BA \dots) + \dots \\ &= A + B + \frac{1}{2}[A, B] + \dots \end{aligned} \quad (\text{B.21})$$

Commutators are of fundamental importance in a *Lie algebra*: a vector space  $\mathfrak{g}$  together with an operation called the Lie bracket, an alternating bilinear map  $\mathfrak{g} \times \mathfrak{g} \rightarrow \mathfrak{g}$ , that satisfies the Jacobi identity. In other words, a Lie algebra is an algebra over a field for which the multiplication operation (called the Lie bracket) is alternating and satisfies the Jacobi identity. The Lie bracket of two vectors  $x$  and  $y$  is denoted  $[x, y]$ . A Lie algebra is typically a non-associative algebra. However, every associative algebra gives rise to a Lie algebra, consisting of the same vector space with the commutator Lie bracket,  $[x, y] = xy - yx$ .

*Lie groups* are smooth differentiable manifolds and as such can be studied using differential calculus, in contrast with the case of more general topological groups. One of the key ideas in the theory of Lie groups is to replace the global object, the group, with its local or linearized version, which Lie himself called its “infinitesimal group” and which has since become known as its Lie algebra or the tangent space to the manifold at the identity.

The following theorem is also of great importance:

**Theorem:** Given two hermitian operators  $A$  and  $B$  which commutes,  $[A, B] = 0$ , they can be diagonalized simultaneously on the same orthonormal base of vectors of the Hilbert space.

## Appendix C

# The Levi-Civita symbol

The Levi-Civita symbol  $\epsilon_{i_1 i_2 \dots i_n}$  is defined as a total antisymmetric  $n$  rank tensor with  $\epsilon_{012\dots n} = 1$ .

In two dimensions

$$\epsilon_{ij}\epsilon_{ik} = \delta_{jk}, \quad (C.1)$$

$$\epsilon_{ij}\epsilon_{ij} = 2, \quad (C.2)$$

where in the first equation we contracted one index and in the second equation we contracted both indexes.

In three dimensions

$$\epsilon_{ijk}\epsilon_{ilm} = \delta_{jl}\delta_{km} - \delta_{jm}\delta_{kl}, \quad (C.3)$$

$$\epsilon_{ijk}\epsilon_{ijl} = 3\delta_{kl} - \delta_{kl} = 2\delta_{kl}, \quad (C.4)$$

$$\epsilon_{ijk}\epsilon_{ijk} = 6. \quad (C.5)$$

In general

$$\epsilon_{i_1 i_2 \dots i_n} \epsilon_{j_1 j_2 \dots j_n} = \det \begin{pmatrix} \delta_{i_1 j_1} & \cdots & \delta_{i_1 j_n} \\ \vdots & \ddots & \\ \delta_{i_n j_1} & & \delta_{i_n j_n} \end{pmatrix}. \quad (C.6)$$

Also for an  $n \times n$  matrix  $\mathbf{A}$  with  $(\mathbf{A})_{ij} = a_{ij}$  we have

$$\det(\mathbf{A}) = \epsilon_{i_1 i_2 \dots i_n} a_{1i_1} a_{2i_2} \dots a_{ni_n}, \quad (C.7)$$

$$\det(\mathbf{A}) \epsilon_{j_1 j_2 \dots j_n} = \epsilon_{i_1 i_2 \dots i_n} a_{i_1 j_1} a_{i_2 j_2} \dots a_{i_n j_n}. \quad (C.8)$$



## Appendix D

# Angular momentum

Consider the angular momentum hermitian operator  $\hat{\mathbf{L}}$ , where the hat denotes the operator. Then the following commutation relations hold

$$[\hat{L}_i, \hat{L}_j] = i\epsilon_{ijk}\hat{L}_k. \quad (\text{D.1})$$

Then define

$$\hat{L}^2 = \sum_{i=1}^3 \hat{L}_i^2, \quad (\text{D.2})$$

$$\hat{L}_\pm = \hat{L}_1 \pm i\hat{L}_2. \quad (\text{D.3})$$

We can then prove the following relations

$$[\hat{L}^2, \hat{L}_i] = 0, \quad (\text{D.4})$$

$$[\hat{L}_+, \hat{L}_-] = 2\hat{L}_3, \quad (\text{D.5})$$

$$[\hat{L}_3, \hat{L}_\pm] = \pm \hat{L}_\pm, \quad (\text{D.6})$$

and

$$\hat{L}^2 = \hat{L}_+ \hat{L}_- + \hat{L}_3^2 - \hat{L}_3 = \hat{L}_- \hat{L}_+ + \hat{L}_3^2 + \hat{L}_3 \quad (\text{D.7})$$

Since  $\hat{L}^2$  commutes with  $\hat{L}_3$  we can diagonalize them simultaneously so that

$$\hat{L}^2 |\psi_{L,M}\rangle = \mathcal{L}^2 |\psi_{L,M}\rangle, \quad (\text{D.8})$$

$$\hat{L}_3 |\psi_{L,M}\rangle = M |\psi_{L,M}\rangle, \quad (\text{D.9})$$

where, since  $\hat{L}^2 - \hat{L}_3^2 = \hat{L}_1^2 + \hat{L}_2^2$ , we called  $L$  the maximum value of  $|M|$  for a given value  $\mathcal{L}$ . Then

$$\hat{L}_3 \hat{L}_\pm |\psi_{L,M}\rangle = (M \pm 1) \hat{L}_\pm |\psi_{L,M}\rangle, \quad (\text{D.10})$$

$$\hat{L}_+ |\psi_{L,L}\rangle = 0. \quad (\text{D.11})$$

From Eq. (D.7) follows

$$0 = \hat{L}_- \hat{L}_+ |\psi_{L,L}\rangle = (\hat{L}^2 - \hat{L}_3^2 - \hat{L}_3) |\psi_{L,L}\rangle, \quad (\text{D.12})$$

or  $\mathcal{L}^2 = L(L + 1)$ . Also  $M$  can assume  $2L + 1$  values, namely  $M = L, L - 1, \dots, -L$ . And  $2L = 0, 1, 2, 3, \dots$

For the orbital angular momentum  $\hat{\mathbf{L}} = \hat{\mathbf{r}} \wedge \hat{\mathbf{p}}$ . In the coordinate representation  $\hat{\mathbf{r}} = \mathbf{r}$  and  $\hat{\mathbf{p}} = -i\boldsymbol{\nabla}_r$ . From the commutation relations for position and momentum

$$[\hat{r}_i, \hat{r}_j] = 0, \quad (\text{D.13})$$

$$[\hat{p}_i, \hat{p}_j] = 0, \quad (\text{D.14})$$

$$[\hat{r}_i, \hat{p}_j] = i\delta_{ij}, \quad (\text{D.15})$$

follows

$$[\hat{L}_i, \hat{r}_j] = i\epsilon_{ijk}\hat{r}_k, \quad (\text{D.16})$$

$$[\hat{L}_i, \hat{p}_j] = i\epsilon_{ijk}\hat{p}_k, \quad (\text{D.17})$$

and again Eq. (D.1). Using spherical coordinates

$$r_1 = r \sin \theta \cos \phi, \quad r_2 = r \sin \theta \sin \phi, \quad r_3 = r \cos \theta, \quad (\text{D.18})$$

we find in particular

$$\hat{L}_3 = -i\frac{\partial}{\partial \phi}. \quad (\text{D.19})$$

So we see that the eigenvalue equation

$$\hat{L}_3 \psi_{L,M}(\mathbf{r}) = M \psi_{L,M}(\mathbf{r}), \quad (\text{D.20})$$

has solution

$$\psi_{L,M} = f(r, \theta) e^{iM\phi}, \quad (\text{D.21})$$

where  $f$  is an arbitrary function. If the function  $\psi_{L,M}$  has to be single valued, it must be periodic in  $\phi$  with period  $2\pi$ . Hence we find that additionally for the orbital case we must have  $M = 0, \pm 1, \pm 2, \dots$ , i.e.  $L$  must be an integer.

If we have to add the angular momentum of two different systems,  $\hat{L} = \widehat{\mathbf{L}^{(1)}} + \widehat{\mathbf{L}^{(2)}}$ , we can either choose the set of commuting operators  $\{\widehat{(L^{(1)})^2}, \widehat{(L^{(2)})^2}, \widehat{L^{(1)}_3}, \widehat{L^{(2)}_3}\}$  or the other one  $\{\widehat{(L^{(1)})^2}, \widehat{(L^{(2)})^2}, \widehat{L^2}, \widehat{L}_3\}$ , since  $[\widehat{L^{(1)}}, \widehat{L^{(2)}}] = 0$ .

## Appendix E

# SU(2)

The special unitary group of degree  $n$ ,  $\text{SU}(n)$ , is the group of  $n \times n$  unitary matrices with determinant 1. Its dimension as a real manifold is  $n^2 - 1 = 3$ . Topologically it is compact and simply connected. Algebraically it is a simple Lie group.

Consider the  $2 \times 2$  complex matrices  $A$  which are unitary  $A^\dagger A = 1$  and with determinant equal to 1. The most general  $2 \times 2$  complex matrix can be written as

$$A = \begin{pmatrix} z_1 & z_2 \\ z_3 & z_4 \end{pmatrix} \quad z_i = \rho_i e^{i\varphi_i}. \quad (\text{E.1})$$

Imposing unitarity is the same as imposing the three following conditions

$$z_1^* z_1 + z_3^* z_3 = 1, \quad (\text{E.2})$$

$$z_2^* z_2 + z_4^* z_4 = 1, \quad (\text{E.3})$$

$$z_1^* z_2 + z_3^* z_4 = 0. \quad (\text{E.4})$$

Imposing that the determinant is 1 amounts to setting

$$z_1 z_4 - z_2 z_3 = 1. \quad (\text{E.5})$$

This four conditions can be rewritten as follows

$$\rho_1^2 + \rho_3^2 = 1, \quad (\text{E.6})$$

$$\rho_2^2 + \rho_4^2 = 1, \quad (\text{E.7})$$

$$\rho_1 \rho_2 e^{i(\varphi_2 - \varphi_1)} + \rho_3 \rho_4 e^{i(\varphi_4 - \varphi_3)} = 0, \quad (\text{E.8})$$

$$\rho_1 \rho_4 e^{i(\varphi_1 + \varphi_4)} - \rho_2 \rho_3 e^{i(\varphi_2 - \varphi_3)} = 1. \quad (\text{E.9})$$

Taking the modulus of Eq. (E.8) gives  $\rho_1 \rho_2 = \rho_3 \rho_4$ . When we use this relation in Eqs. (E.6) and (E.7) we find  $\rho_1 = \rho_4$  and  $\rho_2 = \rho_3$ . Then Eq. (E.8) gives  $\varphi_2 - \varphi_1 + \varphi_3 - \varphi_4 = \pi$  which when used in Eq. (E.9) gives

$$\rho_1^2 + \rho_2^2 = e^{-i(\varphi_1 + \varphi_4)}, \quad (\text{E.10})$$

which in turn is satisfied by  $\rho_1^2 + \rho_2^2 = 1$  and  $\varphi_1 + \varphi_4 = 0$ . Then we end up with matrices of the form

$$A = \begin{pmatrix} \rho_1 e^{i\varphi_1} & \pm \sqrt{1 - \rho_1^2} e^{i\varphi_2} \\ \mp \sqrt{1 - \rho_1^2} e^{-i\varphi_2} & \rho_1 e^{-i\varphi_1} \end{pmatrix}. \quad (\text{E.11})$$

In other words we can say that

$$SU(2) = \left\{ \begin{pmatrix} \alpha & -\beta^* \\ \beta & \alpha^* \end{pmatrix} \mid \alpha, \beta \in \mathbb{C}, \quad |\alpha|^2 + |\beta|^2 = 1 \right\}. \quad (\text{E.12})$$

The Lie algebra  $SU(2)$  of the group is obtained through the exponential map as the  $2 \times 2$  complex matrices  $ia$  such that  $A = e^{ia}$ . Then the unitarity of  $A$  implies that  $a$  be hermitian and the condition for  $A$  to have determinant 1 implies that  $a$  be traceless. It is easy to prove that  $SU(n)$  has dimension  $2n(n-1)/2 + n - 1 = n^2 - 1$  and

$$\mathcal{SU}(2) = \{i\boldsymbol{\theta} \cdot \boldsymbol{\sigma} \mid \boldsymbol{\theta} \in \mathbb{R}^3\}, \quad (\text{E.13})$$

with  $\sigma_i$  the Pauli matrices

$$\sigma_1 = \sigma_x = \begin{pmatrix} 0 & 1 \\ 1 & 0 \end{pmatrix}, \quad (\text{E.14})$$

$$\sigma_2 = \sigma_y = \begin{pmatrix} 0 & -i \\ i & 0 \end{pmatrix}, \quad (\text{E.15})$$

$$\sigma_3 = \sigma_z = \begin{pmatrix} 1 & 0 \\ 0 & -1 \end{pmatrix}. \quad (\text{E.16})$$

If we add to the Pauli matrices the identity matrix

$$1 = \begin{pmatrix} 1 & 0 \\ 0 & 1 \end{pmatrix} = \sigma_1^2 = \sigma_2^2 = \sigma_3^2 = -i\sigma_1\sigma_2\sigma_3, \quad (\text{E.17})$$

we obtain a base for the vector space of hermitian  $2 \times 2$  complex matrices.

The Pauli matrices are unitary and some of their properties are as follows

$$\det(\sigma_i) = -1, \quad (\text{E.18})$$

$$\text{Tr}(\sigma_i) = 0, \quad (\text{E.19})$$

$$\det(\mathbf{a} \cdot \boldsymbol{\sigma}) = -|\mathbf{a}|^2, \quad (\text{E.20})$$

$$[\sigma_i, \sigma_j] = 2i\epsilon_{ijk}\sigma_k, \quad (\text{E.21})$$

$$\{\sigma_i, \sigma_j\} = 2\delta_{ij}1, \quad (\text{E.22})$$

$$(\mathbf{a} \cdot \boldsymbol{\sigma})(\mathbf{b} \cdot \boldsymbol{\sigma}) = (\mathbf{a} \cdot \mathbf{b})1 + i(\mathbf{a} \wedge \mathbf{b}) \cdot \boldsymbol{\sigma}, \quad (\text{E.23})$$

$$e^{ia(\hat{\mathbf{n}} \cdot \boldsymbol{\sigma})} = 1 \cos a + i(\hat{\mathbf{n}} \cdot \boldsymbol{\sigma}) \sin a. \quad (\text{E.24})$$

The Pauli matrices offer a representation for the spin  $1/2$  operator  $s$  as follows

$$s = \frac{\boldsymbol{\sigma}}{2}. \quad (\text{E.25})$$

There exists a  $2 : 1$  group homomorphism between  $SU(2)$  and  $SO(3)$ .

## Appendix F

# Velocity transformations

A velocity transformation with  $\beta = (0, 0, \beta)$  is  $x' = \Lambda x$  with

$$\begin{pmatrix} x'^0 \\ x'^1 \\ x'^2 \\ x'^3 \end{pmatrix} = \begin{pmatrix} \gamma & 0 & 0 & -\gamma\beta \\ 0 & 1 & 0 & 0 \\ 0 & 0 & 1 & 0 \\ -\gamma\beta & 0 & 0 & \gamma \end{pmatrix} \begin{pmatrix} x^0 \\ x^1 \\ x^2 \\ x^3 \end{pmatrix}, \quad (\text{F.1})$$

where  $\gamma = 1/\sqrt{1-\beta^2}$ . The velocity transformation can be cast into another useful form by defining a parameter  $\alpha$  called the *rapidity* (or hyperbolic angle) such that

$$e^\alpha = \gamma(1 + \beta) = \sqrt{\frac{1 + \beta}{1 - \beta}}, \quad (\text{F.2})$$

and thus

$$e^{-\alpha} = \gamma(1 - \beta) = \sqrt{\frac{1 - \beta}{1 + \beta}}. \quad (\text{F.3})$$

So

$$\gamma = \cosh \alpha = \frac{e^\alpha + e^{-\alpha}}{2}, \quad (\text{F.4})$$

$$\beta\gamma = \sinh \alpha = \frac{e^\alpha - e^{-\alpha}}{2}, \quad (\text{F.5})$$

$$(\text{F.6})$$

and therefore

$$\beta = \tanh \alpha. \quad (\text{F.7})$$

We then have

$$\begin{pmatrix} x'^0 \\ x'^1 \\ x'^2 \\ x'^3 \end{pmatrix} = \begin{pmatrix} \cosh \alpha & 0 & 0 & -\sinh \alpha \\ 0 & 1 & 0 & 0 \\ 0 & 0 & 1 & 0 \\ -\sinh \alpha & 0 & 0 & \cosh \alpha \end{pmatrix} \begin{pmatrix} x^0 \\ x^1 \\ x^2 \\ x^3 \end{pmatrix}, \quad (\text{F.8})$$

with

$$\begin{pmatrix} \cosh \alpha & 0 & 0 & -\sinh \alpha \\ 0 & 1 & 0 & 0 \\ 0 & 0 & 1 & 0 \\ -\sinh \alpha & 0 & 0 & \cosh \alpha \end{pmatrix} = \exp \left[ -i\alpha \begin{pmatrix} 0 & 0 & 0 & -i \\ 0 & 0 & 0 & 0 \\ 0 & 0 & 0 & 0 \\ -i & 0 & 0 & 0 \end{pmatrix} \right] \equiv \exp(-i\alpha K^3), \quad (\text{F.9})$$

where the simpler Lie-algebraic hyperbolic rotation generator  $iK^3$  is called a *boost* generator.

# Chapter 3

## The Polaron

### 3.1 Introduction

An electron in a ionic crystal polarizes the lattice in its neighborhood. An electron moving with its accompanying distortion of the lattice has sometimes been called a “polaron” [45, 46]. Since 1933 Landau addresses the possibility whether an electron can be self-trapped (ST) in a deformable lattice [47, 48, 49]. This fundamental problem in solid state physics has been intensively studied for an optical polaron in an ionic crystal [50, 51, 52, 53, 54, 55]. Bogoliubov approached the polaron strong coupling limit with one of his canonical transformations. Feynman used his path integral formalism and a variational principle to develop an all coupling approximation for the polaron ground state [56]. Its extension to finite temperatures appeared first by Osaka [57, 58], and more recently by Castrigiano *et al.* [59, 60, 61]. Recently the polaron problem has gained new interest as it could play a role in explaining the properties of the high  $T_c$  superconductors [62]. The polaron problem has also been studied to describe an impurity in a Bose-Einstein ultracold quantum gas condensate of atoms [63]. In this context evidence for a transition between free and self-trapped optical polarons is found. For the solid state optical polaron no ST state has been found yet [52, 53, 55].

The acoustic modes of lattice vibration are known to be responsible for the appearance of the ST state [64, 65, 45]. Contrary to the optical mode which interacts with the electron through Coulombic force and is dispersionless, the acoustic phonons have a linear dispersion coupled to the electron through a short range potential which is believed to play a crucial role in forming the ST state [66]. Acoustic modes have also been widely studied [45]. Sumi and Toyozawa generalized the optical polaron model by including a coupling to the acoustic modes [67]. Using Feynman’s variational approach, they found that the electron is ST with a very large effective mass as the acoustic coupling exceeds a critical value. Emin and Holstein also reached a similar conclusion within a scaling theory [68] in which the Gaussian trial wave function is essentially identical to the harmonic trial action used in the Feynman’s variational approach in the adiabatic limit [69].

The ST state distinguishes itself from an extended state (ES) where the polaron has lower mass and a bigger radius. A polaronic phase transition separates the two states with a breaking of translational symmetry in the ST one [45]. The variational approach is unable to clearly assess the existence of the phase transition [45]. In particular Gerlach and Löwen [45] concluded that no phase transition exists in a large class of polarons. The three dimensional acoustic polaron is not included in the class but Fisher *et al.* [69] argued that its ground state is delocalized.

In a recent work [70] we employed for the first time a specialized path integral Monte Carlo

(PIMC) method [34, 71] to the continuous, highly non-local, acoustic polaron problem at low temperature which is valid at all values of the coupling strength and solves the problem exactly (in a Monte Carlo sense). The method differs from previously employed methods [72, 73, 74, 75, 76, 77, 78] and hinges on the Lévy construction and the multilevel Metropolis method with correlated sampling. In such work the potential energy was calculated and it was shown that like the effective mass it usefully signals the transition between the ES and the ST state. Properties of ES and ST states were explicitly shown through the numerical simulation.

Aim of the chapter is to give a detailed description of the PIMC method used in that calculation and some additional numerical results in order to complement the brief paper of Ref. [70]. In particular it is presented a calculation of the properties of an acoustic polaron in three dimensions in thermal equilibrium at a given low temperature using the path integral Monte Carlo method. The specialized numerical method used is described in full details, thus complementing Ref. [70], and it appears to be the first time it has been used in this context. These results are in favor of the presence of a phase transition from a localized state to an extended state for the electron as the phonon-electron coupling constant decreases. The phase transition manifests itself with a jump discontinuity in the potential energy as a function of the coupling constant and it affects the properties of the path of the electron in imaginary time: In the weak coupling regime the electron is in an extended state whereas in the strong coupling regime it is found in a self-trapped state.

The chapter is organized as follows: in section 3.2 we describe the acoustic polaron model and Hamiltonian, in section 3.3 we describe the observables we are going to compute in the simulation, in section 3.4 we describe the PIMC numerical scheme employed, in section 3.5 we describe the multilevel Metropolis method for sampling the path, in section 3.6 we describe the choice of the transition probability and the level action, in section 3.7 we describe the correlated sampling. Section 3.8 is for the results, and section 3.9 is for final remarks.

## 3.2 The model

The acoustic polaron can be described by the following quasi-continuous model [51, 67],

$$\hat{H} = \frac{\hat{p}^2}{2m} + \sum_k \hbar\omega_k \hat{a}_k^\dagger \hat{a}_k + \sum_k (i\Gamma_k \hat{a}_k e^{ik\hat{x}} + \text{H.c.}) . \quad (3.1)$$

Here  $\hat{x}$  and  $\hat{p}$  are the electron coordinate and momentum operators respectively and  $\hat{a}_k$  is the annihilation operator of the acoustic phonon with wave vector  $k$ . The first term in the Hamiltonian is the kinetic energy of the electron, the second term the energy of the phonons and the third term the coupling energy between the electron and the phonons. The electron coordinate  $x$  is a continuous variable, while the phonons wave vector  $k$  is restricted by the Debye cut-off  $k_o$ . The acoustic phonons have a dispersion relation  $\omega_k = uk$  ( $u$  being the sound velocity) and they interact with the electron of mass  $m$  through the interaction vertex  $\Gamma_k = \hbar u k_o (S/N)^{1/2} (k/k_o)^{1/2}$  according to the deformation potential analysis of Ref. [79].  $S$  is the coupling constant between the electron and the phonons and  $N$  the number of unit cells in the crystal with  $N/V = (4\pi/3)(k_o/2\pi)^3$  by Debye approximation and  $V$  the crystal volume.

Using the path integral representation (see Ref. [56] section 8.3), the phonon part in the Hamiltonian can be exactly integrated owing to its quadratic form in phonon coordinates, and one can write the partition function for a polaron in thermal equilibrium at an absolute temperature  $T$  ( $\beta = 1/k_B T$ , with  $k_B$  Boltzmann constant) as follows,

$$Z = \int dx \iint_{x=x(0)}^{x=x(\hbar\beta)} e^{-\frac{1}{\hbar}\mathcal{S}[x(t), \dot{x}(t), t]} \mathcal{D}x(t) , \quad (3.2)$$

where the action  $\mathcal{S}$  is given by [80],<sup>1</sup>

$$\begin{aligned}\mathcal{S} &= \frac{m}{2} \int_0^{\hbar\beta} \dot{x}^2(t) dt - \frac{1}{2\hbar} \int_0^{\hbar\beta} dt \int_0^{\hbar\beta} ds \int \frac{dk}{(2\pi)^3} \Gamma_k^2 e^{ik \cdot (x(t) - x(s)) - \omega_k |t-s|} \\ &= \mathcal{S}_f + \mathcal{U} .\end{aligned}\quad (3.3)$$

Here  $\mathcal{S}_f$  is the *free particle action*, and  $\mathcal{U}$  the *inter-action* and we denoted with a dot a time derivative as usual. Using dimensionless units  $\hbar = m = uk_o = k_B = V = 1$  the action becomes,

$$\mathcal{S} = \int_0^\beta \frac{\dot{x}^2(t)}{2} dt + \int_0^\beta dt \int_0^\beta ds V_{eff}(|x(t) - x(s)|, |t-s|) , \quad (3.4)$$

with the electron moving subject to an effective retarded potential,

$$V_{eff} = -\frac{S}{2I_D} \int_{q \leq 1} dq q e^{i\sqrt{\frac{2}{\gamma}}q \cdot (x(t) - x(s)) - q|t-s|} \quad (3.5)$$

$$= -\frac{3S}{2} \sqrt{\frac{\gamma}{2}} \frac{1}{|x(t) - x(s)|} \int_0^1 dq q^2 \sin\left(\sqrt{\frac{2}{\gamma}}q|x(t) - x(s)|\right) e^{-q|t-s|} , \quad (3.6)$$

where  $q = k/k_o$ ,  $I_D = \int_{q \leq 1} dq = 4\pi/3$ , and we have introduced a non-adiabatic parameter  $\gamma$  defined as the ratio of the average phonon energy,  $\hbar k_o$  to the electron band-width,  $(\hbar k_o)^2/2m$ . This parameter is of order of  $10^{-2}$  in typical ionic crystals with broad band so that the ST state is well-defined [67]. In our simulation we took  $\gamma = 0.02$ . Note that the integral in (3.6) can be solved analytically and the resulting function tabulated.

### 3.3 The observables

In particular the internal energy  $E$  of the polaron is given by,

$$E = -\frac{1}{Z} \frac{\partial Z}{\partial \beta} = \frac{1}{Z} \int dx \iint e^{-\mathcal{S}} \frac{\partial \mathcal{S}}{\partial \beta} d\mathcal{S} = \left\langle \frac{\partial \mathcal{S}}{\partial \beta} \right\rangle , \quad (3.7)$$

where the internal energy tends to the ground state energy in the large  $\beta \rightarrow \infty$  limit.

Scaling the Euclidean time  $t = \beta t'$  and  $s = \beta s'$  in Eq. (3.4), deriving  $\mathcal{S}$  with respect to  $\beta$ , and undoing the scaling, we get,

$$\begin{aligned}\frac{\partial \mathcal{S}}{\partial \beta} &= -\frac{1}{\beta} \int_0^\beta \frac{\dot{x}^2}{2} dt - \frac{S}{2I_D} \int_0^\beta dt \int_0^\beta ds \times \\ &\int_{q \leq 1} dq q e^{i\sqrt{\frac{2}{\gamma}}q \cdot (x(t) - x(s)) - q|t-s|} \frac{1}{\beta} (2 - q|t-s|) ,\end{aligned}\quad (3.8)$$

where the first term is the kinetic energy contribution to the internal energy,  $\mathcal{K}$ , and the last term is the potential energy contribution,  $\mathcal{P}$ ,

$$\begin{aligned}\mathcal{P} &= -\frac{3S}{2\beta} \int_0^\beta dt \int_0^\beta ds \int_0^1 dq q^3 \frac{\sin\left(\sqrt{\frac{2}{\gamma}}q|x(t) - x(s)|\right)}{\sqrt{\frac{2}{\gamma}}q|x(t) - x(s)|} e^{-q|t-s|} \times \\ &\quad (2 - q|t-s|) .\end{aligned}\quad (3.9)$$

---

<sup>1</sup>This is an approximation as  $e^{-\beta\omega_k}$  is neglected. The complete form is obtained by replacing  $e^{-\omega_k|t-s|}$  by  $e^{-\omega_k|t-s|}/(1 - e^{-\beta\omega_k}) + e^{\omega_k|t-s|}e^{-\beta\omega_k}/(1 - e^{-\beta\omega_k})$ . But remember that  $\beta$  is large.

So that,

$$E = \langle \mathcal{K} + \mathcal{P} \rangle . \quad (3.10)$$

An expression for  $\mathcal{K}$  not involving the polaron speed, can be obtained by taking the derivative with respect to  $\beta$  after having scaled both the time, as before, and the coordinate  $x = \sqrt{\beta}x'$ . Undoing the scaling in the end one gets,

$$\begin{aligned} \mathcal{K} &= -\frac{S}{4\beta I_D} \int_0^\beta dt \int_0^\beta ds \int_{q \leq 1} dq q e^{i\sqrt{\frac{2}{\gamma}}\mathbf{q} \cdot (\mathbf{x}(t) - \mathbf{x}(s)) - q|t-s|} \times \\ &\quad \left[ i\sqrt{\frac{2}{\gamma}}\mathbf{q} \cdot (\mathbf{x}(t) - \mathbf{x}(s)) \right] \end{aligned} \quad (3.11)$$

$$\begin{aligned} &= -\frac{3S}{4\beta} \int_0^\beta dt \int_0^\beta ds \int_0^1 dq q^3 \left[ \cos\left(\sqrt{\frac{2}{\gamma}}q|\mathbf{x}(t) - \mathbf{x}(s)|\right) - \right. \\ &\quad \left. \frac{\sin\left(\sqrt{\frac{2}{\gamma}}q|\mathbf{x}(t) - \mathbf{x}(s)|\right)}{\sqrt{\frac{2}{\gamma}}q|\mathbf{x}(t) - \mathbf{x}(s)|} \right] e^{-q|t-s|} . \end{aligned} \quad (3.12)$$

In the following we will explain how we calculated the potential energy  $P = \langle \mathcal{P} \rangle$ .

### 3.4 Discrete path integral expressions

Generally we are interested in calculating the density matrix  $\hat{\rho} = \exp(-\beta\hat{H})$  in the electron coordinate basis, namely,

$$\rho(\mathbf{x}_a, \mathbf{x}_b; \beta) = \iint_{\mathbf{x}=\mathbf{x}_a}^{\mathbf{x}=\mathbf{x}_b} e^{-\mathcal{S}} \mathcal{D}\mathbf{x}(t) . \quad (3.13)$$

To calculate the path integral, we first choose a subset of all paths. To do this ,we divide the independent variable, Euclidean time, into *steps* of width

$$\tau = \beta/M . \quad (3.14)$$

This gives us a set of *times*,  $t_k = k\tau$  spaced a distance  $\tau$  apart between 0 and  $\beta$  with  $k = 0, 1, 2, \dots, M$ .

At each time  $t_k$  we select the special point  $x_k = \mathbf{x}(t_k)$ , the  $k^{th}$  *time slice*. We construct a path by connecting all points so selected by straight lines. It is possible to define a sum over all paths constructed in this manner by taking a multiple integral over all values of  $x_k$  for  $k = 1, 2, \dots, M-1$  where  $x_0 = \mathbf{x}_a$  and  $x_M = \mathbf{x}_b$  are the two fixed ends. The resulting equation is,

$$\rho(\mathbf{x}_a, \mathbf{x}_b; \beta) = \lim_{\tau \rightarrow 0} \frac{1}{A} \int_{-\infty}^{\infty} \int_{-\infty}^{\infty} \cdots \int_{-\infty}^{\infty} e^{-\mathcal{S}} \frac{dx_1}{A} \cdots \frac{dx_{M-1}}{A} , \quad (3.15)$$

where the normalizing factor  $A = (2\pi\tau)^{3/2}$ .

The simplest discretized expression for the action can then be written as follows,

$$\mathcal{S} = \sum_{k=1}^M \frac{(\mathbf{x}_{k-1} - \mathbf{x}_k)^2}{2\tau} + \tau^2 \sum_{i=1}^M \sum_{j=1}^M V(t_i, t_j) , \quad (3.16)$$

where  $V(t_i, t_j) = V_{eff}(|x_i - x_j|, |i - j|)$  is a symmetric two variables function,  $V(s, t) = V(t, s)$ . In our simulation we tabulated this function taking  $|x_i - x_j| = 0, 0.1, 0.2, \dots, 10$  and  $|i - j| = 0, 1, \dots, M$ .

In writing Eq. (3.16) we used the following approximate expressions,

$$\dot{x}_k = \frac{x_k - x_{k-1}}{\tau} + O(\tau) , \quad (3.17)$$

$$\int_{t_{k-1}}^{t_k} \dot{x}^2(t) dt = \dot{x}_k^2 \tau + O(\tau^2) , \quad (3.18)$$

$$\int_{t_{i-1}}^{t_i} \int_{t_{j-1}}^{t_j} V(s, t) ds dt = V(t_i, t_j) \tau^2 + O(\tau^3) . \quad (3.19)$$

If we take  $V = 0$  in Eq. (3.16) the  $M - 1$  Gaussian integrals in (3.15) can be done analytically. The result is the exact free particle density matrix,

$$\rho_f(x_a, x_b; \beta) = (2\pi\beta)^{-3/2} e^{\frac{1}{2\beta}(x_a - x_b)^2} . \quad (3.20)$$

Thus approximations (3.17) and (3.18) allow us to rewrite the polaron density matrix as follows,

$$\rho(x_a, x_b; \beta) = \int \cdots \int dx_1 \cdots dx_{M-1} \rho_f(x_a, x_1; \tau) \cdots \rho_f(x_{M-1}, x_M; \tau) \times e^{\tau^2 \sum_i \sum_j V(t_i, t_j)} . \quad (3.21)$$

In the next section we will see that this expression offers a useful starting point for the construction of an algorithm for the sampling of the path: the Lévy construction and the analogy with classical polymer systems or the classical isomorphism described in [34]).

The partition function is the trace of the density matrix,

$$Z = \int dx \rho(x, x; \beta) . \quad (3.22)$$

This restrict the path integral to an integral over closed paths only. In other words the paths we need to consider in calculating  $Z$  (and hence  $F$ ) are closed by the *periodic boundary condition*,  $x_M = x_0 = x$ .

To calculate the internal energy we need then to perform the following  $M$  dimensional integral,

$$E = \frac{1}{Z} \int_{-\infty}^{\infty} \int_{-\infty}^{\infty} \cdots \int_{-\infty}^{\infty} dx_0 dx_1 \cdots dx_{M-1} e^{-S} (\mathcal{P} + \mathcal{K}) \Big|_{x_M = x_0} . \quad (3.23)$$

To do this integral we use the Monte Carlo simulation technique described next.

## 3.5 Sampling the path

The total configuration space to be integrated over is made of elements  $s = [x_0, x_1, \dots, x_M]$  where  $x_k$  are the path time slices subject to the periodic boundary condition  $x_M = x_0$ . In the simulation we wish to sample these elements from the probability distribution,

$$\pi(s) = \frac{e^{-S}}{Z} , \quad (3.24)$$

where the partition function  $Z$  normalizes the function  $\pi$  in this space.

The idea is to find an efficient way to move the path in a random walk sampled by  $\pi$ , through configuration space.

In order to be able to make the random walk diffuse fast through configuration space, as  $\tau$  decreases, is necessary to use multislices moves [34].

In our simulation we chose to use the bisection method (a particular multilevel Monte Carlo sampling method [34]). That's how an  $l$  levels move is constructed. Clip out of the path  $m = 2^l$  subsequent time slices  $x_i, x_{i+1}, \dots, x_{i+m}$  (choosing  $i$  randomly). In the first level we keep  $x_i$  and  $x_{i+m}$  fixed and, following Lévy construction for a Brownian bridge [81], we move the bisecting point at  $i + m/2$  to,

$$x_{i+m/2} = \frac{x_i + x_{i+m}}{2} + \boldsymbol{\eta} \quad (3.25)$$

where  $\boldsymbol{\eta}$  is a normally distributed random vector with mean zero and standard deviation  $\sqrt{\tau m/4}$ . As shown in next section this kind of transition rule samples the path using a transition probability distribution  $T \propto \exp(-\mathcal{S}_f)$ . Thus we will refer to it as *free particle sampling*.

Having sampled  $x_{i+m/2}$ , we proceed to the second level bisecting the two new intervals  $(0, i + m/2)$  and  $(i + m/2, i + m)$  generating points  $x_{i+m/4}$  and  $x_{i+3m/4}$  with the same algorithm. We continue recursively, doubling the number of sampled points at each level, stopping only when the time difference of the intervals is  $\tau$ .

In this way we are able to partition the full configuration  $s$  into  $l$  levels,  $s = (s_0, s_1, \dots, s_l)$  where:  $s_0 = [x_0, \dots, x_i, x_{i+m}, \dots, x_{M-1}]$ , unchanged;  $s_1 = [x_{i+m/2}]$ , changed in level 1;  $s_2 = [x_{i+m/4}, x_{i+3m/4}]$ , changed in level 2;  $\dots$ ;  $s_l = [x_{i+1}, x_{i+2}, \dots, x_{i+m-1}]$  changed in level  $l$ .

To construct the random walk we use the multilevel Metropolis method [82, 83, 34]. Call  $(s'_1, \dots, s'_l)$  the new trial positions in the sense of a Metropolis rejection method, the unprimed ones are the corresponding old positions with  $s_0 = s'_0$ .

In order to decide if the sampling of the path should continue beyond level  $k$ , we need to construct the probability distribution  $\pi_k$  for level  $k$ . This, usually called the *level action*, is a function of  $s_0, s_1, \dots, s_k$  proportional to the reduced distribution function of  $s_k$  conditional on  $s_0, s_1, \dots, s_{k-1}$ . The optimal choice for the level action would thus be,

$$\pi_k^*(s_0, s_1, \dots, s_k) = \int ds_{k+1} \dots ds_l \pi(s) . \quad (3.26)$$

This is only a guideline. Non optimal choices will lead to slower movement through configuration space. One needs to require only that feasible paths (closed ones) have non zero level action, and that the action at the last level be exact,

$$\pi_l(s_0, s_1, \dots, s_l) = \pi(s) . \quad (3.27)$$

Given the level action  $\pi_k(s)$  the optimal choice for the transition probability  $T_k(s_k)$ , for  $s_k$  contingent on the levels already sampled, is given by,

$$T_k^*(s_k) = \frac{\pi_k(s)}{\pi_{k-1}(s)} . \quad (3.28)$$

One can show that  $T_k^*$  will be a normalized probability if and only if  $\pi_k$  is chosen as in (3.26). In general one need to require only that  $T_k$  be a probability distribution non zero for feasible paths. In our simulation we used the free particle transition probability of the Lévy construction as a starting point for a more efficient correlated sampling that will be described in a later section.

Once the partitioning and the sampling rule are chosen, the sampling proceeds past level  $k$  with probability,

$$A_k(s') = \min \left[ 1, \frac{T_k(s_k)\pi_k(s')\pi_{k-1}(s)}{T_k(s'_k)\pi_k(s)\pi_{k-1}(s')} \right] . \quad (3.29)$$

That is we compare  $A_k$  with a uniformly distributed random number in  $(0, 1)$ , and if  $A_k$  is larger, we go on to sample the next level. If  $A_k$  is smaller, we make a new partitioning of the initial path, and start again from level 1. Here  $\pi_0$  needed in the first level can be set equal to 1, since it will cancel out of the ratio.

This acceptance probability has been constructed so that it satisfies a form of “detailed balance” for each level  $k$ ,

$$\frac{\pi_k(s)}{\pi_{k-1}(s)} T_k(s'_k) A_k(s') = \frac{\pi_k(s')}{\pi_{k-1}(s')} T_k(s_k) A_k(s) . \quad (3.30)$$

The moves will always be accepted if the transition probabilities and level actions are set to their optimal values.

The total transition probability for a trial move making it through all  $l$  levels is,

$$P(s \rightarrow s') = \prod_{k=1}^l T_k(s') A_k(s') . \quad (3.31)$$

By multiplying Eq. (3.30) from  $k = 1$  to  $k = l$  and using Eq. (3.27), one can verify that the total move satisfy the detailed balance condition,

$$\pi(s) P(s \rightarrow s') = \pi(s') P(s' \rightarrow s) . \quad (3.32)$$

Thus if there are no barriers or conserved quantities that restrict the walk to a subset of the full configuration space (i.e. assuming the random walk to be ergodic) the algorithm will asymptotically converge to  $\pi$ , independent of the particular form chosen for the transition probabilities,  $T_k$ , and the level actions,  $\pi_k$  [84]. We will call *equilibration time* the number of moves needed in the simulation to reach convergence.

Whenever the last level is reached, one calculates the properties ( $\mathcal{K}$  and  $\mathcal{P}$ ) on the new path  $s'$ , resets the initial path to the new path, and start a new move. We will call Monte Carlo step (MCS) any attempted move.

## 3.6 Choice of $T_k$ and $\pi_k$

In our simulation we started moving the path with the Lévy construction described in the preceding section. We will now show that this means that we are sampling an approximate  $T^*$  with free particle sampling.

For the free particle case ( $\mathcal{U} = 0$ ) one can find analytic expressions for the optimal level action  $\pi_k^*$  and the optimal transition rule  $T_k^*$ . For examples for the first level, Eq. (3.26) gives,

$$\pi_1^*(x_{i+m/2}) \propto \rho_f(x_i, x_{i+m/2}; \tau m/2) \rho_f(x_{i+m/2}, x_{i+m}; \tau m/2) \quad (3.33)$$

$$\propto e^{\frac{1}{m\tau}(x_i - x_{i+m/2})^2} e^{\frac{1}{m\tau}(x_{i+m/2} - x_{i+m})^2} \quad (3.34)$$

$$\propto e^{\frac{2}{m\tau} \left[ x_{i+m/2} - \left( \frac{x_i + x_{i+m}}{2} \right) \right]^2} . \quad (3.35)$$

This justify the Lévy construction and shows that it exactly samples the free particle action (i.e.  $A_k = 1$  for all  $k$ 's). This also imply that for the interacting system we can introduce a *level inter action*,  $\tilde{\pi}_k$  such that,

$$\tilde{\pi}_k = \int ds_{k+1} \dots ds_l \tilde{\pi}(s) , \quad (3.36)$$

with

$$\tilde{\pi}(s) = \frac{e^{-U}}{Z} . \quad (3.37)$$

So that the acceptance probability will have the simplified expression,

$$A_k(s') = \min \left[ 1, \frac{\tilde{\pi}_k(s') \tilde{\pi}_{k-1}(s)}{\tilde{\pi}_k(s) \tilde{\pi}_{k-1}(s')} \right] . \quad (3.38)$$

For the  $k^{th}$  level inter action we chose the following expression,

$$\tilde{\pi}_k \propto \exp \left[ -(\tau \ell_k)^2 \sum_{i=1}^{[M/\ell_k]} \sum_{j=1}^{[M/\ell_k]} V(i\ell_k \tau, j\ell_k \tau) \right] , \quad (3.39)$$

where  $\ell_k = m/2^k$ . In the last level  $\ell_l = 1$  and the level inter action  $\tilde{\pi}_l$  reduces to the exact inter action  $\tilde{\pi}$  thus satisfying Eq. (3.27).

It's important to notice that during the simulation we never need to calculate the complete level inter action since in the acceptance probabilities enter only ratios of level inter actions calculated on the old and on the new path. For example if for the move we clipped out the interval  $t_i, \dots, t_{i+m}$  with  $i+m < M$ <sup>2</sup>, we have,

$$\ln \frac{\tilde{\pi}_k(s')}{\tilde{\pi}_k(s)} = -(\tau \ell_k)^2 \left\{ \sum_{m=0}^{2^k} \sum_{n=0}^{2^k} V(t_i + m\ell_k \tau, t_i + n\ell_k \tau) + \sum_{m=1}^{i-1} \sum_{n=0}^{2^k} V(m\ell_k \tau, t_i + n\ell_k \tau) + \sum_{m=i+m+1}^M \sum_{n=0}^{2^k} V(m\ell_k \tau, t_i + n\ell_k \tau) \right\} , \quad (3.40)$$

which is computationally much cheaper than (3.39).

## 3.7 Correlated sampling

When the path reaches equilibrium (i.e.  $P(s \rightarrow s') \approx \pi(s')$ ) if we calculate,

$$\sigma(t_0/\tau) = \sqrt{\left\langle \left[ x(t) - \left( \frac{x(t+t_0) + x(t-t_0)}{2} \right) \right]^2 \right\rangle} , \quad (3.41)$$

we see that these deviations are generally smaller than the free particle standard deviations used in the Lévy construction (see Fig. 3.1),

---

<sup>2</sup>When  $i+m \geq M$  there is a minor problem with the periodic boundary conditions and Eq. (3.40) will change.

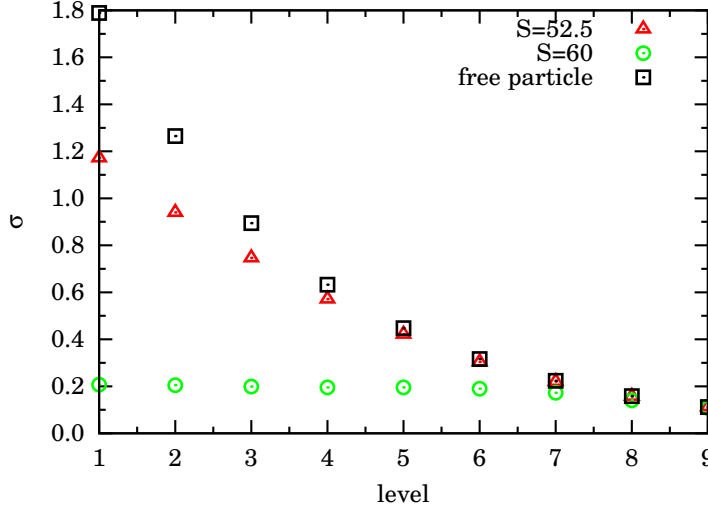


Figure 3.1: Shows the deviations (3.41) for a simulation with  $S = 60$  and  $S = 52.5$ ,  $\tau = 0.025$ ,  $l = 9$ . The free particle standard deviations (3.42) are plotted for comparison. For  $S = 60$  the path is localized while for  $S = 52.5$  is unlocalized i.e. closer to the free particle path.

$$\sigma_f(\ell_k) = \sqrt{\ell_k \tau / 2} . \quad (3.42)$$

As Fig. 3.1 shows, the discrepancy gets bigger as  $\ell_k$  increases.

We thus corrected the sampling rule for the correct deviations. For example for the first level we used,

$$T_1(x_{i+m/2}) \propto e^{-\frac{(x_{i+m/2} - \bar{x})^2}{2\sigma_f^2(m/2)}}, \quad (3.43)$$

where  $\bar{x} = (x_i + x_{i+m})/2$ . Since the level action is given by,

$$\pi_1(x_{i+m/2}) \propto e^{-\frac{(x_{i+m/2} - \bar{x})^2}{2\sigma_f^2(m/2)}} \tilde{\pi}_1(x_{i+m/2}), \quad (3.44)$$

we can define a function,

$$P_1 \propto e^{-\frac{(x_{i+m/2} - \bar{x})^2}{2\sigma_f^2(m/2)} \left[ \frac{1}{\sigma_f^2(m/2)} - \frac{1}{\sigma_f^2(m/2)} \right]}, \quad (3.45)$$

and write the acceptance probability,

$$A_1(s') = \min \left[ 1, \frac{P_1(s)}{P_1(s')} \frac{\tilde{\pi}_1(s') \tilde{\pi}_0(s)}{\tilde{\pi}_1(s) \tilde{\pi}_0(s')} \right] . \quad (3.46)$$

Which is a generalization of Eq. (3.38).

We maintain the acceptance ratios in  $[0.15, 0.65]$  by decreasing (or increasing) the number of levels in the multilevel algorithm as the acceptance ratios becomes too low (or too high).

In the Appendix we report some remarks on the error analysis in our MC simulations.

### 3.8 Numerical Results

We simulated the acoustic polaron fixing the adiabatic coupling constant  $\gamma = 0.02$  and the inverse temperature  $\beta = 15$ . Such temperature is found to be well suited to extract close to ground state properties of the polaron. The path was  $M$  time slices long and the time step was  $\tau = \beta/M$ . For a given coupling constant  $S$  we computed the potential energy  $P$  extrapolating (with a linear  $\chi^2$  square fit) to the continuum time limit,  $\tau \rightarrow 0$ , three points corresponding to time-steps chosen in the interval  $\tau \in [1/100, 1/30]$ . An example of extrapolation is shown in Fig. 3.2 for the particular case  $\beta = 15$ ,  $\gamma = 0.02$ , and  $S = 60$ .

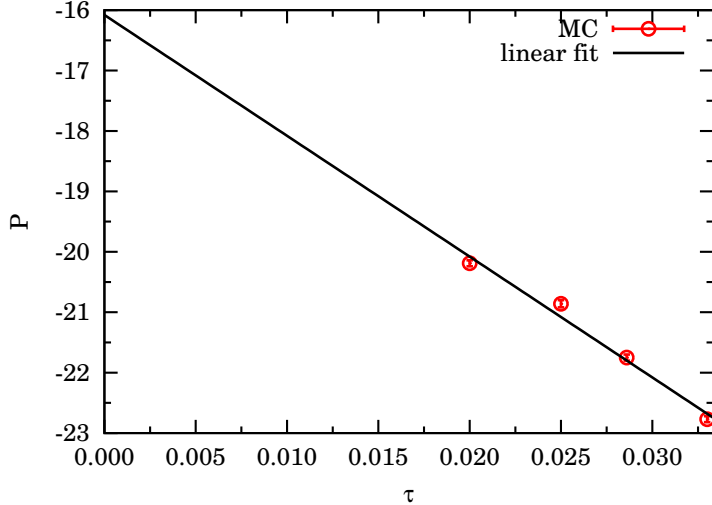


Figure 3.2: Shows the time step,  $\tau$ , extrapolation for the potential energy,  $P = \langle \mathcal{P} \rangle$ . We run at  $\beta = 15$ ,  $\gamma = 0.02$ , and  $S = 60$ . The extrapolated value to the continuum limit is in this case  $P = -16.1(5)$  which is in good agreement with the result of Ref. [76].

In Fig. 3.5 and Tab. 3.1 we show the results for the potential energy as a function of the coupling strength. With the coupling constant  $S = 52.5$  we generated the equilibrium path which turns out to be unlocalized (see Fig. 3.4). Changing the coupling constant to  $S = 60$  and taking the unlocalized path as the initial path we saw the phase transition described in Fig. 3.3. the path after the phase transition is localized (see Fig. 3.4).

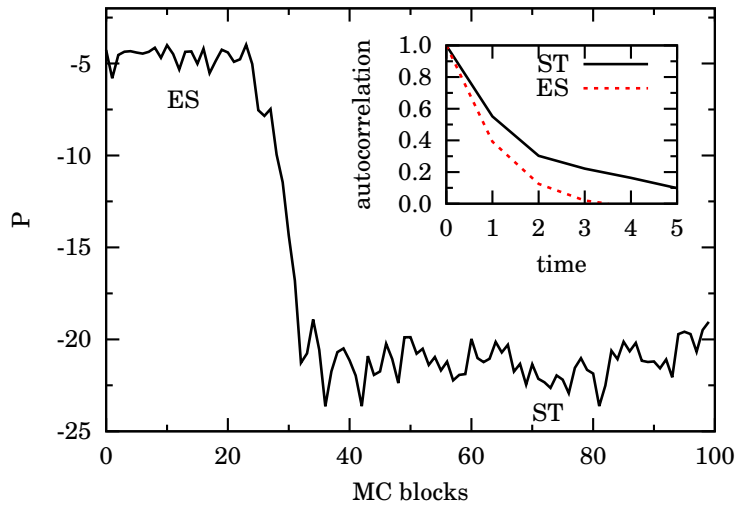


Figure 3.3: At  $S = 60$  the results for the potential energy  $\mathcal{P}$  at each MC block ( $5 \times 10^3$  MCS) starting from an initial unlocalized path obtained by a previous simulation at  $S = 52.5$ . We can see that after about 30 blocks there is a transition from the ES state to the ST state. In the inset is shown the autocorrelation function, defined in Eq. (G.8), for the potential energy, for the two states. The correlation time, in MC blocks, is shorter in the unlocalized phase than in the localized one. The computer time necessary to carry on a given number of Monte Carlo steps is longer for the unlocalized phase.

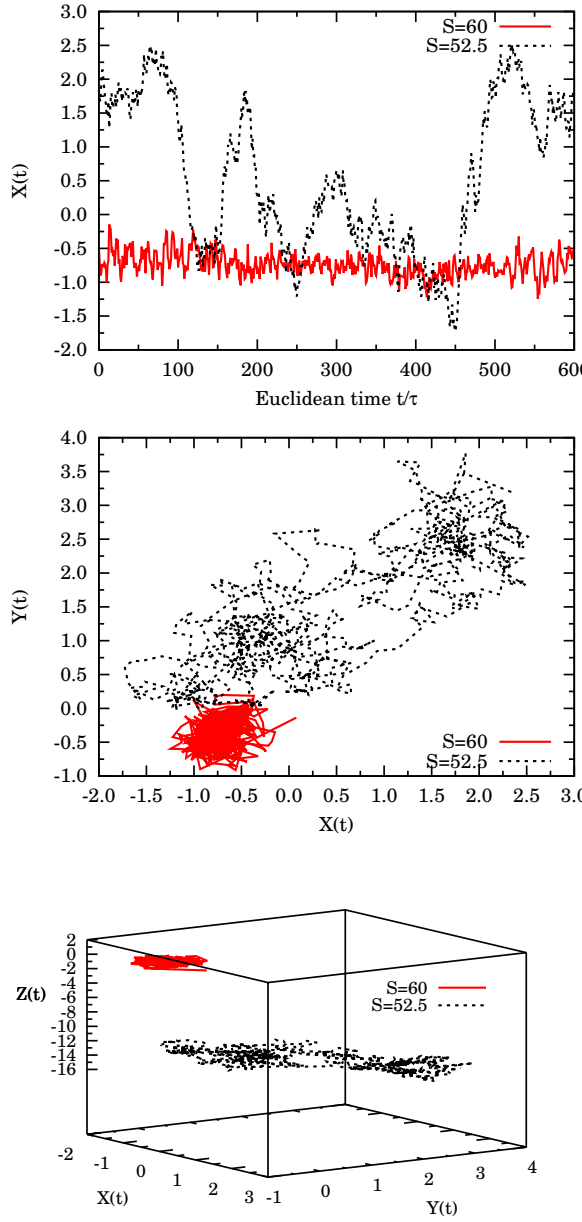


Figure 3.4: The top panel shows the polaron (closed) path  $x(t)$  as a function of Euclidean time  $t$  in units of  $\tau$  at equilibrium during the simulation. The middle panel shows the projection on the  $x - y$  plane of the path. The bottom panel shows the three-dimensional path. We see clearly how both path has moved from the initial path located on the origin but the path at  $S = 52.5$  is much less localized than the one at  $S = 60$ .

Note that since  $S$  and  $\tau$  appear in the combination  $S\tau^2$  in  $\mathcal{U}$  (and  $S\tau$  in  $\mathcal{F}$ ) the same phase

transition from an ES to a ST state will be observed increasing the temperature. With the same Hamiltonian we are able to describe two very different behaviors of the acoustic polaron as the temperature changes.

In Fig. 3.5 we show the behavior of the potential energy as a function of the coupling strength. The numerical results suggests the existence of a phase transition between two different regimes which corresponds to the so called ES and ST states for the weak and strong coupling region respectively. We found that paths related to ES and ST are characteristically distinguishable. Two typical paths for the ES and ST regimes involved in Fig. 3.5 is illustrated in Fig. 3.4. The path in ES state changes smoothly in a large time scale, whereas the path in ST state do so abruptly in a small time scale with a much smaller amplitude which is an indication that the polaron hardly moves. The local fluctuations in the results for the potential energy has an autocorrelation function (defined in Eq. (G.8)) which decay much more slowly in the ES state than in the ST state as shown in the inset of Fig. 3.3. Concerning the critical property of the transition between the ES and ST states our numerical results are in favor of the presence of a discontinuity in the potential energy. In the large  $\beta$  limit at  $\beta = 15$  and fixing the adiabatic coupling constant to  $\gamma = 0.02$ , the ST state appear at a value of the coupling constant between  $S = 52.5$  and  $S = 55$ . With the increase of  $\beta$ , the values for the potential energy  $P = \langle \mathcal{P} \rangle$  increase in the weak coupling regime but decrease in the strong coupling region.

From second order perturbation theory (see Ref. [56] section 8.2) follows that the energy shift  $E(\gamma, S)$  is given by  $-3S\gamma[1/2 - \gamma + \gamma^2 \ln(1 + 1/\gamma)]$  from which one extracts the potential energy shift by taking  $P(\gamma, S) = \gamma dE(\gamma, S)/d\gamma$ . From the Feynman variational approach of Ref. [67] follows that in the weak regime the energy shift is  $-3S\gamma[1/2 - \gamma + \gamma \ln(1 + 1/\gamma)]$  and in the strong coupling regime  $-S + 3\sqrt{S/5\gamma}$ .

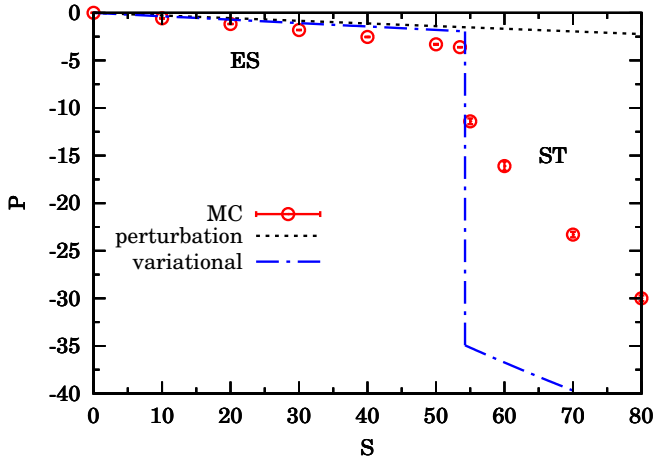


Figure 3.5: Shows the behavior of the potential energy  $P$  as a function of the coupling constant  $S$ . The points are the MC results (see Tab. 3.1), the dashed line is the second order perturbation theory result (perturbation) valid in the weak coupling regime and the dot-dashed line is the variational approach from Ref. [67] (variational) in the weak and strong coupling regimes.

Table 3.1: MC results for  $P$  as a function of  $S$  at  $\beta = 15$  and  $\gamma = 0.02$  displayed in Fig. 3.5. The runs were made of  $5 \times 10^5$  MCS (with  $5 \times 10^4$  MCS for the equilibration) for the ES states and  $5 \times 10^6$  MCS (with  $5 \times 10^5$  MCS for the equilibration) for the ST states.

$S$	$P$
10	-0.573(8)
20	-1.17(2)
30	-1.804(3)
40	-2.53(3)
50	-3.31(4)
53.5	-3.61(1)
55	-11.4(3)
60	-16.1(5)
70	-23.3(3)
80	-30.0(3)

### 3.9 Conclusions

In this chapter we presented a specialized path integral Monte Carlo method to study the low temperature behavior of an acoustic polaron. At an inverse temperature  $\beta = 15$  (close to the ground state of the polaron) and at a non-adiabatic parameter  $\gamma = 0.02$  typical of ionic crystals we found numerical evidence for a phase transition between an extended state in the weak coupling regime and a self-trapped one in the strong coupling regime at a value of the phonons-electron coupling constant  $S = 54.3(7)$ . The transition also appears looking at the potential energy as a function of the coupling constant where a jump discontinuity is observed. Comparison with the perturbation theory and the variational calculation of Ref. [67] is also presented.

The specialized path integral Monte Carlo simulation method used as an unbiased way to study the properties of the acoustic polaron has been presented in full detail. It is based on the Lévy construction and the multilevel Metropolis method with correlated sampling. Some remarks on the estimation of the errors in the Monte Carlo calculation are also given in the Appendix. This complement our previous paper [70] where fewer details on the Monte Carlo method had been given.

This method differs from previously adopted methods [72, 73, 74, 75, 76, 77, 71, 78]. Unlike the method of Ref. [72] this path integral is in real space rather than in Fourier space, Refs. [77, 78] put the polaron on a lattice and not on the continuum as is done here, while Refs. [76] use PIMC single slice move whereas the multilevel PIMC used here instead is a general sampling method which can efficiently make multislice moves. The efficiency  $\xi$  (see the Appendix) for the potential energy increases respect to the single slice sampling because the coarsest movements are sampled and rejected before the finer movements are even constructed. In Ref. [71] the Lévy construction was used as is done here but the Metropolis test was performed after the entire path had been reconstructed, using an effective action, and not at each intermediate level of the reconstruction. In Ref. [71] the simpler Lévy reconstruction scheme was also found to be satisfactory for the efficient sampling of the polaron configuration space even at strong coupling. Even if here it is not implemented the method of Ref. [71] we expect the method presented in this chapter to be of comparable efficiency to the one of these authors. In fact it is true that the Lévy construction is computationally cheap but guiding the path as it is been reconstructed starting already from the first levels as done here should have the advantage of refining the sampling since the path is guided through configuration space starting from the small displacements.

Although these results are of a numerical nature and one only probed the acoustic polaron for one value of the non-adiabatic parameter  $\gamma$  the analysis support the existence of a local-

ization phase transition as the phonons-electron coupling constant  $S$  is increased at constant temperature or as the temperature is decreased at constant  $S$ . More so, considering the fact that the introduction of a cut-off parameter have shown to work successfully in renormalization treatments.



# **Appendices**



## Appendix G

### Estimating errors

Since asymptotic convergence is guaranteed, the main issue is whether configuration space is explored thoroughly in a reasonable amount of computer time. Let us define a measure of the convergence rate and of the efficiency of a given random walk. This is needed to compare the efficiency of different transition rules, to estimate how long the runs should be, and to calculate statistical errors.

The rate of convergence is a function of the property being calculated. Let  $\mathcal{O}(s)$  be a given property, and let its value at step  $k$  of the random walk be  $\mathcal{O}_k$ . Let the estimator for the mean and variance of a random walk with  $N$  MCS be,

$$\bar{\mathcal{O}} = \langle \mathcal{O}_k \rangle = \frac{1}{N} \sum_{k=0}^{N-1} \mathcal{O}_k , \quad (\text{G.1})$$

$$\sigma^2(\mathcal{O}) = \langle (\mathcal{O}_k - \bar{\mathcal{O}})^2 \rangle . \quad (\text{G.2})$$

Then the estimator for the variance of the mean will be,

$$\sigma^2(\bar{\mathcal{O}}) = \langle \left( \frac{1}{N} \sum_k \mathcal{O}_k - \frac{1}{N} \sum_k \bar{\mathcal{O}} \right)^2 \rangle \quad (\text{G.3})$$

$$= \frac{1}{N^2} \langle \left[ \sum_k (\mathcal{O}_k - \bar{\mathcal{O}}) \right]^2 \rangle \quad (\text{G.4})$$

$$= \frac{1}{N^2} \left\{ \sum_k \langle (\mathcal{O}_k - \bar{\mathcal{O}})^2 \rangle + 2 \sum_{i < j} \langle (\mathcal{O}_i - \bar{\mathcal{O}})(\mathcal{O}_j - \bar{\mathcal{O}}) \rangle \right\} \quad (\text{G.5})$$

$$= \frac{\sigma^2(\mathcal{O})}{N} \left\{ 1 + \frac{2}{N\sigma^2(\mathcal{O})} \sum_{i < j} \langle (\mathcal{O}_i - \bar{\mathcal{O}})(\mathcal{O}_j - \bar{\mathcal{O}}) \rangle \right\} \quad (\text{G.6})$$

$$= \frac{\sigma^2(\mathcal{O}) k_{\mathcal{O}}}{N} . \quad (\text{G.7})$$

The quantity  $k_{\mathcal{O}}$  is called the *correlation time* and can be calculated given the autocorrelation function for  $A_k = \mathcal{O}_k - \bar{\mathcal{O}}$ . The estimator for the *autocorrelation function*,  $c_k$ , can be constructed observing that in the infinite random walk,  $\langle A_i A_j \rangle$  has to be a function of  $|i - j|$  only. Thus the estimator can be written,

$$c_k = \frac{\langle A_0 A_k \rangle}{\sigma^2(\mathcal{O})} = \frac{1}{(N - k)\sigma^2(\mathcal{O})} \sum_{n=1}^{N-k} A_n A_{n+k} . \quad (\text{G.8})$$

So that the estimator for the correlation time will be,

$$k_{\mathcal{O}} = 1 + \frac{2}{N} \sum_{k=1}^N (N - k) c_k . \quad (\text{G.9})$$

To determine the true statistical error in a random walk, one needs to estimate this correlation time. To do this, is very important that the total length of the random walk be much greater than  $k_{\mathcal{O}}$ . Otherwise the result and the error will be unreliable. Runs in which the number of steps  $N \gg k_{\mathcal{O}}$  are called *well converged*.

The correlation time gives the average number of steps needed to decorrelate the property  $\mathcal{O}$ . It will depend crucially on the transition rule and has a minimum value of 1 for the optimal rule (while  $\sigma(\mathcal{O})$  is independent of the sampling algorithm).

Normally the equilibration time will be at least as long as the equilibrium correlation time, but can be longer. Generally the equilibration time depends on the choice for the initial path. To lower this time is important to choose a physical initial path. Since the polaron system is isotropic, we chose the initial path with all time slices set to  $\vec{0}$ .

The efficiency of a random walk procedure (for the property  $\mathcal{O}$ ) is defined as how quickly the error bars decrease as a function of the computer time,  $\xi_{\mathcal{O}} = 1/\sigma^2(\mathcal{O})N\mathcal{T} = 1/\sigma^2(\mathcal{O})k_{\mathcal{O}}\mathcal{T}$  where  $\mathcal{T}$  is the computer time per step. The efficiency depends not only on the algorithm but also on the computer and the implementation.

# Chapter 4

## Mendeleev Periodic System

In this chapter we revisit Sections §67 and §73 of [28].

### 4.1 Electron states in the atom

In the non-relativistic approximation,<sup>1</sup> the stationary states of the atom are determined by Schrödinger's equation for the system of electrons, which move in the Coulomb field of the nucleus and interact electrically with one another; the spin operators of the electrons do not appear in this equation. As we know, for a system of particles in a centrally symmetric external field the total orbital angular momentum  $L$  and the parity of the state are conserved. Hence each stationary state of the atom will be characterized by a definite value of the orbital angular momentum  $L$  and by its parity. Moreover, the coordinate wave functions of the stationary states of a system of identical particles have a certain permutational symmetry determined by the total spin  $S$  of the electrons. Hence every stationary state of the atom is characterized also by the total spin  $S$  of the electrons.

The energy level having given values of  $S$  and  $L$  is degenerate to a degree equal to the number of different possible directions in space of the vectors  $S$  and  $L$ . The degree of the degeneracy from the directions of  $L$  and  $S$  is respectively  $2L + 1$  and  $2S + 1$ . Consequently, the total degree of the degeneracy of a level with given  $L$  and  $S$  is equal to the product  $(2L + 1)(2S + 1)$ .

There is a generally accepted notation to denote the atomic energy levels (or, as they are called, the spectral terms of the atoms). States with different values of the total orbital angular

---

<sup>1</sup>The electromagnetic interaction of the electrons contains relativistic effects, which depend on their spins. These effects have the result that the energy of the atom depends not only on the absolute magnitudes of the vectors  $\mathbf{L}$  and  $\mathbf{S}$  but also on their relative positions. Strictly speaking, when the relativistic interactions are taken into account the orbital angular momentum  $\mathbf{L}$  and the spin  $\mathbf{S}$  of the atom are not separately conserved. Only the total angular momentum  $\mathbf{J} = \mathbf{L} + \mathbf{S}$  is conserved; this is a universal and exact law which follows from the isotropy of space relative to a closed system. For this reason, the exact energy levels must be characterized by the values  $J$  of the total angular momentum. However, if the relativistic effects are comparatively small (as often happens), they can be allowed for as a perturbation. Thus, as a result of the relativistic effects, a level with given values of  $L$  and  $S$  is split into a number of levels with different values of  $J$ . This splitting is called the *fine structure* (or the *multiplet splitting*) of the level. Here we will neglect relativistic effects so that we can consider  $L$  and  $S$  as separately conserved quantities.

momentum  $L$  are denoted by capital Latin letters, as follows:

$$\begin{array}{ccccccccccccc} L, l & = & 0 & 1 & 2 & 3 & 4 & 5 & 6 & 7 & 8 & 9 & 10 & \dots \\ l & \rightarrow & s & p & d & f & g & h & i & k & l & m & n & \dots \\ L & \rightarrow & S & P & D & F & G & H & I & K & L & M & N & \dots \end{array}$$

where the lower case letters denote quantum numbers of single electron states and the upper case ones denotes quantum numbers of the many electron states. Above and to the left of this letter is placed the number  $2S + 1$ , called the multiplicity of the term. Below and to the right of the letter is placed the value of the total angular momentum  $J$  (here  $\mathbf{J} = \mathbf{L} + \mathbf{S}$  is the total angular momentum of the system of electrons in the atom). Thus the symbol  $^2P_{1/2}$  denotes the level with  $L = 1, S = 1/2, J = 1/2$ .

An atom with more than one electron is a complex system of mutually interacting electrons moving in the field of the nucleus. For such a system we can, strictly speaking, consider only states of the system as a whole. Nevertheless, it is found that we can, with fair accuracy, introduce the idea of the states of each individual electron in the atom, as being the stationary states of the motion of each electron in some effective centrally symmetric field due to the nucleus and to all the other electrons. These fields are in general different for different electrons in the atom, and they must all be defined simultaneously, since each of them depends on the states of all the other electrons. Such a field is said to be *self-consistent*.

Since the self-consistent field is centrally symmetric, each state of the electron is characterized by a definite value of its orbital angular momentum  $l$ . The states of an individual electron with a given  $l$  are numbered (in order of increasing energy) by the *principal quantum number*  $n$ , which takes the values  $n = l + 1, l + 2, \dots$ ; this choice of the order of numbering is made in accordance with what is usual for the hydrogen atom. However, the sequence of levels of increasing energy for various  $l$  in complex atoms is in general different from that found in the hydrogen atom. In the latter, the energy is independent of  $l$ , so that the states with larger values of  $n$  always have higher energies. In complex atoms, on the other hand, the level with  $n = 5, l = 0$ , for example, is found to lie below that with  $n = 4, l = 2$ .

The states of individual electrons with different values of  $n$  and  $l$  are customarily denoted by a figure which gives the value of the principal quantum number, followed by a letter which gives the value of  $l$ : thus  $4d$  denotes the state with  $n = 4, l = 2$ . A complete description of the atom demands that, besides the values of the total  $L, S$ , and  $J$ , the states of all the electrons should also be enumerated. Thus the symbol  $1s\ 2p\ ^3P_0$  denotes a state of the helium atom in which  $L = 1, S = 1, J = 0$  and the two electrons are in the  $1s$  and  $2p$  states. If several electrons are in states with the same  $l$  and  $n$ , this is usually shown for brevity by means of an index: thus  $3p^2$  denotes two electrons in the  $3p$  state. The distribution of the electrons in the atom among states with different  $l$  and  $n$  is called the *electron configuration*.

For given values of  $n$  and  $l$ , the electron can have different values of the projections of the orbital angular momentum ( $m$ ) and of the spin ( $\sigma$ ) on the  $z$ -axis. For a given  $l$ , the number  $m$  takes  $2l + 1$  values; the number  $\sigma$  is restricted to only two values,  $\pm \frac{1}{2}$ . Hence there are altogether  $2(2l + 1)$  different states with the same  $n$  and  $l$ ; these states are said to be *equivalent*. According to Pauli's principle there can be only one electron in each such state. Thus at most  $2(2l + 1)$  electrons in an atom can simultaneously have the same  $n$  and  $l$ . An assembly of electrons occupying all the states with the given  $n$  and  $l$  is called a *closed shell* of the type concerned.

The difference in energy between atomic levels having different  $L$  and  $S$  but the same electron configuration is due to the electrostatic interaction of the electrons. These energy differences are usually small, and several times less than the distances between the levels of different configurations. The following empirical principle (Hund's rule; F. Hund 1925) is known concerning the

relative position of levels with the same configuration but different  $L$  and  $S$ : The term with the greatest possible value of  $S$  (for the given electron configuration) and the greatest possible value of  $L$  (for this  $S$ ) has the lowest energy.<sup>2</sup> We shall show how the possible atomic terms can be found for a given electron configuration. If the electrons are not equivalent, the possible value of  $L$  and  $S$  are determined immediately from the rule for the addition of angular momenta. Thus, for instance, with the configurations  $np$ ,  $n'p$  ( $n, n'$  being different) the total angular momentum  $L$  can take the values 2, 1, 0, and the total spin  $S = 0, 1$ ; combining these, we obtain the terms  $^{1,3}S$ ,  $^{1,3}P$ ,  $^{1,3}D$ . If we are concerned with equivalent electrons, however, restrictions imposed by Pauli's principle make their appearance.

When Hund's rule is applied to determine the ground term of an atom from a known electron configuration, only the unfilled shell need be considered, since the moments of electrons in closed shells cancel out. For example, let there be four  $d$  electrons outside the closed shells in an atom. The magnetic quantum number of the  $d$  electron can take five values:  $0, \pm 1, \pm 2$ . Hence all four electrons can have the same spin component  $\sigma = \frac{1}{2}$ , and the maximum possible total spin is  $S = 2$ . We must then assign to the electrons different values of  $m$  so as to give the maximum value of  $M_L = \sum m = 2$ . This means that the maximum value of  $L$  for  $S = 2$  is also 2, and the term is  $^5D$ .

## 4.2 Periodic Table

The elucidation of the nature of the periodic variation of properties, observed in the series of elements when they are placed in order of increasing atomic number (D. I. Mendeleev 1869) [85], requires an examination of the peculiarities in the successive completion of the electron shells of atoms. The theory of the periodic system is due to N. Bohr (1922).

When we pass from one atom to the next, the charge is increased by unity and one electron is added to the envelope. At first sight we might expect the binding energy of each of the successively added electrons to vary monotonically as the atomic number increases. The actual variation, however, is entirely different.

In the normal state of the hydrogen atom there is only one electron, in the  $1s$  state. In the atom of the next element, helium, another  $1s$  electron is added; the binding energy of the  $1s$  electrons in the helium atom is, however, considerably greater than in the hydrogen atom. This is a natural consequence of the difference between the field in which the electron moves in the hydrogen atom and the field encountered by an electron added to the  $\text{He}^+$  ion. At large distances these fields are approximately the same, but near the nucleus with charge  $Z = 2$  the field of the  $\text{He}^+$  ion is stronger than that of the hydrogen nucleus with  $Z = 1$ . In the lithium atom ( $Z = 3$ ), the third electron enters the  $2s$  state, since no more than two electrons can be in  $1s$  states at the same time. For a given  $Z$  the  $2s$  energy level<sup>3</sup> lies above the  $1s$  level; as the nuclear charge increases, both levels become lower. In the transition from  $Z = 2$  to  $Z = 3$ , however, the former

<sup>2</sup>The requirement that  $S$  should be as large as possible can be explained as follows. Let us consider, for example, a system of two electrons. Here we can have  $S = 0$  or  $S = 1$ ; the spin 1 corresponds to an antisymmetrical coordinate wave function  $\psi(r_1, r_2)$ . For  $r_1 = r_2$ , this function vanishes; in other words, in the state with  $S = 1$  the probability of finding the two electrons close together is small. This means that their electrostatic repulsion is comparatively small, and hence the energy is less. Similarly, for a system of several electrons, the "most antisymmetrical" coordinate wave function corresponds to the greatest spin.

<sup>3</sup>In an hydrogen-like atom Bohr's formula for the energy levels is as follows:

$$E = -\frac{mZ^2e^4}{2\hbar^2(1 + m/M)} \frac{1}{n^2}, \quad (4.1)$$

where  $Ze$  is the charge of the nucleus,  $M$  its mass,  $m$  the mass of the electron, and  $n$  is the principal quantum number. We notice that the dependence on the mass of the nucleus is only very slight.

effect is predominant, and so the binding energy of the third electron in the lithium atom is considerably less than those of the electrons in the helium atom. Next, in the atoms from Be ( $Z = 4$ ) to Ne ( $Z = 10$ ), first one more  $2s$  electron and then six  $2p$  electrons are successively added. The binding energies of these electrons increase on the average, owing to the increasing nuclear charge. The next electron added, on going to the sodium atom ( $Z = 11$ ), enters the  $3s$  state, and the binding energy again diminishes markedly, since the effect of going to a higher shell predominates over that of the increase of the nuclear charge. This picture of the filling up of the electron envelope is characteristic of the whole sequence of elements. All the electron states can be divided into successively occupied groups such that, as the states of each group are occupied in a series of elements, the binding energy increases on the average, but when the states of the next group begin to be occupied the binding energy decreases noticeably. Figure 4.1 shows those ionization potentials of elements that are known from spectroscopic data; they give the binding energies of the electrons added as we pass from each element to the next.

The different states are distributed as follows into successively occupied groups:

$1s$	2 electrons
$2s\ 2p$	8 electrons
$3s\ 3p$	8 electrons
$4s\ 3d\ 4p$	18 electrons
$5s\ 4d\ 5p$	18 electrons
$6s\ 4f\ 5d\ 6p$	32 electrons
$7s\ 6d\ 5f \dots$	

The first group is occupied in H and He; the occupation of the second and third groups corresponds to the first two (short) periods of the periodic system, containing 8 elements each. Next follow two long periods of 18 elements each, and a long period containing the rare-earth elements and 32 elements in all. The final group of states is not completely occupied in the natural (and artificial transuranic) elements.

To understand the variation of the properties of the elements as the states of each group are occupied, the following property of  $d$  and  $f$  states, which distinguishes them from  $s$  and  $p$  states, is important. The curves of the effective potential energy of the centrally symmetric field (composed of the electrostatic field and the centrifugal field) for an electron in a heavy atom have a rapid and almost vertical drop to a deep minimum near the origin; they then begin to rise, and approach zero asymptotically.<sup>4</sup> For  $s$  and  $p$  states, the rising parts of these curves are very close together. This means that the electron is at approximately the same distance from the nucleus in these states. The curves for the  $d$  states, and particularly for the  $f$  states, on the other hand, pass considerably further to the left; the classically accessible region which they delimit ends considerably closer in than that for the  $s$  and  $p$  states with the same total electron energy. In other words, an electron in the  $d$  and  $f$  states is mainly much closer to the nucleus than in the  $s$  and  $p$  states.

Many properties of atoms (including the chemical properties of elements) depend principally on the outer regions of the electron envelopes. The above characteristic of the  $d$  and  $f$  states

<sup>4</sup>The Schrödinger's equation in a centrally symmetric field being:

$$\frac{\hbar^2}{2\mu} \left[ -\frac{1}{r^2} \frac{\partial}{\partial r} \left( r^2 \frac{\partial \psi}{\partial r} \right) + \frac{l^2}{r^2} \psi \right] + U(r)\psi = E\psi, \quad (4.2)$$

with  $\mu$  is the reduced mass of the two-body problem,  $\psi = R(r)Y_{l,m}(\theta, \phi)\chi_\sigma$ , the spherical harmonics satisfy  $l^2 Y_{l,m} = l(l+1)Y_{l,m}$ , here  $l$  is the orbital angular momentum operator, and  $\chi_\sigma$  is a spin  $\frac{1}{2}$  spinor. In a Coulomb field  $U(r) = -\alpha/r$  where  $\alpha = Ze^2$  and  $\mu = mM/(m+M)$  with  $m$  the electron mass and  $M$  the nucleus mass.

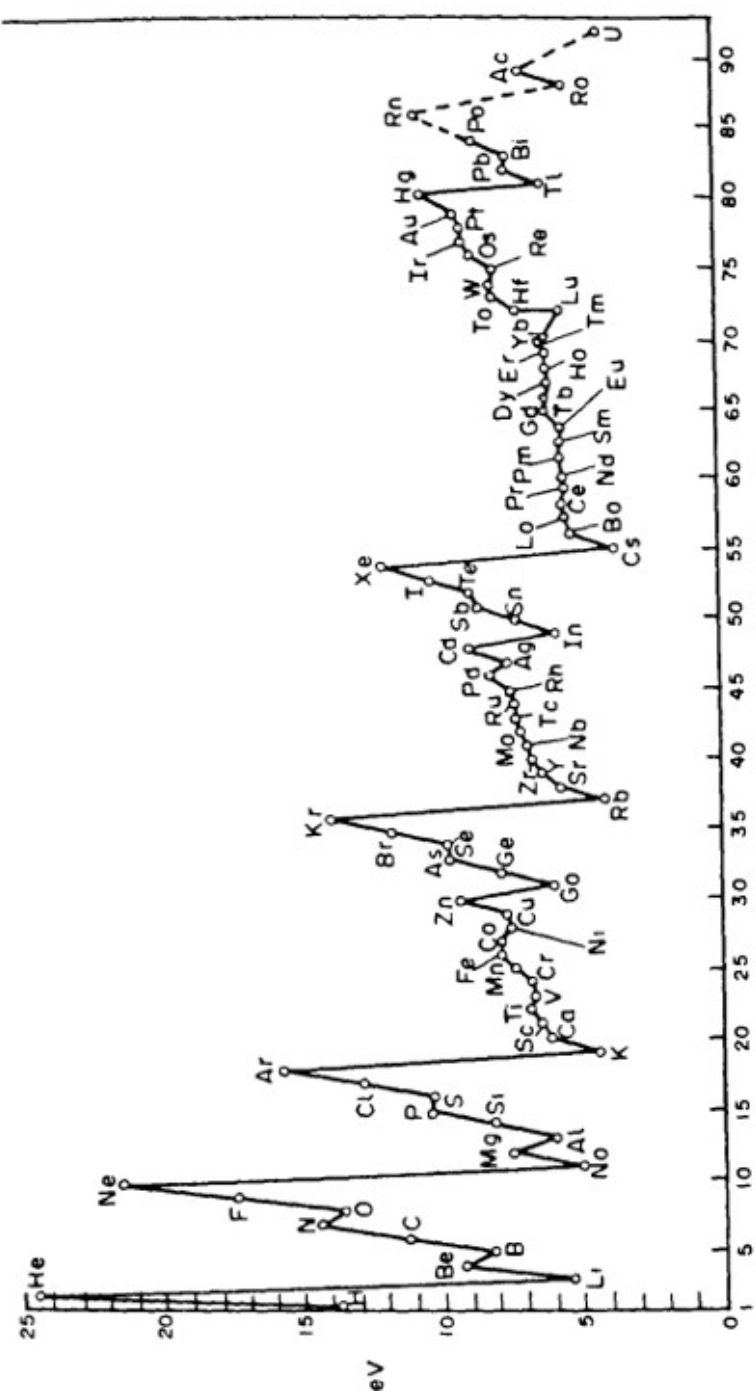


FIG. 24

Figure 4.1: Ionization potentials of elements that are known from spectroscopic data.

is very important in this connection. Thus, for instance, when the  $4f$  states are being filled (in the rare-earth elements; see below), the added electrons are located considerably closer to the nucleus than those in the states previously occupied. As a result, these electrons have practically no effect on the chemical properties, and all the rare-earth elements are chemically very similar.

The elements containing complete  $d$  and  $f$  shells (or not containing these shells at all) are called elements of the *principal groups*; those in which the filling up of these states is actually in progress are called elements of the *intermediate groups*. These groups of elements are conveniently considered separately.

## Chapter 5

# RedOx Chemical Reactions

RedOx (reduction-oxidation or oxidation-reduction) is a type of chemical reaction in which the oxidation states of the reactants change. Oxidation is the loss of electrons or an increase in the oxidation state, while reduction is the gain of electrons or a decrease in the oxidation state. The oxidation and reduction processes occur simultaneously in the chemical reaction.

Oxidation is a process in which a substance loses electrons. Reduction is a process in which a substance gains electrons. The processes of oxidation and reduction occur simultaneously and cannot occur independently. In redox processes, the reductant transfers electrons to the oxidant. Thus, in the reaction, the reductant or reducing agent loses electrons and is oxidized, and the oxidant or oxidizing agent gains electrons and is reduced. The pair of an oxidizing and reducing agent that is involved in a particular reaction is called a redox pair. A redox couple is a reducing species and its corresponding oxidizing form. The oxidation alone and the reduction alone are each called a half-reaction because two half-reactions always occur together to form a whole reaction. In electrochemical reactions the oxidation and reduction processes do occur simultaneously but are separated in space.

Electronegativity, symbolized as  $\chi$ , is the tendency for an atom of a given chemical element to attract shared electrons (or electron density) when forming a chemical bond. An atom's electronegativity is affected by both its atomic number and the distance at which its valence electrons reside from the charged nucleus. The higher the associated electronegativity, the more an atom or a substituent group attracts electrons. Electronegativity serves as a simple way to quantitatively estimate the bond energy, and the sign and magnitude of a bond's chemical polarity, which characterizes a bond along the continuous scale from covalent to ionic bonding. The loosely defined term electropositivity is the opposite of electronegativity: it characterizes an element's tendency to donate valence electrons.

On the most basic level, electronegativity is determined by factors like the nuclear charge (the more protons an atom has, the more "pull" it will have on electrons) and the number and location of other electrons in the atomic shells (the more electrons an atom has, the farther from the nucleus the valence electrons will be, and as a result, the less positive charge they will experience — both because of their increased distance from the nucleus and because the other electrons in the lower energy core orbitals will act to shield the valence electrons from the positively charged nucleus).

The term "electronegativity" was introduced by Jöns Jacob Berzelius in 1811, though the concept was known before that and was studied by many chemists including Avogadro. In spite of its long history, an accurate scale of electronegativity was not developed until 1932, when Linus Pauling proposed an electronegativity scale which depends on bond energies, as a development

of valence bond theory. [86] It has been shown to correlate with a number of other chemical properties. Electronegativity cannot be directly measured and must be calculated from other atomic or molecular properties. Several methods of calculation have been proposed, and although there may be small differences in the numerical values of the electronegativity, all methods show the same periodic trends between elements.

The most commonly used method of calculation is that originally proposed by Linus Pauling. This gives a dimensionless quantity, commonly referred to as the *Pauling scale*, on a relative scale running from 0.79 to 3.98 (hydrogen = 2.20). When other methods of calculation are used, it is conventional (although not obligatory) to quote the results on a scale that covers the same range of numerical values: this is known as an electronegativity in Pauling units.

As it is usually calculated, electronegativity is not a property of an atom alone, but rather a property of an atom in a molecule. [8] Even so, the electronegativity of an atom is strongly correlated with the first ionization energy. The electronegativity is slightly negatively correlated (for smaller electronegativity values) and rather strongly positively correlated (for most and larger electronegativity values) with the electron affinity. It is to be expected that the electronegativity of an element will vary with its chemical environment, [87] but it is usually considered to be a transferable property, that is to say that similar values will be valid in a variety of situations.

Caesium is the least electronegative element (0.79); fluorine is the most (3.98).

## 5.1 Mathematical discovery in 1D

In two Journals of Mathematical Physics, Edwards and Lenard [88, 89] have been able to study a mathematical model of a particularly simplified electron gas, one living in one dimension in the non-quantum limit and made of two oppositely charged species, and to solve its statistical physics exactly analytically. Notwithstanding the simplicity of their model, that could not undergo phase transitions<sup>1</sup>, it turned out to be rich enough to account for and predict chemical bonding. This rather amusing discovery puts them in the position of probably the first chemical physicists to describe a RedOx chemical bond. It was extraordinary how they could carry out this discovery from a purely rigorous mathematically analytic and exact point of view.

The abstract to the first paper of Lenard [88] reads:

---

<sup>1</sup>This is a rather general property shared by one dimensional many impenetrable bodies models in the non-quantum limit [90].

A system consisting of an equal number of positively and negatively charged “sheets” is considered in thermal equilibrium, with motion restricted to one dimension. The configurational part of the partition function can be represented as a sum of terms, each a simple algebraic expression. The summation is performed with the technique of generating functions. The asymptotic form in the limit of an infinite system is obtained from the pole of the generating function closest to the origin. This pole is the solution of a certain transcendental equation for which an explicit analytic representation in terms of an infinite continued fraction is available. It is shown that this equation is identical with the characteristic equation associated with the even Mathieu functions of even order.

In the limit, when the ratio of interparticle force to pressure is small, the system behaves as an ideal gas, the deviations from this state being expandable in powers of the square root of this ratio. In the opposite limit of large ratio, the particles associate in pairs of opposite charge, thus behaving like an ideal gas of neutral “molecules” which have an internal vibrational degree of freedom.

The analysis may be generalized to include the effect of a constant external electric field. For a given pressure there is a critical field which can never be surpassed without disrupting equilibrium.

The abstract to the second paper of Lenard [89] reads:

The statistical mechanics of a one-dimensional system of charged sheets is studied in the formalism of the grand canonical ensemble. It is shown that the grand partition function may be expressed as a Wiener integral, i.e., as an average of a certain functional of Brownian motion paths. This functional integral is then expressed in terms of the fundamental solution of a partial differential equation of diffusion type. This depends on a theorem of Kac whose proof is also given. The generality of this method is discussed. When all charges are integral multiples of a common unit the problem is reduced to the determination of the largest characteristic value of an ordinary differential operator with periodic coefficients. An invariance property of the thermodynamic potential is shown to imply charge neutrality in the infinite system limit: A theorem is proven which, in certain cases, excludes the possibility of a thermodynamic phase transition. The method is generalized to yield exact expressions for the  $n$ -particle reduced density functions. Some properties of the two-particle functions are discussed.

## 5.2 Mathematical discovery in 2D

Two years after Lenard discovery of clustering in a classical two component plasma living in one dimension, Salzberg and Prager [91] observed the same clustering phenomenon in the same classical two component plasma, that they call an electrolyte, but now living in two dimensions. Once again they do this in a completely analytic and exact way. They will write:

---

[Our equation of state] also seems to predict negative pressures below a critical temperature [equal to half the ionic strength]. Before this temperature is reached, however, the [partition function] becomes infinite, specifically when  $2k_B T$  [(here  $k_B$  is Boltzmann constant and  $T$  the absolute temperature)] equals the absolute product of the largest positive and the largest negative charge in the system. Possibly what happens at this point may be interpreted as ion pair formation; in any case, it seems unwise to trust [our classical equation of state] at lower temperatures without further investigation.

# Chapter 6

## The Electron Gas

A gas of electrons would be thermodynamically unstable if not made electrically neutral by introducing a uniform background of opposite charge which gives rise to a harmonic confining potential to the gas which would otherwise explode to infinity. After all we all live in a neutral world. This simplest model of an electron gas is called the *Jellium* in the quantum regime where the Fermi statistics play a role through the Pauli exclusion principle and a One Component Plasma (OCP) in the opposite classical regime where the statistics reduces to the one of Boltzmann. More complicated albeit more realistic models of an electron gas are obtained by a more detailed description of the neutralizing background. This can for example be described by a system of positive charges (ions) which again make the whole system of charges globally neutral. Therefore one can think of a Two Component Plasma (TCP) or more generally of a multicomponent one. Another important complication consists in describing the charges as not ideally pointwise but with finite dimension. The simplest system of this kind is the *primitive model* which consists of uniformly charged hard spheres of  $n$  different species. The spheres belonging to specie  $\mu = 1, 2, \dots, n$  have a diameter  $\sigma_\mu$  and carry a total charge  $z_\mu e$ , where  $e$  is the elementary charge. The spheres are globally neutral,  $\sum_\mu x_\mu z_\mu = 0$ , where  $x_\mu$  is the molar fraction of species  $\mu$ , and move in a continuum medium of dielectric constant  $\epsilon$ . One could for example study the restricted case  $\sigma_\mu = \sigma$  and  $|z_\mu| = z$  for all  $\mu$ .

These have been historically the first models examined. And for these models there exist few exact analytic results, various approximate analytic or numerical results from integral equations theories (like the Percus-Yevick, the Mean-Spherical-Approximation, the Hyper-Netted-Chain, and many others), and various exact numerical results from Monte Carlo methods. [92, 93, 94, 95]

Here we will just mention some of the few exact analytic results. Beginning from the exact solution of the one dimensional OCP of Edwards and Lenard [96] and the TCP of Salzberg and Prager where the chemical bond is analytically seen through the clustering responsible for the molecule formation [97]. An interesting exact analytic solution for the two dimensional OCP at a particular value of the coupling constant  $\Gamma = \beta e^2 = 2$  with  $\beta = 1/k_B T$ ,  $k_B$  Boltzmann constant and  $T$  absolute temperature, is available on various surface of constant curvature: The plane [98], the cylinder [99], the sphere [100], the pseudosphere [101]. And on non-constant curvature surfaces like the Flamm's paraboloid [102] .... Is the two dimensional OCP Exactly Solvable? [103]. These solutions make use of the properties of the Vandermonde determinant. At the same coupling constant a Cauchy identity allows the solution of the TCP.

In the quantum regime we do not know about any analytic exact solution. But the Jellium has been studied with Monte Carlo methods both in its ground state, at zero temperature, or at finite temperature, through path integral. In this chapter we review some recent and less recent

results in these directions on a flat space by David Ceperley and collaborators or on a curved space [104, 105].

The primitive model in the quantum regime and in two dimensions opens the new exotic field of anyons and *fractional statistics* [106, 107].<sup>1</sup>

## 6.1 The model



The *Jellium* model of Wigner [94, 108, 109, 110] is an assembly of  $N_+$  spin up pointwise electrons and  $N_-$  spin down pointwise electrons of charge  $e$  moving in a positive inert background that ensures charge neutrality. The total number of electrons is  $N = N_+ + N_-$  and the average particle number density is  $n = N/\Omega$ , where  $\Omega$  is the volume of the electron fluid. In the volume  $\Omega$  there is a uniform neutralizing background with a charge density  $\rho_b = -en$ . So that the total charge of the system is zero. The fluid polarization is then  $\xi = |N_+ - N_-|/N$ :  $\xi = 0$  in the unpolarized (paramagnetic) case and  $\xi = 1$  in the fully polarized (ferromagnetic) case.

Setting lengths in units of  $a = (4\pi n/3)^{-1/3}$  and energies in Rydberg's units,  $Ry = \hbar^2/2ma_0^2$ , where  $m$  is the electron mass and  $a_0 = \hbar^2/me^2$  is the Bohr radius, the Hamiltonian of Jellium is

$$\mathcal{H} = -\frac{1}{r_s^2} \sum_{i=1}^N \nabla_{\mathbf{r}_i}^2 + V(R), \quad (6.1)$$

$$V = \frac{1}{r_s} \left( 2 \sum_{i < j} \frac{1}{|\mathbf{r}_i - \mathbf{r}_j|} + \sum_{i=1}^N r_i^2 + v_0 \right), \quad (6.2)$$

---

<sup>1</sup>Actually in order to allow for fractional statistics in two dimensions it is sufficient that the particles be impenetrable which may be already assured even by pointwise electrons since the Coulomb repulsion diverges at contact.

where  $R = (r_1, r_2, \dots, r_N)$  with  $r_i$  the coordinate of the  $i$ th electron,  $r_s = a/a_0$ , and  $v_0$  a constant containing the self energy of the background.

The kinetic energy scales as  $1/r_s^2$  and the potential energy (particle-particle, particle-background, and background-background interaction) scales as  $1/r_s$ , so for small  $r_s$  (high electronic densities), the kinetic energy dominates and the electrons behave like an ideal gas. In the limit of large  $r_s$ , the potential energy dominates and the electrons crystallize into a Wigner crystal [111]. No liquid phase is realizable within this model since the pair-potential has no attractive parts even though a superconducting state [112] may still be possible (see chapter 8.9 of Ref. [113] and Ref. [114]).

The Jellium has been solved either by integral equation theories in its ground state [115] or by computer experiments in its ground state [116] and at finite temperature [117].

Some details on the linear response theory for the Jellium can be found in appendixes 4 and 5 of Ref. [94]. Some details on the sum rules for the dielectric function can be found in appendix 6 of Ref. [94]. Some details on the moments of density fluctuation spectrum in the plasma can be found in appendix 7 of Ref. [94]. And some details on the Lindhard theory of dynamic screening can be found in appendix 8 of Ref. [94].

### 6.1.1 Lindhard theory of static screening in Jellium ground state

Suppose we switch on an appropriately screened test charge potential  $\delta V$ , actually the so called Hartree potential, in a free electron gas.<sup>2</sup> The Hartree potential  $\delta V(r)$  created at a distance  $r$  from a static point charge of magnitude  $e$  at the origin, should be evaluated self-consistently from the Poisson equation,

$$\nabla^2 \delta V(r) = -4\pi e^2 [\delta(r) + \delta n(r)] , \quad (6.3)$$

where  $\delta n(r)$  is the change in electronic density induced by the foreign charge. The electron density  $n(r)$  may be written as

$$n(r) = 2 \sum_k |\psi_k(r)|^2 , \quad (6.4)$$

where  $\psi_k(r)$  are single-electron orbitals, the sum over  $k$  is restricted to occupied orbitals ( $|k| \leq k_F$ , where  $k_F$  is the Fermi wave vector) and the factor 2 comes from the sum over spin orientations. We must now calculate how the orbitals in the presence of the foreign charge, differ from plane waves  $\exp(ik \cdot r)$ . We use for this purpose the Schrödinger equation,

$$\nabla^2 \psi_k(r) + [k^2 - \frac{2m}{\hbar^2} \delta V(r)] \psi_k(r) = 0 , \quad (6.5)$$

having imposed that the orbitals reduce to plane waves with energy  $\hbar^2 k^2 / (2m)$  at large distance<sup>3</sup>.

With the aforementioned boundary condition the Schrödinger equation may be converted into an integral equation,

$$\psi_k(r) = \frac{1}{\sqrt{\Omega}} e^{ik \cdot r} + \frac{2m}{\hbar^2} \int G_k(r - r') \delta V(r') \psi_k(r') dr' , \quad (6.6)$$

---

<sup>2</sup>A brief review of the linear response theory to an external perturbation of the fluid is given in Appendix O.

<sup>3</sup>This approach (which lead to the Random-Phase-Approximation, RPA) is approximate insofar as the potential entering the Schrödinger equation has been taken as the Hartree potential, thus neglecting exchange and correlation between an incoming electron and the electronic screening cloud.

with  $G_{\mathbf{k}}(\mathbf{r}) = -\exp(i\mathbf{k} \cdot \mathbf{r})/(4\pi r)$  and  $\Omega$  the volume of the system.

Within linear response theory we can replace  $\psi_{\mathbf{k}}(\mathbf{r})$  by  $\Omega^{-1/2} \exp(i\mathbf{k} \cdot \mathbf{r})$  inside the integral. This yields

$$\delta n(\mathbf{r}) = -\frac{mk_F^2}{2\pi^3 \hbar^2} \int j_1(2k_F|\mathbf{r} - \mathbf{r}'|) \frac{\delta V(\mathbf{r}')}{|\mathbf{r} - \mathbf{r}'|^2} d\mathbf{r}' , \quad (6.7)$$

with  $j_1(x)$  being the first-order spherical Bessel function  $[\sin(x) - x \cos(x)]/x^2$ . Using this result in the Poisson equation we get

$$\nabla^2 \delta V(\mathbf{r}) = -4\pi e^2 \delta(\mathbf{r}) + \frac{2mk_F^2 e^2}{\pi^2 \hbar^2} \int j_1(2k_F|\mathbf{r} - \mathbf{r}'|) \frac{\delta V(\mathbf{r}')}{|\mathbf{r} - \mathbf{r}'|^2} d\mathbf{r}' , \quad (6.8)$$

which is easily soluble in Fourier transform. Writing  $\delta V(k) = 4\pi e^2/[k^2 \varepsilon(k)]$  we find,

$$\varepsilon(k) = 1 + \frac{2mk_F e^2}{\pi k^2 \hbar^2} \left[ 1 + \frac{k_F}{k} \left( \frac{k^2}{4k_F^2} - 1 \right) \ln \left| \frac{k - 2k_F}{k + 2k_F} \right| \right] , \quad (6.9)$$

which is the static dielectric function in RPA.

For  $k \rightarrow 0$  this expression gives  $\varepsilon(k) \rightarrow 1 + k_{TF}^2/k^2$  with  $k_{TF} = 3\omega_p^2/v_F^2$  ( $\omega_p$  being the plasma frequency and  $v_F$  the Fermi velocity) i.e. the result of the Thomas-Fermi theory. However  $\varepsilon(k)$  has a singularity at  $k = \pm 2k_F$ , where its derivative diverges logarithmically <sup>4</sup>. This singularity in  $\delta V(k)$  determines, after Fourier transform, the behavior of  $\delta V(r)$  at large  $r$ .  $\delta V(r)$  turns out to be an oscillating function <sup>5</sup> rather than a monotonically decreasing function as in the Thomas-Fermi theory. Indeed,

$$\delta V(r) = \int \frac{dk}{(2\pi)^3} \frac{4\pi e^2}{k^2 \varepsilon(k)} e^{ik \cdot r} = \frac{e^2}{i\pi r} \int_{-\infty}^{\infty} dk \frac{e^{ikr}}{k \varepsilon(k)} , \quad (6.10)$$

and the integrand has non-analytic behavior at  $q = \pm 2k_F$ ,

$$\left[ \frac{1}{k \varepsilon(k)} \right]_{k \rightarrow \pm 2k_F} = -A(k - (\pm)2k_F) \ln |k - (\pm)2k_F| + \text{regular terms} , \quad (6.11)$$

with  $A = (k_{TF}^2/4k_F^2)/(k_{TF}^2 + 8k_F^2)$ . Hence,

$$\begin{aligned} \delta V(r)|_{r \rightarrow \infty} &= -\frac{Ae^2}{i\pi r} \int_{-\infty}^{\infty} dk e^{ikr} [(k - 2k_F) \ln |k - 2k_F| \\ &\quad + (k + 2k_F) \ln |k + 2k_F|] = -2Ae^2 \frac{\cos(2k_F r)}{r^3} . \end{aligned} \quad (6.12)$$

This result is based on a theorem on Fourier transforms <sup>6</sup>, stating that the asymptotic behavior of  $\delta V(r)$  is determined by the low- $k$  behavior as well as the singularities of  $\delta V(k)$ . Obviously, in the present case the asymptotic contribution from the singularities is dominant over the exponential decay of Thomas-Fermi type. The result implies that the screened ion-ion interaction in a metal has oscillatory character and ranges over several shells of neighbors.

<sup>4</sup>The discontinuity in the momentum distribution across the Fermi surface introduces a singularity in elastic scattering processes with momentum transfer equal to  $2k_F$ .

<sup>5</sup>J. Friedel, *N. Cimento Suppl.* **7**, 287 (1958).

<sup>6</sup>M. Lighthill, "Introduction to Fourier Analysis and Generalized Functions" (University Press, Cambridge 1958)

### 6.1.2 Ewald sums

Periodic boundary conditions are necessary for extrapolating results of the finite system to the thermodynamic limit. Suppose the bare pair-potential, in infinite space, is  $v(r)$ ,

$$v(r) = \int \frac{d\mathbf{k}}{(2\pi)^3} e^{-i\mathbf{k}\cdot\mathbf{r}} \tilde{v}(\mathbf{k}) , \quad \tilde{v}(\mathbf{k}) = \int d\mathbf{r} e^{i\mathbf{k}\cdot\mathbf{r}} v(\mathbf{r}) . \quad (6.13)$$

The best pair-potential of the finite system is given by

$$v_I(\mathbf{r}) = \sum_{\mathbf{L}} v(|\mathbf{r} + \mathbf{L}|) - \tilde{v}(0)/\Omega . \quad (6.14)$$

where the  $\mathbf{L}$  sum is over the Bravais lattice of the simulation cell  $\mathbf{L} = (m_x L, m_y L, m_z L)$  where  $m_x, m_y, m_z$  range over all positive and negative integers and  $\Omega = L^3$ . We have also added a uniform background of the same density but opposite charge. Converting this to  $k$ -space and using the Poisson sum formula we get

$$v_I(\mathbf{r}) = \frac{1}{\Omega} \sum'_{\mathbf{k}} \tilde{v}(\mathbf{k}) e^{-i\mathbf{k}\cdot\mathbf{r}} , \quad (6.15)$$

where the prime indicates that we omit the  $\mathbf{k} = 0$  term; it cancels out with the background. The  $\mathbf{k}$  sum is over reciprocal lattice vectors of the simulation box  $\mathbf{k}_n = (2\pi n_x/L, 2\pi n_y/L, 2\pi n_z/L)$  where  $n_x, n_y, n_z$  range over all positive and negative integers.

Because both sums, Eq. (6.14) and Eq. (6.15), are so poorly convergent [118] we follow the scheme put forward by Natoli *et al.* [119] for approximating the image potential by a sum in  $k$ -space and a sum in  $r$ -space,

$$v_a(\mathbf{r}) = \sum_{\mathbf{L}} v_s(|\mathbf{r} + \mathbf{L}|) + \sum_{|\mathbf{k}| \leq k_c} v_l(k) e^{i\mathbf{k}\cdot\mathbf{r}} - \tilde{v}(0)/\Omega , \quad (6.16)$$

where  $v_s(r)$  is chosen to vanish smoothly as  $r$  approaches  $r_c$ , where  $r_c$  is less than half of the distance across the simulation box in any direction. If either  $r_c$  or  $k_c$  go to infinity then  $v_a \rightarrow v_I$ . Natoli *et al.* show that in order to minimize the error in the potential, it is appropriate to minimize  $\chi^2 = \int_{\Omega} [v_I(r) - v_a(r)]^2 dr/\Omega$ . And choose for  $v_s(r)$  an expansion in a fixed number of radial functions. This same technique has also been applied to treat the pseudo-potential described in section 6.2.3.

Now let us work with  $N$  particles of charge  $e$  in a periodic box and let us compute the total potential energy of the unit cell. Particles  $i$  and  $j$  are assumed to interact with a potential  $e^2 v(r_{ij}) = e^2 v(|\mathbf{r}_i - \mathbf{r}_j|)$ . The potential energy for the  $N$  particle system is

$$V = \sum_{i < j} e^2 v_I(r_{ij}) + \sum_i e^2 v_M , \quad (6.17)$$

where  $v_M = \frac{1}{2} \lim_{r \rightarrow 0} [v_I(r) - v(r)]$  is the interaction of a particle with its own images; it is a Madelung constant [94] for particle  $i$  interacting with the perfect lattice of the simulation cell. If this term were not present, particle  $i$  would only see  $N - 1$  particles in the surrounding cells instead of  $N$ .

## 6.2 Jellium in its ground state

The ground state properties of Jellium has been for the first time found by Ceperley and Alder [116] through a diffusion Monte Carlo method [120]. Since then better wave-functions and

optimization methods have been developed, better schemes to minimize finite-size effect have been devised, and vastly improved computational facilities are available. Today, new modern techniques are available to optimize Slater-Jastrow wave-functions [121] with backflow and three-body correlations [122] and Helmann and Feynman (HF) measures [123] to calculate the RDF, particularly the on-top value, which suffers from poor statistical sampling in its conventional histogram implementation. Other useful tools are the twist-averaged boundary conditions [124] and RPA-based corrections [125] to minimize finite-size effects.

### 6.2.1 Monte Carlo simulation (Diffusion)

Consider the Schrödinger equation for the many-body wave-function,  $\phi(R, t)$  (the wave-function can be assumed to be real, since both the real and imaginary parts of the wave-function separately satisfy the Schrödinger equation), in imaginary time, with a constant shift  $E_T$  in the zero of the energy. This is a diffusion equation in a  $3N$ -dimensional space [126]. If  $E_T$  is adjusted to be the ground-state energy,  $E_0$ , the asymptotic solution is a steady state solution, corresponding to the ground-state eigenfunction  $\phi_0(R)$  (provided  $\phi(R, 0)$  is not orthogonal to  $\phi_0$ ).

Solving this equation by a random-walk process with branching is inefficient, because the branching rate, which is proportional to the total potential  $V(R)$ , can diverge to  $+\infty$ . This leads to large fluctuations in the weights of the diffusers and to slow convergence when calculating averages. However, the fluctuations, and hence the statistical uncertainties, can be greatly reduced [127] by the technique of importance sampling [128].

One simply multiplies the Schrödinger equation by a known trial wave-function  $\Psi(R)$  that approximate the unknown ground-state wave-function, and rewrites it in terms of a new probability distribution

$$f(R, t) = \phi(R, t)\Psi(R) , \quad (6.18)$$

whose normalization is given in Eq. (I.1). This leads to the following diffusion equation

$$-\frac{\partial f(R, t)}{\partial t} = -\lambda \nabla^2 f(R, t) + [E_L(R) - E_T]f(R, t) + \lambda \nabla \cdot [f(R, t)\mathbf{F}(R)] . \quad (6.19)$$

Here  $\lambda = \hbar^2/(2m)$ ,  $t$  is the imaginary time measured in units of  $\hbar$ ,  $E_L(R) = [H\Psi(R)]/\Psi(R)$  is the local energy of the trial wave-function, and

$$\mathbf{F}(R) = \nabla \ln \Psi^2(R) . \quad (6.20)$$

The three terms on the right hand side of Eq. (6.19) correspond, from left to right, to diffusion, branching, and drifting, respectively.

At sufficiently long times the solution to Eq. (6.19) is

$$f(R, t) \approx N_0 \Psi(R) \phi_0(R) \exp[-(E_0 - E_T)t] , \quad (6.21)$$

where  $N_0 = \int \phi_0(R)\phi(R, 0) dR$ . If  $E_T$  is adjusted to be  $E_0$ , the asymptotic solution is a stationary solution and the average  $\langle E_L(R) \rangle_f$  of the local energy over the stationary distribution gives the ground-state energy  $E_0$ . If we set the branching to zero  $E_L(R) = E_T$  then this average would be equal to the expectation value  $\int \Psi(R)H\Psi(R) dR$ , since the stationary solution to Eq. (6.19) would then be  $f = f_{\text{vmc}} = \Psi^2$ . In other words, without branching we would obtain the variational energy of  $\Psi$ , rather than  $E_0$ , as in a Variational Monte Carlo (VMC) calculation.

The time evolution of  $f(R, t)$  is given by

$$f(R', t + \tau) = \int dR G(R', R; \tau) f(R, t) , \quad (6.22)$$

where the Green's function  $G(R', R; \tau) = \Psi(R')\langle R' | \exp[-\tau(H - E_T)]|R\rangle\Psi^{-1}(R)$  is a transition probability for moving the set of coordinates from  $R$  to  $R'$  in a time  $\tau$ . Thus  $G$  is a solution of the same differential equation, Eq. (6.19), but with the initial condition  $G(R', R; 0) = \delta(R' - R)$ . For short times  $\tau$  an approximate solution for  $G$  is

$$G(R', R; \tau) = (4\pi\lambda\tau)^{-3N/2} e^{-|R' - R - \lambda\tau\mathbf{F}(R)|^2/4\lambda\tau} e^{-\tau\{(E_L(R) + E_L(R'))/2 - E_T\}} + O(\tau^2). \quad (6.23)$$

To compute the ground-state energy and other expectation values, the  $N$ -particle distribution function  $f(R, t)$  is represented, in diffusion Monte Carlo, by an average over a time series of generations of walkers each of which consists of a fixed number of  $n_w$  walkers. A walker is a pair  $(R_\alpha, \omega_\alpha)$ ,  $\alpha = 1, 2, \dots, n_w$ , with  $R_\alpha$  a  $3N$ -dimensional particle configuration with statistical weight  $\omega_\alpha$ . At time  $t$ , the walkers represent a random realization of the  $N$ -particle distribution,  $f(R, t) = \sum_{\alpha=1}^{n_w} \omega_\alpha^t \delta(R - R_\alpha^t)$ . The ensemble is initialized with a VMC sample from  $f(R, 0) = \Psi^2(R)$ , with  $\omega_\alpha^0 = 1/n_w$  for all  $\alpha$ . Note that if the trial wave-function were the exact ground-state then there would be no branching and it would be sufficient  $n_w = 1$ . A given walker  $(R^t, \omega^t)$  is advanced in time (diffusion and drift) as  $R^{t+\tau} = R^t + \chi + \lambda\tau\nabla \ln \Psi^2(R^t)$  where  $\chi$  is a normally distributed random  $3N$ -dimensional vector with variance  $2\lambda\tau$  and zero mean [129]. In order to satisfy detailed balance we accept the move with a probability  $A(R, R'; \tau) = \min[1, W(R, R')]$ , where  $W(R, R') = [G(R, R'; \tau)\Psi^2(R')]/[G(R', R; \tau)\Psi^2(R)]$ . This step would be unnecessary if  $G$  were the exact Green's function, since  $W$  would be unity. Finally, the weight  $\omega_\alpha^t$  is replaced by  $\omega_\alpha^{t+\tau} = \omega_\alpha^t \Delta\omega_\alpha^t$  (branching), with  $\Delta\omega_\alpha^t = \exp\{-\tau[(E_L(R_\alpha^t) + E_L(R_\alpha^{t+\tau}))/2 - E_T]\}$ .

However, for the diffusion interpretation to be valid,  $f$  must always be positive, since it is a probability distribution. But we know that the many-fermions wave-function  $\phi(R, t)$ , being antisymmetric under exchange of a pair of particles of the parallel spins, must have nodes, i.e. points  $R$  where it vanishes. In the fixed-nodes approximation one restricts the diffusion process to walkers that do not change the sign of the trial wave-function. One can easily demonstrate that the resulting energy,  $\langle E_L(R) \rangle_f$ , will be an upper bound to the exact ground-state energy; the best possible upper bound with the given boundary condition [130].

A detailed description of the algorithm used for the DMC calculation can be found in Ref. [131].

### 6.2.2 Expectation values in DMC

In a DMC calculation there are various different possibilities to measure the expectation value of a physical observable, as for example the RDF. If  $\langle \mathcal{O} \rangle_f$  is the measure and  $\langle \dots \rangle_f$  the statistical average over the probability distribution  $f$  we will, in the following, use the word *estimator* to indicate the function  $\mathcal{O}$  itself, unlike the more common use of the word to indicate the usual Monte Carlo estimator  $\sum_{i=1}^N \mathcal{O}_i/\mathcal{N}$  of the average, where  $\{\mathcal{O}_i\}$  is the set obtained evaluating  $\mathcal{O}$  over a finite number  $\mathcal{N}$  of points distributed according to  $f$ . Whereas the average from different estimators must give the same result, the variance, the square of the statistical error, can be different for different estimators.

#### The local estimator and the extrapolated measure

To obtain ground-state expectation values of quantities  $\mathcal{O}$  that do not commute with the Hamiltonian we introduce the local estimator  $\mathcal{O}_L(R) = [\mathcal{O}\Psi(R)]/\Psi(R)$  and then compute the average over the DMC walk, the so called mixed measure,  $\overline{\mathcal{O}}^{\text{mix}} = \langle \mathcal{O}_L(R) \rangle_f = \int \phi_0(R) \mathcal{O}\Psi(R) dR / \int \phi_0(R) \Psi(R) dR$ . This is inevitably biased by the choice of the trial wave-function. A way to remedy to this bias is the use of the forward walking method [132, 133] or the reptation quantum

Monte Carlo method [134] to reach pure estimates. Otherwise this bias can be made of leading order  $\delta^2$ , with  $\delta = \phi_0 - \Psi$ , introducing the extrapolated measure

$$\overline{\mathcal{O}}^{\text{ext}} = 2\overline{\mathcal{O}}^{\text{mix}} - \overline{\mathcal{O}}^{\text{var}}, \quad (6.24)$$

where  $\overline{\mathcal{O}}^{\text{var}} = \langle \mathcal{O}_L \rangle_{f_{\text{vmc}}}$  is the variational measure. If the mixed measure equals the variational measure then the trial wave-function has maximum overlap with the ground-state.

### The Hellmann and Feynman measure

Toulouse *et al.* [123, 135] observed that the zero-variance property of the energy [136] can be extended to an arbitrary observable,  $\mathcal{O}$ , by expressing it as an energy derivative through the use of the Hellmann-Feynman theorem.

In a DMC calculation the Hellmann-Feynman theorem takes a form different from the one in a VMC calculation. Namely we start with the eigenvalue expression  $(H^\lambda - E^\lambda)\Psi^\lambda = 0$  for the ground-state of the perturbed Hamiltonian  $H^\lambda = H + \lambda\mathcal{O}$ , take the derivative with respect to  $\lambda$ , multiply on the right by the ground-state at  $\lambda = 0$ ,  $\phi_0$ , and integrate over the particle coordinates to get

$$\int dR \phi_0 (H^\lambda - E^\lambda) \frac{\partial \Psi^\lambda}{\partial \lambda} = \int dR \phi_0 \left( \frac{\partial E^\lambda}{\partial \lambda} - \frac{\partial H^\lambda}{\partial \lambda} \right) \Psi^\lambda. \quad (6.25)$$

Then we notice that due to the Hermiticity of the Hamiltonian, at  $\lambda = 0$  the left hand side vanishes, so that we get [137]

$$\frac{\int dR \phi_0 \mathcal{O} \Psi^\lambda}{\int dR \phi_0 \Psi^\lambda} \Big|_{\lambda=0} = \frac{\partial E^\lambda}{\partial \lambda} \Big|_{\lambda=0}. \quad (6.26)$$

This relation holds only in the  $\lambda \rightarrow 0$  limit unlike the more common form [28] which holds for any  $\lambda$ . Also it resembles Eq. (3) of Ref. [138].

Given  $E^\lambda = \int dR \phi_0(R) H^\lambda \Psi^\lambda(R) / \int dR \phi_0(R) \Psi^\lambda(R)$  the “Hellmann and Feynman” (HF) measure in a DMC calculation is

$$\overline{\mathcal{O}}^{\text{HF}} = \frac{dE^\lambda}{d\lambda} \Big|_{\lambda=0} \approx \langle \mathcal{O}_L(R) \rangle_f + \langle \Delta \mathcal{O}_L^\alpha(R) \rangle_f + \langle \Delta \mathcal{O}_L^\beta(R) \rangle_f. \quad (6.27)$$

The  $\alpha$  correction is [137]

$$\Delta \mathcal{O}_L^\alpha(R) = \left[ \frac{H\Psi'}{\Psi'} - E_L(R) \right] \frac{\Psi'(R)}{\Psi(R)}. \quad (6.28)$$

This expression coincides with Eq. (18) of Ref. [123]. In a VMC calculation this term, usually, does not contribute to the average, with respect to  $f_{\text{vmc}} = \Psi^2$ , due to the Hermiticity of the Hamiltonian. This is of course not true in a DMC calculation. We will then define a Hellmann and Feynman variational (HFv) estimator as  $\mathcal{O}^{\text{HFv}} = \mathcal{O}_L(R) + \Delta \mathcal{O}_L^\alpha(R)$ . The  $\beta$  correction is [137]

$$\Delta \mathcal{O}_L^\beta(R) = [E_L(R) - E_0] \frac{\Psi'(R)}{\Psi(R)}, \quad (6.29)$$

where  $E_0 = E^{\lambda=0}$ . Which differs from Eq. (19) of Ref. [123] by a factor of one half. This term is necessary in a DMC calculation not to bias the measure. The extrapolated Hellmann and Feynman measure will then be

$$\overline{\mathcal{O}}^{\text{HF-ext}} = 2\overline{\mathcal{O}}^{\text{HF}} - \langle \mathcal{O}^{\text{HFv}} \rangle_{f_{\text{vmc}}}. \quad (6.30)$$

Both corrections  $\alpha$  and  $\beta$  to the local estimator depends on the auxiliary function,  $\Psi' = \partial\Psi^\lambda/\partial\lambda|_{\lambda=0}$ . Of course if we had chosen  $\Psi^{\lambda=0}$ , on the left hand side of Eq. (6.27), as the exact ground state wave-function,  $\phi_0$ , instead of the trial wave-function, then both corrections would have vanished. When the trial wave-function is sufficiently close to the exact ground state function a good approximation to the auxiliary function can be obtained from first order perturbation theory for  $\lambda \ll 1$ . So the Hellmann and Feynman measure is affected by the new source of bias due to the choice of the auxiliary function independent from the bias due to the choice of the trial wave-function.

It is convenient to rewrite Eqs. (6.28) and (6.29) in terms of the logarithmic derivative  $Q(R) = \Psi'(R)/\Psi(R)$  as follows

$$\Delta\mathcal{O}_L^\alpha(R) = -\frac{1}{r_s^2} \sum_{k=1}^N [\nabla_{r_k}^2 Q(R) + 2v_k(R) \cdot \nabla_{r_k} Q(R)] , \quad (6.31)$$

$$\Delta\mathcal{O}_L^\beta(R) = [E_L(R) - E]Q(R) , \quad (6.32)$$

where  $v_k(R) = \nabla_{r_k} \ln \Psi(R)$  is the drift velocity of the trial wave-function. For each observable a specific form of  $Q$  has to be chosen.

### 6.2.3 Trial wave-function

We chose the trial wave-function of the Bijl-Dingle-Jastrow [139, 140, 141] or product form

$$\Psi(R) \propto D(R) \exp\left(-\sum_{i < j} u(r_{ij})\right) . \quad (6.33)$$

The function  $D(R)$  is the exact wave-function of the non-interacting fermions (the Slater determinant) and serves to give the trial wave-function the desired antisymmetry

$$D(R) = \frac{1}{\sqrt{N_+!}} \det(\varphi_{n,m}^+) \frac{1}{\sqrt{N_-!}} \det(\varphi_{n,m}^-) , \quad (6.34)$$

where for the fluid phase  $\varphi_{n,m}^\sigma = e^{ik_n \cdot r_m} \delta_{\sigma_m, \sigma} / \sqrt{\Omega}$  with  $k_n$  a reciprocal lattice vector of the simulation box such that  $|k_n| \leq k_F^\sigma$ ,  $\sigma$  the  $z$ -component of the spin ( $\pm 1/2$ ),  $r_m$  the coordinates of particle  $m$ , and  $\sigma_m$  its spin  $z$ -component. For the unpolarized fluid there are two separate determinants for the spin-up and the spin-down states because the Hamiltonian is spin independent. For the polarized fluid there is a single determinant. For the general case of  $N_+$  spin-up particles the polarization will be  $\xi = |N_+ - N_-|/N$  and the Fermi wave-vector for the spin-up (spin-down) particles will be  $k_F^\pm = (1 \pm \xi)^{1/3} k_F$  with  $k_F = (3\pi^2 n)^{1/3} = (9\pi/4)^{1/3} / (a_0 r_s)$  the Fermi wave-vector of the paramagnetic fluid. On the computer we fill closed shells so that  $N_\sigma$  is always odd. We only store  $k_n$  for each pair  $(k_n, -k_n)$  and use sines and cosines instead of  $\exp(ik_n \cdot r_i)$  and  $\exp(-ik_n \cdot r_j)$ .

The second factor (the Jastrow factor) includes in an approximate way the effects of particle correlations, through the “pseudo-potential”,  $u(r)$ , which is repulsive.

In the crystal phase, the orbitals are Gaussians centered around body-centered-cubic lattice sites with a width chosen variationally.

#### The pseudo-potential

Here we will consider a system where the particles interact with a bare potential

$$v_\mu(r) = \frac{\text{erf}(\mu r)}{r} , \quad (6.35)$$

whose Fourier transform is

$$\tilde{v}_\mu(k) = \frac{4\pi}{k^2} e^{-k^2/4\mu^2}, \quad (6.36)$$

so that for  $\mu \rightarrow \infty$  we recover the Jellium and in the opposite limit  $\mu \rightarrow 0$  we recover the non-interacting electron gas.

Neglecting the cross term between the Jastrow and the Slater determinant in Eq. (I.6) (third term) and the Madelung constant, the variational energy per particle can be approximated as follows,

$$\begin{aligned} e_V &= \frac{\langle E_L(R) \rangle_f}{N} = \frac{\int \Psi(R) H \Psi(R) dR}{N} \approx e_F + \frac{1}{2\Omega} \sum'_k [e^2 \tilde{v}_\mu(k) - 2\lambda k^2 \tilde{u}(k)] [S(k) - 1] + \\ &\quad \frac{1}{N\Omega^2} \sum'_{k,k'} \lambda \mathbf{k} \cdot \mathbf{k}' \tilde{u}(k) \tilde{u}(k') \langle \rho_{k+k'} \rho_{-\mathbf{k}-\mathbf{k}'} \rangle_f + \dots , \end{aligned} \quad (6.37)$$

where  $e_F = (3/5)\lambda \sum_\sigma N_\sigma(k_F^\sigma)^2/N$  is the non-interacting fermions energy per particle,  $\tilde{u}(k)$  is the Fourier transform of the pseudo-potential  $u(r)$ ,  $\tilde{v}_\mu(k) = 4\pi \exp(-k^2/4\mu^2)/k^2$  is the Fourier transform of the bare pair-potential,  $S(k)$  is the static structure factor for a given  $u(r)$  (see Sec. 6.2.4),  $\rho_k = \sum_{i=1}^N \exp(i\mathbf{k} \cdot \mathbf{r}_i)$  is the Fourier transform of the total number density  $\rho(\mathbf{r}) = \sum_i \delta(\mathbf{r} - \mathbf{r}_i)$ , and the trailing dots stand for the additional terms coming from the exclusion of the  $j = k$  term in the last term of Eq. (I.6). Next we make the Random-Phase-Approximation [56] and we keep only the terms with  $k + k' = \mathbf{0}$  in the last term. This gives

$$e_V \approx e_F + \frac{1}{2\Omega} \sum'_k \left\{ [e^2 \tilde{v}_\mu(k) - 2\lambda k^2 \tilde{u}(k)] [S(k) - 1] - 2n\lambda [k \tilde{u}(k)]^2 S(k) \right\} + \dots . \quad (6.38)$$

In the limit  $k \rightarrow 0$  we have to cancel the Coulomb singularity and we get  $\tilde{u}^2(k) = me^2 \tilde{v}_\mu(k) / (\hbar^2 n k^2) \simeq [(4\pi e^2/k^2) / (\hbar \omega_p)]^2$  (where  $\omega_p = \sqrt{4\pi n e^2/m}$  is the plasmon frequency) or in adimensional units

$$\tilde{u}(k) = \sqrt{\frac{r_s}{3}} \frac{4\pi}{k^2}, \quad \text{small } k . \quad (6.39)$$

This determines the correct behavior of  $\tilde{u}(k)$  as  $k \rightarrow 0$  or the long range behavior of  $u(r)$

$$u(r) = \sqrt{\frac{r_s}{3}} \frac{1}{r}, \quad \text{large } r . \quad (6.40)$$

Now to construct the approximate pseudo-potential, we start from the expression

$$\epsilon = e_F + \frac{1}{2\Omega} \sum'_k [e^2 \tilde{v}_\mu(k) - \mathcal{A} \lambda k^2 \tilde{u}(k)] [S(k) - 1], \quad (6.41)$$

and use the following perturbation approximation, for how  $S(k)$  depends on  $\tilde{u}(k)$  [142, 143],

$$\frac{1}{S(k)} = \frac{1}{S^x(k)} + \mathcal{B} n \tilde{u}(k), \quad (6.42)$$

where  $\mathcal{A}$  and  $\mathcal{B}$  are constant to be determined and  $S^x(k)$  the structure factor for the non-interacting fermions (see Eq. (K.5)), which is  $S^x = \sum_\sigma S_{\sigma,\sigma}^x$  with

$$S_{\sigma,\sigma}^x(k) = \begin{cases} \frac{n_\sigma}{n} \frac{y_\sigma}{2} (3 - y_\sigma^2) & y_\sigma < 1 \\ \frac{n_\sigma}{n} & \text{else} \end{cases} \quad (6.43)$$

where  $n_\sigma = N_\sigma/\Omega$  and  $y_\sigma = k/(2k_F^\sigma)$ .

Minimizing  $\epsilon$  with respect to  $u(k)$ , we obtain [144]

$$\mathcal{B}n\tilde{u}(k) = -\frac{1}{S^x(k)} + \left[ \frac{1}{S^x(k)} + \frac{\mathcal{B}ne^2\tilde{v}_\mu(k)}{\lambda\mathcal{A}k^2} \right]^{1/2}, \quad (6.44)$$

This form is optimal at both long and short distances but not necessarily in between. In particular, for any value of  $\xi$ , the small  $k$  behavior of  $\tilde{u}(k)$  is  $\sqrt{2r_s/3\mathcal{A}\mathcal{B}}(4\pi/k^2)$  which means that

$$u(r) = \sqrt{\frac{2r_s}{3\mathcal{A}\mathcal{B}}} \frac{1}{r}, \quad \text{large } r. \quad (6.45)$$

The large  $k$  behavior of  $\tilde{u}(k)$  is  $(r_s/\mathcal{A})\tilde{v}_\mu(k)/k^2$ , for any value of  $\xi$ , which in  $r$  space translates into

$$\frac{du(r)}{dr} \Big|_{r=0} = \begin{cases} -\frac{r_s}{2\mathcal{A}} & \mu \rightarrow \infty \\ 0 & \mu \text{ finite} \end{cases} \quad (6.46)$$

In order to satisfy the cusp condition for particles of antiparallel spins (any reasonable pseudo-potential has to obey to the cusp conditions (see Ref. [121] Section IVF) which prevent the local energy from diverging whenever any two electrons ( $\mu = \infty$ ) come together) we need to choose  $\mathcal{A} = 1$ , then the correct behavior at large  $r$  (6.39) is obtained fixing  $\mathcal{B} = 2$ <sup>7</sup>. We will call this Jastrow  $\mathcal{J}_1$  in the following.

It turns out that, at small  $\mu$ , but not for the Coulomb case, a better choice is given by [145]

$$2n\tilde{u}(k) = -\frac{1}{S^x(k)} + \left[ \left( \frac{1}{S^x(k)} \right)^2 + \frac{2ne^2\tilde{v}_\mu(k)}{\lambda k^2} \right]^{1/2}, \quad (6.47)$$

which still has the correct long (6.45) and short (6.46) range behaviors. We will call this Jastrow  $\mathcal{J}_2$  in the following. This is expected since, differently from  $\mathcal{J}_1$ ,  $\mathcal{J}_2$  satisfies the additional exact requirement  $\lim_{\mu \rightarrow 0} u(r) = 0$ , as immediately follows from the definition (6.47). Then at small  $\mu$  (and any  $r_s$ ), the trial wave-function is expected to be very close to the stationary solution of the diffusion problem.

### The backflow and three-body correlations

As shown in Appendix I, the trial wave-function of Eq. (6.33) can be further improved by adding three-body (3B) and backflow (BF) correlations [146, 122] as follows

$$\Psi(R) = \tilde{D}(R) \exp \left[ -\sum_{i < j} \tilde{u}(r_{ij}) - \sum_{l=1}^N \mathbf{G}(l) \cdot \mathbf{G}(l) \right]. \quad (6.48)$$

Here

$$\tilde{D}(R) = \frac{1}{\sqrt{N_+!}} \det(\tilde{\varphi}_{n,m}^+) \frac{1}{\sqrt{N_-!}} \det(\tilde{\varphi}_{n,m}^-), \quad (6.49)$$

---

<sup>7</sup>Note that the probability distribution in a variational calculation is (from Eq. (6.33))  $\Psi^2(R) \propto D^2(R) \exp[-2U(R)]$  with  $U(R) = \sum_{i < j} u(r_{ij})$ . Then if one formally writes  $D^2(R) = \exp[-2W(R)]$ ,  $\Psi^2$  becomes the probability distribution for a classical fluid with potential  $W + U$  at an inverse temperature  $\beta = 2$ . Then one sees that with the choice  $\mathcal{B} = 2$ , Eq (6.42) coincides with the well known Random-Phase-Approximation in the theory of classical fluids (see Ref. [95] Section 6.5) where  $W$  is the potential of the reference fluid and  $U$  the perturbation.

with  $\tilde{\varphi}_{n,m}^\sigma = e^{ik_n \cdot x_m} \delta_{\sigma_m, \sigma} / \sqrt{\Omega}$  and  $x_m$  quasi-particle coordinates defined as

$$\mathbf{x}_i = \mathbf{r}_i + \sum_{j \neq i}^N \eta(r_{ij})(\mathbf{r}_i - \mathbf{r}_j) . \quad (6.50)$$

The displacement of the quasi-particle coordinates  $\mathbf{x}_i$  from the real coordinate  $\mathbf{r}_i$  incorporates effects of hydrodynamic backflow [147], and changes the nodes of the trial wave-function. The backflow correlation function  $\eta(r)$ , is parametrized as [122]

$$\eta(r) = \lambda_B \frac{1 + s_B r}{r_B + w_B r + r^4} , \quad (6.51)$$

which has the long-range behavior  $\sim 1/r^3$ .

Three-body correlations are included through the vector functions

$$\mathbf{G}(i) = \sum_{j \neq i}^N \xi(r_{ij})(\mathbf{r}_i - \mathbf{r}_j) . \quad (6.52)$$

We call  $\xi(r)$  the three-body correlation function which is parametrized as [148]

$$\xi(r) = a \exp \{-[(r - b)c]^2\} . \quad (6.53)$$

To cancel the two-body term arising from  $\mathbf{G}(l) \cdot \mathbf{G}(l)$ , we use  $\tilde{u}(r) = u(r) - 2\xi^2(r)r^2$

The backflow and three-body correlation functions are then chosen to decay to zero with a zero first derivative at the edge of the simulation box.

#### 6.2.4 The radial distribution function

The radial distribution function (RDF) is proportional to the probability of finding another particle of the fluid inside a spherical shell of radius  $r$  and thickness  $dr$  centered on any one particle on which you sit. This observable gives us informations about the structure of the fluid. We will see here how it can be measured in a DMC calculation. In appendix K we give some details on the determination of the RDF for the ideal gas and in appendix L we give some details on exact relationships that must be satisfied by the RDF of the interacting fluid, the *sum rules*.

##### Definition of the radial distribution function

The spin-resolved RDF is defined as [149, 93]

$$g_{\sigma, \sigma'}(\mathbf{r}, \mathbf{r}') = \frac{\left\langle \sum_{i, j \neq i} \delta_{\sigma, \sigma_i} \delta_{\sigma', \sigma_j} \delta(\mathbf{r} - \mathbf{r}_i) \delta(\mathbf{r}' - \mathbf{r}_j) \right\rangle}{n_\sigma(\mathbf{r}) n_{\sigma'}(\mathbf{r}')} , \quad (6.54)$$

$$n_\sigma(\mathbf{r}) = \left\langle \sum_{i=1}^N \delta_{\sigma, \sigma_i} \delta(\mathbf{r} - \mathbf{r}_i) \right\rangle , \quad (6.55)$$

where here, and in the following,  $\langle \dots \rangle$  will denote the expectation value respect to the ground-state. Two exact conditions follow immediately from the definition: i. the zero-moment sum rule

$$\sum_{\sigma, \sigma'} \int d\mathbf{r} d\mathbf{r}' n_\sigma(\mathbf{r}) n_{\sigma'}(\mathbf{r}') [g_{\sigma, \sigma'}(\mathbf{r}, \mathbf{r}') - 1] = -N , \quad (6.56)$$

also known as the charge (monopole) sum rule in the sequence of multipolar sum rules in the framework of charged fluids [110], ii.  $g_{\sigma,\sigma}(r, r) = 0$  due to the Pauli exclusion principle.

For the homogeneous and isotropic fluid  $n_\sigma(r) = N_\sigma/\Omega$  where  $N_\sigma$  is the number of particles of spin  $\sigma$  and  $g_{\sigma,\sigma'}$  depends only on the distance  $r = |\mathbf{r} - \mathbf{r}'|$ , so that

$$g_{\sigma,\sigma'}(r) = \frac{1}{4\pi r^2} \frac{\Omega}{N_\sigma N_{\sigma'}} \left\langle \sum_{i,j \neq i} \delta_{\sigma,\sigma_i} \delta_{\sigma',\sigma_j} \delta(r - r_{ij}) \right\rangle . \quad (6.57)$$

The total (spin-summed) radial distribution function will be

$$\begin{aligned} g(r) &= \frac{1}{n^2} \sum_{\sigma,\sigma'} n_\sigma n_{\sigma'} g_{\sigma,\sigma'}(r) \\ &= \left(\frac{1+\xi}{2}\right)^2 g_{+,+}(r) + \left(\frac{1-\xi}{2}\right)^2 g_{-,-}(r) + \frac{1-\xi^2}{2} g_{+,-}(r) . \end{aligned} \quad (6.58)$$

### From the structure to the thermodynamics

As it is well known the knowledge of the RDF gives access to the thermodynamic properties of the system. The mean potential energy per particle can be directly obtained from  $g(r)$  and the bare pair-potential  $v_\mu(r)$  as follows

$$e_p = \sum_{\sigma,\sigma'} \frac{n_\sigma n_{\sigma'}}{2n} \int dr e^2 v_\mu(r) [g_{\sigma,\sigma'}(r) - 1] , \quad (6.59)$$

where we have explicitly taken into account of the background contribution. Suppose that  $e_p(r_s)$  is known as a function of the coupling strength  $r_s$ . The virial theorem for a system with Coulomb interactions ( $v_\infty(r) = 1/r$ ) gives  $N(2e_k + e_p) = 3P\Omega$  with  $P = -d(Ne_0)/d\Omega$  the pressure and  $e_0 = e_k + e_p$  the mean total ground-state energy per particle. We then find

$$e_p(r_s) = 2e_0(r_s) + r_s \frac{de_0(r_s)}{dr_s} = \frac{1}{r_s} \frac{d}{dr_s} [r_s^2 e_0(r_s)] , \quad (6.60)$$

which integrates to

$$e_0(r_s) = e_F + \frac{1}{r_s^2} \int_0^{r_s} dr'_s r'_s e_p(r'_s) . \quad (6.61)$$

We can rewrite the ground-state energy per particle of the ideal Fermi gas, in reduced units, as

$$e_F = \left(\frac{9\pi}{4}\right)^{2/3} \frac{3}{10} \phi_5(\xi) \frac{1}{r_s^2} , \quad (6.62)$$

where  $\phi_n(\xi) = (1-\xi)^{n/3} + (1+\xi)^{n/3}$ . And for the exchange potential energy per particle in the Coulomb case

$$e_p^x = - \left(\frac{2}{3\pi^5}\right)^{1/3} \frac{9\pi}{8} \phi_4(\xi) \frac{1}{r_s} , \quad (6.63)$$

which follows from Eq. (6.59) and Eqs. (K.2)-(K.3). The expression for finite  $\mu$  can be found in Ref. [150] (see their Eqs. (15)-(16)).

### Definition of the static structure factor

If we introduce the microscopic spin dependent number density

$$\rho_\sigma(\mathbf{r}) = \sum_{i=1}^N \delta_{\sigma,\sigma_i} \delta(\mathbf{r} - \mathbf{r}_i) , \quad (6.64)$$

and its Fourier transform  $\rho_{\mathbf{k},\sigma}$ , then the spin-resolved static structure factors are defined as  $S_{\sigma,\sigma'}(\mathbf{k}) = \langle \rho_{\mathbf{k},\sigma} \rho_{-\mathbf{k},\sigma'} \rangle / N$ , which, for the homogeneous and isotropic fluid, can be rewritten as

$$S_{\sigma,\sigma'}(\mathbf{k}) = \frac{n_\sigma}{n} \delta_{\sigma,\sigma'} + \frac{n_\sigma n_{\sigma'}}{n} \int [g_{\sigma,\sigma'}(\mathbf{r}) - 1] e^{-i\mathbf{k}\cdot\mathbf{r}} d\mathbf{r} + \frac{n_\sigma n_{\sigma'}}{n} (2\pi)^3 \delta(\mathbf{k}) , \quad (6.65)$$

From now on we will ignore the delta function at  $\mathbf{k} = 0$ . The total (spin-summed) static structure factor is  $S = \sum_{\sigma,\sigma'} S_{\sigma,\sigma'}$ . Due to the charge sum rule (6.56) we must have  $\lim_{k \rightarrow 0} S(k) = 0$ . In Sec. L.2 we will show that the small  $k$  behavior of  $S(k)$  has to start from the term of order  $k^2$ .

### 6.2.5 Results for the radial distribution function and structure factor

The radial distribution function and structure factor have been calculated through DMC by Ortiz and Ballone [151]. In Fig. 6.1 we show their results for the radial distribution function and in Fig. 6.2 their results for the structure factor.

### 6.2.6 Results for the internal energy

The behavior of the internal energy of the Jellium in its ground state has been determined through DMC by Ceperley and Alder [116]. Their result is shown in Fig. 6.3. Three phases of the fluid appeared, for  $r_s < 75$  the stable phase is the one of the unpolarized Jellium, for  $75 < r_s < 100$  the one of the polarized fluid, and for  $r_s > 100$  the one of the Wigner crystal. The Wigner formula of Eq. (K.11) turns out to be a rather good approximation. They used systems from  $N = 38$  to  $N = 246$  electrons.

## 6.3 Jellium at finite temperature

For the Jellium at finite temperature it is convenient to introduce the *electron degeneracy parameter*  $\Theta = T/T_F$ , where  $T_F$  is the Fermi temperature

$$T_F = T_D \frac{(2\pi)^2}{2[(2 - \xi)\alpha_3]^{2/3}}, \quad (6.66)$$

here  $\xi$  is the polarization of the fluid that can be either  $\xi = 0$ , for the unpolarized case, and  $\xi = 1$ , for the fully polarized case,  $\alpha_3 = 4\pi/3$ , and

$$T_D = \frac{n^{2/3} \hbar^2}{m k_B}, \quad (6.67)$$

is the degeneracy temperature, for temperatures higher than  $T_D$  quantum effects are less relevant.

The state of the fluid will then depend also upon the *Coulomb coupling parameter*,  $\Gamma = e^2/r_s a_0 k_B T$  [117].

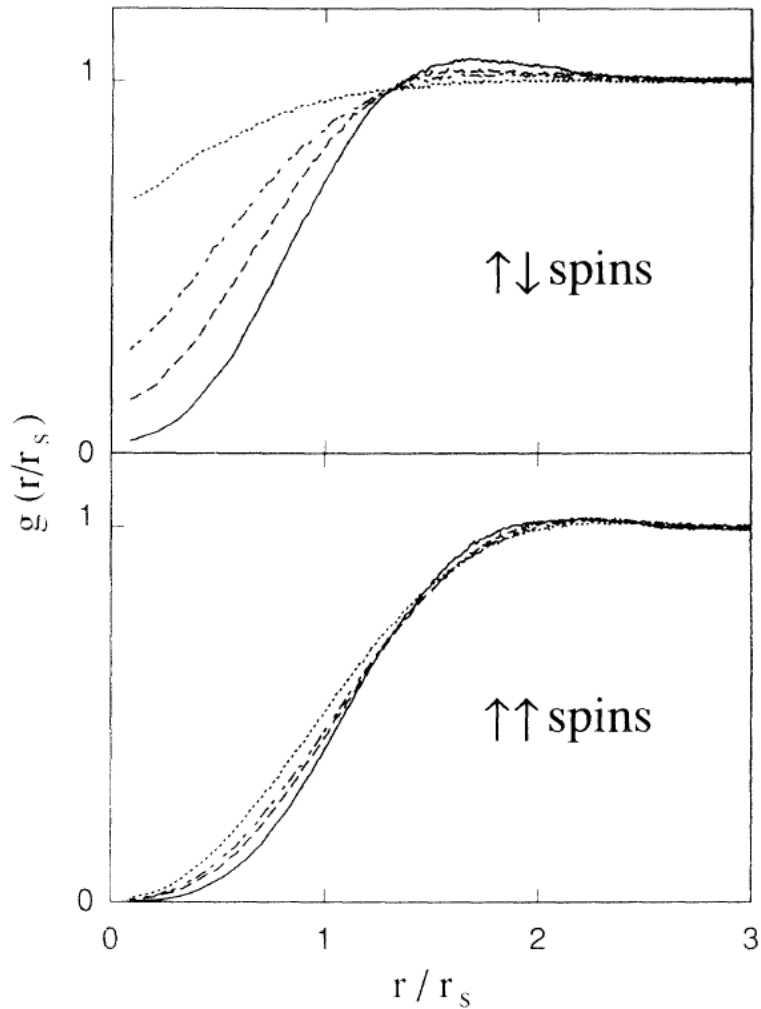


Figure 6.1: Radial distribution function  $g(r)$  computed by DMC method (mixed estimator) for the unpolarized  $\xi = 0$  case and the fully polarized  $\xi = 1$  case.  $r_s = 1$  (dotted line),  $r_s = 3$  (dash-dotted line),  $r_s = 5$  (dashed line), and  $r_s = 10$  (full line).  $r$  is in units of a Bohr radius. (Figure reproduced here by courtesy of the authors of Ref. [151])

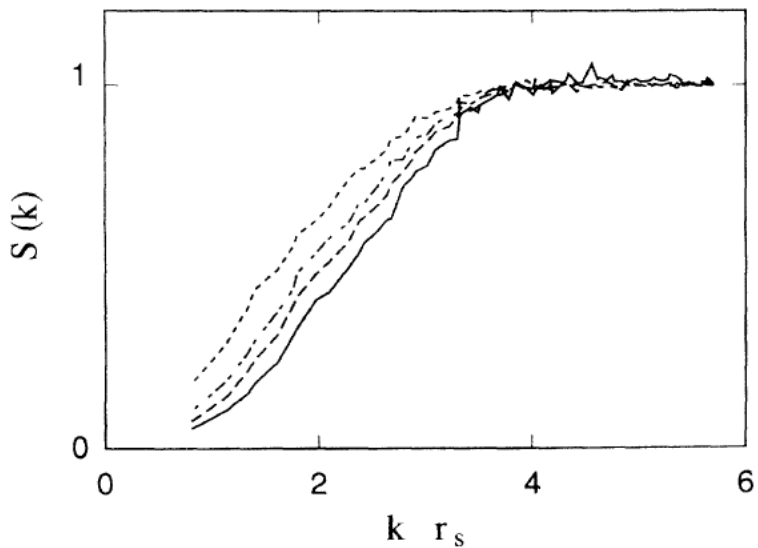


Figure 6.2: Structure factor  $S(k)$  computed by the DMC method (mixed estimator). The  $r_s$  considered and the symbols are the same as those of Fig. 6.1. (Figure reproduced here by courtesy of the authors of Ref. [151])

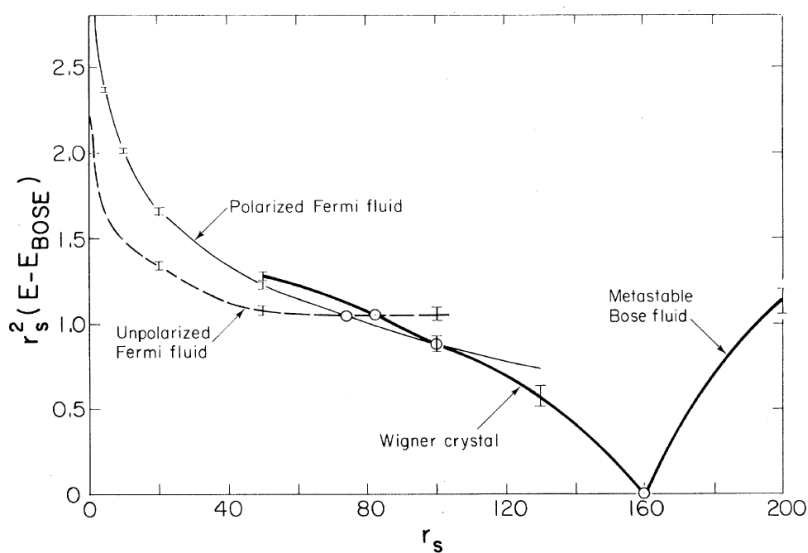


Figure 6.3: The energy of the four phases studied relative to that of the lowest boson state times  $r_s^2$  in Rydbergs as a function of  $r_s$  in Bohr radii. The boson system undergoes Wigner crystallization at  $r_s = 160 \pm 10$ . The fermion system has two phase transitions, crystallization at  $r_s = 100 \pm 20$  and depolarization at  $r_s = 75 \pm 5$ . (Figure reproduced here by courtesy of the authors of Ref. [116])

### 6.3.1 Monte Carlo simulation (Path Integral)

The *density matrix* of a many-fermion system at temperature  $k_B T = \beta^{-1}$  can be written as an integral over all paths  $\{R_t\}$

$$\rho_F(R_\beta, R_0; \beta) = \frac{1}{N!} \sum_{\mathcal{P}} (-1)^{\mathcal{P}} \oint_{\mathcal{P} R_0 \rightarrow R_\beta} dR_t \exp(-S[R_t]). \quad (6.68)$$

the path  $R(t)$  begins at  $\mathcal{P} R_0$  and ends at  $R_\beta$  and  $\mathcal{P}$  is a permutation of particles labels. For nonrelativistic particles interacting with a potential  $V(R)$  the *action* of the path,  $S[R_t]$ , is given by (see appendix M)

$$S[R_t] = \int_0^\beta dt \left[ \frac{r_s^2}{4} \left| \frac{dR(t)}{dt} \right|^2 + V(R_t) \right]. \quad (6.69)$$

Thermodynamic properties, such as the energy, are related to the diagonal part of the density matrix, so that the path returns to its starting place or to a permutation  $\mathcal{P}$  after a time  $\beta$ .

To perform Monte Carlo calculations of the integrand, one makes imaginary time discrete, so that one has a finite (and hopefully small) number of time slices and thus a classical system of  $N$  particles in  $M$  time slices; an equivalent  $NM$  particle classical system of “polymers” [34].

Note that in addition to sampling the path, the permutation is also sampled. This is equivalent to allowing the ring polymers to connect in different ways. This macroscopic “percolation” of the polymers is directly related to superfluidity as Feynman [152, 153, 154] first showed. Any permutation can be broken into cycles. Superfluid behavior can occur at low temperature when the probability of exchange cycles on the order of the system size is non-negligible. The *superfluid fraction* can be computed in a path integral Monte Carlo calculation as described in Ref. [114]. The same method could be used to calculate the *superconducting fraction* in Jellium at low temperature. However, the straightforward application of those techniques to Fermi systems means that odd permutations subtract from the integrand. This is the “fermions sign problem” [130] which will be discussed in the next section.

Thermodynamic properties are averages over the thermal  $N$ -fermion density matrix which is defined as a thermal occupation of the exact eigenstates  $\phi_i(R)$

$$\rho_F(R, R'; \beta) = \sum_i \phi_i^*(R) e^{-\beta E_i} \phi_i(R'). \quad (6.70)$$

The partition function is the trace of the density matrix

$$Z(\beta) = e^{-\beta F} = \int dR \rho_F(R, R; \beta) = \sum_i e^{-\beta E_i}. \quad (6.71)$$

Other thermodynamic averages are obtained as

$$\langle \mathcal{O} \rangle = Z(\beta)^{-1} \int dR dR' \langle R | \mathcal{O} | R' \rangle \rho(R', R; \beta). \quad (6.72)$$

Note that for any density matrix the diagonal part is always positive

$$\rho(R, R; \beta) \geq 0, \quad (6.73)$$

so that  $Z^{-1} \rho(R, R; \beta)$  is a proper probability distribution. It is the diagonal part which we need for many observables, so that probabilistic ways of calculating those observables are, in principle, possible.

Path integrals are constructed using the product property of density matrices

$$\rho(R_2, R_0; \beta_1 + \beta_2) = \int dR_1 \rho(R_2, R_1; \beta_2) \rho(R_1, R_0; \beta_1), \quad (6.74)$$

which holds for any sort of density matrix. If the product property is used  $M$  times we can relate the density matrix at a temperature  $\beta^{-1}$  to the density matrix at a temperature  $M\beta^{-1}$ . The sequence of intermediate points  $\{R_1, R_2, \dots, R_{M-1}\}$  is the path, and the time step is  $\tau = \beta/M$ . As the time step gets sufficiently small the Trotter theorem tells us that we can assume that the kinetic  $\mathcal{T}$  and potential  $\mathcal{V}$  operator commute so that:  $e^{-\tau\mathcal{H}} = e^{-\tau\mathcal{T}}e^{-\tau\mathcal{V}}$  and the primitive approximation for the Boltzmann density matrix is found [34]. The Feynman-Kac formula for the Boltzmann density matrix results from taking the limit  $M \rightarrow \infty$ . The price we have to pay for having an explicit expression for the density matrix is additional integrations; all together  $3N(M-1)$ . Without techniques for multidimensional integration, nothing would have been gained by expanding the density matrix into a path. Fortunately, simulation methods can accurately treat such integrands. It is feasible to make  $M$  rather large, say in the hundreds or thousands, and thereby systematically reduce the time-step error.

In addition to the internal energy and the static structure of the Jellium one could also measure its dynamic structure, the “superconducting fraction”, the specific heat, and the pressure [34].

### The direct path integral method

In the *direct fermion method* one sums over permutations just as bosonic systems. Odd permutations then contribute with a negative weight. The direct method has a major problem because of the cancellation of positive and negative permutations. This was first noted by Feynman and Hibbs [80] who after describing the path integral theory for boson superfluid  $^4\text{He}$ , noted: “The [path integral] expression for Fermi particles, such as  $^3\text{He}$ , is also easily written down. However in the case of liquid  $^3\text{He}$ , the effect of the potential is very hard to evaluate quantitatively in an accurate manner. The reason for this is that the contribution of a cycle to the sum over permutations is either positive or negative depending whether the cycle has an odd or an even number of atoms in its length  $L$ . At very low temperature, the contributions of cycles such as  $L = 51$  and  $L = 52$  are very nearly equal but opposite in sign, and therefore they very nearly cancel. It is necessary to compute the difference between such terms, and this requires very careful calculation of each term separately. It is very difficult to sum an alternating series of large terms which are decreasing slowly in magnitude when a precise analytic formula for each term is not available.”

Progress could be made in this problem if it were possible to arrange the mathematics describing a Fermi system in a way that corresponds to a sum of positive terms. Some such schemes have been tried, but the resulting terms appear to be much too hard to evaluate even qualitatively.

[...]

The [explanation] of the superconducting state was first answered in a convincing way by Bardeen, Cooper, and Schrieffer. The path integral approach played no part in their analysis and *in fact has never proved useful for degenerate Fermi systems. [D. M. Ceperley *italics*]“*

When we measure a property  $\mathcal{O}$  in a Monte Carlo calculation [130, 155]

$$\langle \mathcal{O} \rangle = \frac{\int \Pi \mathcal{O}}{\int \Pi}, \quad (6.75)$$

where  $\pi$  is a function with both positive and negative pieces and the integrals are not only over coordinates but a sum over permutations is also tacitly assumed.

One introduces the distribution function for the importance sampling  $P$

$$\langle \mathcal{O} \rangle = \frac{\int P[\Pi \mathcal{O}/P]}{\int P[\Pi/P]} , \quad (6.76)$$

and calculates

$$\langle \mathcal{O} \rangle = \frac{\sum_i \omega_i \mathcal{O}_i}{\sum_i \omega_i} , \quad (6.77)$$

where  $\omega_i = \Pi_i/P_i$  and the sums are over  $M$  points distributed according to  $P$ . Then the variance of the measure is

$$\begin{aligned} \sigma_{\mathcal{O}}^2 &= \left\langle \left( \frac{\sum_i \omega_i \mathcal{O}_i}{\sum_i \omega_i} - \langle \mathcal{O} \rangle \right)^2 \right\rangle_P \\ &= \frac{1}{(\sum_i \omega_i)^2} \left\langle \left[ \sum_i \omega_i (\mathcal{O}_i - \langle \mathcal{O} \rangle) \right]^2 \right\rangle_P \\ &\approx \frac{1}{(\sum_i \omega_i)^2} \left\langle \sum_i \omega_i^2 (\mathcal{O}_i - \langle \mathcal{O} \rangle)^2 \right\rangle_P \\ &= \frac{1}{M (\int \Pi)^2} \langle \omega^2 (\mathcal{O} - \langle \mathcal{O} \rangle)^2 \rangle_P \\ &= \frac{1}{M (\int \Pi)^2} \int \frac{\Pi^2 (\mathcal{O} - \langle \mathcal{O} \rangle)^2}{P} , \end{aligned} \quad (6.78)$$

where we assumed that the sampled points were uncorrelated. Choosing  $P = q^2/\int q^2$  and solving  $\delta\sigma_{\mathcal{O}}^2/\delta q = 0$  we find as the optimal distribution

$$P^* \propto |\Pi(\mathcal{O} - \langle \mathcal{O} \rangle)| . \quad (6.79)$$

The usually one chooses  $P = |\Pi|/\int |\Pi|$ . For bosons there are no problems since  $\Pi$  is everywhere positive, but for fermions one finds

$$\sigma_F^2 = \sigma_B^2/\xi , \quad (6.80)$$

where the efficiency is

$$\xi = \left[ \frac{\int \Pi}{\int |\Pi|} \right]^2 = \left[ \frac{M_+ - M_-}{M} \right]^2 = \left[ \frac{\Theta_F}{\Theta_B} \right]^2 = e^{-2\beta(\Omega_F - \Omega_B)} . \quad (6.81)$$

The average time that the simulation spend in the positive region of  $P$  is  $M_+/M$  and  $M_-/M$  is the average time spent in the negative region. The efficiency for the fermionic case is proportional to the square of the average sign: the positive sampled points in excess over the negative ones. From the expressions for the grand-thermodynamic potentials for the ideal Bose,  $\Omega_B$ , and Fermi,  $\Omega_F$ , gas we find for example

$$\xi = \begin{cases} e^{-N\rho^3\Lambda^3/(\sqrt{2}g)} & z \rightarrow 0 \\ e^{-N\rho 2g(b_{5/2}(1) - f_{5/2}(1))/\Lambda^3} & z \rightarrow 1 \end{cases} , \quad (6.82)$$

where  $b_{5/2}(1) - f_{5/2}(1) \approx 0.4743$ . We then see that for any  $z$  the efficiency becomes exponentially small in the number of particles. Moreover for a fixed  $N$  we find  $\xi = e^{-2\beta(F_F - F_B)}$ , with  $F_B$  the Helmholtz free energy of the Bose gas and  $F_F$  the one of the Fermi gas, and in the high temperature limit we find [156]

$$\xi \approx e^{-2\rho N(2\pi\lambda\beta)^{3/2}/g}. \quad (6.83)$$

Whereas in the low temperature limit

$$F_F = F_F^0 - \frac{1}{4\lambda} \frac{N}{\beta^2} \left( \frac{\pi}{3\rho} \right)^{2/3}, \quad (6.84)$$

$$F_B = -\frac{N}{\beta} \frac{b_{5/2}(1)}{b_{3/2}(1)} \left( \frac{T}{T_c} \right)^{3/2}, \quad (6.85)$$

where  $T_c \simeq T_D 2\pi/(2.612g)^{2/3}$  is the Bose-Einstein condensation temperature,  $F_F^0 = N\epsilon_F + \Omega_F^0$  with  $\epsilon_F = \mu$  the Fermi energy and  $\Omega_F^0 = -gV\epsilon_F^{5/2}/(15\pi^2\lambda^{3/2})$ , and  $N = gV(2m\epsilon_F)^{3/2}/6\pi^2\hbar^3$ . So that in the limit  $\beta \rightarrow \infty$  we find

$$\xi = e^{-2\beta F_F^0}, \quad (6.86)$$

with  $F_F^0 = g(1/6 - 1/15)V\epsilon_F^{5/2}/(\pi^2\lambda^{3/2}) > 0$ , which shows how the efficiency of a direct Monte Carlo calculation on fermions becomes exponentially small as  $\beta$  and  $N$  increases. Exactly where the physics becomes more interesting.

### Restricted Path Integral Monte Carlo

The Fermion density matrix is defined [130, 155] by the Bloch equation which describes its evolution in imaginary time

$$\frac{\partial}{\partial\beta}\rho_F(R, R_0; \beta) = -\mathcal{H}\rho_F(R, R_0; \beta), \quad (6.87)$$

$$\rho_F(R, R_0; 0) = \mathcal{A}\delta(R - R_0), \quad (6.88)$$

where  $\beta = 1/k_B T$  with  $T$  the absolute temperature and  $\mathcal{A}$  is the operator of antisymmetrization. The reach of  $R_0$ ,  $\gamma(R_0, t)$ , is the set of points  $\{R_t\}$  for which

$$\rho_F(R_{t'}, R_0; t') > 0 \quad 0 \leq t' \leq t, \quad (6.89)$$

where  $t$  is the imaginary thermal time. Note that

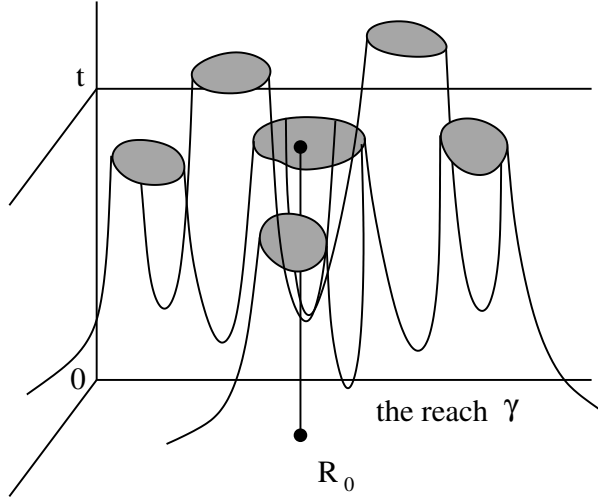
$$\rho_F(R_0, R_0; t) > 0, \quad (6.90)$$

and clearly

$$\rho_F(R, R_0; t)|_{R \in \partial\gamma(R_0, t)} = 0. \quad (6.91)$$

We want to show that (6.91) uniquely determines the solution. Suppose  $\delta(R, t)$  satisfies the Bloch equation

$$\left( \mathcal{H} + \frac{\partial}{\partial t} \right) \delta(R, t) = 0, \quad (6.92)$$

Figure 6.4: Illustration of the reach  $\gamma(R_0, t)$  of the fermion density matrix.

in a space-time domain  $\alpha = \{t_1 \leq t \leq t_1, R \in \Omega_t\}$ . And the two conditions

$$\delta(R, t_1) = 0, \quad (6.93)$$

$$\delta(R, t)|_{R \in \partial \Omega_t} = 0 \quad t_1 \leq t \leq t_2, \quad (6.94)$$

are also satisfied. Consider

$$\int_{t_1}^{t_2} dt \int_{\Omega_t} dR e^{2V_0 t} \delta(R, t) \left( \mathcal{H} + \frac{\partial}{\partial t} \right) \delta(R, t) = 0, \quad (6.95)$$

where  $V_0$  is a lower bound for  $V(R)$ .

We have

$$\frac{\partial}{\partial t} [e^{2V_0 t} \delta^2(R, t)] = 2V_0 e^{2V_0 t} \delta^2(R, t) + 2e^{2V_0 t} \delta(R, t) \frac{\partial}{\partial t} \delta(R, t). \quad (6.96)$$

Since

$$\begin{aligned} \int_{t_1}^{t_2} dt \int_{\Omega_t} dR \frac{\partial}{\partial t} \left( \frac{e^{2V_0 t}}{2} \delta^2(R, t) \right) &= \int_{t_1}^{t_2} dt \frac{\partial}{\partial t} \left( \frac{e^{2V_0 t}}{2} \int_{\Omega_t} dR \delta^2(R, t) \right) \\ &= \frac{e^{2V_0 t_2}}{2} \int_{\Omega_{t_2}} dR \delta^2(R, t_2), \end{aligned} \quad (6.97)$$

where in the last equality we used Eq. (6.93). Then from Eq. (6.95) follows

$$\frac{e^{2V_0 t}}{2} \int_{\Omega_{t_2}} dR \delta^2(R, t_2) - e^{2V_0 t} \int_{t_1}^{t_2} dt \int_{\Omega_t} dR [V_0 \delta^2(R, t) - \delta(R, t) \mathcal{H} \delta(R, t)] = 0. \quad (6.98)$$

Then using Eq. (6.94) we find

$$\frac{e^{2V_0 t}}{2} \int_{\Omega_{t_2}} dR \delta^2(R, t_2) + e^{2V_0 t} \int_{t_1}^{t_2} dt \int_{\Omega_t} dR [(V(R) - V_0) \delta^2(R, t) + \lambda (\nabla \delta(R, t))^2] = 0. \quad (6.99)$$

Each term in Eq. (6.99) is non-negative so it must be

$$\delta(R, t) = 0 \quad \text{in } \alpha. \quad (6.100)$$

Let  $\rho_1$  and  $\rho_2$  be two solutions of the restricted path problem and let  $\delta = \rho_1 - \rho_2$ . Then  $\delta(R, t)|_{R \in \partial\gamma(R_0, t)} = 0$  for  $t_1 \leq t \leq t_2$ . By taking  $t_2$  to infinity and  $t_1$  to zero we conclude that the fermion density matrix is the unique solution.

Eq (6.99) also shows that the reach  $\gamma$  has the *tiling* property [130]. Suppose it did not. Then there would exist a space-time domain with the density matrix non-zero inside and from which it is only possible to reach  $R_0$  or any of its images  $\mathcal{P}R_0$ , with  $\mathcal{P}$  any permutation of the particles, crossing the nodes of the density matrix. But such a domain cannot extend to  $t = 0$  because in the classical limit there are no nodes. Then this density matrix satisfies for some  $t_1 > 0$  the boundary conditions (6.93) and (6.94) and as a consequence it must vanish completely inside the domain contradicting the initial hypothesis.

We now derive the restricted path identity. Suppose  $\rho_F$  is the density matrix corresponding to some set of quantum numbers which is obtained by using the projection operator  $\mathcal{A}$  on the distinguishable particle density matrix. Then it is a solution to the Bloch equation (6.87) with boundary condition (6.88). Thus we have proved the *Restricted Path Integral* identity

$$\rho_F(R_\beta, R_0; \beta) = \int dR' \rho_F(R', R_0; 0) \oint_{R' \rightarrow R_\beta \in \gamma(R_0)} dR_t e^{-S[R_t]}, \quad (6.101)$$

where the subscript means that we restrict the path integration to paths starting at  $R'$ , ending at  $R_\beta$  and node-avoiding. The weight of the walk is  $\rho_F(R', R_0; 0)$ . It is clear that the contribution of all the paths for a single element of the density matrix will be of the same sign; positive if  $\rho_F(R', R_0; 0) > 0$ , negative otherwise.

Important in this argument is that the random-walk is a continuous process so we can say definitely that if sign of the density matrix changed, it had to have crossed the nodes at some point.

The restricted path identity is one solution to Feynman's task of rearranging terms to keep only positive contributing paths for diagonal expectation values.

The problem we now face is that the unknown density matrix appears both on the left-hand side and on the right-hand side of Eq. (6.101) since it is used to define the criterion of node-avoiding paths. To apply the formula directly, we would somehow have to self-consistently determine the density matrix. In practice what we need to do is make an *ansatz*, which we call  $\rho_T$ , for the nodes of the density matrix needed for the restriction. The *trial density matrix*,  $\rho_T$ , is used to define trial nodal cells:  $\gamma_T(R_0)$ .

Then if we know the reach of the fermion density matrix we can use the Monte Carlo method to solve the fermion problem restricting the path integral (RPIMC) to the space-time domain where the density matrix has a definite sign (this can be done, for example, using a trial density matrix whose nodes approximate well the ones of the true density matrix) and then using the antisymmetrization operator to extend it to the whole configuration space. This will require the complicated task of sampling the permutation space of the  $N$ -particles [34]. Recently it has been devised an intelligent method to perform this sampling through a new algorithm called the *worm* algorithm [157]. In order to sample the path in coordinate space one generally uses various generalizations of the Metropolis rejection algorithm [158] and the *bisection method* [34] in order to accomplish multislice moves which becomes necessary as  $\tau$  decreases.

The *pair-product approximation* was used [117] (see appendix N) to write the many-body density matrix as a product of high-temperature two-body density matrices [34]. The pair Coulomb density matrix was determined using the results of Pollock [159] even if these could

be improved using the results of Vieillefosse [160, 161]. This procedure comes with an error that scales as  $\sim \tau^3/r_s^2$  where  $\tau = \beta/M$  is the time step, with  $M$  the number of imaginary time discretizations. A more dominate form of time step error originates from paths which cross the nodal constraint in a time less than  $\tau$ . To help alleviate this effect, Brown *et al.* [117] use an image action to discourage paths from getting too close to nodes. Additional sources of error are the finite size one and the sampling error of the Monte Carlo algorithm itself. For the highest density points, statistical errors are an order of magnitude higher than time step errors.

The results at a given temperature  $T$  where obtained starting from the density matrix in the classical limit, at small thermal times, and using repetitively the *squaring* method

$$\rho_F(R_1, R_2; \beta) = \int dR' \rho_F(R_1, R'; \beta/2) \rho_F(R', R_2; \beta/2). \quad (6.102)$$

Time doubling is an improvement also because if we have accurate nodes down to a temperature  $T$ , we can do accurate simulations down to  $T/2$ . Eq. (6.102) is clearly symmetric in  $R_1$  and  $R_2$ . The time doubling cannot be repeated without reintroducing the sign problem.

Brown *et al.* [117] use  $N = 33$  electrons for the fully spin polarized system and  $N = 66$  electrons for the unpolarized system.

### 6.3.2 Results for the radial distribution function and structure factor

In the classical Debye-Hückel limit one has [95, 162]

$$g_{DH}(r) = \exp\left[-\frac{\Gamma}{r} \exp(-k_D r_s a_0 r)\right], \quad (6.103)$$

where  $k_D = \sqrt{4\pi\beta ne^2}$ . And for the structure factor, after linearizing Eq. (6.103) for  $r \gg 1/k_D r_s a_0$ ,

$$S_{DH}(k) = \frac{k^2}{k^2 + 3\Gamma}. \quad (6.104)$$

A serious weakness of the linearized approximation is the fact that it allows  $g(r)$  to become negative at small  $r$ . This failing is rectified in the non-linear version (6.103).

In the ground state the radial distribution function and structure factor have been calculated by Ortiz and Ballone [151].

In Fig. 6.5 we present the RPIMC results of Brown *et al.* [117].

### 6.3.3 Results for the internal energy

Given the total internal energy per particle of the fluid  $e_{tot}$ , the exchange and correlation energy per particle is

$$e_{xc}(T) = e_{tot}(T) - e_0(T). \quad (6.105)$$

where  $e_0(T)$  is the kinetic energy of a free Fermi gas at temperature  $T$ . And

$$e_{xc}(T) = e_x(T) + e_c(T). \quad (6.106)$$

where  $e_x(T)$  is the Hartree-Fock exchange energy for a Fermi gas at temperature  $T$  (see Eq. (7) of Ref. [163]).

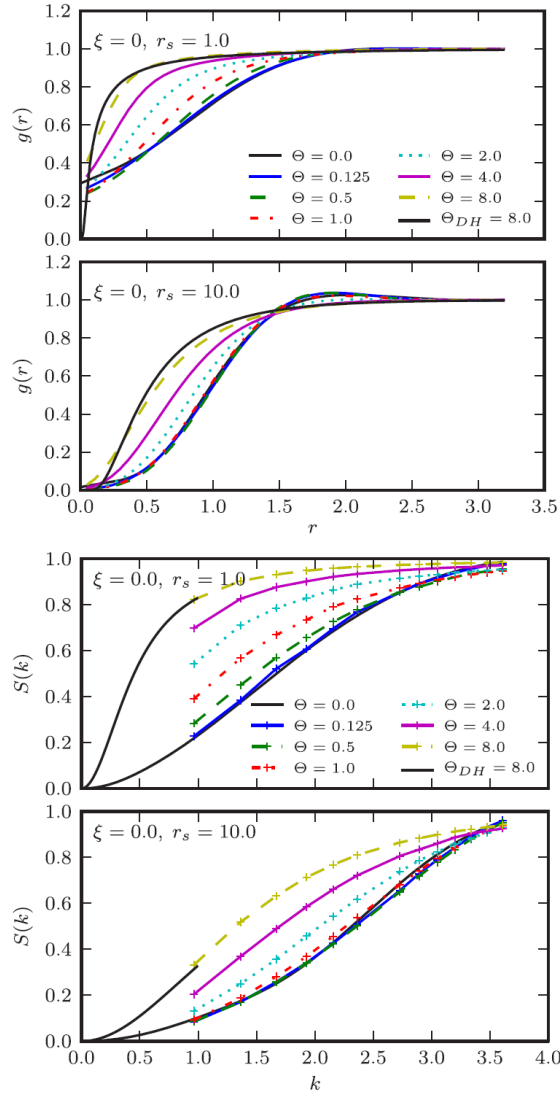


Figure 6.5: Pair correlation functions (on the left) for  $r_s = 1.0$  and  $r_s = 10.0$  in the unpolarized state. Also shown is the small  $r$  part of the classical Debye-Hückel limit at  $\Theta = 8.0$ ; see Eq. (6.103). The Debye-Hückel limit is not yet reached at  $\Theta = 8.0$  for the lower density  $r_s = 10.0$ . Static structure factors (on the right) for  $r_s = 1.0$  and  $r_s = 10.0$  in the unpolarized state. Also shown is the small  $k$  part of the classical Debye-Hückel limit at  $\Theta = 8.0$ ; see Eq. (6.104). (Figure reproduced here by courtesy of the authors of Ref. [117])

For fixed polarizations  $\xi = 0$ , the unpolarized case, and for  $\xi = 1$ , the fully polarized case, one has

$$e_0 = (2 - \xi) \frac{r_s^3}{3\pi\beta^{5/2}} \frac{1}{Ry^{5/2}} I(3/2, \kappa), \quad (6.107)$$

$$e_x = -(2 - \xi) \frac{r_s^3}{6\pi^2\beta^2} \frac{1}{Ry^2} \int_0^\infty \frac{dx}{1 + e^{x-\kappa}} \int_0^\infty \frac{dy}{1 + e^{y-\kappa}} \int_{-1}^1 \frac{dz}{\sqrt{x/y} + \sqrt{y/x} - 2z}, \quad (6.108)$$

where

$$I(\nu, \kappa) = \int_0^\infty \frac{x^\nu}{1 + e^{x-\kappa}} dx, \quad (6.109)$$

and  $\kappa$  is determined from

$$I(1/2, \kappa) = \frac{2}{3} \Theta^{-3/2}. \quad (6.110)$$

For the expressions at an intermediate polarization  $0 < \xi < 1$  see the appendix H. It is still missing an analysis of the finite temperature Jellium at intermediate polarizations. This would be important for a clearer determination of the Jellium phase diagram.

In Fig. 6.6 we present the RPIMC results of Brown *et al.* [117].

In Ref. [165] a comparison is given between these calculations to previous estimations of the Jellium correlation energy. Such parameterizations generally fall into two categories: those which extend down from the classical regime and those which assume some interpolation between the  $T = 0$  and high- $T$  regimes. From the former group, in Fig. 6.7, Brown *et al.* plot  $e_c$  coming from Debye-Hückel (DH) theory which solves for the Poisson-Boltzmann equations for the classical one component plasma and the quantum corrections of Hansen *et al.* [162, 166] of the Coulomb system both with Wigner-Kirkwood corrections (H+WK) and without (H). Clearly these methods do not perform well in the quantum regime below the Fermi temperature since they lack quantum exchange.

The Random-Phase-Approximation (RPA) [167, 168] is a reasonable approximation in the low-density, high-temperature limit (where it reduces to DH) and the low-temperature, high-density limit, since these are both weakly interacting regimes. Its failure, however, is most apparent in its estimation of the equilibrium, radial distribution function  $g(r)$  which becomes negative for stronger coupling. Extensions of the RPA into intermediate densities and temperatures have largely focused on constructing local-field corrections (LFC) through interpolation since diagrammatic resummation techniques often become intractable in strongly-coupled regimes. Singwi *et al.* [115] introduced one such strategy. Tanaka and Ichimaru [169] (TI) extended this method to finite temperatures and provided the shown parameterization of the Jellium correlation energy. This method appears to perform marginally better than the RPA at all temperatures, though it still fails to produce a positive-definite  $g(r)$  at values of  $r_s > 2$ . A third, more recent approach introduced by Perrot and Dharma-wardana (PDW) [170] relies on a classical mapping where the distribution functions of a classical system at temperature  $T_{cf}$ , solved for through the hypernetted-chain equation, reproduce those for the quantum system at temperature  $T$ . In a previous work, PDW showed such a temperature  $T_q$  existed for the classical system to reproduce the correlation energy of the quantum system at  $T = 0$  [171]. To extend this work to finite temperature quantum systems, they use the simple interpolation formula  $T_{cf} = \sqrt{T^2 + T_q^2}$ . This interpolation is clearly valid in the low- $T$  limit where Fermi liquid theory gives the quadratic dependence of the energy on  $T$ . Further in the high- $T$  regime,  $T$  dominates over  $T_q$  as the system becomes increasingly classical. The PDW line in Fig. 6.7 clearly matches

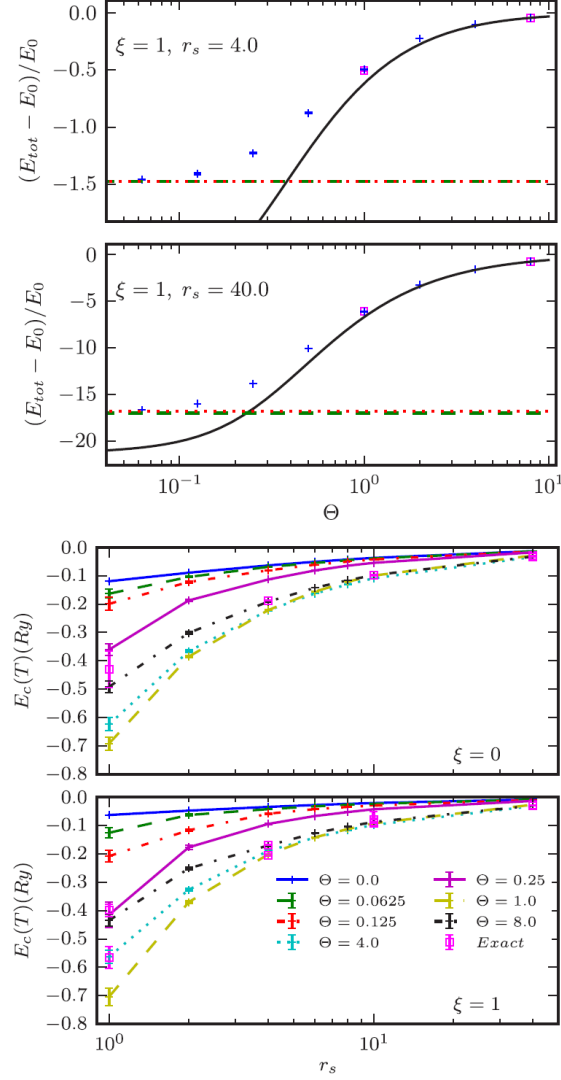


Figure 6.6: Excess energies  $E_{xc} = e_{xc}$  (on the left) for  $r_s = 4.0$  and  $r_s = 40.0$  for the polarized state ( $E_0 = e_0$ ). For both densities the high temperature results fall smoothly on top of previous Monte Carlo energies for the classical electron gas [164] (solid line). Differences from the classical Coulomb gas occur for  $\Theta < 2.0$  for  $r_s = 4.0$  and  $\Theta < 4.0$  for  $r_s = 40.0$ . Simulations with the Fermion sign (squares) confirm the fixed-node results at  $\Theta = 1.0$  and  $8.0$ . The zero-temperature limit (dotted line) smoothly extrapolates to the ground state QMC results of Ceperley-Alder [116] (dashed line). Correlation energy  $E_c(T) = e_c(T)$  (on the right) of the 3D Jellium at several temperatures and densities for the unpolarized (top) and fully spin-polarized (bottom) states. Exact (signful) calculations (squares) confirm the fixed-node results where possible ( $\Theta = 8.0$  for  $\xi = 0$  and  $\Theta = 4.0, 8.0$  for  $\xi = 1$ ). (Figure reproduced here by courtesy of the authors of Ref. [117])

well with the RPIMC results in these two limits. It is not surprising, however, that in the intermediate temperature regime, where correlation effects are greatest, the quadratic interpolation fails. A contemporary, but similar approach by Dutta and Dufty [172] uses the same classical mapping as PDW which relies on matching the  $T = 0$  pair correlation function instead of the correlation energy. While we expect this to give more accurate results near  $T = 0$ , we would still expect a breakdown of the assumed Fermi liquid behavior near the Fermi temperature. Future Jellium work will include creating a new parameterization of the correlation energy which uses the RPIMC data directly. In doing so, simulations at higher densities and both lower and higher temperatures may be necessary in order to complete the interpolation between the ground state and classical limits.

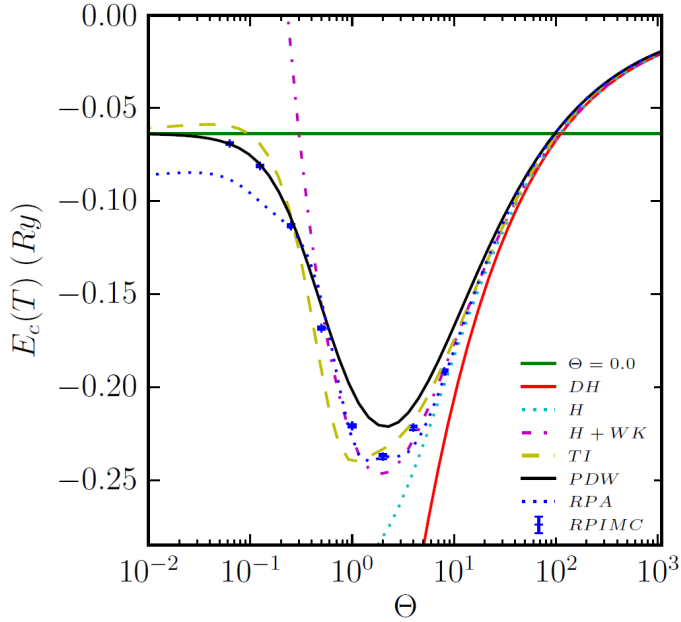


Figure 6.7: Correlation energy  $E_c(T) = e_c(T)$  of the Jellium at  $r_s = 4.0$  for the unpolarized  $\xi = 0$  state from the RPIMC calculations (RPIMC) and several previous parameterizations as a function of  $\Theta$ . The latter include Debye-Hückel (DH), Hansen (H), Hansen+Wigner-Kirkwood (H+WK), Random-Phase-Approximation (RPA), Tanaka and Ichimaru (TI), and Perrot and Dharma-wardana (PDW). Also included is the ground state  $\Theta = 0.0$  result for comparison. (Figure reproduced here by courtesy of the authors of Ref. [165])

### 6.3.4 Phase diagram

The *worm-dense* regime for both the fully spin-polarized  $\xi = 1$  and unpolarized  $\xi = 0$  systems has been studied through RPIMC by Brown *et al.* [117]. This study complements the previous Monte Carlo studies on the classical one component plasma [164] and the inclusion of first order quantum mechanical effects by Jancovici [173] and Hansen and Vieillefosse [166]. However, the accuracy of these results quickly deteriorates as the temperature is lowered and quantum correlations play a greater role [174]. This breakdown is most apparent in the *warm-dense* regime where both  $\Gamma$  and  $\Theta$  are close to unity as shown in Fig. 6.8.

In the RPIMC of Brown *et al.* [117] the trial density matrix was taken as the free electron density matrix

$$\rho_T(R, R'; \tau) = (4\pi\tau/r_s^2)^{-3N/2} \mathcal{A} \exp \left[ -\frac{(R - R')^2}{4\tau/r_s^2} \right], \quad (6.111)$$

where  $\tau = \beta/M$  with  $M$  the number of imaginary time discretizations. This approximation should be best at high temperature and low density when correlation effects are weak. The free-particle nodal approximation performs well for the densities studied by Brown *et al.* [117]. Further investigation is needed at even smaller values of  $r_s$  and lower temperatures in order to determine precisely where this approximation begins to fail. Such studies will necessarily require algorithmic improvements, however, because of difficulty in sampling paths at low density and low temperature.

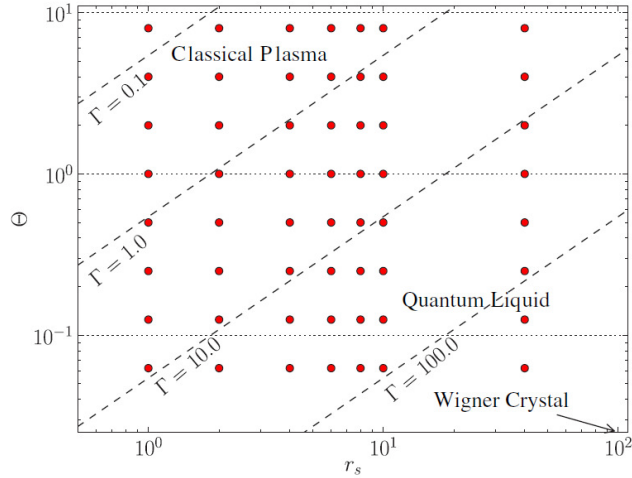


Figure 6.8: Temperature-density phase diagram showing the points considered in Ref. [117]. Several values of the Coulomb coupling parameter  $\Gamma$  (dashed lines) and the electron degeneracy parameter  $\Theta$  (dotted lines) are also shown. (Figure reproduced here by courtesy of the authors of Ref. [117])

## 6.4 Some physical realizations and phenomenology

The Jellium model is a system of pointwise electrons of charge  $e$  and number density  $n$  in the three dimensional Euclidean space filled with an uniform neutralizing background of charge density  $-en$ . The zero temperature, ground-state, properties of the statistical mechanical system thus depends just on the electronic density  $n$ , or the Wigner-Seitz radius  $r_s = (3/4\pi n)^{1/3}/a_0$  where  $a_0$  is Bohr radius, or the Coulomb coupling parameter  $\Gamma$ .

The model can be used for example as a first approximation to describe free electrons in metallic elements [35] ( $2 \lesssim r_s \lesssim 4$ ) or the interior of a white dwarf [38] ( $r_s \simeq 0.01$ ). More

generally it is an essential ingredient for the study of ionic liquids (see Ref. [95] Chapter 10 and 11): *molten-salts*, *liquid-metals*, and *ionic-solutions*. In molten alkali halides the masses of the cation and the anion are comparable whereas in liquid metals the anions are replaced by electrons from the valence or conduction bands. The very small mass of the electron leads to a pronounced disymmetry between the two species present in the metal. In particular, whereas the behavior of the cations can be discussed in the framework of classical statistical mechanics, the electron form a degenerate Fermi gas for which a quantum-mechanical treatment is required. Restricting to the class of simple metals in which the electronic valence states are well separated in energy from the tightly-bound core states; their properties are reasonably well described by the nearly-free-electron model. Metals that are classified in this sense include the alkali metals, magnesium, zinc, mercury, gallium, and aluminium. Other liquid metals (noble and transition metals, alkaline earths, lanthanides, and actinides) have more complicated electronic structures, and the theory of such systems is correspondingly less well advanced. Molten-salt solutions are mixtures of liquid metals and molten salts. Ionic-solutions are liquids consisting of a solvent formed by neutral, polar molecules, and a solute that dissociates into positive and negative ions. They vary widely in complexity: in the classic electrolyte solutions, the cations and anions are comparable in size and absolute charge, whereas macromolecular ionic solutions contain both macroions (charged polymers chains or coils, micelles, charged colloidal particles, etc.) and microscopic counterions.

Experimentally, Wigner crystallization was first unambiguously observed to occur in a quasi-classical, quasi-two-dimensional fluid of electrons floating on top of liquid  ${}^4\text{He}$  substrate [175]. Such quasi-two-dimensional electron systems are currently realized in the laboratory in various semiconductors structures, but is has proven difficult to reach the very low temperatures needed for Wigner crystallization of electrons in the quantal regime without losing their collective behavior through the unavoidable presence of impurities. Furthermore, the application of a strong magnetic field to a quasi-two-dimensional electron fluid in semiconductor structures provides a very effective way to squeeze out the translational kinetic energy without going to very low densities. The Wigner crystallization in the exactly-two-dimensional Jellium has been found by DMC calculations to be past  $r_s = 37 \pm 5$  [176].

Whereas the finite temperature properties of Jellium depends additionally on the electron degeneracy parameter  $\Theta$ . Apart from its purely speculative interest, the temperature dependence of the Jellium properties are certainly of great astrophysical relevance. Examples are dense plasmas in the interior of giant planets [177] and brown dwarfs atmospheres. Other uses could be in highly compressed laboratory plasmas, such as laser plasmas [178], inertial confinement fusion plasmas [179], and pressure-induced modifications of solids, such as insulator-metal transitions [180]. These examples justify the growing interest recently emerged in matter under extreme conditions in the warm-dense regime [181].

It would be desirable to perform a full quantum Monte Carlo simulation for the Restricted Primitive Model (RPM), an electrically neutral fluid of particles of opposite charge made thermodynamically stable by preventing the particles collapse through the inclusion of a hard core of a certain radius centered on each particle. Some attempts have been made for large mass asymmetries between the positive and negative charges requiring a mixed MC (classical) - DMC (quantum) treatment [182, 183] where one treats the slow ions through the Born-Oppenheimer approximation and the fast ones at zero temperature. Other alternatives could be a mixed MC - PIMC or more generally a full PIMC one.

Follows an excerpt from the last March and Tosi book [184].

### 6.4.1 Molten halides and some alloys of metallic elements

Unlike monatomic fluid like liquid argon already for liquid sodium it is necessary to view it as formed of positive ions and conduction electrons. More obviously, one has to start from an ionic picture in describing a sodium chloride melt or liquid lithium iodide.

The crystal structures of halide compounds arise from electronic charge transfer and local compensation of positive and negative ionic charges through chemical order. Nature achieves charge compensation in two qualitatively distinct ways. The first involves halogen sharing and high coordination for the metal ions, as for example in alkali, alkaline-earth and lanthanide metal halides. In the second type charge compensation takes place within well defined molecular units, either monomeric ones as for example in  $\text{HgCl}_2$  and  $\text{SbCl}_3$  or dimeric ones as in  $\text{AlBr}_3$ .

Neutron diffraction studies of metal halide melts have shown that melting usually preserves the type of chemical order found in the crystal. For example, the melting of  $\text{MgCl}_2$  or  $\text{YC}_3$  can be viewed as a transition from an ionic crystal to an ionic liquid (ionic-to-ionic, in short) and that of  $\text{SbCl}_3$  or  $\text{AlBr}_3$  as a molecular-to-molecular transition. However,  $\text{AlBr}_3$  and  $\text{FeCl}_3$  are known instances of ionic-to-molecular melting. Intermediate-range order (IRO), extending over distances of 5 to 10 Å say, has been revealed in both network-type and molecular-type melts. This type of order is well known in glassy materials.

#### Alkali halide vapours

Even for alkali halides, the vapour at coexistence with the hot melt is made of molecular monomers and dimers. The same basic ionic model can account for cohesion in these molecules as in the solid and dense liquid states, provided that distortions of the electron shells of the ions from electrical and overlap effects are accounted for.

#### Coulomb ordering in monohalides and dihalides

##### Alkali halides

The nature of Coulomb ordering in a molten salt like  $\text{NaCl}$  is such that the distribution of the screening charge density around any given ion oscillates in space, rather than being a monotonic function of distance as in the Debye-Hückel theory. Nevertheless, a meaningful definition of screening length in a dense ionic fluid can be based on the Debye-Hückel concept of the potential drop across the dipole layer formed by an ion and by the screening charge distribution.

##### Noble-metal halides

The monovalent  $\text{Cu}^+$  and  $\text{Ag}^+$  ions, with an outer shell of ten  $d$ -electrons, have small ionic radius and large electronic polarisability in comparison with the corresponding alkali ions. These properties lead to some hybridisation and covalent binding in copper and silver halides, tending to favor low coordination of first neighbors and promoting remarkable transport behaviors.

The ionic conductivity of solid  $\text{CuBr}$  and  $\text{CuI}$  increases rapidly with temperature, already reaching values of  $\approx 0.1 \Omega^{-1}\text{cm}^{-1}$  before attaining, through two structural phase transitions, fast-ion (superionic) behavior of the  $\text{Cu}^+$  ions before melting. A phase transition is also exhibited by  $\text{AgI}$  at  $147^\circ\text{C}$  and is accompanied by a jump in ionic conductivity to a values of  $\approx 1 \Omega^{-1}\text{cm}^{-1}$ , typical of ionic melts. The  $\text{Ag}^+$  ions in the a phase are disordered over many interstitial sites. Solid  $\text{CuCl}$ ,  $\text{AgCl}$  and  $\text{AgBr}$  also show premelting phenomena, with the ionic conductivity rising to values of  $0.1 - 0.5 \Omega^{-1}\text{cm}^{-1}$ .

These materials melt at relatively low temperature with a relatively low entropy change, while the ionic conductivity of the melt is comparable to that of molten alkali halides. Excess entropy

has been released in the crystal before melting through the massive disordering of the metal ions. Diffraction data are available for all melts of this family: overall, their liquid structure can be described in term of a random close-packing of halogens, accommodating the metal ions in tetrahedral-like coordinations.

### Fluorite-type superionic conductors

Fluorite-type materials such as SrCl<sub>2</sub> undergo a diffuse transition to a high-conductivity state before melting. The ionic conductivity and the entropy increase rapidly but continuously with temperature across the transition, whereas the heat capacity shows a peak. A high dynamic concentration of anionic Frenkel defects (interstitial-vacancy pairs) is gradually created across the transition, as revealed by neutron diffraction and diffuse quasi-elastic scattering studies on a variety of materials including SrCl<sub>2</sub>, CaF<sub>2</sub>, PbF<sub>2</sub> and UO<sub>2</sub>. In other materials, such as BaCl<sub>2</sub> and SrBr<sub>2</sub>, a superionic state is attained through a structural phase transition to the fluorite structure.

The liquid structure of BaCl<sub>2</sub> and SrCl<sub>2</sub> has been determined by neutron diffraction using isotopic substitution. In both melts, within the frame of the divalent cations, the halogen ion component is more weakly ordered. The liquid structure thus shows a remnant of the fast-ion conducting state that the solid attains through an extensive disordering of the anions.

The observed short-range ordering in molten SrCl<sub>2</sub> and BaCl<sub>2</sub> suggests that freezing may be viewed as a process in which the cationic component is independently crystallising and at the same time modulating the anions into the lattice periodicity. The anionic component in the hot crystal near melting may thus be described as a modulated “lattice liquid”. In turn, the diffuse transition from the superionic to the “normal” state on cooling the SrCl<sub>2</sub> crystal may be viewed as a continuous process of anionic freezing inside the periodic force field of the metal-ion lattice.

### Tetrahedral-network structure in ZnCl<sub>2</sub>

The pair structure is also experimentally known for a number of other dihalide melts. The evolution of the liquid structure with increasing covalency versus ionicity of the bonding brings it from a cation-dominated structure to one in which the anions provide a “deformable frame” accommodating the doubly-charged cations. The C1<sup>-</sup>-C1<sup>-</sup> structural correlations are not especially affected: the C1-C1 bond length stays in the range 3.6 to 3.8 Å.

The state of pronounced IRO in molten ZnCl<sub>2</sub> arises from strongly stable local tetrahedral structures through the formation of a network of chlorines. The partial distribution functions can be interpreted as describing a disordered close-packed arrangement of chlorine ions which provides tetrahedral sites for the Zinc ions. Such a structural arrangement is very similar to that of the glassy state of ZnCl<sub>2</sub>: the Zn-C1 bond length is practically the same in the two states and the average coordination number of Zn is reported as 3.8 in the glass and  $\approx 4$  in the melt.

#### 6.4.2 Structure of trivalent-metal halides

Two main trends emerge from liquid structure studies on trichlorides: (i) the trend from cation-dominated Coulomb ordering to loose octahedral-network structures across the series of lanthanide compounds including YCl<sub>3</sub>, and (ii) the stabilization of molecular structures with strong intermolecular correlations leading to IRO. The overall structural evolution is governed by the increasing weight of covalency versus ionicity.

### Octahedral-network formation in lanthanide chlorides

X-ray diffraction data on the series of molten rare-earth trichlorides show similar structural characters. The  $d_{MCl}$  bond length lies in the range 2.7-2.9 Å while the second-neighbor bond lengths are  $d_{MM} \approx 5$  Å and  $d_{ClCl} \approx 4$  Å, indicating a Coulomb ordering primarily ruled by the repulsion between the cations as discussed earlier for SrC<sub>12</sub>. Ionic conductivity and Raman scattering data suggest that the coordination of the metal ions is becoming more stable through the series, leading to a liquid structure which resembles a loose network of Cl-sharing octahedra.

### Ionic-to-molecular melting in AlCl<sub>3</sub> and FeCl<sub>3</sub>

YCl<sub>3</sub> is structurally isomorphous to AlCl<sub>3</sub> in the crystal phase. The octahedral coordination of the Y, Al and Fe ions in the crystal is apparent, which is basically preserved in YCl<sub>3</sub> on melting. The upper cluster illustrates the cooperative mechanism of metal-ion displacements by which the Al<sub>2</sub>C<sub>16</sub> and Fe<sub>2</sub>Cl<sub>6</sub> molecules can form on melting, each dimer being in the shape of two tetrahedra sharing an edge. In AlBr<sub>3</sub> such an arrangement of Al ions in tetrahedral sites already exists in the crystal. The melting of AlCl<sub>3</sub> and FeCl<sub>3</sub> also involves expansion of the chlorine packing.

### Liquid haloaluminates

In AlCl<sub>3</sub> and AlBr<sub>3</sub>, while the pure melt is a molecular liquid, molten-salt behavior emerges on mixing with alkali halides. Complex anions are formed with the alkalis playing the role of counterions. Thus, starting from neutral Al<sub>2</sub>C<sub>16</sub> dimers in the AlCl<sub>3</sub> liquid, the (Al<sub>2</sub>C<sub>17</sub>)<sup>-</sup> anion in the shape of two tetrahedra sharing a corner has been identified in mixtures with alkali chlorides. This anion is ultimately replaced by (AlC<sub>14</sub>)<sup>-</sup> anions at 1 : 1 stoichiometry.

The fluoroaluminates behave quite differently. The Na<sub>3</sub>AlF<sub>4</sub> compound, known as cryolite, presents special interest because of its role in the industrial Haïl-Héroult process for the electrodeposition of Al metal from alumina. The Raman spectra of molten (AlF<sub>3</sub>)<sub>c</sub>, (NaF)<sub>l-c</sub> and other Al-alkali fluoride mixtures give evidence for a gradual conversion of (AlF<sub>4</sub>)<sup>-</sup> into (AlFs)<sup>2-</sup> and (AlF<sub>6</sub>)<sup>-</sup> as the solution becomes more basic with *c* decreasing below 0.5.

### Molecular-to-molecular melting in GaCl<sub>3</sub> and SbCl<sub>3</sub>

For other trihalides, such as GaCl<sub>3</sub> and SbCl<sub>3</sub> molecular units can be recognized as constituents in the crystal structure. Crystalline GaCl<sub>3</sub> can be viewed as composed of Ga<sub>2</sub>C<sub>16</sub> dimers. The crystal structure of SbCl<sub>3</sub> is instead built by packing chains of monomers in the shape of trigonal pyramids with metal ions at the apices. The stable molecular units in the vapour phase are the Ga<sub>2</sub>C<sub>16</sub> dimer and the SbCl<sub>3</sub> monomer.

The liquid structure of SbCl<sub>3</sub> at 80 °C has been studied by a combination of X-ray and neutron diffraction. It can be described as arising from separate monomeric units with strong intermolecular correlations. Each metal ion has three additional chlorine neighbors from other molecules: such a strongly distorted octahedral arrangement could result from stacking the monomers in chains like umbrellas, the dipole axes of molecules within a chain being strongly correlated over at least one or two molecular diameters.

The neutron diffraction patterns measured for molten AlBr<sub>3</sub>, GaBr<sub>3</sub> and GaI<sub>3</sub> show three peaks at approximately 1.0, 1.9 and 3.4 Å<sup>-1</sup>. The corresponding pair distribution functions exhibit a very well defined coordination shell of first neighbors, with coordination number  $4.0 \pm 0.2$  for AlBr<sub>3</sub> and GaBr<sub>3</sub> and  $3.75 \pm 0.2$  for GaI<sub>3</sub>. The intermolecular correlations between halogens are quite significant, the corresponding coordination number being in the range typical of a random close-packing in the liquid state.

### 6.4.3 Chemical short-range order in liquid alloys

Fully ionized salts with a large band gap, like the alkali halides, remain ionic across melting. At the opposite extreme, melting of covalent semiconductors such as Ge and InSb involves a collapse of the covalent structure, which is directly revealed by an increase of coordination from 4 to values in the range 6-8 and by a sharp increase in electrical conductivity to an essentially metallic type. Between these extremes a number of systems have been identified which show a variety of intermediate electronic behavior in the liquid phase.

#### The CsAu compound

The stoichiometric CsAu compound crystallizes in the CsCl-type structure and is a strongly polar semiconductor with an optical band gap of 2.6 eV at room temperature. Its electrical conductivity drops on melting to a value which is comparable to molten salts. Electromigration experiments give evidence that Cs migrates to the cathode and Au to the anode, one  $\text{Cs}^+$  and one  $\text{Au}^-$  being transported per elementary charge to the electrodes.

A neutron diffraction study of the liquid structure of the Cs-Au alloy shows a structure in the neutron structure factor at  $k = 1.2 \text{ \AA}^{-1}$ , which is interpreted as the “Coulomb prepeak” characteristic of chemical order. After Fourier transform of these data, the Cs-Au first neighbor distance at  $3.6 \text{ \AA}$  can be followed up to 80% Cs, while the Cs-Cs distance at  $5.3 \text{ \AA}$  characteristic of the pure Cs metal start emerging at 70% Cs.

#### Other alkali-based alloys with chemical short-range order

Interspecies ordering as shown by the Cs-Au system has been reported for a number of other alkali-based alloys, the alloying partners being elements of group III, IV or V. The formation of chemical short-range order at certain compositions is signalled by anomalies in electronic properties such as the electrical resistivity and the magnetic susceptibility, which reflect a minimum in the electron density of states at the Fermi level if not the opening of a gap due to full charge transfer. Three different kinds of compound formation can be identified: (i) compound formation near the electronic octet composition  $\text{A}_4\text{B}$  as in Li-Pb or Li-Sn; (ii) compound formation near the equimolar composition AB, as in K-Pb or Rb-Pb; and (iii) compound formation near both these compositions, as in Li-Si, Li-Ge or Na-Sn. The data show increasing stability of the octet composition through the sequence Si, Ge, Sn and Pb, and decreasing stability through the sequence from Li to Cs.

A neutron diffraction measurement of the Bhatia-Thornton<sup>8</sup> concentration-structure factor in  $\text{Li}_4\text{Pb}$  has shown chemical order extending over a range of about  $20 \text{ \AA}$  in the corresponding  $g_{cc}(r)$  distribution function. With regard to alkali-group IV alloys in the second and third classes mentioned above, such as K-Pb or Na-Sn, it has proposed a model for order at equimolar composition which invokes formation of essentially tetrahedral  $\text{Pb}_4$  or  $\text{Sn}_4$  polyanions. Such tetrahedral “Zintl ions” are seen in the crystal structure of the equiatomic compound. In such a tetrahedral cluster the p-type electron states of Pb, say, would be split into bonding and antibonding states and the former could be filled by electron transfer from the alkali atoms.

The presence of polyanions in Zintl alloys also has dynamical consequences. A striking case is NaSn, in which the  $\text{Sn}_4$  polyanions are observed to undergo jump reorientations and thereby to enhance the diffusivity of the Na cations by a paddle-wheel mechanism. These two types of disorder appear simultaneously as the melting point is approached.

---

<sup>8</sup>A. B. Bhatia and D. E. Thornton, *Phys. Rev. B* **2**, 3004 (1970)

#### 6.4.4 Liquid metals

Some properties of simple liquid metals having conduction electrons in  $s$  and  $p$  states, that specifically reflect their nature as two component liquids of ions and electrons are: (i) the effective interaction between pairs of ions as determined by screening of their bare Coulomb repulsions by the conduction electrons; (ii) the structural correlation functions involving the conduction electrons and supplementing the nuclear structure factor  $S(k)$  in a full description of the liquid-metal structure; and (iii) the theory of electrical resistivity and viscosity of liquid metals. For a general account of liquid metals the book of March [185] may be consulted. in the limit when the effects of the ionic cores become negligible, we shall call the plasma particles “Jellium”.



# **Appendices**



## Appendix H

# Ideal gas energy and exchange energy as a function of polarization

For the general case of  $N_+$  spin-up particles the Fermi wave-vector for the spin-up (spin-down) particles will be

$$k_F^\pm = (1 \pm \xi)^{1/3} k_F, \quad (\text{H.1})$$

with

$$k_F = (3\pi^2 n)^{1/3} = (9\pi/4)^{1/3}/a_0 r_s, \quad (\text{H.2})$$

the Fermi wave-vector of the unpolarized fluid.

The Fermi energy will be

$$k_B T_F = \sum_{\sigma} \frac{(\hbar k_F^{\sigma})^2}{2m} \quad (\text{H.3})$$

$$= \frac{\hbar^2 [(1 + \xi)^{2/3} + (1 - \xi)^{2/3}] k_F^2}{2m}. \quad (\text{H.4})$$

The degeneracy parameter will then be

$$\Theta = \frac{2m}{\hbar^2} \left( \frac{1}{3\pi^2 n} \right)^{2/3} \left( \frac{k_B T}{[(1 + \xi)^{2/3} + (1 - \xi)^{2/3}]} \right). \quad (\text{H.5})$$

Then finding  $\kappa^+$  and  $\kappa^-$  from the following equations

$$I(1/2, \kappa^+) = \frac{2}{3} \Theta^{-3/2} \frac{(1 + \xi)}{[(1 + \xi)^{2/3} + (1 - \xi)^{2/3}]^{3/2}}, \quad (\text{H.6})$$

$$I(1/2, \kappa^-) = \frac{2}{3} \Theta^{-3/2} \frac{(1 - \xi)}{[(1 + \xi)^{2/3} + (1 - \xi)^{2/3}]^{3/2}}, \quad (\text{H.7})$$

we can determine the kinetic energy per particle of the partially polarized,  $0 < \xi < 1$ , ideal Fermi gas

$$e_0 = \frac{2r_s^3}{3\pi\beta^{5/2}} \frac{1}{Ry^{5/2}} \left[ \frac{I(3/2, \kappa^+)}{(1+\xi)} + \frac{I(3/2, \kappa^-)}{(1-\xi)} \right]. \quad (\text{H.8})$$

The exchange energy on the other hand will be

$$e_x = -\frac{r_s^3}{3\pi^2\beta^2} \frac{1}{Ry^2} \left[ \begin{aligned} & \frac{1}{(1+\xi)} \int_0^\infty \frac{dx}{1+e^{x-\kappa^+}} \int_0^\infty \frac{dy}{1+e^{y-\kappa^+}} \int_{-1}^1 \frac{dz}{\sqrt{x/y} + \sqrt{y/x} - 2z} \\ & + \frac{1}{(1-\xi)} \int_0^\infty \frac{dx}{1+e^{x-\kappa^-}} \int_0^\infty \frac{dy}{1+e^{y-\kappa^-}} \int_{-1}^1 \frac{dz}{\sqrt{x/y} + \sqrt{y/x} - 2z} \end{aligned} \right] \quad (\text{H.9})$$

## Appendix I

# Jastrow, backflow, and three-body

In terms of the stochastic process governed by  $f(R, t)$  one can write, using Kac theorem [186, 187]

$$\int dR f(R, \tau) = \left\langle \exp \left[ - \int_0^\tau dt E_L(R^t) \right] \right\rangle_{\text{DRW}}, \quad (\text{I.1})$$

where  $\langle \dots \rangle_{\text{DRW}}$  means averaging with respect to the diffusing and drifting random-walk. Choosing a complete set of orthonormal wave-functions  $\Psi_i$  we can write for the true time dependent many-body wave-function

$$\begin{aligned} \phi(R, \tau) &= \sum_i \Psi_i(R) \int dR' \Psi_i(R') \phi(R', \tau) \approx \Psi(R) \int dR f(R, \tau) \\ &= \Psi(R) \left\langle \exp \left[ - \int_0^\tau dt E_L(R^t) \right] \right\rangle_{\text{DRW}}, \end{aligned} \quad (\text{I.2})$$

where  $\Psi$  is the wave-function, of the set, of maximum overlap with the true ground-state, the trial wave-function. Assuming that at time zero we are already close to the stationary solution, for sufficiently small  $\tau$  we can approximate

$$\left\langle \exp \left[ - \int_0^\tau dt E_L(R^t) \right] \right\rangle_{\text{DRW}} \approx e^{-\tau E_L(R^\tau)}. \quad (\text{I.3})$$

By antisymmetrising we get the Fermion wave-function

$$\phi_F(R, \tau) \approx \mathcal{A} \left[ e^{-\tau E_L(R)} \Psi(R) \right], \quad (\text{I.4})$$

where given a function  $f(R)$  we define the operator (a symmetry of the Hamiltonian)

$$\mathcal{A}[f(R)] = \frac{1}{N_{\mathcal{P}}} \sum_{\mathcal{P}} (-1)^{\mathcal{P}} f(\mathcal{P}R), \quad (\text{I.5})$$

here  $N_{\mathcal{P}} = N_+!N_-!$  is the total number of allowed permutations  $\mathcal{P}$ .

This is called the local energy method to improve a trial wave-function. Suppose we start from a simple unsymmetrical product of single particle plane waves of  $N_+$  spin-up particles with

$k < k_F^+$  occupied and  $N_-$  spin-up particles with  $k < k_F^-$  occupied, for the zeroth order trial wave-function. Equation (I.4) will give us a first order wave-function of the Slater-Jastrow type (see equation (6.33)). If we start from an unsymmetrical Hartree-Jastrow trial wave-function the local energy with the Jastrow factor has the form

$$E_L = V - \lambda \sum_i \left[ -k_i^2 - 2ik_i \cdot \nabla_i \sum_{j < k} u(r_{jk}) - \nabla_i^2 \sum_{j < k} u(r_{jk}) + \left| \nabla_i \sum_{j < k} u(r_{jk}) \right|^2 \right], \quad (\text{I.6})$$

where  $V = V(R)$  is the total potential energy and  $r_{ij} = |\mathbf{r}_{ij}| = |\mathbf{r}_i - \mathbf{r}_j|$ . Then the antisymmetrized second order wave-function has the form in Eq. (6.48), which includes backflow (see the third term), which is the correction inside the determinant and which affects the nodes, and three-body boson-like correlations (see last term) which do not affect the nodes.

## Appendix J

# The Random-Phase-Approximation

In this Appendix we will work on an unpolarized system.

Within the linear density response theory [95]<sup>1</sup> one introduces the space-time Fourier transform,  $\chi(\mathbf{k}, \omega)$ , of the linear density response function. Which is related through the fluctuation dissipation theorem,  $S(\mathbf{k}, \omega) = -(2\hbar/n)\Theta(\omega)\text{Im}\chi(\mathbf{k}, \omega)$ , to the space-time Fourier transform,  $S(\mathbf{k}, \omega)$  (dynamic structure factor), of the van Hove correlation function [188],  $\langle \rho(\mathbf{r}, t)\rho(\mathbf{0}, 0) \rangle/n$ , where  $\rho(\mathbf{r}, t) = \exp(iHt/\hbar)\rho(\mathbf{r})\exp(-iHt/\hbar)$ .

In the Random-Phase-Approximation (RPA) we have [92]

$$\frac{1}{\chi_{RPA}(\mathbf{k}, \omega)} = \frac{1}{\chi_0(\mathbf{k}, \omega)} - e^2 \tilde{v}_\mu(\mathbf{k}), \quad (\text{J.1})$$

where  $\chi_0$  is the response function of the non-interacting Fermions (ideal Fermi gas), known as the Lindhard susceptibility [189]. This corresponds to taking the “proper polarizability” (the response to the Hartree potential) equal to the response of the ideal Fermi gas [190]. With the help of the fluctuation dissipation theorem,  $S_0(\mathbf{k}, \omega) = -(2\hbar/n)\Theta(\omega)\text{Im}\chi_0(\mathbf{k}, \omega)$  gives the differential cross-section for inelastic scattering from the ideal Fermi gas (at energy transfer  $\omega \geq 0$ ). Scattering is due to the excitation of single particle-hole pairs

$$S_0(\mathbf{k}, \omega) = 2\pi \sum_{\mathbf{q}, \sigma} n_{\mathbf{q}}^0 [1 - n_{\mathbf{q}+\mathbf{k}}^0] \delta \left[ \omega - \frac{1}{\hbar} (e_{\mathbf{q}+\mathbf{k}} - e_{\mathbf{q}}) \right], \quad (\text{J.2})$$

where  $e_{\mathbf{k}} = \hbar^2 k^2/(2m)$  and  $n_{\mathbf{k}}^0 = \Theta(|\mathbf{k}| - k_F)$  is the momentum distribution of the ideal Fermi gas. We thus find

$$S_0(\mathbf{k}, \omega) = \begin{cases} \hbar\pi\nu_F \frac{\omega}{kv_F} & 0 \leq \omega \leq -\omega_2(k) \\ \hbar\pi\nu_F \frac{k_F}{2k} \left[ 1 - \left( \frac{\omega}{kv_F} - \frac{k}{2k_F} \right)^2 \right] & |\omega_2(k)| \leq \omega \leq \omega_1(k) \\ 0 & \omega \geq \omega_1(k) \end{cases} \quad (\text{J.3})$$

with  $\nu_F = mk_F/(n\pi^2\hbar^2)$  the density of states for particles at the Fermi level,  $v_F = \hbar k_F/m$  the velocity of a free particle on the Fermi surface,  $\omega_1(k) = \hbar(kk_F + k^2/2)/m$ , and  $\omega_2(k) = \hbar(-kk_F + k^2/2)/m$ . Naturally we also have  $S^x(\mathbf{k}) = \int S_0(\mathbf{k}, \omega)d\omega/(2\pi)$ .

---

<sup>1</sup>Note that, unlike in the classical case, in quantum statistical physics even the linear response to a static perturbation requires the use of imaginary time correlation functions [110].

The RPA static structure factor is then recovered through

$$S_{RPA}(k) = -\frac{\hbar}{n} \int_0^\infty \frac{d\omega}{\pi} \text{Im}\chi(k, \omega). \quad (\text{J.4})$$

where

$$\text{Im}\chi = \frac{\text{Im}\chi_0}{(1 - e^2 \tilde{v}_\mu \text{Re}\chi_0)^2 + (e^2 \tilde{v}_\mu \text{Im}\chi_0)^2}, \quad (\text{J.5})$$

and

$$\text{Im}\chi_0 = -\frac{n}{2\hbar} S_0, \quad \omega > 0, \quad (\text{J.6})$$

$$\text{Re}\chi_0 = -n\nu_F \left\{ \frac{1}{2} + \frac{1 - (x - y)^2}{8y} \ln \left| \frac{x - 1 - y}{x + 1 - y} \right| + \frac{1 - (x + y)^2}{8y} \ln \left| \frac{x + 1 + y}{x - 1 + y} \right| \right\}, \quad (\text{J.7})$$

where  $x = \omega/kv_F$  and  $y = k/2k_F$ . In deriving Eq. (J.7) we used the fact that  $\text{Im}\chi_0(k, \omega)$  is an odd function of  $\omega$  and the Kramers-Kronig relations.

## Appendix K

# Analytic expressions for the non-interacting fermions ground state

Usually  $g_{\sigma,\sigma'}$  is conventionally divided into the (known) exchange and the (unknown) correlation terms

$$g_{\sigma,\sigma'} = g_{\sigma,\sigma'}^x + g_{\sigma,\sigma'}^c , \quad (\text{K.1})$$

where the exchange term corresponds to the uniform system of non-interacting fermions.

### K.1 Radial distribution function

We thus have (from the definition of the RDF (6.54) and using Slater determinants for the wave-function)

$$g_{+-}^x(r) = 1 , \quad (\text{K.2})$$

$$g_{\sigma,\sigma}^x(r) = 1 - \left[ \frac{3j_1(k_F^\sigma r)}{k_F^\sigma r} \right]^2 , \quad (\text{K.3})$$

where  $j_1(x) = [\sin(x) - x \cos(x)]/x^2$  is the spherical Bessel function of the first kind and  $(k_F^\sigma)^3 = 6\pi^2 n_\sigma$  is the Fermi wave-number for particles of spin  $\sigma$ .

### K.2 Static structure factor

Again we will have the splitting  $S_{\sigma,\sigma'} = S_{\sigma,\sigma'}^x + S_{\sigma,\sigma'}^c$  into the exchange and the correlation parts. So that for the non-interacting fermions we get

$$S_{+-}^x(k) = 0 , \quad (\text{K.4})$$

$$\begin{aligned} S_{\sigma,\sigma}^x(k) &= \frac{n_\sigma}{n} - \frac{n_\sigma^2}{n} \Theta(2k_F^\sigma - k) \frac{3\pi^2}{(k_F^\sigma)^3} \left(1 - \frac{k}{2k_F^\sigma}\right)^2 \left(2 + \frac{k}{2k_F^\sigma}\right) \\ &= \frac{n_\sigma}{n} \begin{cases} 1 & k > 2k_F^\sigma \\ \frac{3}{4} \frac{k}{k_F^\sigma} - \frac{1}{16} \left(\frac{k}{k_F^\sigma}\right)^3 & k < 2k_F^\sigma \end{cases} , \end{aligned} \quad (\text{K.5})$$

where  $\Theta(x)$  is the Heaviside step function.

### K.3 Internal energy

The Hartree-Fock approximation [191, 192, 193] for the ground state of a system of interacting fermions assumes that the many-body wave function is a Slater determinant built from single-particle states, which are to be determined self-consistently by minimization of the expectation value of the Hamiltonian. Whereas for an inhomogeneous many-electron system (e.g. an atom or a molecule) the solution of the Hartree-Fock self-consistent problem can usually be obtained only in a numerical form involving further approximations, the exact Hartree-Fock solution is immediate in the case of a homogeneous fluid: in this case the self-consistent single-particle states are necessarily plane waves, from translational invariance. Hence, the Hartree-Fock wave function for the ground-state of a homogeneous fluid is the same as the ground-state wave function of the ideal Fermi gas.

Including explicitly the spin indices we get

$$E_g^{\text{HF}} = \sum_{\mathbf{k},\sigma} n_{\mathbf{k},\sigma}^0 \left[ \epsilon_{\mathbf{k}} + \frac{1}{2} \Sigma_{\text{HF}}(\mathbf{k}) \right], \quad (\text{K.6})$$

where  $n_{\mathbf{k},\sigma}^0$  is the ideal Fermi distribution,  $\epsilon_{\mathbf{k}} = \hbar^2 k^2 / 2m$  and for an unpolarized system

$$\Sigma_{\text{HF}}(\mathbf{k}) = v_0 + \frac{1}{N} \sum_{\mathbf{q}} v_{\mathbf{q}} n_{\mathbf{k}+\mathbf{q},\sigma}^0 \quad (\text{K.7})$$

$$= -\frac{e^2 k_F}{\pi} \left[ 1 + \frac{k_F^2 - k^2}{2k k_F} \ln \left| \frac{k + k_F}{k - k_F} \right| \right], \quad (\text{K.8})$$

here  $v_0 = v_{\mathbf{q}=0}$  and  $v_{\mathbf{q}} = 4\pi e^2/q^2$ . So that

$$E_g^{\text{HF}} = E_g^{\text{HF}}/N = \left( \frac{3}{5\alpha^2 r_s^2} - \frac{3}{2\pi\alpha r_s} \right) \text{Ry} = \left( \frac{2.21}{r_s^2} - \frac{0.916}{r_s} \right) \text{Ry}, \quad (\text{K.9})$$

with  $\alpha = (9\pi/4)^{-1/3}$ . As already remarked, the gain in potential energy found in Hartree-Fock derives from the fact that the exclusion principle is built into the many-body wave function and keeps apart pairs of electrons with parallel spins, thus lowering their Coulomb repulsive interaction energy on average. Notice that the ratio between potential and kinetic energy is proportional to  $r_s$ : this dimensionless length gives a measure of the coupling strength, which increases with decreasing density. The main problem with the Hartree-Fock approximation is that, by including exchange between electrons with parallel spins but neglecting correlations due to the Coulomb repulsions (which are most effective for electrons with antiparallel spins), it includes neither dielectric screening nor the collective plasma excitation. As shown in section 6.2.4 the Hartree-Fock ground-state can be determined from the exchange part of the radial distribution function (see Eqs. (K.2)-(K.3)).

When one proceeds to evaluate the ground-state energy of Jellium by perturbation theory beyond first order (i.e. beyond Hartree-Fock), one meets divergences arising from the long-range character of the Coulomb interactions. On summing to infinite order the most strongly divergent terms of the perturbative expansion (corresponding to the RPA theory), screening introduces a cut-off as the lower end of integrals over wave vector space and cures the divergences [194]. Such a calculation, supplemented by the inclusion of a contribution from second-order exchange

processes, yields the low  $r_s$  expansion

$$e_g(r_s) = \left[ \frac{2.21}{r_s^2} - \frac{0.916}{r_s} + 0.0622 \ln r_s - 0.096 + \dots \right] \text{Ry}, \quad (\text{K.10})$$

plus terms going like  $r_s$ ,  $r_s \ln r_s$ , etc. The results of such a truncated expansion is reasonably accurate only up to  $r_s = 1$ , whereas the values of  $r_s$  that are relevant in the physics of normal metals extend up to  $r_s = 6$ .

In the thirties Wigner [111, 195] had already noticed that an optimal value  $e_{\text{pot}} = -(1.8/r_s)\text{Ry}$  is obtained for the potential energy if the electrons are placed on the sites of a crystalline lattice having body-centered-cubic (bcc) structure. The gain by a factor  $\approx 2$  over the potential energy in Hartree-Fock is clearly related to the fact that in the crystal all pairs of electrons keep apart irrespectively of their relative spin orientation. Using the crystalline result at large  $r_s$  in combination with an estimate of the correlation energy at low  $r_s$ , Wigner proposed the interpolation formula

$$e_g^W = \left[ \frac{2.21}{r_s^2} - \frac{0.916}{r_s} - \frac{0.88}{7.8 + r_s} \right] \text{Ry}, \quad (\text{K.11})$$

as approximately valid at metallic densities.



## Appendix L

# Radial distribution functions sum rules for the electron gas ground state

Both the behavior of the RDF at small  $r$  and at large  $r$  has to satisfy to general exact relations or sum rules.

### L.1 Cusp conditions

When two electrons ( $\mu = \infty$ ) get closer and closer together, the behavior of  $g_{\sigma,\sigma'}(r)$  is governed by the exact cusp conditions [196, 197, 198]

$$\frac{d}{dr} g_{\sigma,\sigma}(r) \Big|_{r \rightarrow 0} = 0 , \quad (\text{L.1})$$

$$\frac{d^3}{dr^3} g_{\sigma,\sigma}(r) \Big|_{r \rightarrow 0} = \frac{3}{2a_0} \frac{d^2}{dr^2} g_{\sigma,\sigma}(r) \Big|_{r \rightarrow 0} , \quad (\text{L.2})$$

$$\frac{d}{dr} g_{+,-}(r) \Big|_{r \rightarrow 0} = \frac{1}{a_0} g_{+,-}(0) , \quad (\text{L.3})$$

where in the adimensional units  $a_0 \rightarrow 1/r_s$ . For finite  $\mu$  we only have the condition  $g_{\sigma,\sigma}(0) = 0$  due to Pauli exclusion principle.

### L.2 The Random-Phase-Approximation (RPA) and the long range behavior of the RDF

The small  $k$  behavior of the RPA, summarized in Appendix J, is exact [92]. One finds

$$S_{RPA}(k) = \frac{\hbar k^2}{2m\omega_p} , \quad k \ll k_F , \quad (\text{L.4})$$

where  $\omega_p = \sqrt{4\pi ne^2/m}$  is the plasmon frequency [113]. This is also known as the second-moment sum rule for the exact RDF and can be rewritten as  $n \int dr r^2 [g(r) - 1] = -6(\hbar/2m\omega_p)$ .

We can then say that  $g(r) - 1$  has to decay faster than  $r^{-5}$  at large  $r$ . The fourth-moment (or compressibility) sum rule links the thermodynamic compressibility,  $\chi = [nd(n^2 de_0/dn)/dn]^{-1}$ , [190] to the fourth-moment of the RDF. For the equivalent classical system it is well known that the correlation functions have to decay faster than any inverse power of the distance [199, 110, 200] (in accord with the Debye-Hückel theory). To the best of our knowledge we do not know, yet, the exact decay for the zero temperature quantum case.

## Appendix M

# The primitive action

Suppose the Hamiltonian is split into two pieces  $\mathcal{H} = \mathcal{T} + \mathcal{V}$ , where  $\mathcal{C}\text{al}t$  and  $\mathcal{V}$  are the kinetic and potential operators. Recall the exact Baker-Campbell-Hausdorff formula to expand  $\exp(-\tau\mathcal{H})$  into the product  $\exp(-\tau\mathcal{T})\exp(-\tau\mathcal{V})$ . As  $\tau \rightarrow 0$  the commutator terms which are of order higher than  $\tau^2$  become smaller than the other terms and thus can be neglected. This is known as the *primitive approximation*

$$e^{-\tau(\mathcal{T}+\mathcal{V})} \approx e^{-\tau\mathcal{T}}e^{-\tau\mathcal{V}}. \quad (\text{M.1})$$

hence we can approximate the exact density matrix by product of the density matrices for  $\mathcal{T}$  and  $\mathcal{V}$  alone. One might worry that this would lead to an error as  $M \rightarrow \infty$ , with small errors building up to a finite error. According to the Trotter [201] formula, one does not have to worry

$$e^{-\beta(\mathcal{T}+\mathcal{V})} = \lim_{M \rightarrow \infty} [e^{-\tau\mathcal{T}}e^{-\tau\mathcal{V}}]^M. \quad (\text{M.2})$$

The Trotter formula holds if the three operators  $\mathcal{T}$ ,  $\mathcal{V}$ , and  $\mathcal{T} + \mathcal{V}$  are self-adjoint and make sense separately, for example, if their spectrum is bounded below [202]. This is the case for the Hamiltonian describing Jellium.

Let us now write the primitive approximation in position space

$$\rho(R_0, R_2; \tau) \approx \int dR_1 \langle R_0 | e^{-\tau\mathcal{T}} | R_1 \rangle \langle R_1 | e^{-\tau\mathcal{V}} | R_2 \rangle, \quad (\text{M.3})$$

and evaluate the kinetic and potential density matrices. Since the potential operator is diagonal in the position representation, its matrix elements are trivial

$$\langle R_1 | e^{-\tau\mathcal{V}} | R_2 \rangle = e^{-\tau V(R_1)} \delta(R_2 - R_1). \quad (\text{M.4})$$

The kinetic matrix can be evaluated using the eigenfunction expansion of  $\mathcal{T}$ . Consider, for example, the case of distinguishable particles in a cube of side  $L$  with periodic boundary conditions. Then the exact eigenfunctions and eigenvalues of  $\mathcal{T}$  are  $L^{-3N/2}e^{iK_n R}$  and  $\lambda K_n^2$ , with  $K_n = 2\pi n/L$  and  $n$  a  $3N$ -dimensional integer vector. We are using here dimensional units. Then

$$\langle R_0 | e^{-\tau\mathcal{T}} | R_1 \rangle = \sum_n L^{-3N} e^{-\tau \lambda K_n^2} e^{-iK_n(R_0 - R_1)} \quad (\text{M.5})$$

$$= (4\pi\lambda\tau)^{-3N/2} \exp\left[-\frac{(R_0 - R_1)^2}{4\lambda\tau}\right], \quad (\text{M.6})$$

where  $\lambda = \hbar^2/2m$ . Eq. (M.6) is obtained by approximating the sum by an integral. This is appropriate only if the thermal wavelength of one step is much less than the size of the box,  $\lambda\tau \ll L^2$ . In some special situations this condition could be violated, in which case one should use Eq. (M.5) or add periodic “images” to Eq. (M.6). The exact kinetic density matrix in periodic boundary conditions is a theta function,  $\prod_{i=1}^{3N} \theta_3(z_i, q)$ , where  $z = \pi(R_0^i - R_1^i)/L$ ,  $R^i$  is the  $i$ th component of the  $3N$  dimensional vector  $R$ , and  $q = e^{-\lambda\tau(2\pi/L)^2}$  (see chapter 16 of Ref. [203]). Errors from ignoring the boundary conditions are  $O(q)$ , exponentially small at large  $M$ .

A *link*  $m$  is a pair of time slices  $(R_{m-1}, R_m)$  separated by a *time step*  $\tau = \beta/M$ . The action  $S^m$  of a link is defined as minus the logarithm of the exact density matrix. Then the exact path integral expression becomes

$$\rho(R_0, R_M; \beta) = \int dR_1 \dots dR_{M-1} \exp \left[ - \sum_{m=1}^M S^m \right], \quad (\text{M.7})$$

It is convenient to separate out the *kinetic action* from the rest of the action. The exact kinetic action for link  $m$  will be denoted  $K^m$

$$K^m = \frac{3N}{2} \ln(4\pi\lambda\tau) + \frac{(R_{m-1} - R_m)^2}{4\lambda\tau}, \quad (\text{M.8})$$

The *inter-action* is then defined as what is left

$$U^m = U(R_{m-1}, R_m; \tau) = S^m - K^m. \quad (\text{M.9})$$

In the primitive approximation the inter-action is

$$U_1^m = \frac{\tau}{2} [V(R_{m-1}) + V(R_m)], \quad (\text{M.10})$$

where we have symmetrized  $U_1^m$  with respect to  $R_{m-1}$  and  $R_m$ , since one knows that the exact density matrix is symmetric and thus the symmetrized form is more accurate.

A capital letter  $U$  refers to the total link inter-action. One should not think of the exact  $U$  as being strictly the potential action. That is true for the primitive action but, in general, is only correct in the small- $\tau$  limit. The exact  $U$  also contains kinetic contributions of higher order in  $\tau$ . If a subscript is present on the inter-action, it indicates the order of approximation; the primitive approximation is only correct to order  $\tau$ . No subscript implies the exact inter-action.

The *residual energy* of an approximate density matrix is defined as

$$E_A(R, R'; t) = \frac{1}{\rho_A(R, R'; t)} \left[ \mathcal{H} + \frac{\partial}{\partial t} \right] \rho_A(R, R'; t). \quad (\text{M.11})$$

The residual energy for an exact density matrix vanishes; it is a local measure of the error of an approximate density matrix. The Hamiltonian  $\mathcal{H}$  is a function of  $R$ ; thus the residual energy is not symmetric in  $R$  and  $R'$ .

It is useful to write the residual energy as a function of the inter-action. We find

$$E_A(R, R'; t) = V(R) - \frac{\partial U_A}{\partial t} - \frac{(R - R') \cdot \nabla U_A}{t} + \lambda \nabla^2 U_A - \lambda (\nabla U_A)^2. \quad (\text{M.12})$$

The terms on the right hand side are ordered in powers of  $\tau$ , keeping in mind that  $U(R)$  is of order  $\tau$ , and  $|R - R'|$  is of order  $\tau^{1/2}$ . One obtains the primitive action by setting the residual energy to zero and dropping the last three terms on the right hand side.

The residual energy of the primitive approximation is

$$E_1(R, R'; t) = \frac{1}{2} [V(R) - V(R')] - \frac{1}{2} (R - R') \cdot \nabla V + \frac{\lambda t}{2} \nabla^2 V - \frac{\lambda t^2}{4} (\nabla V)^2. \quad (\text{M.13})$$

With a leading error of  $\sim \lambda\tau^2$ .

## Appendix N

# The pair-product action

An often useful method to determine the many-body action is to use the exact action for two electrons [204]. To justify this approach, first assume that the potential energy can be broken into a pairwise sum of terms

$$V(R) = \sum_{i < j} v(|\mathbf{r}_i - \mathbf{r}_j|), \quad (\text{N.1})$$

with  $|\mathbf{r}_i - \mathbf{r}_j| = r_{ij}$ . Next, apply the Feynman-Kac formula for the inter-action

$$e^{-U(R_0, R_F; \tau)} = \left\langle \exp \left[ - \int_0^\tau dt V(R(t)) \right] \right\rangle_{\text{RW}}, \quad (\text{N.2})$$

where the notation  $\langle \dots \rangle_{\text{RW}}$  means the average over all Gaussian random-walks from  $R_0$  to  $R_F$  in a “time”  $\tau$ . So that

$$e^{-U(R_0, R_F; \tau)} = \left\langle \exp \left[ - \int_0^\tau dt \sum_{i < j} v(r_{ij}(t)) \right] \right\rangle_{\text{RW}} \quad (\text{N.3})$$

$$= \left\langle \prod_{i < j} \exp \left[ - \int_0^\tau dt v(r_{ij}(t)) \right] \right\rangle_{\text{RW}} \quad (\text{N.4})$$

$$\approx \prod_{i < j} \left\langle \exp \left[ - \int_0^\tau dt v(r_{ij}(t)) \right] \right\rangle_{\text{RW}} \quad (\text{N.5})$$

$$= \prod_{i < j} \exp [-u_2(r_{ij}, r'_{ij}; \tau)] \quad (\text{N.6})$$

$$= \exp \left[ - \sum_{i < j} u_2(r_{ij}, r'_{ij}; \tau) \right] = e^{-U_2(R_0, R_F; \tau)}, \quad (\text{N.7})$$

where  $U_2$  is the *pair-product* action and  $u_2$  is the exact action for a pair of electrons. At low temperatures the pair action approaches the solution of the two particle wave equation. The result is the pair-product or Jastrow ground-state wave function, which is the ubiquitous choice for a correlated wave function because it does such a good job of describing most ground-state correlations.

The residual energy (see Eq. (M.11)) for the pair-product action is less singular than for other forms. We have that

$$u_2(r_{ij}, r'_{ij}; \tau) = -\ln \left\langle \exp \left( - \int_0^\tau dt v(r_{ij}(t)) \right) \right\rangle_{\text{RW}}, \quad (\text{N.8})$$

is of order  $\tau^2$  since the two body problem can be factorized into a center-of-mass term and a term that is a function of the relative coordinates. Moreover we must have

$$\frac{\partial u_2}{\partial \tau} = v(r_{ij}(\tau)), \quad (\text{N.9})$$

so that

$$\frac{\partial U_2}{\partial \tau} = V(R(\tau)), \quad (\text{N.10})$$

which tells that only the last three terms on the right hand side of Eq. (M.12) contribute to the residual energy. We also have

$$\nabla U_2 = \sum_i \sum_{i \neq j} \nabla_i u_2(r_{ij}, r'_{ij}; \tau), \quad (\text{N.11})$$

where the indices run over the particles. So the leading error of the pair-product action is  $\sim \lambda \tau^3$ .

## Appendix O

# Linear-Response-Theory

Linear response theory [205, 94, 95] is a well known framework to describe the approach to thermal equilibrium in response to an external perturbation acting on a many-body quantum fluid.

Let us introduce the density linear response function  $K(\mathbf{r} - \mathbf{r}', t - t')$  for a homogeneous fluid. Let us indicate with  $V_b$  the “bare” potential in vacuum.

The coupling of the fluid to the perturbing potential is described by the Hamiltonian

$$H'(t) = \int d\mathbf{r} \rho(\mathbf{r}) V_b(\mathbf{r}, t), \quad (\text{O.1})$$

where  $\rho(\mathbf{r})$  is the density operator (here we implicitly assume that the mean value of the density has been subtracted from  $\rho(\mathbf{r})$ ). We will just consider the linear effect of this perturbation. The change in density is given by

$$\delta n(\mathbf{r}, t) = \langle \rho(\mathbf{r}) \rangle - \langle \rho(\mathbf{r}) \rangle_0 = \text{tr}\{[w(t) - w_0]\rho(\mathbf{r})\}, \quad (\text{O.2})$$

where  $\text{tr}$  denotes the trace,  $w(t) = \int \psi^*(\mathbf{R}, t)\psi(\mathbf{R}, t) d^{3N}R$  is the perturbed density matrix whose unperturbed counterpart is  $w_0 = \exp(-\beta H_0)/\text{tr}\{\exp(-\beta H_0)\}$ , and  $\beta = 1/k_B T$  with  $k_B$  the Boltzmann constant and  $T$  the absolute temperature. We are indicating with  $\psi(\mathbf{R}, t)$  the many-body wave function of the fluid with particles at positions  $\mathbf{R} = (\mathbf{r}_1, \mathbf{r}_2, \dots, \mathbf{r}_N)$  at time  $t$ . This satisfies to the Schrödinger equation

$$i\hbar \frac{\partial \psi(\mathbf{R}, t)}{\partial t} = [H_0 + H'(t)]\psi(\mathbf{R}, t), \quad (\text{O.3})$$

where  $H$  is the Hamiltonian of the unperturbed fluid. Then the perturbed density matrix satisfies to

$$\begin{aligned} i\hbar \frac{\partial w(t)}{\partial t} &= [H_0 + H'(t), w(t)] \\ &\approx [H_0, w(t) - w_0] + [H'(t), w_0], \end{aligned} \quad (\text{O.4})$$

where  $[A, B]$  denotes the commutator  $AB - BA$  and in the last step we have linearized the effect of the perturbation and used  $[H_0, w_0] = 0$ . This equation is subject to the initial condition

$$\lim_{t \rightarrow -\infty} w(t) = w_0, \quad (\text{O.5})$$

representing a state of thermal equilibrium.

The linearized equation (O.4) has the following solution

$$w(t) - w_0 = (i\hbar)^{-1} \int_{-\infty}^t dt' \exp\{-iH_0(t-t')/\hbar\} [H'(t'), w_0] \exp\{iH_0(t-t')/\hbar\}. \quad (\text{O.6})$$

Inserting this result into Eq. (O.2) and using the cyclic invariance of the trace,  $\text{tr}\{AB\} = \text{tr}\{BA\}$ , we can write the desired result as follows

$$\delta n(\mathbf{r}, t) = (-i/\hbar) \int d\mathbf{r}' \int_{-\infty}^t dt' \langle [\rho(\mathbf{r}, t), \rho(\mathbf{r}', t')] \rangle_0 V_b(\mathbf{r}', t). \quad (\text{O.7})$$

Again the angle parenthesis  $\langle A \rangle_0 = \text{tr}\{w_0 A\}$  denotes the mean value on the equilibrium state and  $\rho(\mathbf{r}, t)$  is the Heisenberg operator

$$\rho(\mathbf{r}, t) = \exp(iH_0 t/\hbar) \rho(\mathbf{r}) \exp(-iH_0 t/\hbar). \quad (\text{O.8})$$

So

$$K(\mathbf{r} - \mathbf{r}', t - t') = (-i/\hbar) \theta(t - t') \langle [\rho(\mathbf{r}, t), \rho(\mathbf{r}', t')] \rangle_0. \quad (\text{O.9})$$

This result clearly embodies the causality property through the Heaviside step function  $\theta$ .

Introducing the notation

$$\chi''(k, t - t') = (1/2\hbar) \int d(\mathbf{r} - \mathbf{r}') \exp[-ik \cdot (\mathbf{r} - \mathbf{r}')] \langle [\rho(\mathbf{r}, t), \rho(\mathbf{r}', t')] \rangle_0, \quad (\text{O.10})$$

we see, from Eq. (O.9) that the Fourier transform of  $K$  is the convolution integral of the Fourier transform of  $\chi''(k, t)$ , that we will indicate with  $\chi''(k, \omega)$ , and of the Heaviside step function, that is equal to  $i/(\omega + i\eta)$  with  $\eta$  a small positive quantity. We can then write the space-time Fourier transform of  $K$  like so

$$\chi(k, \omega) = - \int_{-\infty}^{\infty} \frac{d\omega'}{\pi} \chi''(k, \omega') / (\omega - \omega' + i\eta). \quad (\text{O.11})$$

Using the rule  $(\omega + i\eta)^{-1} = P(1/\omega) - i\pi\delta(\omega)$ , where  $P$  denotes the Cauchy principal part, this can be written like so

$$\chi(k, \omega) = -P \int_{-\infty}^{\infty} \frac{d\omega'}{\pi} \chi''(k, \omega') / (\omega - \omega') + i\chi''(k, \omega). \quad (\text{O.12})$$

Since  $\chi''(k, t)$  is written in terms of the commutator of Hermitian operators it can be readily shown that  $\chi''(k, \omega)$  must be real. So we can write

$$\text{Im}\chi(k, \omega) = \chi''(k, \omega). \quad (\text{O.13})$$

## O.1 Fluctuation-dissipation theorem

We now worry about the relationship between the density response function and the van Hove dynamic response  $S(k, \omega)$ . Let us define the autocorrelation density function as

$$G(\mathbf{r} - \mathbf{r}', t - t') = \frac{1}{n} \langle \rho(\mathbf{r}, t) \rho(\mathbf{r}', t') \rangle_0, \quad (\text{O.14})$$

whose space-time Fourier transform is  $S(\mathbf{k}, \omega)$ . The connection between  $G$  e  $K$  that gush from Eq. (O.9) can be rewritten in Fourier transform like so

$$\chi(\mathbf{k}, \omega) = (n/\hbar) \int_{-\infty}^{\infty} \frac{d\omega'}{2\pi} [S(\mathbf{k}, \omega) - S(-\mathbf{k}, -\omega)] / (\omega - \omega' + i\eta). \quad (\text{O.15})$$

This has the same form of Eq. (O.11) so that

$$\text{Im}\chi(\mathbf{k}, \omega) = (-n/2\hbar)[S(\mathbf{k}, \omega) - S(-\mathbf{k}, -\omega)]. \quad (\text{O.16})$$

For a fluid in thermodynamic equilibrium we must have

$$S(-\mathbf{k}, -\omega) = \exp(-\hbar\beta\omega)S(\mathbf{k}, \omega). \quad (\text{O.17})$$

In order to prove this property we observe that its inverse space-time Fourier transform reads

$$G(-\mathbf{r}, -t) = \exp\left(-i\hbar\beta\frac{\partial}{\partial t}\right) G(\mathbf{r}, t), \quad (\text{O.18})$$

since under time Fourier transform  $\partial/\partial t \rightarrow -i\omega$ . But Eq. (O.18) can readily be proven through the following steps (where, once again we use the cyclic invariance of the trace and the definition of the Heisenberg operator, Eq. (O.8))

$$\begin{aligned} \text{tr}\{\exp(-\beta H_0)\rho(\mathbf{0}, 0)\rho(\mathbf{r}, t)\} &= \text{tr}\{\rho(\mathbf{r}, t)\exp(-\beta H_0)\rho(\mathbf{0}, 0)\} \\ &= \text{tr}\{\exp(-\beta H_0)\rho(\mathbf{r}, t - i\hbar\beta)\rho(\mathbf{0}, 0)\} \\ &= \exp(-i\hbar\beta\partial/\partial t)\text{tr}\{\exp(-\beta H_0)\rho(\mathbf{r}, t)\rho(\mathbf{0}, 0)\}. \end{aligned} \quad (\text{O.19})$$

In the classical limit, for  $\beta$  small, Eq. (O.16) becomes

$$\text{Im}\chi(\mathbf{k}, \omega) = (-n\beta\omega/2)S(\mathbf{k}, \omega). \quad (\text{O.20})$$

## O.2 Kramers-Kronig relations

Causality imposes that the response function  $K(\mathbf{r}, t)$  vanish for  $t < 0$ . In other words the fluid is influenced only by the action of the external perturbation in the past. Introducing the “intermediate” response function  $\chi(\mathbf{k}, t)$  as the space Fourier transform of  $K(\mathbf{r}, t)$ , we have

$$\chi(\mathbf{k}, t) = 0 \quad \text{for } t < 0. \quad (\text{O.21})$$

On the other hand

$$\chi(\mathbf{k}, t) = \int_{-\infty}^{\infty} \frac{d\omega}{2\pi} \exp(-i\omega t)\chi(\mathbf{k}, \omega). \quad (\text{O.22})$$

Extending the definition of  $\chi(\mathbf{k}, \omega)$  from real to complex frequencies, we can calculate this integral through contour methods and for  $t < 0$  we can close the contour with the semicircle at infinity above the real axis. The contribution from the integration on the semicircle vanishes since  $\chi(\mathbf{k}, \omega) \propto \omega^{-2}$  at high frequency. So the causality property (O.21) is guaranteed if  $\chi(\mathbf{k}, \omega)$  is analytic in the upper part of the complex frequency plane.

Let us now consider the integral

$$\oint \frac{\chi(\mathbf{k}, \omega')}{\omega - \omega'} d\omega' = 0, \quad (\text{O.23})$$

on the contour  $\Gamma$  shown in Fig. O.1. This contour integral vanishes due to the analyticity of  $\chi(\mathbf{k}, \omega)$ . The contribution from the semicircle at infinity is again zero, so that

$$P \int_{-\infty}^{\infty} d\omega' \frac{\chi(\mathbf{k}, \omega')}{\omega' - \omega} - i\pi\chi(\mathbf{k}, \omega) = 0, \quad (\text{O.24})$$

where again  $P$  denotes the Cauchy principal part of the integral on the real frequency axis and the second term comes from the integration over the small semicircle around the point  $\omega$ . If we now separate  $\chi(\mathbf{k}, \omega)$  into its real and imaginary parts we find

$$P \int_{-\infty}^{\infty} d\omega' \frac{\text{Re}\chi(\mathbf{k}, \omega')}{\omega' - \omega} + \pi\text{Im}\chi(\mathbf{k}, \omega) = 0, \quad (\text{O.25})$$

and

$$P \int_{-\infty}^{\infty} d\omega' \frac{\text{Im}\chi(\mathbf{k}, \omega')}{\omega' - \omega} - \pi\text{Re}\chi(\mathbf{k}, \omega) = 0. \quad (\text{O.26})$$

These are the Kramers-Kronig relations.

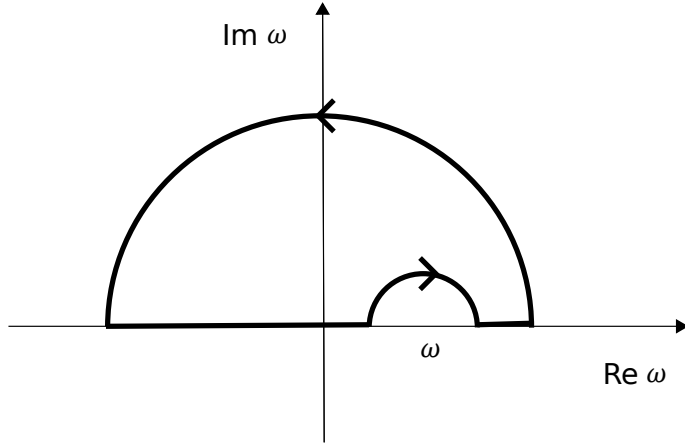


Figure O.1: Integration contour on the complex  $\omega$  plane.

### O.3 The dielectric function

In a Coulomb liquid, the connection with the longitudinal dielectric function  $\epsilon(\mathbf{k}, \omega)$ , becomes apparent from the Poisson equations

$$\nabla \cdot \mathbf{D}(\mathbf{r}, t) = -4\pi e n_e(\mathbf{r}, t), \quad (\text{O.27})$$

$$\nabla \cdot \mathbf{E}(\mathbf{r}, t) = -4\pi e [n_e(\mathbf{r}, t) + \delta n(\mathbf{r}, t)], \quad (\text{O.28})$$

which yield

$$\frac{1}{\epsilon(\mathbf{k}, \omega)} = \frac{\mathbf{k} \cdot \mathbf{E}(\mathbf{k}, \omega)}{\mathbf{k} \cdot \mathbf{D}(\mathbf{k}, \omega)} = 1 + \frac{\delta n(\mathbf{k}, \omega)}{n_e(\mathbf{k}, \omega)} = 1 + \frac{4\pi e^2}{k^2} \chi(\mathbf{k}, \omega), \quad (\text{O.29})$$

since from Eqs. (O.7) and (O.9) follows  $\delta n(\mathbf{k}, \omega) = \chi(\mathbf{k}, \omega)V_b(\mathbf{k}, \omega)$  where  $\chi(\mathbf{k}, \omega)$  is the Fourier transform of  $K(|\mathbf{r} - \mathbf{r}'|, t - t')$  and

$$V_b(\mathbf{k}, \omega) = \frac{4\pi e^2}{k^2} n_e(\mathbf{k}, \omega). \quad (\text{O.30})$$

Of course the field  $\mathbf{E}$  and the associated screened or “Hartree” potential  $V_H(\mathbf{k}, \omega) = V_b(\mathbf{k}, \omega)/\epsilon(\mathbf{k}, \omega)$  would be experienced by a second test charge introduced into the plasma, rather than by the particles of the plasma. The latter also experience effects which involve the precise “hole” a particle of the plasma digs around itself. This latter effect brings about the so called local field corrections.

In addition to  $\chi(\mathbf{k}, \omega)$  which relates the displaced charge density to the potential *in vacuo*, it is useful to introduce yet another longitudinal response function,  $\tilde{\chi}(\mathbf{k}, \omega)$  say, by exploiting further the analogy with elementary electrostatics. This relates  $n(\mathbf{k}, \omega)$  directly to the Hartree potential through

$$n(\mathbf{k}, \omega) = \tilde{\chi}(\mathbf{k}, \omega)V_H(\mathbf{k}, \omega). \quad (\text{O.31})$$

We then have

$$\epsilon(\mathbf{k}, \omega) = 1 - \frac{4\pi e^2}{k^2} \tilde{\chi}(\mathbf{k}, \omega). \quad (\text{O.32})$$

The expression  $\chi(\mathbf{k}, \omega) = \tilde{\chi}(\mathbf{k}, \omega)/\epsilon(\mathbf{k}, \omega)$  accounts at one stroke for the *long range* effects of the Coulomb interactions (the resonance at the plasma frequency, determined by  $\epsilon(\mathbf{k}, \omega) = 0$ , is brought about explicitly in the denominator).

The simplest useful approximation to the dielectric function of the plasma is obtained by approximating  $\tilde{\chi}$  by the density response function of an ideal gas. This corresponds to the Vlasov theory for the classical plasma and to the Lindhard theory for the degenerate electron fluid. Refinements of these theories aims at incorporating the effects of “exchange and correlation” in  $\tilde{\chi}$ . This expression being an abbreviation for the short range effects arising from the statistics (“exchange”) and long range effect arising from the Coulomb interaction (“correlation”). Of course the exchange effects are absent in the classical limit.



# Chapter 7

## The White Dwarf

In this chapter we study the effect of having a finite temperature on the equation of state and structure of a white dwarf. In order to keep the treatment as general as possible we carry on our discussion for ideal quantum gases obeying to both the Fermi-Dirac and the Bose-Einstein statistics even if we will only use the results for the free electron gas inside a white dwarf. We discuss the effect of temperature on the stability of the star and on the Fermi hole.

### 7.1 Introduction

A white dwarf below the regime of neutron drip, at mass densities less than  $4 \times 10^{11} \text{ g cm}^{-3}$ , are stars which emit light of a white color due to their relatively high surface temperature of about  $10^4 \text{ K}$ . Because of their small radii  $R$ , luminous white dwarfs, radiating away their residual thermal energy, are characterized by much higher effective temperatures,  $T$ , than normal stars even though they have lower luminosities (which varies as  $R^2 T^4$ ). In other words, white dwarfs are much “whiter” than normal stars, hence their name [206, 207, 208].

White dwarfs life begins when a star dies, they are therefore *compact objects* [38]. Star death begins when most of the nuclear fuel has been consumed. White dwarfs has about one solar mass  $M_\odot$  with characteristic radii of about 5000km and mean densities of around  $10^6 \text{ g cm}^{-3}$ . They are no longer burning nuclear fuel and are slowly cooling down as they radiate away their residual thermal energy.

They support themselves against gravity by the pressure of cold electrons, near their degenerate, zero temperature, state. In 1932 L. D. Landau [209] presented an elementary explanation of the equilibrium of a white dwarf which had been previously discovered by Chandrasekhar in 1931 [210, 211, 212] building on the formulation of the Fermi-Dirac statistics in August 1926 [213] and the work of R. H. Fowler in December 1926 [214], on the role of the *electron degeneracy pressure* to keep the white dwarf from gravitational collapse. Landau explanation can be found in §3.4 of the book of Shapiro and Teukolsky [38], and fixes the equilibrium maximum mass of the white dwarf to  $M_{\max} \sim 1.5 M_\odot$ . Whereas Chandrasekhar result was  $M_{\text{Ch}} = 1.456 M_\odot$  for completely ionized matter made of elements with a ratio between mass number and atomic number equal to 2. Strictly speaking one would have a matter made of a fluid of electrons and a fluids of nuclei. In the work of Chandrasekhar the fluid of electrons is treated as an ideal gas where the electrons are not interacting among themselves and the nuclei thousands times heavier are neglected.

Despite the high surface temperature these stars are still considered cold, however, because on a first approximation temperature does not affect the equation of state of its matter. White dwarfs are described as faint stars below the main sequence in the Hertzsprung-Russell diagram.

In other words, white dwarfs are less luminous than main-sequence stars of corresponding colors. While slowly cooling, the white dwarfs are changing in color from white to red and finally to black. White dwarfs can be considered as one possibility of a final stage of stellar evolution since they are considered static over the lifetime of the Universe.

White dwarfs were established in the early 20<sup>th</sup> century and have been studied and observed ever since. They comprise an estimated 3% of all the stars of our galaxy. Because of their low luminosity, white dwarfs (except the very nearest ones) have been very difficult to detect at any reasonable distance and that is why there was very little observational data supporting the theory in the time of them being discovered. The companion of Sirius, discovered in 1915 by W. S. Adams [215, 216], was among the earliest to become known. The cooling of white dwarfs is not only a fascinating phenomenon but in addition offers information of many body physics in a new setting since the circumstances of an original star can not be built up in a laboratory. Moreover, the evolution and the equation of state for white dwarfs can be useful on Earth providing us more understanding of matter and physics describing the Universe.

In this chapter, we discuss how the Chandrasekhar analysis at zero temperature should be changed in order to take into account the effect of having a quantum ideal gas at finite (non-zero) temperature. For the sake of generality we will treat in parallel the case of the Fermi and the Bose ideal gases. Even if only the Fermi case is appropriate for the description of the white dwarf interior made of ionized matter characterized by a sea of free cold electrons (as Chandrasekhar did, we will neglect the Coulomb interaction between the electrons and disregards the nuclei in order to keep the treatment analytically solvable. We will also use Newtonian gravity to study the star stability disregarding general relativistic effects). At the typical surface temperature and density of a white dwarf the momentum thermal average fraction of particles having momentum  $\hbar k$  and a full relativistic dispersion relation ( $C_k/C_0$  where  $C_k$  is given by Eq. (7.25) below) varies appreciably over a  $k$  range which is a fraction of 0.933 <sup>1</sup> of the  $k$  range where it is different from zero. So we generally expect the effect of temperature to play a role on the behavior of the ideal quantum gas. We will pursue our analysis for both the thermodynamic properties, as the validity of the various polytropic adiabatic equation of state as a function of density, and for the structural properties, as the Fermi hole.

The chapter is organized as follows: In section 7.2 we review the thermodynamic properties of the ideal quantum gases at finite temperatures. This section contains three subsections, in the first one 7.2.1 we discuss the importance of a full relativistic treatment at high densities, in the second one 7.2.2 we discuss the onset of quantum statistics as the star collapses, and in the third one 7.2.3 we present the revised Chandrasekhar analysis. In the second section 7.3 we present our study of the structure of the ideal quantum gases at finite temperature and in the full relativistic regime.

## 7.2 The thermodynamics of the ideal quantum gas

We want to find the thermodynamic grand potential of a system of many free fermions or bosons with a rest mass  $m$  in thermodynamic equilibrium at an inverse temperature  $\beta = 1/k_B T$ .

The Hamiltonian of the system is

$$\mathcal{H} = \sum_i (-\hbar^2 c^2 \Delta_i + m^2 c^4)^{1/2}, \quad (7.1)$$

with  $\Delta$  the Laplacian and  $c$  the speed of light.

---

<sup>1</sup>This value will get smaller as the star cools down in view of Eq. (7.20) and eventually become close to zero as the momentum thermal average fraction approaches a step function

Assuming the many particles are distinguishable (Boltzmannons) the density matrix operator,  $\hat{\rho}_D$ , satisfies to the Bloch equation

$$\frac{\partial \hat{\rho}_D(\beta)}{\partial \beta} = -\mathcal{H}\hat{\rho}_D(\beta), \quad (7.2)$$

$$\hat{\rho}_D(0) = \mathcal{I}, \quad (7.3)$$

where  $\mathcal{I}$  is the identity operator. The solution of Eq. (7.2) in coordinate representation  $\mathbf{R} = (\mathbf{r}_1, \dots, \mathbf{r}_N)$ , where  $\mathbf{r}_i$  is the position of  $i$ th spinless particle in the three dimensional space, has the following solution

$$\rho_D(\mathbf{R}_0, \mathbf{R}_1; \beta) = \langle \mathbf{R}_0 | e^{-\beta \mathcal{H}} | \mathbf{R}_1 \rangle = \int \frac{d\mathbf{K}}{(2\pi)^{3N}} e^{-i\mathbf{K} \cdot (\mathbf{R}_0 - \mathbf{R}_1)} e^{-\beta \sum_i (\hbar^2 c^2 \mathbf{k}_i^2 + m^2 c^4)^{1/2}}, \quad (7.4)$$

where  $\mathbf{K} = (\mathbf{k}_1, \dots, \mathbf{k}_N)$  and  $\mathbf{R}_n = (\mathbf{r}_1^n, \dots, \mathbf{r}_N^n)$ . A very simple calculation yields the propagator  $\rho_D$  in closed form. The result can be cast in the following form

$$\rho_D = \prod_i \mathcal{R}(\mathbf{r}_i^1, \mathbf{r}_i^0), \quad (7.5)$$

where  $\mathcal{R}$  in one dimension is

$$\mathcal{R}_{1d}(\mathbf{r}^1, \mathbf{r}^0) = \frac{mc^2 \beta}{\pi \Psi^{1/2}} K_1\left(\frac{mc}{\hbar} \Psi^{1/2}\right), \quad (7.6)$$

where  $\Psi = (\mathbf{r}^1 - \mathbf{r}^0)^2 + (\hbar c \beta)^2$  and  $K_\nu$  is the familiar modified Bessel functions of order  $\nu$ . In three dimensions we thus find

$$\begin{aligned} \mathcal{R}(\mathbf{r}^1, \mathbf{r}^0) &= -\frac{1}{2\pi |\mathbf{r}^1 - \mathbf{r}^0|} \frac{d\mathcal{R}_{1d}(\mathbf{r}^1, \mathbf{r}^0)}{d|\mathbf{r}^1 - \mathbf{r}^0|} \\ &= \frac{mc^2 \beta}{4\pi^2 \Psi^{3/2}} \left[ \frac{mc}{\hbar} \Psi^{1/2} K_0\left(\frac{mc}{\hbar} \Psi^{1/2}\right) + 2K_1\left(\frac{mc}{\hbar} \Psi^{1/2}\right) + \frac{mc}{\hbar} \Psi^{1/2} K_2\left(\frac{mc}{\hbar} \Psi^{1/2}\right) \right], \end{aligned} \quad (7.7)$$

Note that for the non relativistic gas, when  $\mathcal{H} = -\lambda \sum_i \Delta_i$ ,  $\rho_D$  would have been the usual Gaussian  $\Lambda^{-3N} e^{-(\mathbf{R}_1 - \mathbf{R}_0)^2/4\lambda\beta}$ , with  $\lambda = \hbar^2/2m$  and  $\Lambda = \sqrt{4\pi\beta\lambda}$  the de Broglie thermal wavelength.

Taking care of the indistinguishability of the particles we can describe a system of bosons and fermions with spin  $s = (g - 1)/2$  through density matrices,  $\hat{\rho}_{B,F}$ , that are obtained from the distinguishable one opportunely symmetrized or antisymmetrized, respectively. The corresponding grand canonical partition functions can then be found through a standard procedure [56] from  $\Theta_{B,F} = e^{-\beta\Omega_{B,F}} = \sum_{N=0}^{\infty} Z_{B,F}^N e^{N\mu\beta}$  where  $Z_{B,F}^N = e^{-\beta F_{B,F}^N}$  is the trace of  $\hat{\rho}_{B,F}$ . Here  $\mu = (\ln z)/\beta$  is the chemical potential,  $F$  is the Helmholtz free energy, and  $\Omega$  is the grand thermodynamic potential.

If  $V$  is the volume occupied by the system of particles, the pressure is given by  $P = -\Omega/V$ , and the average number of particles,  $N = nV = -z\partial\beta\Omega/\partial z$ , where  $n$  is the number density. We find for bosons

$$\beta P = \frac{gm^2 c}{2\pi^2 \beta \hbar^3} \sum_{\nu=1}^{\infty} \frac{z^\nu}{\nu^2} K_2(\beta mc^2 \nu), \quad (7.8)$$

$$n = \frac{gm^2 c}{2\pi^2 \beta \hbar^3} \sum_{\nu=1}^{\infty} \frac{z^\nu}{\nu} K_2(\beta mc^2 \nu), \quad (7.9)$$

and for fermions

$$\beta P = \frac{gm^2c}{2\pi^2\beta\hbar^3} \sum_{\nu=1}^{\infty} \frac{(-1)^{\nu-1}z^\nu}{\nu^2} K_2(\beta mc^2\nu) , \quad (7.10)$$

$$n = \frac{gm^2c}{2\pi^2\beta\hbar^3} \sum_{\nu=1}^{\infty} \frac{(-1)^{\nu-1}z^\nu}{\nu} K_2(\beta mc^2\nu) . \quad (7.11)$$

Clearly in the zero temperature limit ( $\beta \rightarrow \infty$ ) these reduce to (see §2.3 of Ref. [38] and our appendix P)

$$P = \frac{g}{2} \frac{mc^2}{\lambda^3} \phi(x) , \quad (7.12)$$

$$n = \frac{g}{2} \frac{x^3}{3\pi^2\lambda^3} , \quad (7.13)$$

$$\phi(x) = \frac{1}{8\pi^2} \left[ x\sqrt{1+x^2} \left( \frac{2}{3}x^2 - 1 \right) + \ln \left( x + \sqrt{1+x^2} \right) \right] , \quad (7.14)$$

where  $\lambda = \hbar/mc$ , with  $m$  the electron mass, is the electron Compton wavelength.

We can then introduce the polylogarithm,  $b_\mu$ , of order  $\mu$  and the companion  $f_\mu$  function,

$$b_\mu(z) = \sum_{\nu=1}^{\infty} \frac{z^\nu}{\nu^\mu} , \quad (7.15)$$

$$f_\mu(z) = \sum_{\nu=1}^{\infty} \frac{(-1)^{\nu-1}z^\nu}{\nu^\mu} = -b_\mu(-z) = (1 - 2^{1-x}) b_\mu(z) . \quad (7.16)$$

At finite temperatures, in the extreme relativistic case, we find for bosons

$$\beta P = \frac{g}{\pi^2(\beta\hbar c)^3} b_4(z) , \quad (7.17)$$

$$n = \frac{g}{\pi^2(\beta\hbar c)^3} b_3(z) , \quad (7.18)$$

where we used the property  $zdb_\mu(z)/dz = b_{\mu-1}(z)$ , and for fermions

$$\beta P = \frac{g}{\pi^2(\beta\hbar c)^3} f_4(z) , \quad (7.19)$$

$$n = \frac{g}{\pi^2(\beta\hbar c)^3} f_3(z) , \quad (7.20)$$

In agreement with §61 of Landau [156]. And in the non relativistic case, we find for bosons

$$\beta P = \frac{g}{\Lambda^3} b_{5/2}(z) , \quad (7.21)$$

$$n = \frac{g}{\Lambda^3} b_{3/2}(z) , \quad (7.22)$$

and for fermions

$$\beta P = \frac{g}{\Lambda^3} f_{5/2}(z) , \quad (7.23)$$

$$n = \frac{g}{\Lambda^3} f_{3/2}(z) , \quad (7.24)$$

In agreement with §56 of Landau [156]. Recalling that the internal energy of the system is given by  $E = -\partial \ln \Theta / \partial \beta$  we find in the extreme relativistic case  $E = 3PV$  and in the non relativistic case  $E = 3PV/2$ . At very low density  $n$ , and high temperature  $T$ , when  $n/T^{3/2}$  is very small,  $b_{3/2}(z) \approx f_{3/2}(z)$  is very small and  $z$  is also very small. In this case  $b_{3/2}(z) \approx b_{5/2}(z) \approx f_{3/2}(z) \approx f_{5/2}(z) \approx z$  and we find for the quantum gas  $E/V \approx (3/2)K_B T n$ . That is the non relativistic classical limit. For the bosons, as the temperature gets small at fixed density  $b_{3/2}(z)$  increases (see Eq. (7.22)) and  $z$  gets close to 1.  $b_\mu(z)$  is a monotonically increasing function of  $z$  which is only defined in  $0 \leq z \leq 1$ , so the bosons ideal gas must have a chemical potential less than zero.  $b_{3/2}(1) = \zeta(3/2) \approx 2.612$  and  $b_{5/2}(1) = \zeta(5/2) \approx 1.341$  where  $\zeta$  is the Riemann zeta function. The temperature  $T_c = \frac{2\pi\hbar^2}{mk_B} \left( \frac{n/g}{\zeta(3/2)} \right)^{2/3}$  at which  $z = 1$  is called the *critical temperature* for the Bose-Einstein condensation in the non relativistic case. For  $T < T_c$  the number of bosons with energy greater than zero will then be  $N_> = N(T/T_c)^{3/2}$ . The rest  $N_0 = N[1 - (T/T_c)^{3/2}]$  bosons are in the lowest energy state, i.e. have zero energy. For the fermions the activity is allowed to vary in  $0 \leq z < \infty$  and the functions  $f_\mu(z)$  can be extended at  $z > 1$  by using the following integral representation  $f_x(z) = [\int_0^\infty dy y^{x-1} / (e^y/z + 1)]/\Gamma(x)$ , where  $\Gamma$  is the usual gamma function.

Given the entropy  $S = -\partial \Omega / \partial T$  we immediately see that, in both the extreme relativistic and the non relativistic cases,  $S/N$  must be a homogeneous function of order zero in  $z$  and that along an adiabatic process ( $S/N$  constant) we must have  $z$  constant. Then on an adiabatic, in the extreme relativistic case,  $P \propto n^{1+1/3}$ , a polytrope of index 3, and in the non relativistic case,  $P \propto n^{1+2/3}$ , a polytrope of index 3/2. This conclusions clearly continue to hold at zero temperature when  $z \rightarrow \infty$  and the entropy is zero.

### 7.2.1 Relativistic effects at high density in a gas of fermions

The thermal average fraction of particles having momentum  $p = \hbar k$  is given by

$$\mathcal{C}_k = \frac{g}{N} \frac{1}{e^{\beta[\epsilon(k)-\mu]} - \xi} = \frac{g}{N\xi} b_0 (\xi z e^{-\beta\epsilon_k}) , \quad V \int \frac{dk}{(2\pi)^3} \mathcal{C}_k = 1 , \quad (7.25)$$

where  $\xi = +1, -1, 0$  refer to the Bose, Fermi, and Boltzmann gas respectively.

In a degenerate ( $T = 0$ ) Fermi gas we can define a Fermi energy as  $\epsilon_F = \mu = \sqrt{p_F^2 c^2 + m^2 c^4}$ , in terms of the Fermi momentum  $p_F$ . From Eq. (7.25) follows that the thermal average fraction of particles having momentum  $p = \hbar k$  is  $\mathcal{C}_k = (g/N)\Theta[\mu - \epsilon(k)]$ , where  $\Theta$  is the Heaviside unit step function and  $\epsilon(k) = \sqrt{\hbar^2 k^2 c^2 + m^2 c^4}$  is the full relativistic dispersion relation. We will then have for the density

$$n = \frac{g}{h^3} \int_0^{p_F} 4\pi p^2 dp = \frac{4\pi g}{3h^3} p_F^3 . \quad (7.26)$$

We then see immediately that at high density the Fermi momentum is also large and as a consequence the Fermi gas becomes relativistic. On the contrary the degenerate Bose gas will undergo the Bose Einstein condensation and have all the particles in the zero energy state.

At finite temperature from the results of the previous section we find that since  $f_\mu(z)$  is a monotonously increasing function of  $z$  then at large density  $n$  also  $z$  is large and at fixed temperature this implies that the chemical potential  $\mu$  is also large. In view of Eq. (7.25) this means that in the gas there are fermions of ever increasing momentum so that a relativistic treatment becomes necessary.

From Eqs. (7.10) and (7.11) it is possible (see appendix P) to extract the full relativistic adiabatic equation of state as a function of temperature and observe the transition from the low

density regime to the high density extreme relativistic one. In Fig. 7.1 we show the exponent  $\Gamma = d \ln P / d \ln n$  for the adiabatic full relativistic equation of state as a function of density. For the sake of the calculation it may be convenient to use natural units  $\hbar = c = k_B = 1$ . From the figure we see how at high density (which implies high activity)  $\Gamma \rightarrow 4/3$ . This figure should be compared with Fig. 2.3 of Ref. [38] for the degenerate Fermi gas. In particular we see how at a temperature of  $T = 20000\text{K}$  the Fermi gas can be considered extremely relativistic already at an electron number density  $n \gtrsim 10^{25}\text{cm}^{-3}$ . While we know (see Ref. [38] and Eqs. (7.12)-(7.14)) that the completely degenerate gas becomes extremely relativistic for  $n \gtrsim 10^{31}\text{cm}^{-3}$ .

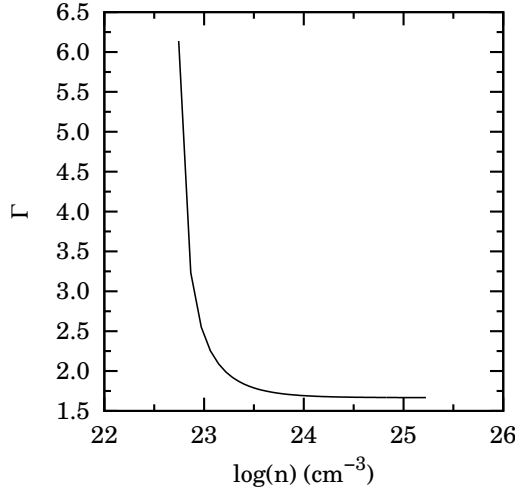


Figure 7.1: The exponent  $\Gamma = d \ln P / d \ln n$  for the adiabatic full relativistic equation of state as a function of density. We chose a temperature  $T = 20000\text{K}$  and zero entropy,  $g = 2$ , and  $m$  is the mass of an electron.  $n$  is in  $\text{cm}^{-3}$ .

### 7.2.2 The onset of quantum statistics

For a spherically symmetric distribution of matter, the mass interior to a radius  $r$  is given by

$$m(r) = \int_0^r \rho 4\pi r'^2 dr' , \quad \text{or} \quad \frac{dm(r)}{dr} = 4\pi r^2 \rho . \quad (7.27)$$

Here, since as we are considering non relativistic matter made of completely ionized elements of atomic number  $Z$  and mass number  $A$ ,  $\rho = \rho_0 = \mu_e m_u n$  is the rest mass density with  $\mu_e = A/Z$  the mean molecular weight per electron and  $m_u = 1.66 \times 10^{-24}\text{g}$  the atomic mass unit. If the star is in a steady state, the gravitational force balances the pressure force at every point. To derive the *hydrostatic equilibrium* equation, consider an infinitesimal fluid element lying between  $r$  and  $r + dr$  and having an area  $dA$  perpendicular to the radial direction. The gravitational attraction between  $m(r)$  and the mass  $dm = \rho dA dr$  is the same as if  $m(r)$  were concentrated in a point at the center, while the mass outside exerts no force on  $dm$ . The net outward pressure force on  $dm$  is  $-[P(r + dr) - P(r)]dA$ , where  $P$  is the pressure. So in equilibrium

$$\frac{dP}{dr} = -\frac{Gm(r)\rho}{r^2} , \quad (7.28)$$

where  $G$  is the universal gravitational constant.<sup>2</sup>

A consequence of the hydrostatic equilibrium is the *virial theorem*. The gravitational potential energy of the star of radius  $R$  is

$$\begin{aligned} W &= - \int_0^R \frac{Gm(r)}{r} \rho 4\pi r^2 dr \\ &= \int_0^R \frac{dP}{dr} 4\pi r^3 dr \\ &= -3 \int_0^R P 4\pi r^2 dr , \end{aligned} \quad (7.29)$$

where we have integrated by parts.

Now we assume that the gas of fermions is characterized by an adiabatic equation of state

$$P = K\rho_0^\Gamma, \quad K, \Gamma = 1 + \frac{1}{n} \text{ constants} , \quad (7.30)$$

which is also called a *polytrope* of polytropic index  $n$ . For example for fermions in the extreme relativistic limit we find

$$K = \frac{P}{\rho^{4/3}} = \frac{\pi^{2/3} \hbar c}{g^{1/3} (\mu_e m_u)^{4/3}} \frac{f_4(z)}{f_3^{4/3}(z)} , \quad (7.31)$$

where  $z$  depends on the temperature and density and goes to infinity in the degenerate limit ( $\lim_{z \rightarrow \infty} f_4(z)/f_3^{4/3}(z) = 3^{1/3}/2^{5/3}$ ). At the temperature and density typical of a white dwarf  $z$  is very large so the equation of state is practically indistinguishable from the one in the degenerate limit.

Calling  $u'$  the energy density of the gas, excluding the rest mass energy, we must have from the first law of thermodynamics, assuming adiabatic changes,

$$d(u/\rho_0) = -Pd(1/\rho_0) , \quad (7.32)$$

and integration leads to

$$u = \rho_0 c^2 + \frac{P}{\Gamma - 1} , \quad (7.33)$$

which gives  $u' = P/(\Gamma - 1)$ . Now Eq. (7.29) can be rewritten as

$$W = -3(\Gamma - 1)U , \quad (7.34)$$

where  $U = \int_0^R u' 4\pi r^2 dr$  is the total internal energy of the star. The total energy of the star,  $E = W + U$ , is then

$$E = -\frac{3\Gamma - 4}{3(\Gamma - 1)} |W| . \quad (7.35)$$

If Eq. (7.30) holds everywhere inside the star of total mass  $M$  and constant density, then the gravitational potential energy is given by

$$W = -3 \int_0^M \frac{P}{\rho} dm(r) = -\frac{3(\Gamma - 1)}{5\Gamma} \frac{GM^2}{R} , \quad (7.36)$$

---

<sup>2</sup>Here we are assuming Newtonian theory of gravity. For the general relativistic stability analysis see for example §6.9 of Ref. [38].

where we used  $d(P/\rho) = [(\Gamma - 1)/\Gamma]Gm(r)d(1/r)$  and integrated by parts using  $\Gamma > 1$ .

Without nuclear fuel,  $E$  decreases due to radiation. According to Eqs. (7.35) and (7.36),  $\Delta E < 0$  implies  $\Delta R < 0$  whenever  $\Gamma > 4/3$ . That is the star contracts and the gas will soon become quantum (see Ref. [38] §3.2). Can the star contract forever, extracting energy from the infinite supply of gravitational potential energy until  $R$  goes to zero or until the star undergoes total collapse? The answer is no for stars with  $M \sim M_\odot$ , as is demonstrated by Chandrasekhar [217] or in the book of Shapiro and Teukolsky [38]. We will reproduce their treatments in the next section.

### 7.2.3 The Chandrasekhar limit

The hydrostatic equilibrium Eqs. (7.27) and (7.28) can be combined to give

$$\frac{1}{r^2} \frac{d}{dr} \left( \frac{r^2}{\rho} \frac{dP}{dr} \right) = -4\pi G\rho . \quad (7.37)$$

Substituting the equation of state (7.30) and reducing the result to dimensionless form with

$$\rho = \rho_c \theta^n , \quad (7.38)$$

$$r = a\eta , \quad (7.39)$$

$$a = \sqrt{\frac{(n+1)K\rho_c^{1/n-1}}{4\pi G}} , \quad (7.40)$$

where  $\rho_c = \rho(r=0)$  is the central density, we find

$$\frac{1}{\eta^2} \frac{d}{d\eta} \eta^2 \frac{d\theta}{d\eta} = -\theta^n . \quad (7.41)$$

This is the *Lane-Emden equation* for the structure of a polytrope of index  $n$ . The boundary conditions at the center of a polytropic star are

$$\theta(0) = 1 , \quad (7.42)$$

$$\theta'(0) = 0 . \quad (7.43)$$

The condition (7.42) follows directly from Eq. (7.38). Eq. (7.43) follows from the fact that near the center  $m(r) \approx 4\pi\rho_cr^3/3$ , so that by Eq. (7.27)  $d\rho/dr = 0$ .

Eq. (7.41) can be easily integrated numerically, starting at  $\eta = 0$  with the boundary conditions (7.42) and (7.43). One finds that for  $n < 5$  ( $\Gamma > 6/5$ ), the solutions decreases monotonically and have a zero at a finite value  $\eta = \eta_n$ :  $\theta(\eta_n) = 0$ . This point corresponds to the surface of the star, where  $P = \rho = 0$ . Thus the radius of the star is

$$R = a\eta_n , \quad (7.44)$$

while the mass is

$$\begin{aligned} M &= \int_0^R 4\pi r^2 \rho dr \\ &= 4\pi a^3 \rho_c \int_0^{\eta_n} \eta^2 \theta^n d\eta \\ &= -4\pi a^3 \rho_c \int_0^{\eta_n} \frac{d}{d\eta} \left( \eta^2 \frac{d\theta}{d\eta} \right) d\eta \\ &= 4\pi a^3 \rho_c \eta_n |\theta'(\eta_n)| . \end{aligned} \quad (7.45)$$

Eliminating  $\rho_c$  between Eqs. (7.44) and (7.45) gives the mass-radius relation for polytropes

$$M = 4\pi R^{(3-n)/(1-n)} \left[ \frac{(n+1)K}{4\pi G} \right]^{n/(n-1)} \eta_n^{(3-n)/(1-n)} \eta_n^2 |\theta'(\eta_n)| . \quad (7.46)$$

The solutions we are particularly interested in are

$$\Gamma = \frac{5}{3}, \quad n = \frac{3}{2}, \quad \eta_{3/2} = 3.65375, \quad \eta_{3/2}^2 |\theta'(\eta_{3/2})| = \omega_{3/2} = 2.71406, \quad (7.47)$$

$$\Gamma = \frac{4}{3}, \quad n = 3, \quad \eta_3 = 6.89685, \quad \eta_3^2 |\theta'(\eta_3)| = \omega_3 = 2.01824, \quad (7.48)$$

which as explained in section 7.2.1 corresponds to the low density non relativistic case and to the high density relativistic case respectively. Note that for  $\Gamma = 4/3$ ,  $M$  is independent of  $\rho_c$  and hence  $R$ . We conclude that as  $\rho_c \rightarrow \infty$ , the electrons become more and more relativistic throughout the star, and the mass asymptotically approaches the value

$$M_{\text{Ch}} = 4\pi \omega_3 \left( \frac{K}{\pi G} \right)^{3/2}, \quad (7.49)$$

as  $R \rightarrow 0$ . The mass limit (7.49) is called *Chandrasekhar limit* (see Eq. (36) in Re. [210], Eq. (58) in [218], or Eq. (43) in [219]) and represents the maximum possible mass of a white dwarf.

In Fig. 7.2 we show the temperature dependence of the Chandrasekar limit at  $\mu_e = 2$ .

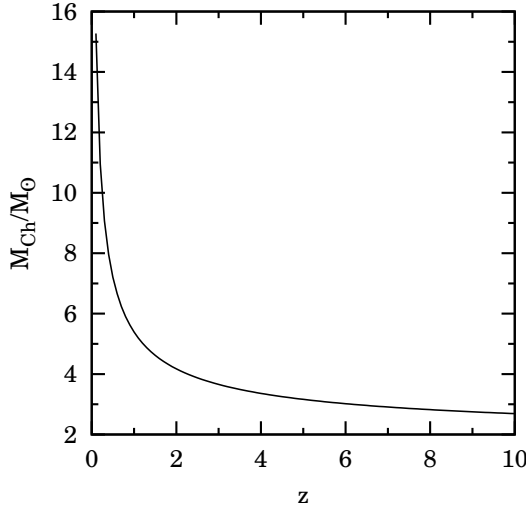


Figure 7.2: Temperature dependence of the Chandrasekar limit at  $\mu_e = 2$ . We recall that  $z = e^{\beta\mu}$ .

For the dependence of the star mass on the central density as it develops through the various polytropes, as shown in Fig. (7.1), see for example Fig. 3.2 of Ref. [38]. Clearly in the high  $\rho_c \rightarrow \infty$  limit we will have in the degenerate limit  $z \rightarrow \infty$ , from Eq. (7.31),

$$M \rightarrow M_{\text{Ch}} = 1.45639 \left( \frac{2}{\mu_e} \right)^2 M_\odot, \quad (7.50)$$

where  $\mu_e$  can be taken approximately equal to 2 or to 56/26 assuming that all the elements have been subject to nuclear fusion into the stable iron  $^{56}_{26}\text{Fe}$ .

The star will not become a black hole if  $R > r_s$  (see Fig. 1.1 of Ref. [38]), with  $r_s = 2GM_{\text{Ch}}/c^2$  the Schwarzschild radius in the Chandrasekhar limit, i.e.

$$K < \frac{\eta_3 c^2}{2^3 \omega_3 \rho_c^{1/3}}, \quad (7.51)$$

where  $K$  is given by (7.31). This suggests that at high enough central densities the star fate is to become a black hole. The critical central density is given in the degenerate  $z \rightarrow \infty$  limit by  $\bar{\rho}_c = g(\mu_e/2)^4 (2.3542 \times 10^{17} \text{ g cm}^{-3})$  which is well above the one required for the neutron drip.

If the star has a mass lower than  $M_{\text{Ch}}$  it will not reach the Chandrasekhar limit but will remain on a polytrope with  $n < 3$ . If the star has a mass higher than  $M_{\text{Ch}}$  it will eventually evolve through a supernovae explosion into a more compact object as a neutron star (when electrons are captured by protons to form neutrons by  $\beta^+$  decay), a quark star, or a black hole.

### 7.3 The structure of the ideal quantum gas

The radial distribution function  $g(r)$  is related to the structure factor  $S(k)$  by the following Fourier transform

$$n[g(r) - 1] = \frac{1}{V} \sum_k e^{ik \cdot r} [S(k) - 1]. \quad (7.52)$$

Taking into account that the operator of the particle number  $N_0$  is a constant of motion, the fluctuation-dissipation theorem (see appendix 5 of Ref. [94])  $\chi''(k, \omega) = (n\pi/\hbar)(1 - e^{-\beta\hbar\omega})S(k, \omega)$ , can be solved for the van Hove function

$$S(k, \omega) = \frac{\hbar}{n\pi} [1 - \delta_k] \frac{\chi''(k, \omega)}{1 - e^{-\beta\hbar\omega}} + \left\langle \frac{(\delta N)^2}{N} \right\rangle \delta_k \delta(\omega), \quad (7.53)$$

where  $\langle \dots \rangle$  represents averaging in the grand canonical ensemble. The static structure factor  $S(k) = \int_{-\infty}^{\infty} d\omega S(k, \omega)$  then is

$$S(k) = \frac{\hbar}{n\pi} [1 - \delta_k] \int_0^{\infty} d\omega \chi''(k, \omega) \coth\left(\frac{\beta\hbar\omega}{2}\right) + \left\langle \frac{(\delta N)^2}{N} \right\rangle \delta_k \delta(\omega), \quad (7.54)$$

where the last term does not contribute in the thermodynamic limit [220]. We substitute (see appendix 8 of Ref. [94])

$$\chi''(k, \omega) = N\pi \int \frac{dk'}{(2\pi)^3} \mathcal{C}_{k'} \{ \delta[\hbar\omega - \Delta_{k'}(\mathbf{k})] - \delta[\hbar\omega + \Delta_{k'}(\mathbf{k})] \}, \quad (7.55)$$

with  $\Delta_{k'}(\mathbf{k}) = \epsilon(|\mathbf{k}' + \mathbf{k}|) - \epsilon(\mathbf{k}')$ , and obtain for  $\mathbf{k} \neq \mathbf{0}$

$$S(k) = V \int \frac{dk'}{(2\pi)^3} \mathcal{C}_{k'} \coth\left\{\frac{1}{2}\beta[\epsilon(|\mathbf{k}' + \mathbf{k}|) - \epsilon(\mathbf{k}')]\right\}, \quad k > 0, \quad (7.56)$$

where  $\mathcal{C}_k$  denotes the thermal average fraction of particles having momentum  $\hbar\mathbf{k}$  defined in Eq. (7.25).

For further analytical manipulation we rewrite

$$\frac{\beta}{2}[\epsilon(k) - \mu] = \ln \sqrt{\frac{g}{N\mathcal{C}_k} + \xi} , \quad (7.57)$$

One rewrites Eq. (7.56) changing variables first  $\mathbf{k} + \mathbf{k}' \rightarrow \mathbf{k}$  and subsequently  $\mathbf{k} \rightarrow -\mathbf{k}$  to find

$$S(k) = V \int \frac{d\mathbf{k}'}{(2\pi)^3} \mathcal{C}_{|\mathbf{k}+\mathbf{k}'|} \coth \left\{ \frac{1}{2}\beta[\epsilon(k) - \epsilon(|\mathbf{k} + \mathbf{k}'|)] \right\} . \quad (7.58)$$

Adding Eqs. (7.56) and (7.58) and making use of the fact that the hyperbolic cotangent is an odd function, one finds

$$2S(k) = V \int \frac{d\mathbf{k}'}{(2\pi)^3} (\mathcal{C}_{\mathbf{k}'} - \mathcal{C}_{|\mathbf{k}+\mathbf{k}'|}) \coth \left\{ \frac{1}{2}\beta[\epsilon(|\mathbf{k}' + \mathbf{k}|) - \epsilon(\mathbf{k}')] \right\} . \quad (7.59)$$

Now using Eq. (7.57) we find

$$\begin{aligned} S(k) &= \frac{V}{2} \int \frac{d\mathbf{k}'}{(2\pi)^3} (\mathcal{C}_{\mathbf{k}'} - \mathcal{C}_{|\mathbf{k}+\mathbf{k}'|}) \coth \left[ \ln \sqrt{\frac{g}{N\mathcal{C}_{|\mathbf{k}+\mathbf{k}'|}}} + \xi - \ln \sqrt{\frac{g}{N\mathcal{C}_{\mathbf{k}'}}} + \xi \right] \\ &= \frac{V}{2} \int \frac{d\mathbf{k}'}{(2\pi)^3} \left( \mathcal{C}_{\mathbf{k}'} + \mathcal{C}_{|\mathbf{k}+\mathbf{k}'|} + \frac{2N\xi}{g} \mathcal{C}_{\mathbf{k}'} \mathcal{C}_{|\mathbf{k}+\mathbf{k}'|} \right) \\ &= 1 + \frac{VN\xi}{g} \int \frac{d\mathbf{k}'}{(2\pi)^3} \mathcal{C}_{\mathbf{k}'} \mathcal{C}_{|\mathbf{k}+\mathbf{k}'|} , \quad k > 0 , \end{aligned} \quad (7.60)$$

where  $\coth[\ln \sqrt{x}] = (x+1)/(x-1)$  was used in the middle step. From this follows

$$\frac{1}{V} \sum_{\mathbf{k} \neq \mathbf{0}} e^{i\mathbf{k} \cdot \mathbf{r}} [S(k) - 1] = \frac{n\xi}{g} \left\{ 2\mathcal{C}_0 \sum_{\mathbf{k} \neq \mathbf{0}} \mathcal{C}_k e^{i\mathbf{k} \cdot \mathbf{r}} + \left| \sum_{\mathbf{k} \neq \mathbf{0}} \mathcal{C}_k e^{i\mathbf{k} \cdot \mathbf{r}} \right|^2 \right\} , \quad (7.61)$$

where  $\mathcal{C}_0 = \delta_{\xi,1} \Theta(T_c - T) N_0 / N$ , with  $\Theta$  the Heaviside step function, denotes the fraction of particles which occupy the zero momentum state. We then introduce the function  $F(r) = \sum_k \mathcal{C}_k e^{i\mathbf{k} \cdot \mathbf{r}}$ . This assume the following forms

$$F_r(r) = \mathcal{C}_0(T) + \frac{g}{2\pi^2 n (\beta \hbar c)^2 \xi} \int_0^\infty \kappa d\kappa b_0 \left( \xi z e^{-\sqrt{\kappa^2 + \beta^2 m^2 c^4}} \right) \sin \left( \frac{1}{\beta \hbar c} \kappa r \right) / r , \quad (7.62)$$

$$F_{er}(r) = \mathcal{C}_0(T) + \frac{g}{2\pi^2 n (\beta \hbar c)^2 \xi} \int_0^\infty \kappa d\kappa b_0 \left( \xi z e^{-\kappa} \right) \sin \left( \frac{1}{\beta \hbar c} \kappa r \right) / r , \quad (7.63)$$

$$F_{nr}(r) = \mathcal{C}_0(T) + \frac{2g}{\pi n \Lambda^2 \xi} \int_0^\infty \kappa d\kappa b_0 \left( \xi z e^{-\kappa^2} \right) \sin \left( \frac{2\sqrt{\pi}}{\Lambda} \kappa r \right) / r . \quad (7.64)$$

in the relativistic  $\epsilon(k) = \sqrt{\hbar^2 k^2 c^2 + m^2 c^4}$ , extreme relativistic  $\epsilon(k) = c\hbar k$ , and non relativistic  $\epsilon(k) = \lambda k^2$  cases respectively. Inserting Eq. (7.60) into Eq. (7.52) we find

$$g(r) = 1 + \frac{\xi}{g} [F^2(r) - \mathcal{C}_0^2(T)] . \quad (7.65)$$

which generalizes Eq. (117.8) of Landau [156]. In Fig. 7.3 we show the radial distribution function for fermions in the relativistic and the non relativistic cases. From the figure we see how the Fermi hole becomes larger in the non relativistic case at smaller number densities.

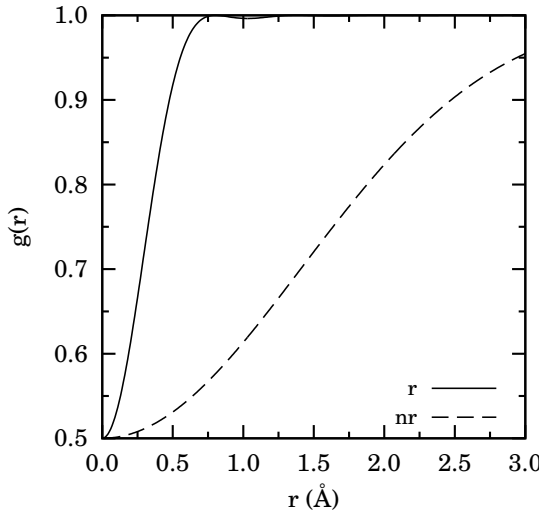


Figure 7.3: The radial distribution function for ideal electrons ( $\xi = -1, g = 2$ ) in the relativistic and the non relativistic cases. Here we chose  $T = 20000\text{K}$  and  $n = 1.04 \times 10^{22}\text{cm}^{-3}$  in the non relativistic case and  $n = 5.93 \times 10^{24}\text{cm}^{-3}$  in the relativistic case.  $r$  is in Angstroms.

Increasing the temperature by one order of magnitude (see Fig. 3.3 of Ref. [38]) keeping the density fixed produces a change in the radial distribution function of the order of  $10^{-2}$ , with the Fermi hole getting smaller.

For the electron gas we should include the Coulomb interaction between the particles: the *jellium*. The radial distribution function of jellium cannot of course be calculated exactly analytically, for a Monte Carlo simulation of the degenerate ( $T = 0$ ) jellium see for example Ref. [221] and for jellium at finite temperature see for example Ref. [222].

Actually a more accurate result could be found by treating the white dwarf matter as a binary mixture of electrons and nuclei which can today be done exactly with Monte Carlo simulations techniques like the one devised in Ref. [182].

From these numerical studies one could extract a more accurate value for the constant  $K$  in the adiabatic equation of state and thus the critical central density  $\bar{\rho}_c = (\eta_3 c^2 / 2^3 \omega_3 K)^3$ .

## 7.4 Conclusions

In this chapter we studied the importance of temperature dependence on ideal Quantum gases relevant for white dwarfs interior. Even if the temperature of the star is six orders of magnitudes smaller than the Fermi energy of the electron gas inside the star, we find that the temperature effects are quite relevant at the white dwarf densities and temperatures. In particular we show that the adiabatic equation of state becomes extremely relativistic, with  $\Gamma = 4/3$ , at densities six orders of magnitude lower than the ones required for the completely degenerate,  $T = 0$ , case. Even if the polytropic form of the adiabatic equation of state remains the same as that at zero temperature, the proportionality constant  $K$  changing by just a  $10^{-10}$  relative factor between the finite temperature case and the zero temperature case, we think that an accurate analysis of the star evolution, at least at the level of the ideal electron gas approximation in absence of

the nuclei, should properly take into account the temperature effects. This gives us a complete exactly solvable analytic approximation for the compact star interior at a finite temperature. We could comment that the temperature effects are smaller than the corrections necessary to take into account of the Coulomb interactions between the electrons and of the presence of the nuclei, but from a calculation point of view it is still desirable to keep under control the magnitude of the temperature corrections alone. Since this can be done analytically we think that their analysis is relevant by itself.

We gave the generalization to finite temperature of all the zero temperature results used by Chandrasekhar and in order to keep the treatment as general as possible we studied in parallel the Fermi and the Bose gas. Clearly only the Fermi gas results were used for the description of the ideal electron gas in the star interior.

We then studied the structure of the ideal quantum gas as a function of temperature. We found the Fermi hole for the cold electron gas in a white dwarf which turned out to be of the order of 1Å in the full relativistic regime at a number density of the order of  $n \sim 10^{26} \text{ cm}^{-3}$  and bigger in the non relativistic regime at smaller densities and fixed temperature. The radial distribution function is also affected by the temperature and the Fermi hole gets smaller as the temperature increases at fixed density.

We also point out that in order to correct our result for the Coulomb interaction among the electrons and for the presence of the nuclei, it is necessary to abandon the analytic treatment in favor of the numerical simulation. We gave some relevant references of Monte Carlo methods which are important to adopt to solve this fascinating subject. These corrections to the Chandrasekhar result or to our temperature dependent treatment are important more from a philosophical point of view rather than an experimental or observational point of view. They would lead us to the exact knowledge of the properties of a mixture of electrons and nuclei at astrophysical conditions such as the ones found in white dwarfs.

More over let us observe that only a general relativistic statistical physics theory would give us fully correct results for the stability of a white dwarf. But since this theory has not yet been formulated [223] we will have to wait till the theory becomes available.



# **Appendices**



## Appendix P

# The adiabatic equation of state for a relativistic ideal electron gas at finite temperature

Using the dispersion relation  $\epsilon(k) = \sqrt{\hbar^2 k^2 c^2 + m^2 c^4}$ , with  $m$  the rest mass of an electron, we find the pressure and the density from,

$$\beta P = g \int \frac{dk}{(2\pi)^3} \ln \left( 1 + ze^{-\beta\epsilon(k)} \right), \quad (\text{P.1})$$

$$n = g \int \frac{dk}{(2\pi)^3} \frac{1}{e^{\beta\epsilon(k)}/z + 1}. \quad (\text{P.2})$$

Integrating by parts the pressure equation and changing variable  $\kappa = \beta\hbar ck$  we find

$$\beta P = \frac{g}{(\beta\hbar c)^3} \frac{1}{2\pi^2} \frac{1}{3} \int d\kappa \frac{\kappa^3 / \sqrt{\kappa^2 + (\beta mc^2)^2}}{e^{\sqrt{\kappa^2 + (\beta mc^2)^2}/z} + 1}, \quad (\text{P.3})$$

$$n = \frac{g}{(\beta\hbar c)^3} \frac{1}{2\pi^2} \int d\kappa \frac{\kappa^2}{e^{\sqrt{\kappa^2 + (\beta mc^2)^2}/z} + 1}. \quad (\text{P.4})$$

These equations are equivalent to Eqs. (7.10) and (7.11) in the main text. Then the entropy is given by

$$S/Vk_B = g \int \frac{dk}{(2\pi)^3} \ln \left( 1 + ze^{-\beta\epsilon(k)} \right) - g \int \frac{dk}{(2\pi)^3} \frac{\ln z - \beta\epsilon(k)}{e^{\beta\epsilon(k)}/z + 1}. \quad (\text{P.5})$$

On an adiabatic the entropy per particle  $s = S/Nk_B$  is constant, and from Eq. (P.1) follows

$$\beta P = g \int \frac{dk}{(2\pi)^3} \frac{\ln z - \beta\epsilon(k)}{e^{\beta\epsilon(k)}/z + 1} + sn. \quad (\text{P.6})$$



## Chapter 8

# The Renormalization Group

We review some of the ideas of the renormalization group in the statistical physics of classical and quantum fluids theory. The origin, the nature, the basis, the formulation, the critical exponents and scaling, relevance, irrelevance, and marginality, universality, and Wilson's concept of flows and fixed point in a space of Hamiltonians.

In a recent Review of Modern Physics, M. E. Fisher [224] presented, to a wide audience, the ideas of the Renormalization Group (RG) theory behind statistical mechanics of matter physics and Quantum Field Theory (QFT).

We will also follow the lectures given by N. Goldenfeld [225] at the University of Illinois at Urbana-Champaign in 1992.

Despite its name the theory is not really about a group but about a *semigroup* since the set of transformations involved is not necessarily invertible. The theory is thought as one of the underlying ideas in the theoretical structure of QFT even if the roots of RG theory has to be looked upon the theory of critical phenomena of the statistical mechanics of matter physics.

### 8.1 Notation

In specifying critical behavior (and asymptotic variation more generally) a little more precision than normally used is really called for. Following well established custom, we use  $\simeq$  for “approximately equals” in a rough and ready sense, as in  $\pi^2 \simeq 10$ . But to express “ $f(x)$  varies like  $x^\lambda$  when  $x$  is small and positive” i.e., just to specify a critical exponent, we write:

$$f(x) \sim x^\lambda \quad (x \rightarrow 0^+). \quad (8.1)$$

Then the precise implication is

$$\lim_{x \rightarrow 0^+} \ln |f(x)| / \ln x = \lambda. \quad (8.2)$$

We define  $\approx$  as “asymptotically equals” so that

$$f(x) \approx g(x) \quad (x \rightarrow 0^+), \quad (8.3)$$

implies

$$\lim_{x \rightarrow 0^+} f(x)/g(x) = 1. \quad (8.4)$$

We define the  $o(\cdot)$  symbol as follows:

$$f = o(g) \quad (x \rightarrow 0), \tag{8.5}$$

means that  $|f| < c|g|$  for some constant  $c$  and  $|x|$  small enough.

## 8.2 The origin of RG

The history of the RG has to be reckoned on the work of Lev D. Landau who can be regarded as the founder of systematic effective field theories and of the concept of the *order parameter* ([226] sec. 135). That is one recognizes that there is a microscopic level of description and believes it should have certain general, overall properties especially as regards locality and symmetry. Those then serve to govern the most characteristic behavior on scales greater than atomic. Known the nature of the order parameter, suppose, for example, it is a complex number and like a wave function, then one knows much about the macroscopic nature of a physical system.

Traditionally, one characterizes statistical mechanics as directly linking the *microscopic* world of nuclei and atoms (on length scales of  $10^{-13}$  to  $10^{-8}$  cm) to the *macroscopic* world of say, millimeters to meters. But the order parameter, as a dynamic, fluctuating object in many cases intervenes on an intermediate or *mesoscopic* level characterized by scales of tens or hundreds of angstroms up to microns. A major collaborator of Landau and developer of the concept was V. L. Ginzburg [227, 228] in particular for the theory of superconductivity.

Landau's concept of the order parameter brought light, clarity, and form to the general theory of phase transitions, leading eventually, to the characterization of multicritical points and the understanding of many characteristic features of ordered states. But in 1944 Lars Onsager, by a mathematical tour de force, computed exactly the partition function and thermodynamic properties of the simplest model of a ferromagnet or a fluid [229, 230, 231]. This model, the Ising model, exhibited a sharp critical point: But the explicit properties, in particular, the nature of the critical singularities disagreed profoundly with essentially all the detailed predictions of the Landau theory (and of all foregoing, more specific theories). From this challenge, and from experimental evidence pointing in the same direction [232], grew the ideas of universal but nontrivial critical exponents [233, 234], special relations between different exponents [235], and then, scaling descriptions of the region of a critical point [236, 237, 238, 239, 240]. These insights served as stimulus and inspiration to Kenneth Wilson in his pursuit of an understanding of QFTs [241]. Indeed, once one understood the close mathematical analogy between doing statistical mechanics with effective Hamiltonians and doing quantum field theory (especially with the aid of Feynman's path integral) the connections seemed almost obvious. Needless to say, however, the realization of the analogy did not come overnight: In fact, Wilson himself was the individual who first understood clearly the analogies at the deepest levels.

In 1971, Wilson, having struggled with the problem of the systematic integrating out of appropriate degrees of freedom and the resulting RG flows for four or five years, was able to cast his RG ideas into a conceptually effective framework [242, 243, 241]. Effective in the sense that one could do certain calculations with it. And Franz Wegner, very soon afterwards [244, 245], further clarified the foundations and exposed their depth and breadth. An early paper by Kadanoff and Wegner [246] showing when and how universality could fail was particularly significant in demonstrating the richness of Wilson's conception. Their focus on *relevant*, *irrelevant*, and *marginal* operators (or perturbations) has played a central role [247, 248]. The advent of Wilson's concept of the RG gave more precise meaning to the effective ("coarse-grained") Hamiltonians that stemmed from the work of Landau and Ginzburg. One now pictures the Landau-Ginzburg-Wilson (LGW) Hamiltonians as true but significantly renormalized Hamiltonians in which finer microscopic degrees of freedom have been integrated out.

So our understanding of “anomalous” i.e., non-Landau-type but, in reality, standard critical behaviour was greatly enhanced. The epsilon expansion (see chapter 12 of the Goldenfeld book [225]), which used as a small, perturbation parameter the deviation of the spatial dimensionality,  $d$ , from four dimensions, namely,  $\epsilon = 4 - d$ , provided a powerful and timely tool [249]. It had the added advantage, if one wanted to move ahead, that the method looked something like a cookbook so that “any fool” could do or check the calculations, whether they really understood, at a deeper level, what they were doing or not. But in practice that also has a real benefit in that a lot of calculations do get done, and some of them turn up new and interesting things or answer old or new questions in instructive ways. A few calculations reveal apparent paradoxes and problems which serve to teach one and advance understanding.

The foundations of RG theory are in the *critical exponent relations* and the crucial *scaling concepts* developed in 1963-66 [235, 236, 237, 239, 250].

Some antedating reviews on RG theory are to be found in the following Refs. [233, 232, 251, 252, 253]. Retrospective reviews can be found in the following books [254, 255, 234]. Introductory accounts in an informal lecture style are presented by M. E. Fisher in Refs. [232, 256].

### 8.3 The decay of correlation functions

Consider a locally defined microscopic variable which we will denote  $\psi(r)$ . In a ferromagnet this might well be the local magnetization,  $M(r)$ , or spin vector,  $S(r)$ , at point  $r$  in ordinary  $d$ -dimensional (Euclidean) space; in a fluid it might be the deviation  $\delta\rho(r)$ , of the fluctuating density at  $r$  from the mean density. In QFT the local variables  $\psi(r)$  are the basic quantum fields which are “operator valued”. For a magnetic system, in which quantum mechanics was important,  $M(r)$  and  $S(r)$  would, likewise, be operators. However, the distinction is of relatively minor importance so that we may, for ease, suppose  $\psi(r)$  is a simple classical variable. It will be most interesting when  $\psi$  is closely related to the order parameter for the phase transition and critical behavior of concern.

By means of a scattering experiment (using light, x rays, neutrons, electrons, etc.) one can often observe the corresponding pair correlation function (or basic “two-point function”)

$$G(r) = \langle \psi(\mathbf{0})\psi(r) \rangle, \quad (8.6)$$

where the angular brackets  $\langle \cdot \rangle$  denote a statistical average over the thermal fluctuations that characterize all equilibrium systems at nonzero temperature. (Also understood, when  $\psi(r)$  is an operator, are the corresponding quantum-mechanical expectation values).

Physically,  $G(r)$  is important since it provides a direct measure of the influence of the leading microscopic fluctuations at the origin  $\mathbf{0}$  on the behavior at a point distance  $r = |r|$  away. But, almost by definition, in the vicinity of an appropriate critical point, for example the Curie point of a ferromagnet when  $\psi = M$  or the gas-liquid critical point when  $\psi = \delta\rho$ , a strong “ordering” influence or correlation spreads out over, essentially, macroscopic distances. As a consequence, precisely at criticality one rather generally finds a power-law decay, namely,

$$G_c(r) \approx D/r^{d-2+\eta} \quad \text{as } r \rightarrow \infty, \quad (8.7)$$

which is characterized by the critical exponent (or critical index)  $d - 2 + \eta$ .

Now all the theories one first encounters, the so-called “classical” or Landau-Ginzburg or van der Waals theories, etc., predict, quite unequivocally, that  $\eta$  vanishes. In QFT this corresponds to the behavior of a free massless particle. Mathematically, the reason underlying this prediction is that the basic functions entering the theory have (or are assumed to have) a smooth, analytic, nonsingular character so that, following Newton, they may be freely differentiated and, thereby

expanded in Taylor series with positive integral powers even at the critical point. In QFT the classical exponent value  $d - 2$  (implying  $\eta = 0$ ) can often be determined by naive dimensional analysis or “power counting”: Then  $d - 2$  is said to represent the “canonical dimension” while  $\eta$ , if nonvanishing, represents the “dimensional anomaly”. Physically, the prediction  $\eta = 0$  typically results from a neglect of fluctuations or, more precisely as Wilson emphasized, from the assumption that only fluctuations on much smaller scales can play a significant role: In such circumstances the fluctuations can be safely incorporated into effective (or renormalized) parameters (masses, coupling constants, etc.) with no change in the basic character of the theory.

But a power-law dependence on distance implies a lack of a definite length scale and, hence, a *scale invariance*. To illustrate this, let us rescale distances by a factor  $b$  so that  $r \rightarrow r' = br$ , and, at the same time, rescale the order parameter  $\psi$  by some “covariant” factor  $b^\omega$  where  $\omega$  will be a critical exponent characterizing  $\psi$ . Then we have that if one has  $\omega = \frac{1}{2}(d - 2 + \eta)$ , the factors of  $b$  drop out and the form in Eq. (8.7) is recaptured. In other words  $G_c(r)$  is *scale invariant* (or covariant): Its variation reveals no characteristic lengths, large, small, or intermediate.

Since power laws imply scale invariance and the absence of well separated scales, the classical theories should be suspect at (and near) criticality. Indeed, one finds that the “anomaly”  $\eta$  does *not* normally vanish (at least for dimensions  $d$  less than 4, which is the only concern in a physics of matter laboratory). In particular, from the work of Kaufman and Onsager [231] one can show analytically that  $\eta = \frac{1}{4}$  for the  $d = 2$  Ising model. Consequently, the analyticity and Taylor expansions presupposed in the classical theories are *not* valid. Therein lies the challenge to theory. Indeed, it proved hard even to envisage the nature of a theory that would lead to  $\eta \neq 0$ . The power of the renormalization group is that it provides a conceptual and, in many cases, a computational framework within which anomalous values for  $\eta$  (and for other exponents like  $\omega$  and its analogs for all local quantities such as the energy density  $\mathcal{E}$ ) arise naturally.

In applications to matter physics, it is clear that the power law in Eq. (8.7) can hold only for distances relatively large compared to atomic lengths or lattice spacings which we will denote  $a$ . In this sense the scale invariance of correlation functions is only *asymptotic* hence the symbol  $\approx$ , for “asymptotically equals”, and the proviso  $r \rightarrow \infty$  in Eq. (8.7). A more detailed description would account for the effects of nonvanishing  $a$ , at least in leading order. By contrast, in QFT the microscopic distance  $a$  represents an “ultraviolet” cutoff which, since it is in general unknown, one normally wishes to remove from the theory. If this removal is not done with surgical care, which is what the renormalization program in QFT is all about, the theory remains plagued with infinite divergencies arising when  $a \rightarrow 0$ , i.e., when the “cutoff is removed”. But in statistical physics one always anticipates a short-distance cutoff that sets certain physical parameters such as the value of  $T_c$ ; infinite terms *per se* do not arise and certainly do not drive the theory as in QFT.

One may, however, provide a more concrete illustration of scale dependence by referring again to the power law Eq. (8.7). If the exponent  $\eta$  vanishes, or equivalently, if  $\psi$  has its canonical dimension, so that  $\omega = \omega_{\text{can}} = \frac{1}{2}(d - 2)$ , one may regard the amplitude  $D$  as a fixed, measurable parameter which will typically embody some real physical significance. Suppose, however,  $\eta$  does not vanish but is nonetheless relatively small: Indeed, for many ( $d = 3$ )-dimensional systems, one has  $\eta \simeq 0.035$  [257, 256, 254, 234]. Then we can introduce a “renormalized” or “scale-dependent” parameter

$$\tilde{D}(r) \approx D/r^\eta \quad \text{as} \quad r \rightarrow \infty, \quad (8.8)$$

and rewrite the original result simply as

$$G_c(r) = \tilde{D}(r)/r^{d-2}. \quad (8.9)$$

Since  $\eta$  is small we see that  $\tilde{D}(r)$  varies slowly with the scale  $r$  on which it is measured. In many cases in QFT the dimensions of the field  $\psi$  (alias the order parameter) are subject only to marginal perturbations (see below) which translate into a  $\ln r$  dependence of the renormalized parameter  $\tilde{D}(r)$ ; the variation with scale is then still weaker than when  $\eta \neq 0$ .

## 8.4 The challenges posed by critical phenomena

Physics is an experimental science. So let us briefly review a few experimental findings that serves to focus attention on the principal theoretical challenges faced by, and rather fully met by RG theory.

In 1869 Andrews reported to the Royal Society his observations of carbon dioxide sealed in a (strong) glass tube at a mean overall density,  $\rho$ , close to  $0.5 \text{ gm cm}^{-3}$ . At room temperatures the fluid breaks into two phases: A liquid of density  $\rho_{\text{liq}}(T)$  that coexists with a lighter vapor or gas phase of density  $\rho_{\text{gas}}(T)$  from which it is separated by a visible meniscus or interface; but when the temperature,  $T$ , is raised and reaches a sharp critical temperature,  $T_c \simeq 31.04^\circ\text{C}$ , the liquid and gaseous phases become identical, assuming a common density  $\rho_{\text{liq}} = \rho_{\text{gas}} = \rho_c$  while the meniscus disappears in a “mist” of “critical opalescence”. For all  $T$  above  $T_c$  there is a complete “continuity of state”, i.e., no distinction whatsoever remains between liquid and gas (and there is no meniscus). A plot of  $\rho_{\text{liq}}(T)$  and  $\rho_{\text{gas}}(T)$ , as illustrated somewhat schematically in Fig. 8.1(d), represents the so-called gas-liquid coexistence curve or *binodal*: The two halves,  $\rho_{\text{liq}} > \rho_c$  and  $\rho_{\text{gas}} < \rho_c$ , meet smoothly at the critical point  $(T_c, \rho_c)$ , shown as a small circle in Fig. 8.1: The dashed line below  $T_c$  represents the diameter defined by  $\rho(T) = \frac{1}{2}[\rho_{\text{liq}}(T) + \rho_{\text{gas}}(T)]$ .

The same phenomena occur in all elemental and simple molecular fluids and in fluid mixtures. The values of  $T_c$ , however, vary widely: e.g., for helium-four one finds 5.20 K while for mercury  $T_c \simeq 1764$  K. The same is true for the critical densities and concentrations: These are thus “nonuniversal parameters” directly reflecting the atomic and molecular properties, i.e., the physics on the scale of the cutoff  $a$ . Hence, in Fig. 8.1,  $\rho_{\text{max}}$  (which may be taken as the density of the corresponding crystal at low  $T$ ) is of order  $1/a^3$ , while the scale of  $k_B T_c$  is set by the basic microscopic potential energy of attraction denoted  $\varepsilon$ . While of considerable chemical, physical, and engineering interest, such parameters will be of marginal concern to us here. The point, rather, is that the shapes of the coexistence curves,  $\rho_{\text{liq}}(T)$  and  $\rho_{\text{gas}}(T)$  versus  $T$ , become asymptotically universal in character as the critical point is approached.

To be more explicit, note first an issue of symmetry. In QFT, symmetries of many sorts play an important role: They may (or must) be built into the theory but can be “broken” in the physically realized vacuum state(s) of the quantum field. In the physics of fluids the opposite situation pertains. There is no real physical symmetry between coexisting liquid and gas: They are just different states, one a relatively dense collection of atoms or molecules, the other a relatively dilute collection, see Fig. 8.1(d). However, if one compares the two sides of the coexistence curve, gas and liquid, by forming the ratio

$$R(T) = [\rho_c - \rho_{\text{gas}}(T)]/[\rho_c - \rho_{\text{liq}}(T)], \quad (8.10)$$

one discovers an extraordinarily precise asymptotic symmetry. Explicitly, when  $T$  approaches  $T_c$  from below or, introducing a convenient notation,

$$t \equiv (T - T_c)/T_c \rightarrow 0^-, \quad (8.11)$$

one finds  $R(T) \rightarrow 1$ . This simply means that the physical fluid builds for itself an exact mirror symmetry in density (and other properties) as the critical point is approached. And this is a

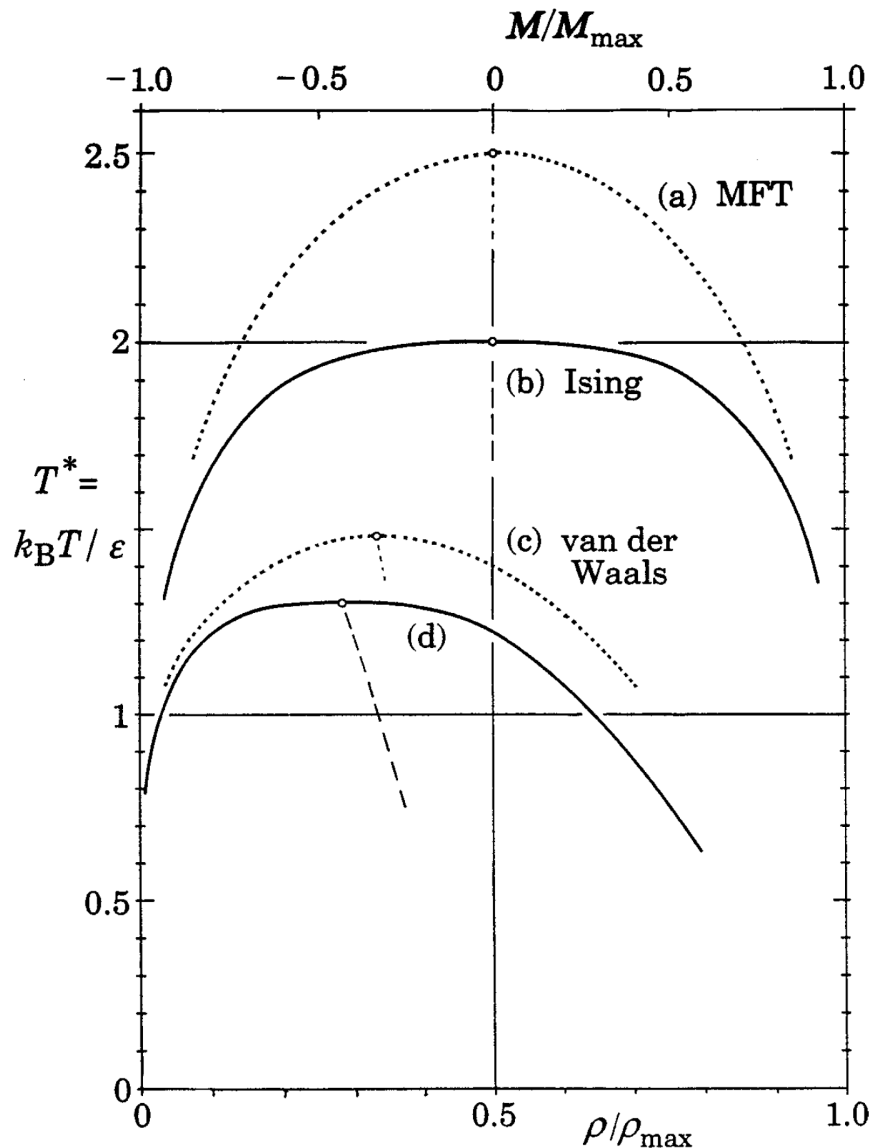


Figure 8.1: Temperature variation of gas-liquid coexistence curves (temperature,  $T$ , versus density,  $\rho$ ) and corresponding spontaneous magnetization plots (magnetization,  $M$ , versus  $T$ ). The solid curves, (b) and (d), represent (semiquantitatively) observation and modern theory, while the dotted curves (a) and (c) illustrate the corresponding “classical” predictions (mean-field theory and van der Waals approximation). These latter plots are parabolic through the critical points (small open circles) instead of obeying a power law with the universal exponent  $\beta \simeq 0.325$ : See Eqs. (8.12) and (11). The energy scale  $\varepsilon$ , and the maximal density and magnetization,  $\rho_{\max}$  and  $M_{\max}$ , are nonuniversal parameters particular to each physical system; they vary widely in magnitude.

universal feature for all fluids near criticality. (This symmetry is reflected in Fig. 8.1(d) by the high, although not absolutely perfect, degree of asymptotic linearity of the coexistence-curve diameter,  $\bar{\rho}(T)$ , the dashed line described above).

More striking than the (asymptotic) symmetry of the coexistence curve is the universality of its shape close to  $T_c$ , visible in Fig. 8.1(d) as a flattening of the graph relative to the parabolic shape of the corresponding classical prediction, see plot (c) in Fig. 8.1, which is derived from the famous van der Waals equation of state. Rather generally one can describe the shape of a fluid coexistence curve in the critical region via the power law

$$\Delta\rho \equiv \frac{1}{2}[\rho_{\text{liq}}(T) - \rho_{\text{gas}}(T)] \approx B|t|^\beta \quad \text{as } t \rightarrow 0^-, \quad (8.12)$$

where  $B$  is a *nonuniversal* amplitude while the critical exponent  $\beta$  takes a *universal* value

$$\beta \simeq 0.325, \quad (8.13)$$

(in which the last figure is uncertain). To stress the point:  $\beta$  is a nontrivial number, not known exactly, but it is the same for all fluid critical points! This contrasts starkly with the classical prediction  $\beta = \frac{1}{2}$  [corresponding to a parabola: See Fig. 8.1(c)]. The value in Eq. (8.13) applies to ( $d = 3$ )-dimensional systems. Classical theories make the same predictions for all  $d$ . On the other hand, for  $d = 2$ , Onsager's work [230] on the square-lattice Ising model leads to  $\beta = \frac{1}{8}$ . This value has since been confirmed experimentally by Kim and Chan [258] for a “two-dimensional fluid” of methane ( $\text{CH}_4$ ) adsorbed on the flat, hexagonal-lattice surface of graphite crystals.

Not only does the value in Eq. (8.13) for  $\beta$  describe many types of fluid system, it also applies to anisotropic magnetic materials, in particular to those of Ising-type with one “easy axis”. For that case, in vanishing magnetic fields,  $H$ , below the Curie or critical temperature,  $T_c$ , a ferromagnet exhibits a spontaneous magnetization and one has  $M = \pm M_0(T)$ . The sign, + or −, depends on whether one lets  $H$  approach zero from positive or negative values. Since, in equilibrium, there is a full, natural physical symmetry under  $H \rightarrow -H$  and  $M \rightarrow -M$  (in contrast to fluid systems) one clearly has  $M_c = 0$ : Likewise, the asymptotic symmetry corresponding to Eq. (8.10) is, in this case exact for all  $T$ : See Fig. 8.1, plots (a) and (b). Thus, as is evident in Fig. 8.1, the global shape of a spontaneous magnetization curve does not closely resemble a normal fluid coexistence curve. Nevertheless, in the asymptotic law

$$M_0(T) \approx B|t|^\beta \quad \text{as } t \rightarrow 0^-, \quad (8.14)$$

the exponent value in Eq. (8.13) still applies for  $d = 3$ : See Fig. 8.1(b); the corresponding classical “mean-field theory” in plot (a), again predicts  $\beta = \frac{1}{2}$ . For  $d = 2$  the value  $\beta = \frac{1}{8}$  is once more valid.

And, beyond fluids and anisotropic ferromagnets many other systems belong, more correctly their critical behavior belongs, to the “Ising universality class”. Included are other magnetic materials (antiferromagnets and ferrimagnets), binary metallic alloys (exhibiting order-disorder transitions), certain types of ferroelectrics, and so on.

For each of these systems there is an appropriate order parameter and, via Eq. (8.7), one can then define (and usually measure) the correlation decay exponent  $\eta$  which is likewise universal. Indeed, essentially any measurable property of a physical system displays a universal critical singularity. Of particular importance is the exponent  $\alpha \simeq 0.11$  (Ising,  $d = 3$ ) which describes the divergence to infinity of the specific heat via

$$c(T) \approx A^\pm/|t|^\alpha \quad \text{as } t \rightarrow 0^\pm, \quad (8.15)$$

(at constant volume for fluids or in zero field,  $H = 0$ , for ferromagnets, etc.). The amplitudes  $A^+$  and  $A^-$  are again nonuniversal; but their dimensionless ratio,  $A^+/A^-$ , is universal, taking a

value close to 0.52. When  $d = 2$ , as Onsager [229] found,  $A^+/A^- = 1$  and  $|t|^{-\alpha}$  is replaced by  $\ln |t|$ . But classical theory merely predicts a jump in specific heat,  $\Delta c = c_c^- - c_c^+ > 0$  for all  $d$ .

Two other central quantities are a divergent isothermal compressibility  $\chi(T)$  (for a fluid) or isothermal susceptibility,  $\chi(T) \propto (\partial M / \partial H)_T$  (for a ferromagnet) and, for all systems, a *divergent correlation length*,  $\xi(T)$ , which measures the growth of the “range of influence” or of correlation observed say, via the decay of the correlation function  $G(r; T)$ , see Eq. (8.6) above, to its long-distance limit. For these functions we write

$$\chi(T) \approx C^\pm / |t|^\gamma \quad \text{and} \quad \xi(t) \approx \xi_0^\pm / |t|^\nu, \quad (8.16)$$

as  $t \rightarrow 0^\pm$ , and find, for  $d = 3$  Ising-type systems,

$$\gamma \simeq 1.24 \quad \text{and} \quad \nu \simeq 0.63, \quad (8.17)$$

(while  $\gamma = 1\frac{3}{4}$  and  $\nu = 1$  for  $d = 2$ ).

As hinted, there are other universality classes known theoretically although relatively few are found experimentally [259, 260]. Indeed, one of the early successes of RG theory was delineating and sharpening our grasp of the various important universality classes. To a significant degree one found that only the vectorial or tensorial character of the relevant order parameter (e.g., scalar, complex number alias two-component vector, threecomponent vector, etc.) plays a role in determining the universality class. But the whys and the wherefores of this self-same issue represent, as does the universality itself, a prime challenge to any theory of critical phenomena.

## 8.5 The critical exponents

It has been believed for a long time that the critical exponents were the same above and below the critical temperature. It has now been shown that this is not necessarily true: When a continuous symmetry is explicitly broken down to a discrete symmetry by irrelevant (in the renormalization group sense) anisotropies, then the exponents  $\gamma$  and  $\gamma'$  are not identical [261]. Here we indicate with a prime the critical exponents for  $t < 0$  (ordered phase) and without the prime the critical exponent for  $t > 0$  (disordered phase).

### 8.5.1 The classical exponent values

The classical Landau theory (aka mean-field theory) values of the critical exponents for a scalar field are given by (see chapter 5 of Goldenfeld book [225])

$$\alpha = 0, \quad (8.18)$$

$$\beta = \frac{1}{2}, \quad (8.19)$$

$$\gamma = 1, \quad (8.20)$$

$$\delta = 3, \quad (8.21)$$

adding derivative terms turning it into a mean-field Ginzburg-Landau theory, we get

$$\eta = 0, \quad (8.22)$$

$$\nu = \frac{1}{2}. \quad (8.23)$$

They are valid for  $d > d_{uc} = 4$ , the upper critical dimension [249, 262, 263, 259, 256].

The problem with mean-field theory is that the critical exponents do not depend on the space dimension. This leads to a quantitative discrepancy in space dimensions 2 and 3, where the true critical exponents differ from the mean-field values. It leads to a qualitative discrepancy in space dimension 1, where a critical point in fact no longer exists, even though mean-field theory still predicts there is one. The space dimension where mean-field theory becomes qualitatively incorrect is called the lower critical dimension.

### 8.5.2 The Ising exponent values

We list in Table 8.1 the critical exponents of the ferromagnetic transition in the Ising model (see also Goldenfeld book [225] p. 111).

Table 8.1: This table lists the critical exponents of the ferromagnetic transition in the Ising model. In statistical physics, the Ising model describes a continuous phase transition with scalar order parameter. The critical exponents of the transition are universal values and characterize the singular properties of physical quantities. The ferromagnetic transition of the Ising model establishes an important universality class, which contains a variety of phase transitions as different as ferromagnetism close to the Curie point and critical opalescence of liquid near its critical point.

	$d = 2$	$d = 3$	$d = 4$
$\alpha$	0	0.11008(1)	0
$\beta$	1/8	0.326419(3)	1/2
$\gamma$	7/4	1.237075(10)	1
$\delta$	15	4.78984(1)	3
$\eta$	1/4	0.036298(2)	0
$\nu$	1	0.629971(4)	1/2
$\omega$	2	0.82966(9)	0

### 8.5.3 Exponent relations

Critical exponents obey the following *exponent relations* independently of the universality class

$$\nu d = 2 - \alpha = 2\beta + \gamma = \beta(\delta + 1) = \gamma \frac{\delta + 1}{\delta - 1}, \quad (8.24)$$

$$2 - \eta = \frac{\gamma}{\nu} = d \frac{\delta - 1}{\delta + 1}. \quad (8.25)$$

These equations imply that there are only two independent exponents, e.g.,  $\nu$  and  $\eta$ . All this follows from the theory of the RG.

The relations [264, 265, 266, 251, 235]

$$\gamma = (2 - \eta)\nu, \quad (8.26)$$

$$\alpha + 2\beta + \gamma = 2, \quad (8.27)$$

hold exactly for the  $d = 2$  Ising models and are valid when  $d = 3$  to within the experimental accuracy or the numerical precision (of the theoretical estimates [251, 254, 234]). They are even obeyed exactly by the classical exponent values (which, today, we understand as valid for  $d > 4$ ).

The first relation (8.26) pertains just to the basic correlation function  $G(r; T)$  as defined previously in Eq. (8.6). It follows from the assumption [264, 265], supported in turn by an

examination of the structure of Onsager's matrix solution to the Ising model [229, 231] that in the critical region all lengths (much larger than the lattice spacing  $a$ ) scale like the correlation length  $\xi(T)$ , introduced in Eq. (8.16). Formally one expresses this principle by writing, for  $t \rightarrow 0$  and  $r \rightarrow \infty$ ,

$$G(r; T) \approx \frac{D}{r^{d-2+\eta}} \mathcal{G} \left( \frac{r}{\xi(T)} \right), \quad (8.28)$$

where, for consistency with (8.7), the scaling function,  $\mathcal{G}(x)$ , satisfies the normalization condition  $\mathcal{G}(0) = 1$ . Integrating  $r$  over all space yields the compressibility/susceptibility  $\chi(T)$  and, thence, the relation  $\gamma = (2 - \eta)\nu$ . This scaling law highlights the importance of the correlation length  $\xi$  in the critical region, a feature later stressed and developed further, especially by Widom [236, 237], Kadanoff [239, 247], and Wilson [241, 262]. It is worth remarking that in QFT the inverse correlation length  $\xi^{-1}$ , is basically equivalent to the *renormalized mass* of the field  $\psi$ : Masslessness then equates with *criticality* since  $\xi^{-1} \rightarrow 0$ .

The second relation (8.27) is proven in section 8.8.

## 8.6 The Gaussian model and the upper critical dimension

See chapters 6 and 7 of the book of Goldenfeld [225].

## 8.7 The task of RG

One would wish the RG theory to:

- (i) explain the ubiquity of *power laws* at and near critical points (as opposed to the exponential laws which governs, for example, the decay of correlation in Coulomb liquids [267, 268]);
- (ii) explain the values of the leading *thermodynamic and correlation exponents*,  $\alpha, \beta, \gamma, \delta, \nu, \eta$ , and  $\omega$ ;
- (iii) clarify why and how the classical values are in error, including the existence of *borderline dimensionalities*, like  $d_{uc} = 4$ , above which classical theories become valid;
- (iv) find the *correction-to-scaling exponent*  $\theta$  (and, ideally, the higher-order correction exponents);
- (v) give a method to compute *crossover exponents*,  $\phi$ , to check for the relevance or *irrelevance* of a multitude of possible perturbations;
- (vi) give understanding of *universality* with nontrivial exponents;
- (vii) give a derivation of *scaling*;
- (viii) allow to understand the *breakdown* of universality and scaling in certain circumstances;
- (ix) handle effectively *logarithmic* and more exotic dependences on temperature.

We may start by supposing that one has a set of microscopic, fluctuating, mechanical variables: In QFT these would be the various quantum fields,  $\psi(r)$ , defined at all points in a Euclidean (or Minkowski) space. In statistical physics the phase space variables  $PS = \{R^N, P^N\}$

of  $N$  particles of coordinates  $R^N = \{r_1, \dots, r_N\}$  and momenta  $P^N = \{p_1, \dots, p_N\}$  in a volume  $V$ .

In terms of the basic variables  $PS$  one can form various “local operators” (or “physical quantities” or “observables”) like, for a real fluid, the pressure  $P$ , the energy density  $\mathcal{E}$ , the specific heat  $c$ , the isothermal compressibility  $\chi$ , etc. or, for the Ising model, the pressure  $P$ , the spontaneous magnetization  $M$ , the energy density  $\mathcal{E}$ , the specific heat  $c$ , the isothermal magnetic susceptibility  $\chi$ , etc. For a mapping between the Ising model and a real fluid see Goldenfeld book [225] section 2.12.

A physical system of interest is then specified by its *Hamiltonian*  $\mathcal{H}[PS; L]$  which is usually just a spatially uniform sum of local operators made up from the phase space operators and the coupling constant  $L = \{L\}$ . The crucial function is the “reduced Hamiltonian”

$$\bar{\mathcal{H}}[PS; K] = -\mathcal{H}[PS; L]/k_B T, \quad (8.29)$$

where  $k_B$  is Boltzmann constant,  $T$  the absolute temperature, and  $K = \{T, L\}$ , are the various “thermodynamic fields” (or coupling constants in QFT). We may suppose that one or more of the thermodynamic fields, in particular the temperature, can be controlled directly by the experimenter; but others may be “given” since they will, for example, embody details of the physical system that are “fixed by nature”.

An important feature of Wilson’s approach, however, is to regard any “physical Hamiltonian” as merely specifying a subspace in a very large space of possible (reduced) Hamiltonians,  $\mathcal{H}$ . This change in perspective proves crucial to the proper formulation of a renormalization group: In principle, it enters also in QFT although in practice, it is usually given little attention.

The partition function will be

$$Z_N[\bar{\mathcal{H}}] = \text{Tr}_N \left\{ e^{\bar{\mathcal{H}}[PS]} \right\}, \quad (8.30)$$

where the trace operator  $\text{Tr}_N \{\cdot\}$ , denotes a summation or integration over the possible values of all the  $2dN$  variables  $PS$ . Then the thermodynamics follow from the total free energy density, which is given by

$$f[\bar{\mathcal{H}}] \equiv f(K) = \lim_{N, V \rightarrow \infty} \frac{\ln Z_N[\bar{\mathcal{H}}]}{V}, \quad (8.31)$$

where  $N$  and  $V$  becomes infinite maintaining the ratio  $V/N = a^d$  fixed: In QFT this corresponds to an infinite system with an ultraviolet lattice cutoff.

To the degree that one can actually perform the trace operation in Eq. (8.30) for a particular model system and take the “thermodynamic limit” in Eq. (8.31) one will obtain the precise critical exponents, scaling functions, and so on. This was Onsager’s (1944) [229] route in solving the  $d = 2$ , spin 1/2 Ising models in zero magnetic field. At first sight one then has no need of RG theory. While one knows for sure that  $\alpha = 0$  ( $\ln$ ),  $\beta = \frac{1}{8}$ ,  $\gamma = 1\frac{3}{4}$ ,  $\nu = 1$ ,  $\eta = \frac{1}{4}$ , ... for the planar Ising models one does not know why the exponents have these values. Indeed, the seemingly inevitable mathematical complexities of solving even such physically oversimplified models exactly [269] serve to conceal almost all traces of general, underlying mechanisms and principles that might “explain” the results. Also, should one ever achieve truly high precision in simulating critical systems on a computer (a prospect which still seems some decades away [34]) the same problem would remain. Thus it comes to pass that even a rather crude and approximate solution of a two-dimensional Ising model by a RG method can be truly instructive.

## 8.8 The basis and formulation

At the heart of (real space<sup>1</sup>) RG theory there is the renormalization of the spatial scale via  $r \rightarrow r' = br$  which produces on the reduced Hamiltonian the following *renormalization transformation*

$$\bar{\mathcal{H}}'[PS'; K'] = \mathcal{R}_b \bar{\mathcal{H}}[PS, K], \quad (8.32)$$

where we have elected to keep track of the spatial rescaling factor,  $b$ , as a subscript of the RG operator  $\mathcal{R}$ . Thus successive renormalizations with scaling factors  $b_1$  and  $b_2$  yield the quite general relation  $\mathcal{R}_{b_2} \mathcal{R}_{b_1} = \mathcal{R}_{b_2 b_1}$ , which essentially defines a unitary *semigroup* of transformations. The formal algebraic definition [270] of a unitary semigroup (or “monoid”) is a set  $M$  of elements,  $u, v, w, x, \dots$  with a binary operation,  $xy = w \in M$ , which is associative, so  $v(wx) = (vw)x$ , and has a unit  $u$ , obeying  $ux = xu = x$  (for all  $x \in M$ ). In RG theory, the unit transformation corresponds simply to  $b = 1$ .

It is more fruitful to iterate the transformation so obtaining a sequence,  $\bar{\mathcal{H}}^{(l)}$ , of renormalized Hamiltonians, namely,

$$\bar{\mathcal{H}}^{(l)} = \mathcal{R}_b \bar{\mathcal{H}}^{(l-1)} = \mathcal{R}_{b^l} \bar{\mathcal{H}}. \quad (8.33)$$

Hille [271] and Riesz and Sz.-Nagy [272] describe semigroups within a continuum, functional analysis context and discuss the existence of an infinitesimal generator when the flow parameter  $l$  is defined for continuous values  $l \geq 0$ . One may regard

$$l = \log_b(|r'|/|r|), \quad (8.34)$$

as measuring, logarithmically, the scale on which the system is being described; but note that, in general, the form of the Hamiltonian is also changing as the “scale” is changed or  $l$  increases. Thus a partially renormalized Hamiltonian can be expected to take on a more-or-less generic, mesoscopic form: Hence it represents an appropriate candidate to give meaning to a Landau-Ginzburg or, now, LGW effective Hamiltonian.

It is also worth mentioning that by letting  $b \rightarrow 1^+$ , one can derive a *differential* or continuous RG flow and rewrite the recursion relation (8.33) as

$$\frac{d}{dl} \bar{\mathcal{H}} = \mathcal{B} \bar{\mathcal{H}}. \quad (8.35)$$

In this form the RG semigroup can typically be extended to an Abelian group [270]. But as already stressed this fact plays a negligible role. Such continuous flows are illustrated in Fig. 8.2.<sup>2</sup>

The recursive application of an RG transformation  $\mathcal{R}_b$  induces a *flow* in the space of Hamiltonians,  $\mathcal{H}$ . Then one observes that “sensible”, “reasonable”, or, better, “well-designed” RG transformations are *smooth*, so that points in the original physical manifold,  $\mathcal{H}^{(0)}$ , that are close, say in temperature, remain so in  $\mathcal{H}^{(1)}$ , i.e., under renormalization, and likewise as the flow parameter  $l$  increases, in  $\mathcal{H}^{(l)}$ .

Thanks to the smoothness of the RG transformation, if one knows the free energy  $f_l \equiv f[\mathcal{H}^{(l)}]$  at the  $l$ -th stage of renormalization, then one knows the original free energy  $f[\mathcal{H}]$  and its critical behavior: Explicitly one has

$$f(K) \equiv f[\bar{\mathcal{H}}] = b^{-dl} f[\bar{\mathcal{H}}^{(l)}] \equiv b^{-dl} f_l(K^{(l)}). \quad (8.36)$$

<sup>1</sup>As opposed to the *momentum-shell* RG [249].

<sup>2</sup>If it happens that  $\bar{\mathcal{H}}$  can be represented, in general only approximately, by a single coupling constant, say,  $g$ , then  $\mathcal{B}$  reduces to the so-called beta-function  $\beta(g)$  of QFT.

Furthermore, the smoothness implies that all the universal critical properties are preserved under renormalization. Similarly one finds [242, 262, 256] that the critical point of  $\bar{\mathcal{H}}^{(0)} \equiv \bar{\mathcal{H}}$  maps on to that of  $\bar{\mathcal{H}}^{(1)} \equiv \bar{\mathcal{H}}'$ , and so on, as illustrated by the flow lines in Fig. 8.2. Thus it is instructive to follow the *critical trajectories* in  $\mathcal{H}$ , i.e., those RG flow lines that emanate from a physical critical point. In principle, the topology of these trajectories could be enormously complicated and even chaotic: In practice, however, for a well-designed or “apt” RG transformation, one most frequently finds that the critical flows terminate, or, more accurately, come to an asymptotic halt, at a *fixed point*  $\bar{\mathcal{H}}^*$ , of the RG: See Fig. 8.2. Such a fixed point is defined simply by

$$\mathcal{R}_b \bar{\mathcal{H}}^* = \bar{\mathcal{H}}^* \quad \text{or} \quad \mathcal{B} \bar{\mathcal{H}}^* = 0. \quad (8.37)$$

One then searches for fixed-point solutions.

Why are the fixed points so important? Some, in fact, are *not*, being merely *trivial*, corresponding to *no interactions* or to all spins frozen, etc. But the *nontrivial* fixed points represent critical states; furthermore, the nature of their criticality, and of the free energy in their neighborhood, must, as explained, be *identical* to that of all those distinct Hamiltonians whose critical trajectories converge to the same fixed point. In other words, a particular fixed point defines a *universality class*<sup>3</sup> of critical behavior which “governs” or “attracts” all those systems whose critical points eventually map onto it: See Fig. 8.2.

Here, then we at last have the natural explanation of universality: Systems of quite different physical character may, nevertheless, belong to the domain of attraction of the same fixed point  $\bar{\mathcal{H}}^*$  in  $\mathcal{H}$ . The distinct sets of inflowing trajectories reflect their varying physical content of associated irrelevant variables and the corresponding nonuniversal rates of approach to the asymptotic power laws dictated by  $\bar{\mathcal{H}}^*$ .

From each critical fixed point, there flow at least two “unstable” or outgoing trajectories. These correspond to one or more relevant variables, specifically, for the case illustrated in Fig. 8.2, to the temperature or thermal field,  $t = (T - T_c)/T_c$ , with  $T_c$  the critical temperature, and the magnetic or ordering field,  $h$ . If there are further relevant trajectories then one can expect crossover to different critical behavior. In the space  $\mathcal{H}$ , such trajectories will then typically lead to distinct fixed points describing (in general) completely new universality classes. A skeptical reader may ask: “But what if no fixed points are found?” This can well mean, as it has frequently meant in the past, simply that the chosen RG transformation was poorly designed or “not apt”.

---

<sup>3</sup>This retrospective statement may, perhaps, warrant further comment. First, the terms “universal” and “universality class” came into common usage only after 1974 when the concept of various types of RG fixed point had been well recognized (see Fisher Ref. [259]). Kadanoff [247] deserves credit not only for introducing and popularizing the terms but especially for emphasizing, refining, and extending the concepts. On the other hand, Domb’s [233] review made clear that all (short-range) Ising models should have the same critical exponents irrespective of lattice structure but depending strongly on dimensionality. The excluded-volume problem for polymers was known to have closely related but distinct critical exponents from the Ising model, depending similarly on dimensionality but not lattice structure [273]. And, as regards the Heisenberg model, which possesses what we would now say is an ( $n = 3$ )-component vector or  $O(3)$  order parameter, there were strong hints that the exponents were again different [274, 275]. On the experimental front matters might, possibly be viewed as less clear-cut: Indeed, for ferromagnets, nonclassical exponents were unambiguously revealed only in 1964 by Kouvel and Fisher [276]. However, a striking experiment by Heller and Benedek [277] had already shown that the order parameter of the antiferromagnet MnF<sub>2</sub>, namely, the sublattice magnetization  $M_0^\dagger(T)$ , vanishes as  $|t|^\beta$  with  $\beta = 0.335$ . Furthermore, for fluids, the work of the Dutch school under Michels and the famous analysis of coexistence curves by Guggenheim [278] allowed little doubt, see Rowlinson book [279], Chap. 3, especially, pp. 91-95 that all reasonably simple atomic and molecular fluids displayed the same but nonclassical critical exponents with  $\beta \simeq \frac{1}{3}$ : And, also well before 1960, Widom and Rice [280] had analyzed the critical isotherms of a number of simple fluids and concluded that the corresponding critical exponent  $\delta$  (see, e.g., Ref. [251]) took a value around 4.2 in place of the van der Waals value  $\delta = 3$ . In addition, evidence was in hand showing that the consolute point in binary fluid mixtures was similar (see Rowlinson book [279], pp. 165-166).

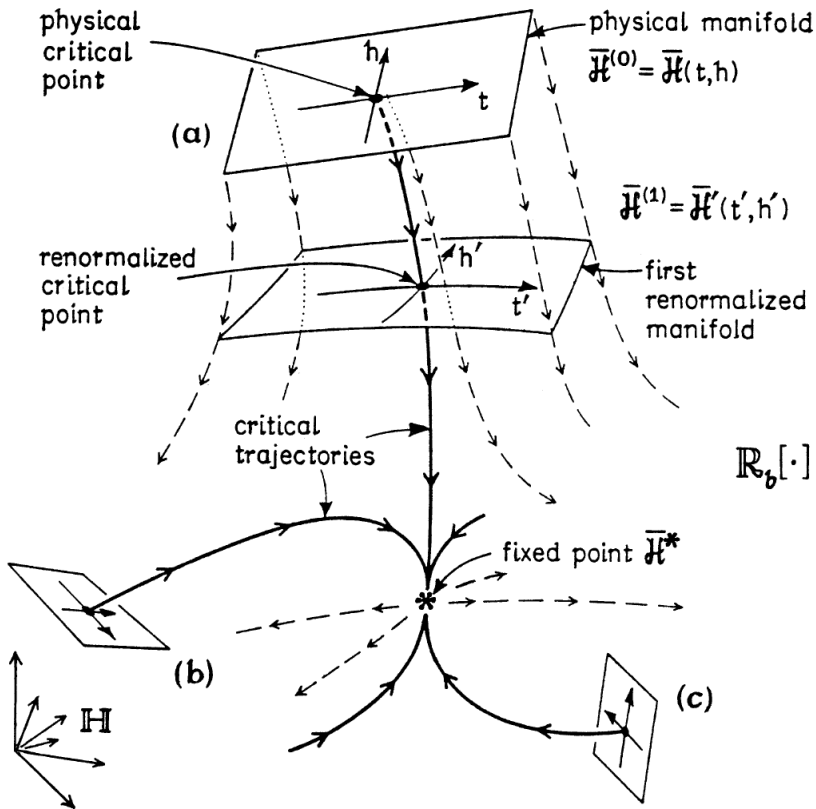


Figure 8.2: A depiction of the space of Hamiltonians  $\mathcal{H}$  showing initial or physical manifolds,  $K = \{t, h\}$  with  $t = (T - T_c)/T_c$  and  $T_c$  the critical temperature, [labelled (a), (b), ...] and the flows induced by repeated application of a discrete RG transformation  $\mathcal{R}_b$  with a spatial rescaling factor  $b$  (or induced by a corresponding continuous or differential RG). Critical trajectories are shown bold: They all terminate, in the region of  $\mathcal{H}$  shown here, at a fixed point  $\bar{\mathcal{H}}^*$ . The full space contains, in general, other nontrivial, critical fixed points, describing multicritical points and distinct critical-point universality classes; in addition, trivial fixed points, including high-temperature ‘‘sinks’’ with no outflowing or relevant trajectories, typically appear. Lines of fixed points and other more complex structures may arise and, indeed, play a crucial role in certain problems. [After Ref. [256]]

On the other hand, a fixed point represents only the simplest kind of asymptotic flow behavior: Other types of asymptotic flow may well be identified and translated into physical terms.

But what about *power laws and scaling*?

The smoothness of a well-designed RG transformation means that it can always be expanded locally, to at least some degree, in a Taylor series [242, 262, 259, 244, 245, 248, 247]. It is worth stressing that it is this very property that fails for free energies in a critical region: To regain this ability, the large space of Hamiltonians is crucial. Near a fixed point satisfying Eq. (8.36) we can, therefore, rather generally expect to be able to *linearize* by writing

$$\mathcal{R}_b[\bar{\mathcal{H}}^* + g\mathcal{Q}] = \bar{\mathcal{H}}^* + g\mathcal{L}_b\mathcal{Q} + o(g), \quad (8.38)$$

as  $g \rightarrow 0$ , or in differential form,

$$\frac{d}{dl}(\bar{\mathcal{H}}^* + g\mathcal{Q}) = g\mathcal{B}\mathcal{Q} + o(g). \quad (8.39)$$

Now  $\mathcal{L}_b$  and  $\mathcal{B}$  are *linear operators* (albeit acting in a large space  $\mathcal{H}$ ). As such we can seek eigenvalues and corresponding “eigenoperators”, say  $\mathcal{Q}_k$  (which will be “partial Hamiltonians”). Thus, we may write

$$\mathcal{L}_b\mathcal{Q}_k = \Lambda_k(b)\mathcal{Q}_k \quad \text{or} \quad \mathcal{B}\mathcal{Q}_k = \lambda_k\mathcal{Q}_k, \quad (8.40)$$

where, in fact, (by the semigroup property) the eigenvalues must be related by  $\Lambda_k(b) = b^{\lambda_k}$ . As in any such linear problem, knowing the spectrum of eigenvalues and eigenoperators or, at least, its dominant parts, tells one much of what one needs to know. Reasonably, the  $\mathcal{Q}_k$  should form a basis for a general expansion

$$\bar{\mathcal{H}} \cong \bar{\mathcal{H}}^* + \sum_{k \geq 1} g_k \mathcal{Q}_k. \quad (8.41)$$

Physically, the expansion coefficient  $g_k$  ( $\equiv g_k^{(0)}$ ) then represents the thermodynamic field (reduced, as always, by the factor  $1/k_B T$ ) conjugate to the “critical operator”  $\mathcal{Q}_k$  which, in turn, will often be close to some combination of *local* operators. Indeed, in a characteristic critical-point problem one finds two *relevant operators*, say  $\mathcal{Q}_1$  and  $\mathcal{Q}_2$  with  $\lambda_1, \lambda_2 > 0$ . Invariably, one of these operators can, say by its symmetry, be identified with the local energy density,  $\mathcal{Q}_1 \cong \mathcal{E}$ , so that  $g_1 \cong t$  is the thermal field; the second then characterizes the order parameter,  $\mathcal{Q}_2 \cong \Psi$  with field  $g_2 \cong h$ . Under renormalization each  $g_k$  varies simply as  $g_k^{(l)} \approx b^{\lambda_k l} g_k^{(0)}$ .

Finally, one examines the flow equation (8.36) for the free energy. The essential point is that the degree of renormalization,  $b^l$ , can be chosen as large as one wishes. When  $t \rightarrow 0$ , i.e., in the critical region which it is our aim to understand, a good choice proves to be  $b^l = 1/|t|^{1/\lambda_1}$ , which clearly diverges at  $\infty$ . One then finds that Eq. (8.36) leads to the following *basic scaling relation*

$$f_s(t, h, \dots, g_j, \dots) \approx |t|^{2-\alpha} \mathcal{F} \left( \frac{h}{|t|^\Delta}, \dots, \frac{g_j}{|t|^{\phi_j}}, \dots \right), \quad (8.42)$$

where  $f_s$  is the “singular part” of the free energy found by subtracting from the free energy all the analytic terms.  $\alpha$  is the specific heat exponent introduced while the exponent,  $\Delta$ , which determines how  $h$  scales with  $t$ , is given by

$$\Delta = \beta + \gamma, \quad (8.43)$$

Widom observed, incidentally, that the classical theories themselves obey scaling: One then has  $\alpha = 0, \Delta = 1\frac{1}{2}, \phi = -\frac{1}{2}$ . The exponent,  $\phi$ , did not appear in the original critical-point scaling

formulations [236, 237, 238, 239, 240, 251, 253]; neither did the argument  $g/|t|^\phi$  appear in the scaling function  $\mathcal{F}$ . It is really only with the appreciation of RG theory that we know that such a dependence should in general be present and, indeed, that a full spectrum  $\{\phi_j\}$  of such higher-order exponents with  $\phi \equiv \phi_1 > \phi_2 > \phi_3 > \dots$  must normally appear [242, 263].

Eq. (8.42) is the essential result. Recall, for example, that: (i) it very generally implies the thermodynamic exponent relation Eq. (8.27) connecting  $\alpha$ ,  $\beta$ , and  $\gamma$  (since the derivative of the free energy with respect to  $h$  is proportional to minus the magnetization); and (ii) since all leading exponents are determined entirely by the two exponents  $\alpha$  and  $\Delta$  ( $= \beta + \gamma$ ), it predicts similar exponent relations for any other exponents one might define, such as  $\delta$  specified on the critical isotherm by  $H \sim M^\delta$ . Beyond that, (iii) if one fixes  $P$  (or  $g$ ) and similar parameters and observes the free energy or, in practice, the equation of state, the data one collects amount to describing a function, say  $M(T, H)$ , of two variables. Typically this would be displayed as sets of isotherms: i.e., many plots of  $M$  vs.  $H$  at various closely spaced, fixed values of  $T$  near  $T_c$ . But according to the scaling law Eq. (8.42) if one plots the scaled variables  $f_s/|t|^{2-\alpha}$  or  $M/|t|^\beta$  vs. the scaled field  $h/|t|^\Delta$ , for appropriately chosen exponents and critical temperature  $T_c$ , one should find that all these data “collapse” (in Stanley’s [253] picturesque terminology) onto a single curve, which then just represents the scaling function  $x = \mathcal{F}(y)$  itself. This collapse is sometimes also called law of corresponding states (see for instance section 4.1 in Ref. [95]).

Now, however, the critical exponents can be expressed directly in terms of the RG eigenexponents  $\lambda_k$  (for the fixed point in question). Specifically one finds

$$2 - \alpha = \frac{d}{\lambda_1}, \quad \Delta = \frac{\lambda_2}{\lambda_1}, \quad \phi_j = \frac{\lambda_j}{\lambda_1}, \quad \nu = \frac{1}{\lambda_1}. \quad (8.44)$$

Then, the sign of a given  $\phi_j$  and, hence, of the corresponding  $\lambda_j$  determines the relevance (for  $\lambda_j > 0$ ), marginality (for  $\lambda_j = 0$ ), or irrelevance (for  $\lambda_j < 0$ ) of the corresponding critical operator  $Q_j$  (or “perturbation”) and of its conjugate field  $g_j$ : This field might, but for most values of  $j$  will not, be under direct experimental control. The first and last of the equations (8.44) yield the hyperscaling relation:  $d\nu = 2 - \alpha$  which explicitly involve the spatial dimensionality [263]. This relation holds exactly for the  $d = 2$  Ising model and also for all other exactly soluble models when  $d < 4$  [256, 269].<sup>4</sup>

When a coupling constant  $g$  is irrelevant then  $z = g/|t|^\phi \rightarrow 0$  on approaching the critical point. Consequently,  $\mathcal{F}(y, z)$  can be replaced simply by  $\mathcal{F}(y, 0)$  which is a function of just a single variable. Furthermore, asymptotically when  $T \rightarrow T_c$  we get the same function whatever the actual value of  $g$ . Clearly this is an example of universality.<sup>5</sup> Then one can, fairly generally, hope to expand the scaling function  $\mathcal{F}(y, z)$  in powers of  $z$  and thereby obtain the so called “correction-to-scaling” exponent  $\theta$ , which is also universal (for  $d = 3$  Ising-type systems one finds  $\theta \simeq 0.54$  [282]).

<sup>4</sup>Unlike the previous exponent relations (all being independent of  $d$ ) hyperscaling fails for the classical theories unless  $d = 4$ . And since one knows (rigorously for certain models) that the classical exponent values are valid for  $d > 4$ , it follows that hyperscaling cannot be generally valid. Thus something is certainly missing from Kadanoff’s picture. Now, thanks to RG insights, we know that the breakdown of hyperscaling is to be understood via the second argument in the “fuller” scaling form Eq. (8.42): when  $d$  exceeds the appropriate borderline dimension,  $d_{uc}$ , a “dangerous irrelevant variable” appears and must be allowed for (see Fisher in Ref. [281] p. 66 where a “dangerous irrelevant variable” is characterized as a “hidden relevant variable” and Ref. [256], appendix D). In essence one finds that the scaling function limit  $\mathcal{F}(y, z \rightarrow 0, \dots)$ , previously accepted without question, is no longer well defined but, rather, diverges as a power of  $z$ : asymptotic scaling survives but  $d^* \equiv (2 - \alpha)/\nu$  sticks at the value 4 for  $d > d_{uc} = 4$ .

<sup>5</sup>Note that  $T_c$  for example, will usually be a function of any irrelevant parameter such as  $g_j$ . This comes about because, in a full scaling formulation, the variables  $t$ ,  $h$ , and  $\{g_j\}$  appearing in Eq. (8.42) must be replaced by nonlinear scaling fields  $t(t, h, \{g_j\})$ ,  $h(t, h, \{g_j\})$ , and  $g_j(t, h, \{g_j\})$  which are smooth functions of  $t$ ,  $h$ , and  $g_j$  [244, 245, 248, 256]. By the same token it is usually advantageous to introduce a prefactor  $A_0$  in Eq. (8.42) and “metrical factors”  $E_j$  in the arguments of  $\mathcal{F}$  (see, e.g., Ref. [256]).

When a coupling constant  $g$  is relevant then when  $t \rightarrow 0$  the scaled variable  $g/|t|^\phi$  grows larger and larger. Two possibilities then arise: *Either* the critical point may be destroyed altogether. This is, in fact, the effect of the magnetic field, which must itself be regarded as a relevant perturbation since  $\phi \equiv \Delta = \beta + \gamma > 0$ . *Alternatively*, when  $z$  grows, the true, asymptotic critical behavior may crossover [259, 260] to a new, quite *distinct* universality class with different exponents and a new asymptotic scaling function, say,  $\mathcal{F}_\infty(y)$ .<sup>6</sup>

When a coupling constant  $g$  is marginal then when  $t \rightarrow 0$  this may lead to *logarithmic* modifications of the classical critical power laws (by factors diverging as  $\ln |t|$  to various powers). The predicted logarithmic behavior has, in fact, been verified experimentally by Ahlers et al. [283]. In other cases, especially for  $d = 2$ , marginal variables lead to continuously variable exponents such as  $\alpha(g)$ , and to quite different thermal variation, like  $\exp(A/|t|^\nu)$ ; such results have been checked both in exactly solved statistical mechanical models and in physical systems such as superfluid helium films [284, 246].

Because of the multifaceted character of matter physics these are rather different and more diverse than those aspects of RG theory of significance for QFT. When there are no marginal variables and the least negative  $\phi_j$  is larger than unity in magnitude, a simple scaling description will usually work well and the Kadanoff picture almost applies. When there are no relevant variables and only one or a few marginal variables, field-theoretic perturbative techniques of the Gell-Mann-Low [285], Callan-Symanzik [286, 287, 288, 289] or so-called “parquet diagram” varieties [290] may well suffice (assuming the dominating fixed point is sufficiently simple to be well understood). There may then be little incentive for specifically invoking general RG theory. This seems, more or less, to be the current situation in QFT and it applies also in certain physics of matter problems.

Within RG theory the general mechanism of universality is as follows: In a very large (generally infinitely large) space of Hamiltonians  $\mathcal{H}$ , parametrized by  $t, h$ , and all the  $g_j$ , there is a controlling critical point (a fixed point) about which each variable enters with a characteristic exponent. All systems with Hamiltonians differing only through the values of the  $g_j$  (within suitable bounds) will exhibit the same critical behavior determined by the same free-energy scaling function  $\mathcal{F}$ , dropping the irrelevant arguments. Different universality classes will be associated with different controlling critical points in the space of Hamiltonians with, once one recognizes the concept of RG flows, different “domains of attraction” under the flow. Indeed, the expectation of a general form of scaling is frequently the most important consequence of RG theory for the practicing experimentalist or theorist.

---

<sup>6</sup>Formally, one might write  $\mathcal{F}_\infty(y) = \mathcal{F}(y, z \rightarrow z_\infty)$  where  $z_\infty$  is a critical value which could be  $\infty$ ; but a more subtle relationship is generally required since the exponent  $\alpha$  in the prefactor in Eq. (8.42) changes



# List of Figures

1.1	Radiation zone of a current system. The shaded area is where are the currents. The origin of the coordinate system $O$ is chosen inside this region. $Q$ is any point of the currents. $P$ is where we measure the electromagnetic field radiated out. $d$ is the linear extension of the current system. . . . .	8
3.1	deviations . . . . .	97
3.2	Shows the time step, $\tau$ , extrapolation for the potential energy, $P = \langle \mathcal{P} \rangle$ . We run at $\beta = 15$ , $\gamma = 0.02$ , and $S = 60$ . The extrapolated value to the continuum limit is in this case $P = -16.1(5)$ which is in good agreement with the result of Ref. [76]. . . . .	98
3.3	At $S = 60$ the results for the potential energy $\mathcal{P}$ at each MC block ( $5 \times 10^3$ MCS) starting from an initial unlocalized path obtained by a previous simulation at $S = 52.5$ . We can see that after about 30 blocks there is a transition from the ES state to the ST state. In the inset is shown the autocorrelation function, defined in Eq. (G.8), for the potential energy, for the two states. The correlation time, in MC blocks, is shorter in the unlocalized phase than in the localized one. The computer time necessary to carry on a given number of Monte Carlo steps is longer for the unlocalized phase. . . . .	99
3.4	The top panel shows the polaron (closed) path $x(t)$ as a function of Euclidean time $t$ in units of $\tau$ at equilibrium during the simulation. The middle panel shows the projection on the $x - y$ plane of the path. The bottom panel shows the three-dimensional path. We see clearly how both path has moved from the initial path located on the origin but the path at $S = 52.5$ is much less localized than the one at $S = 60$ . . . . .	100
3.5	Shows the behavior of the potential energy $P$ as a function of the coupling constant $S$ . The points are the MC results (see Tab. 3.1), the dashed line is the second order perturbation theory result (perturbation) valid in the weak coupling regime and the dot-dashed line is the variational approach from Ref. [67] (variational) in the weak and strong coupling regimes. . . . .	101
4.1	Ionization potentials of elements that are known from spectroscopic data. . . . .	113
6.1	Radial distribution function $g(r)$ computed by DMC method (mixed estimator) for the unpolarized $\xi = 0$ case and the fully polarized $\xi = 1$ case. $r_s = 1$ (dotted line), $r_s = 3$ (dash-dotted line), $r_s = 5$ (dashed line), and $r_s = 10$ (full line). $r$ is in units of a Bohr radius. (Figure reproduced here by courtesy of the authors of Ref. [151]) . . . . .	133

6.2	Structure factor $S(k)$ computed by the DMC method (mixed estimator). The $r_s$ considered and the symbols are the same as those of Fig. 6.1. (Figure reproduced here by courtesy of the authors of Ref. [151]) . . . . .	134
6.3	The energy of the four phases studied relative to that of the lowest boson state times $r_s^2$ in Rydbergs as a function of $r_s$ in Bohr radii. The boson system undergoes Wigner crystallization at $r_s = 160 \pm 10$ . The fermion system has two phase transitions, crystallization at $r_s = 100 \pm 20$ and depolarization at $r_s = 75 \pm 5$ . (Figure reproduced here by courtesy of the authors of Ref. [116]) . . . . .	135
6.4	Illustration of the reach $\gamma(R_0, t)$ of the fermion density matrix. . . . .	140
6.5	Pair correlation functions (on the left) for $r_s = 1.0$ and $r_s = 10.0$ in the unpolarized state. Also shown is the small $r$ part of the classical Debye-Hückel limit at $\Theta = 8.0$ ; see Eq. (6.103). The Debye-Hückel limit is not yet reached at $\Theta = 8.0$ for the lower density $r_s = 10.0$ . Static structure factors (on the right) for $r_s = 1.0$ and $r_s = 10.0$ in the unpolarized state. Also shown is the small $k$ part of the classical Debye-Hückel limit at $\Theta = 8.0$ ; see Eq. (6.104). (Figure reproduced here by courtesy of the authors of Ref. [117]) . . . . .	143
6.6	Excess energies $E_{xc} = e_{xc}$ (on the left) for $r_s = 4.0$ and $r_s = 40.0$ for the polarized state ( $E_0 = e_0$ ). For both densities the high temperature results fall smoothly on top of previous Monte Carlo energies for the classical electron gas [164] (solid line). Differences from the classical Coulomb gas occur for $\Theta < 2.0$ for $r_s = 4.0$ and $\Theta < 4.0$ for $r_s = 40.0$ . Simulations with the Fermion sign (squares) confirm the fixed-node results at $\Theta = 1.0$ and $8.0$ . The zero-temperature limit (dotted line) smoothly extrapolates to the ground state QMC results of Ceperley-Alder [116] (dashed line). Correlation energy $E_c(T) = e_c(T)$ (on the right) of the 3D Jellium at several temperatures and densities for the unpolarized (top) and fully spin-polarized (bottom) states. Exact (signful) calculations (squares) confirm the fixed-node results where possible ( $\Theta = 8.0$ for $\xi = 0$ and $\Theta = 4.0, 8.0$ for $\xi = 1$ ). (Figure reproduced here by courtesy of the authors of Ref. [117]) . . . . .	145
6.7	Correlation energy $E_c(T) = e_c(T)$ of the Jellium at $r_s = 4.0$ for the unpolarized $\xi = 0$ state from the RPIMC calculations (RPIMC) and several previous parameterizations as a function of $\Theta$ . The latter include Debye-Hückel (DH), Hansen (H), Hansen+Wigner-Kirkwood (H+WK), Random-Phase-Approximation (RPA), Tanaka and Ichimaru (TI), and Perrot and Dharma-wardana (PDW). Also included is the ground state $\Theta = 0.0$ result for comparison. (Figure reproduced here by courtesy of the authors of Ref. [165]) . . . . .	146
6.8	Temperature-density phase diagram showing the points considered in Ref. [117]. Several values of the Coulomb coupling parameter $\Gamma$ (dashed lines) and the electron degeneracy parameter $\Theta$ (dotted lines) are also shown. (Figure reproduced here by courtesy of the authors of Ref. [117]) . . . . .	147
O.1	. . . . .	176
7.1	The exponent $\Gamma = d \ln P / d \ln n$ for the adiabatic full relativistic equation of state as a function of density. We chose a temperature $T = 20000\text{K}$ and zero entropy, $g = 2$ , and $m$ is the mass of an electron. $n$ is in $\text{cm}^{-3}$ . . . . .	184
7.2	Temperature dependence of the Chandrasekar limit at $\mu_e = 2$ . We recall that $z = e^{\beta\mu}$ . . . . .	187

- 7.3 The radial distribution function for ideal electrons ( $\xi = -1, g = 2$ ) in the relativistic and the non relativistic cases. Here we chose  $T = 20000\text{K}$  and  $n = 1.04 \times 10^{22}\text{cm}^{-3}$  in the non relativistic case and  $n = 5.93 \times 10^{24}\text{cm}^{-3}$  in the relativistic case.  $r$  is in Angstroms. . . . . 190
- 8.1 Temperature variation of gas-liquid coexistence curves (temperature,  $T$ , versus density,  $\rho$ ) and corresponding spontaneous magnetization plots (magnetization,  $M$ , versus  $T$ ). The solid curves, (b) and (d), represent (semiquantitatively) observation and modern theory, while the dotted curves (a) and (c) illustrate the corresponding “classical” predictions (mean-field theory and van der Waals approximation). These latter plots are parabolic through the critical points (small open circles) instead of obeying a power law with the universal exponent  $\beta \simeq 0.325$ : See Eqs. (8.12) and (11). The energy scale  $\varepsilon$ , and the maximal density and magnetization,  $\rho_{\max}$  and  $M_{\max}$ , are nonuniversal parameters particular to each physical system; they vary widely in magnitude. . . . . 202
- 8.2 A depiction of the space of Hamiltonians  $\mathcal{H}$  showing initial or physical manifolds,  $K = \{t, h\}$  with  $t = (T - T_c)/T_c$  and  $T_c$  the critical temperature, [labelled (a), (b), ...] and the flows induced by repeated application of a discrete RG transformation  $\mathcal{R}_b$  with a spatial rescaling factor  $b$  (or induced by a corresponding continuous or differential RG). Critical trajectories are shown bold: They all terminate, in the region of  $\mathcal{H}$  shown here, at a fixed point  $\bar{\mathcal{H}}^*$ . The full space contains, in general, other nontrivial, critical fixed points, describing multicritical points and distinct critical-point universality classes; in addition, trivial fixed points, including high-temperature “sinks” with no outflowing or relevant trajectories, typically appear. Lines of fixed points and other more complex structures may arise and, indeed, play a crucial role in certain problems. [After Ref. [256]] . . . . . 210

*LIST OF FIGURES*

---

# Bibliography

- [1] G. F. R. Ellis. Top-down causation and emergence: some comments on mechanisms. *Interface Focus*, 2011. [doi:10.1098/rsfs.2011.0062](https://doi.org/10.1098/rsfs.2011.0062).
- [2] E. J. Eichten, M. E. Peskin, and M. Peskin. New Tests for Quark and Lepton Substructure. *Phys. Rev. Lett.*, 50:811, 1983. [doi:10.1103/PhysRevLett](https://doi.org/10.1103/PhysRevLett).
- [3] S. Navas et al. Review of particle physics. *Phys. Rev. D*, 110(3):030001, 2024. [doi:10.1103/PhysRevD.110.030001](https://doi.org/10.1103/PhysRevD.110.030001).
- [4] W. V. Farrar. Richard Laming and the Coal-Gas Industry, with His Views on the Structure of Matter. *Annals of Science*, 25:243, 1969. [doi:10.1080/00033796900200141](https://doi.org/10.1080/00033796900200141).
- [5] J. J. Thomson. Cathode Rays. *Philosophical Magazine*, 44:293, 1897. [doi:10.1080/14786449708621070](https://doi.org/10.1080/14786449708621070).
- [6] M. Agostini. Test of electric charge conservation with Borexino. *Phys. Rev. Lett.*, 115:231802, 2015. [doi:10.1103/PhysRevLett.115.231802](https://doi.org/10.1103/PhysRevLett.115.231802).
- [7] W. Pauli. *Electrodynamics*, volume 1 of *Pauli Lectures on Physics*. MIT Press, Cambridge, Massachusetts, first edition, 1973.
- [8] L. C. Pauling. *The Nature of the Chemical Bond and the Structure of Molecules and Crystals: an introduction to modern structural chemistry*. Cornell University Press, 1960. pp. 88–107.
- [9] R. A. Millikan. The isolation of an ion, a precision measurement of its charge, and the correction of Stokes's law. *Science*, 32:436, 1910. [doi:10.1126/science.32.822.436](https://doi.org/10.1126/science.32.822.436).
- [10] S. Glashow. The renormalizability of vector meson interactions. *Nucl. Phys.*, 10:107, 1959.
- [11] A. Salam and J. C. Ward. Weak and electromagnetic interactions. *Nuovo Cimento*, 11:568, 1959. [doi:10.1007/BF02726525](https://doi.org/10.1007/BF02726525).
- [12] S. Weinberg. A Model of Leptons. *Phys. Rev. Lett.*, 19:1264, 1967. [doi:10.1103/PhysRevLett.19.1264](https://doi.org/10.1103/PhysRevLett.19.1264).
- [13] P. W. Higgs. Broken Symmetries and the Masses of Gauge Bosons. *Phys. Rev. Lett.*, 12:132, 1964. [doi:10.1103/PhysRevLett.13.508](https://doi.org/10.1103/PhysRevLett.13.508).
- [14] R. Fantoni and J. R. Klauder. Affine quantization of  $(\varphi^4)_4$  succeeds while canonical quantization fails. *Phys. Rev. D*, 103:076013, 2021. [doi:10.1103/PhysRevD.103.076013](https://doi.org/10.1103/PhysRevD.103.076013).

---

## BIBLIOGRAPHY

---

- [15] R. Fantoni. Monte Carlo evaluation of the continuum limit of  $(\phi^{12})_3$ . *J. Stat. Mech.*, page 083102, 2021. [doi:10.1088/1742-5468/ac0f69](https://doi.org/10.1088/1742-5468/ac0f69).
  - [16] R. Fantoni and J. R. Klauder. Monte Carlo evaluation of the continuum limit of the two-point function of the Euclidean free real scalar field subject to affine quantization. *J. Stat. Phys.*, 184:28, 2021. [doi:10.1007/s10955-021-02818-x](https://doi.org/10.1007/s10955-021-02818-x).
  - [17] R. Fantoni and J. R. Klauder. Monte Carlo evaluation of the continuum limit of the two-point function of two Euclidean Higgs real scalar fields subject to affine quantization. *Phys. Rev. D*, 104:054514, 2021. [doi:10.1103/PhysRevD.104.054514](https://doi.org/10.1103/PhysRevD.104.054514).
  - [18] R. Fantoni and J. R. Klauder. Eliminating Nonrenormalizability Helps Prove Scaled Affine Quantization of  $\varphi_4^4$  is Nontrivial. *Int. J. Mod. Phys. A*, 37:2250029, 2022. [doi:10.1142/S0217751X22500294](https://doi.org/10.1142/S0217751X22500294).
  - [19] R. Fantoni and J. R. Klauder. Kinetic Factors in Affine Quantization and Their Role in Field Theory Monte Carlo. *Int. J. Mod. Phys. A*, 37(14):2250094, 2022. [doi:10.1142/S0217751X22500944](https://doi.org/10.1142/S0217751X22500944).
  - [20] R. Fantoni and J. R. Klauder. Scaled Affine Quantization of  $\varphi_4^4$  in the Low Temperature Limit. *Eur. Phys. J. C*, 82:843, 2022. [doi:10.1140/epjc/s10052-022-10807-x](https://doi.org/10.1140/epjc/s10052-022-10807-x).
  - [21] R. Fantoni and J. R. Klauder. Scaled Affine Quantization of Ultralocal  $\varphi_2^4$  a comparative Path Integral Monte Carlo study with scaled Canonical Quantization. *Phys. Rev. D*, 106:114508, 2022. [doi:10.1103/PhysRevD.106.114508](https://doi.org/10.1103/PhysRevD.106.114508).
  - [22] J. R. Klauder and R. Fantoni. The Magnificent Realm of Affine Quantization: valid results for particles, fields, and gravity. *Axioms*, 12:911, 2023. [doi:10.3390/axioms12100911](https://doi.org/10.3390/axioms12100911).
  - [23] R. Fantoni. Scaled Affine Quantization of  $\varphi_3^{12}$  is Nontrivial. *Mod. Phys. Lett. A*, 38:2350167, 2023. [doi:10.1142/S0217732323501675](https://doi.org/10.1142/S0217732323501675).
  - [24] R. Fantoni. Continuum limit of the Green function in scaled affine  $\varphi_4^4$  quantum Euclidean covariant relativistic field theory. *Quantum Rep.*, 6:134, 2024. [doi:10.3390/quantum6020010](https://doi.org/10.3390/quantum6020010).
  - [25] S. L. Glashow. Partial-symmetries of weak interactions. *Nucl. Phys.*, 22:579, 1961. [doi:10.1016/0029-5582\(61\)90469-2](https://doi.org/10.1016/0029-5582(61)90469-2).
  - [26] J. Schwinger. On Quantum-Electrodynamics and the Magnetic Moment of the Electron. *Phys. Rev.*, 73:416, 1948. [doi:10.1103/PhysRev.73.416](https://doi.org/10.1103/PhysRev.73.416).
  - [27] C. W. Misner, K. S. Thorne, and J. A. Wheeler. *Gravitation*. C. W. Misner and K. S. Thorne and J. A. Wheeler, New York, 1970.
  - [28] L. D. Landau and E. M. Lifshitz. *Quantum Mechanics. Non-relativistic Theory*, volume 3. Pergamon Press Ltd, Oxford, 1977. Course of Theoretical Physics.
  - [29] J. R. Klauder. Continuous-Representation Theory. I. Postulates of Continuous-Representation Theory. *J. Math. Phys.*, 4:1055, 1963. [doi:10.1063/1.1704034](https://doi.org/10.1063/1.1704034).
  - [30] J. R. Klauder. Continuous-Representation Theory. II. Generalized Relation between Quantum and Classical Dynamics. *J. Math. Phys.*, 4:1058, 1963. [doi:10.1063/1.1704035](https://doi.org/10.1063/1.1704035).
-

---

## BIBLIOGRAPHY

---

- [31] J. R. Klauder. Continuous Representation Theory. III. On Functional Quantization of Classical Systems. *J. Math. Phys.*, 5:177, 1964. [doi:10.1063/1.1704107](https://doi.org/10.1063/1.1704107).
  - [32] J. McKenna and J. R. Klauder. Continuous Representation Theory. IV. Structure of a Class of Function Spaces Arising from Quantum Mechanics. *J. Math. Phys.*, 5:878, 1964. [doi:10.1063/1.1704190](https://doi.org/10.1063/1.1704190).
  - [33] J. R. Klauder and J. McKenna. Continuous Representation Theory. V. Construction of a Class of Scalar Boson Field Continuous Representations. *J. Math. Phys.*, 6:68, 1965. [doi:10.1063/1.1704265](https://doi.org/10.1063/1.1704265).
  - [34] D. M. Ceperley. Path integrals in the theory of condensed helium. *Rev. Mod. Phys.*, 67:279, 1995. [doi:10.1103/RevModPhys.67.279](https://doi.org/10.1103/RevModPhys.67.279).
  - [35] N. W. Ashcroft and N. D. Mermin. *Solid State Physics*. Thomson Learning Inc, Australia, 1976.
  - [36] G. Grossi and G. P. Parravicini. *Solid State Physics*. Academic Pr., 2013.
  - [37] R. M. Martin, L. Reining, and D. M. Ceperley. *Interacting Electrons, Theory and Computational Approaches*. Cambridge, 2016.
  - [38] S. L. Shapiro and S. A. Teukolsky. *Black Holes, White Dwarfs, and Neutron Stars. The Physics of Compact Objects*. John Wiley & Sons Inc, New York, 1983.
  - [39] V. B. Berestetskiĭ, E. M. Lifshitz, and L. P. Pitaevskiĭ. *Relativistic Quantum Theory*. Pergamon Press Ltd, Oxford, 1971.
  - [40] Y. M. Shirokov. A Group-Theoretical Consideration on the Basis of Relativistic Quantum Mechanics. I. The General Properties of the Inhomogeneous Lorentz Group. *JETP*, 6:664, 1958.
  - [41] Y. M. Shirokov. A Group-Theoretical Consideration on the Basis of Relativistic Quantum Mechanics. II. Classification of the Irreducible Representations of the Inhomogeneous Lorentz Group. *JETP*, 6:919, 1958.
  - [42] Y. M. Shirokov. A Group-Theoretical Consideration on the Basis of Relativistic Quantum Mechanics. III. Irreducible Representations of the Classes  $P_0$  and  $O_0$ , and the Non-Completely-Reducible Representations of the Inhomogeneous Lorentz Group. *JETP*, 6:929, 1958.
  - [43] Y. M. Shirokov. A Group-Theoretical Consideration of the Basis of Relativistic Quantum Mechanics. IV. Space Reflections in Quantum Theory. *JETP*, 7:493, 1958.
  - [44] Y. M. Shirokov. A Group-Theoretical Consideration of the Basis of Relativistic Quantum Mechanics. V. *JETP*, 9:620, 1959.
  - [45] B. Gerlach and H. Löwen. Analytical properties of polaron systems or: Do polaronic phase transitions exist or not? *Rev. Mod. Phys.*, 63:63, 1991. [doi:10.1103/RevModPhys.63.63](https://doi.org/10.1103/RevModPhys.63.63).
  - [46] J. T. Devreese and A. S. Alexandrov. Fröhlich polaron and bipolaron: recent developments. *Rep. Prog. Phys.*, 72:066501, 2009. [doi:10.1088/0034-4885/72/6/066501](https://doi.org/10.1088/0034-4885/72/6/066501).
  - [47] L. D. Landau. The Movement of Electrons in the Crystal Lattice. *Phys. Z. Sowjetunion*, 3:644, 1933. [doi:10.1016/b978-0-08-010586-4.50015-8](https://doi.org/10.1016/b978-0-08-010586-4.50015-8).
-

---

## BIBLIOGRAPHY

---

- [48] L. D. Landau and S. Pekar. *Zh. eksper. teor. Fiz.*, 16:341, 1946.
  - [49] L. D. Landau and S. I. Pekar. *Zh. Eksp. Teor. Fiz.*, 18:419, 1948.
  - [50] H. Fröhlich, H. Pelzer, and S. Zienau. Properties of slow electrons in polar materials. *Phil. Mag.*, 41:221, 1950. [doi:10.1080/14786445008521794](https://doi.org/10.1080/14786445008521794).
  - [51] H. Fröhlich. Electrons in lattice fields. *Adv. Phys.*, 3:325, 1954. [doi:10.1080/00018735400101213](https://doi.org/10.1080/00018735400101213).
  - [52] R. P. Feynman. Slow Electrons in a Polar Crystal. *Phys. Rev.*, 97:660, 1955. [doi:10.1103/PhysRev.97.660](https://doi.org/10.1103/PhysRev.97.660).
  - [53] F. M. Peeters and J. T. Devreese. On the Existence of a Phase Transition for the Fröhlich Polaron. *Phys. Stat. Sol.*, 112:219, 1982. [doi:10.1002/pssb.2221120125](https://doi.org/10.1002/pssb.2221120125).
  - [54] B. A. Mason and S. Das Sarma. Path-integral study of localization in the generalized polaron problem. *Phys. Rev. B*, 33:1412, 1986. [doi:10.1103/PhysRevB.33.1412](https://doi.org/10.1103/PhysRevB.33.1412).
  - [55] T. K. Mitra, A. Chatterjee, and S. Mukhopadhyay. Polarons. *Phys. Rep.*, 91:153, 1987. [doi:10.1016/0370-1573\(87\)90087-1](https://doi.org/10.1016/0370-1573(87)90087-1).
  - [56] R. P. Feynman. *Statistical Mechanics: A Set of Lectures*. Addison-Wesley Publishing Company Inc, Reading, 1972. Section 9.6; Chapter 8.
  - [57] Y. Ōsaka. Polaron State at a Finite Temperature. *Prog. Theor. Phys.*, 22:437, 1959. [doi:10.1143/PTP.22.437](https://doi.org/10.1143/PTP.22.437).
  - [58] Y. Osaka. Polaron Mobility at Finite Temperature (Weak Coupling Limit). *J. Phys. Soc. Jpn.*, 21:423, 1965. [doi:10.1143/JPSJ.21.423](https://doi.org/10.1143/JPSJ.21.423).
  - [59] D. P. L. Castrigiano and N. Kokianonis. Classical paths for a quadratic action with memory and exact evaluation of the path integral. *Phys. Lett. A*, 96:55, 1983. [doi:10.1016/0375-9601\(83\)90588-1](https://doi.org/10.1016/0375-9601(83)90588-1).
  - [60] D. P. L. Castrigiano, N. Kokianonis, and H. Stierstorfer. Free energy and effective mass of the polaron at finite temperatures. *Phys. Lett. A*, 104:364, 1984. [doi:10.1016/0375-9601\(84\)90818-1](https://doi.org/10.1016/0375-9601(84)90818-1).
  - [61] D. C. Khandekar and S. V. Lawande. Feynman path integrals: Some exact results and applications. *Phys. Rep.*, 137:115, 1986. [doi:10.1016/0370-1573\(86\)90029-3](https://doi.org/10.1016/0370-1573(86)90029-3).
  - [62] Proceedings of the International Conference on Materials & Mechanism of Superconductivity, High Temperature Superconductors V. In Y-Sheng He, Pei-Heng Wu, Li-Fang Xu, and Zong-Xian Zhao, editor, *Physica*, volume 282C-287C, Amsterdam, 1997.
  - [63] J. Tempere, W. Casteels, M. K. Oberthaler, S. Knoop, E. Timmermans, and J. T. Devreese. Feynman path-integral treatment of the BEC-impurity polaron. *Phys. Rev. B*, 80:184504, 2009. [doi:10.1103/PhysRevB.80.184504](https://doi.org/10.1103/PhysRevB.80.184504).
  - [64] Y. Toyozawa. Self-Trapping of an Electron by the Acoustical Mode of Lattice Vibration. I. *Prog. Theor. Phys.*, 26:29, 1961. [doi:10.1143/PTP.26.29](https://doi.org/10.1143/PTP.26.29).
  - [65] C. G. Kuper and G. D. Whitfield, editors. *Polarons and Excitons*. Oliver and Boyd, Edinburgh, 1963. page 211.
-

---

## BIBLIOGRAPHY

---

- [66] F. M. Peeters and J. T. Devreese. Acoustical polaron in three dimensions: The ground-state energy and the self-trapping transition. *Phys. Rev. B*, 32:3515, 1985. [doi:10.1103/PhysRevB.32.3515](#).
  - [67] A. Sumi and Y. Toyozawa. Discontinuity in the Polaron Ground State. *J. Phys. Soc. Jpn.*, 35:137, 1973. [doi:10.1143/JPSJ.35.137](#).
  - [68] D. Emin and T. Holstein. Adiabatic Theory of an Electron in a Deformable Continuum. *Phys. Rev. Lett.*, 36:323, 1976. [doi:10.1103/PhysRevLett.36.323](#).
  - [69] M. P. A. Fisher and W. Zwerger. Ground-state symmetry of a generalized polaron. *Phys. Rev. B*, 34:5912, 1986. [doi:10.1103/PhysRevB.34.5912](#).
  - [70] R. Fantoni. Localization of acoustic polarons at low temperatures: A path-integral Monte Carlo approach. *Phys. Rev. B*, 86:144304, 2012. [doi:10.1103/PhysRevB.86.144304](#).
  - [71] J. T. Titantah, C. Pierleoni, and S. Ciuchi.
  - [72] C. Alexandrou, W. Fleischer, and R. Rosenfelder. Fourier path integrals, partial averaging, and the polaron problem. *Phys. Rev. Lett.*, 65:2615, 1990. [doi:10.1103/PhysRevLett.65.2615](#).
  - [73] C. Alexandrou and R. Rosenfelder. Stochastic solution to highly nonlocal actions: the polaron problem. *Phys. Rep.*, 215:1, 1992. [doi:10.1016/0370-1573\(92\)90150-X](#).
  - [74] M. Creutz and B. Freedman. A statistical approach to quantum mechanics. *Ann. Phys.*, 132:427, 1981. [doi:10.1016/0003-4916\(81\)90074-9](#).
  - [75] M. Takahashi and M. Imada. Monte Carlo Calculation of Quantum Systems. *J. Phys. Soc. Jpn.*, 53:963, 1983. [doi:10.1143/JPSJ.53.963](#).
  - [76] X. Wang. *Mod. Phys. Lett. B*, 12:775, 1998.
  - [77] P. E. Kornilovitch. Trotter-number scaling in Monte Carlo studies of the small polaron. *J. Phys.: Condens. Matter*, 9:10675, 1997. [doi:10.1088/0953-8984/9/48/011](#).
  - [78] P. E. Kornilovitch. Path-integral approach to lattice polarons. *J. Phys.: Condens. Matter*, 19:255213, 2007. [doi:10.1088/0953-8984/19/25/255213](#).
  - [79] J. Bardeen and W. Shockley. Deformation Potentials and Mobilities in Non-Polar Crystals. *Phys. Rev.*, 80:72, 1950. [doi:10.1103/PhysRev.80.72](#).
  - [80] R. P. Feynman and A. R. Hibbs. *Quantum Mechanics and Path Integrals*. McGraw-Hill Inc, New York, 1965. pp. 292-293.
  - [81] P. Lévy. Sur certains processus stochastiques homogènes. *Compositio Math.*, 7:283, 1939.
  - [82] D. M. Ceperley and E. L. Pollock. Path-integral computation of the low-temperature properties of liquid  $^4\text{He}$ . *Phys. Rev. Lett.*, 56:351, 1986. [doi:10.1103/PhysRevLett.56.351](#).
  - [83] D. M. Ceperley and E. L. Pollock. Path-integral simulation of the superfluid transition in two-dimensional  $^4\text{He}$ . *Phys. Rev. B*, 39:2084, 1989. [doi:10.1103/PhysRevB.39.2084](#).
  - [84] J. M. Hammersley and C. D. Handscomb. *Monte Carlo Methods*. Chapman and Hall, London, 1964.
-

---

## BIBLIOGRAPHY

---

- [85] D. Mendeleev. The natural system of elements and its application to the indication of the properties of undiscovered elements. *Journal of the Russian Chemical Society*, 3:25, 1871.
  - [86] L. Pauling. The Nature of the Chemical Bond. IV. The Energy of Single Bonds and the Relative Electronegativity of Atoms. *Journal of the American Chemical Society*, 54:3570, 1932. [doi:10.1021/ja01348a011](https://doi.org/10.1021/ja01348a011).
  - [87] N. N. Greenwood and A. Earnshaw. *Chemistry of the Elements*. Pergamon, 1960. p. 30.
  - [88] A. Lenard. Exact Statistical Mechanics of a One Dimensional System with Coulomb Forces. *J. Math. Phys.*, 2:682, 1961. [doi:10.1063/1.1703757](https://doi.org/10.1063/1.1703757).
  - [89] S. F. Edards and A. Lenard. Exact Statistical Mechanics of a One Dimensional System with Coulomb Forces. II. The Method of Functional Integration. *J. Math. Phys.*, 3:778, 1961. [doi:10.1063/1.1724281](https://doi.org/10.1063/1.1724281).
  - [90] G. Gallavotti, S. Miracle-Sole, and D. Ruelle. Absence of phase transitions in one-dimensional systems with hard cores. *Physics Letters A*, 26:350, 1968. [doi:10.1016/0375-9601\(68\)90367-8](https://doi.org/10.1016/0375-9601(68)90367-8).
  - [91] A. M. Salzberg and S. Prager. Equation of State for a Two-Dimensional Electrolyte. *J. Chem. Phys.*, 38:2587, 1963. [doi:10.1063/1.1733553](https://doi.org/10.1063/1.1733553).
  - [92] D. Pines and P. Nozières. *Theory of Quantum Liquids*. W. A. Benjamin Inc, New York, 1966.
  - [93] E. Feenberg. *Theory of Quantum Fluids*. Academic Press Inc, New York, 1969.
  - [94] N. H. March and M. P. Tosi. *Coulomb Liquids*. Academic Press Inc Ltd, London, 1984.
  - [95] J. P. Hansen and I. R. McDonald. *Theory of Simple Liquids*. Academic Press, Amsterdam, 1986.
  - [96] R. Fantoni. Exact results for one dimensional fluids through functional integration. *J. Stat. Phys.*, 163:1247, 2016. [doi:10.1007/s10955-016-1510-3](https://doi.org/10.1007/s10955-016-1510-3).
  - [97] R. Fantoni. Two component plasma in a Flamm's paraboloid. *J. Stat. Mech.*, page P04015, 2012. [doi:10.1088/1742-5468/2012/04/P04015](https://doi.org/10.1088/1742-5468/2012/04/P04015).
  - [98] B. Jancovici. Exact Results for the Two-Dimensional One-Component Plasma. *Phys. Rev. Lett.*, 46:386, 1981. [doi:10.1103/PhysRevLett.46.386](https://doi.org/10.1103/PhysRevLett.46.386).
  - [99] Ph. Choquard. The two-dimensional one-component plasma on a periodic strip. *Helv. Phys. Acta*, 54:332, 1981.
  - [100] J. M. Caillol. Exact results for a two-dimensional one-component plasma on a sphere. *J. Phys. (Paris) -Lett.*, 42:L-245, 1981.
  - [101] R. Fantoni, B. Jancovici, and G. Téllez. Pressures for a One-Component Plasma on a Pseudosphere. *J. Stat. Phys.*, 112:27, 2003. [doi:10.1023/A:1023671419021](https://doi.org/10.1023/A:1023671419021).
  - [102] R. Fantoni and G. Téllez. Two dimensional one-component plasma on a Flamm's paraboloid. *J. Stat. Phys.*, 133:449, 2008. [doi:10.1007/s10955-008-9616-x](https://doi.org/10.1007/s10955-008-9616-x).
  - [103] L. Šamaj. Is the Two-Dimensional One-Component Plasma Exactly Solvable? *J. Stat. Phys.*, 117:131, 2004. [doi:10.1023/B:JOSS.0000044056.19438.2c](https://doi.org/10.1023/B:JOSS.0000044056.19438.2c).
-

---

## BIBLIOGRAPHY

---

- [104] R. Fantoni. One-component fermion plasma on a sphere at finite temperature. *Int. J. Mod. Phys. C*, 29:1850064, 2018. [doi:10.1142/S012918311850064X](https://doi.org/10.1142/S012918311850064X).
- [105] R. Fantoni. One-component fermion plasma on a sphere at finite temperature. The anisotropy in the paths conformations. *J. Stat. Mech.*, page 083103, 2023. [doi:10.1088/1742-5468/aceb54](https://doi.org/10.1088/1742-5468/aceb54).
- [106] R. Fantoni. How Should We Choose the Boundary Conditions in a Simulation Which Could Detect Anyons in One and Two Dimensions? *J. Low Temp. Phys.*, 202:247, 2021. [doi:10.1007/s10909-020-02532-0](https://doi.org/10.1007/s10909-020-02532-0).
- [107] A. Lerda. *Anyons. Quantum Mechanics of Particles with Fractional Statistics*. Springer-Verlag, Berlin, 1992.
- [108] K. S. Singwi and M. P. Tosi. *Sol. State Phys.*, 36:177, 1981. ed. H. Ehrenreich, F. Seitz and D. Turnbull (Academic, New York, 1981) Vol. 36, p. 177.
- [109] S. Ichimaru. Strongly coupled plasmas: high-density classical plasmas and degenerate electron liquids. *Rev. Mod. Phys.*, 54:1017, 1982. [doi:10.1103/RevModPhys.54.1017](https://doi.org/10.1103/RevModPhys.54.1017).
- [110] Ph. A. Martin. Sum rules in charged fluids. *Rev. Mod. Phys.*, 60:1075, 1988. [doi:10.1103/RevModPhys.60.1075](https://doi.org/10.1103/RevModPhys.60.1075).
- [111] E. P. Wigner. On the Interaction of Electrons in Metals. *Phys. Rev.*, 46:1002, 1934. [doi:10.1103/PhysRev.46.1002](https://doi.org/10.1103/PhysRev.46.1002).
- [112] A. J. Leggett. A theoretical description of the new phases of liquid  $^3\text{He}$ . *Rev. Mod. Phys.*, 47:331, 1975. [doi:10.1103/RevModPhys.47.331](https://doi.org/10.1103/RevModPhys.47.331).
- [113] G. F. Giuliani and G. Vignale. *Quantum Theory of the Electron Liquid*. Cambridge University Press, Cambridge, 2005.
- [114] E. L. Pollock and D. M. Ceperley. Path-integral computation of superfluid densities. *Phys. Rev. B*, 36:8343, 1987. [doi:10.1103/PhysRevB.36.8343](https://doi.org/10.1103/PhysRevB.36.8343).
- [115] K. S. Singwi, M. P. Tosi, R. H. Land, and A. Sjölander. Electron Correlations at Metallic Densities. *Phys. Rev.*, 176:589, 1968. [doi:10.1103/PhysRev.176.589](https://doi.org/10.1103/PhysRev.176.589).
- [116] D. M. Ceperley and B. J. Alder. Ground State of the Electron Gas by a Stochastic Method. *Phys. Rev. Lett.*, 45:566, 1980. [doi:10.1103/PhysRevLett.45.566](https://doi.org/10.1103/PhysRevLett.45.566).
- [117] E. W. Brown, B. K. Clark, J. L. DuBois, and D. M. Ceperley. Path-Integral Monte Carlo Simulation of the Warm Dense Homogeneous Electron Gas. *Phys. Rev. Lett.*, 110:146405, 2013. [doi:10.1103/PhysRevLett.110.146405](https://doi.org/10.1103/PhysRevLett.110.146405).
- [118] M. P. Allen and D. J. Tildesley. *Computer Simulation of Liquids*. Oxford University Press Inc, New York, 1987.
- [119] V. Natoli and D. M. Ceperley. An Optimized Method for Treating Long-Range Potentials. *Comput. Phys.*, 117:171, 1995. [doi:10.1006/jcph.1995.1054](https://doi.org/10.1006/jcph.1995.1054).
- [120] J. Kolorenc and L. Mitas. Applications of quantum Monte Carlo methods in condensed systems. *Rep. Prog. Phys.*, 74:026502, 2011. [doi:10.1088/0034-4885/74/2/026502](https://doi.org/10.1088/0034-4885/74/2/026502).
- [121] W. M. C. Foulkes, L. Mitas, R. J. Needs, and G. Rajagopal. Quantum Monte Carlo simulations of solids. *Rev. Mod. Phys.*, 73:33, 2001. [doi:10.1103/RevModPhys.73.33](https://doi.org/10.1103/RevModPhys.73.33).

---

## BIBLIOGRAPHY

---

- [122] Y. Kwon, D. M. Ceperley, and R. M. Martin. Effects of backflow correlation in the three-dimensional electron gas: Quantum Monte Carlo study. *Phys. Rev. B*, 58:6800, 1998. [doi:10.1103/PhysRevB.58.6800](https://doi.org/10.1103/PhysRevB.58.6800).
- [123] J. Toulouse, R. Assaraf, and C. J. Umrigar. Zero-variance zero-bias quantum Monte Carlo estimators of the spherically and system-averaged pair density. *J. Chem. Phys.*, 126:244112, 2007. [doi:10.1063/1.2746029](https://doi.org/10.1063/1.2746029).
- [124] C. Lin, F. H. Zong, and D. M. Ceperley. Twist-averaged boundary conditions in continuum quantum Monte Carlo algorithms. *Phys. Rev. E*, 64:016702, 2001. [doi:10.1103/PhysRevE.64.016702](https://doi.org/10.1103/PhysRevE.64.016702).
- [125] S. Chiesa, D. M. Ceperley, R. M. Martin, and M. Holzmann. Finite-Size Error in Many-Body Simulations with Long-Range Interactions. *Phys. Rev. Lett.*, 97:076404, 2006. [doi:10.1103/PhysRevLett.97.076404](https://doi.org/10.1103/PhysRevLett.97.076404).
- [126] J. B. Anderson. Quantum chemistry by random walk.  $H\ ^2P$ ,  $H_3^+ \ D_{3h} \ ^1A'_1$ ,  $H_2 \ ^3\Sigma_u^+$ ,  $H^4 \ ^1\Sigma_g^+$ ,  $Be \ ^1S$ . *J. Chem. Phys.*, 65:4121, 1976. [doi:10.1063/1.432868](https://doi.org/10.1063/1.432868).
- [127] M. H. Kalos, D. Levesque, and L. Verlet. Helium at zero temperature with hard-sphere and other forces. *Phys. Rev. A*, 9:2178, 1974. [doi:10.1103/PhysRevA.9.2178](https://doi.org/10.1103/PhysRevA.9.2178).
- [128] J. M. Hammersley and D. C. Handscomb. *Monte Carlo Methods*. Fletcher & Son Ltd, Norwich, 1964. pp. 57-59.
- [129] M. H. Kalos and P. A. Whitlock. *Monte Carlo Methods*. John Wiley & Sons Inc, New York, 1986.
- [130] D. M. Ceperley. Fermion nodes. *J. Stat. Phys.*, 63:1237, 1991. [doi:10.1007/BF01030009](https://doi.org/10.1007/BF01030009).
- [131] C. J. Umrigar, M. P. Nightingale, and K. J. Runge. A diffusion Monte Carlo algorithm with very small time-step errors. *J. Chem. Phys.*, 99:2865, 1993. [doi:10.1063/1.465195](https://doi.org/10.1063/1.465195).
- [132] K. S. Liu, M. H. Kalos, and G. V. Chester. Quantum hard spheres in a channel. *Phys. Rev. A*, 10:303, 1974. [doi:10.1103/PhysRevA.10.303](https://doi.org/10.1103/PhysRevA.10.303).
- [133] R. N. Barnett, P. J. Reynolds, and Jr. W. A. Lester. *J. Comp. Phys.*, 96:258, 1991.
- [134] S. Baroni and S. Moroni. Reptation Quantum Monte Carlo: A Method for Unbiased Ground-State Averages and Imaginary-Time Correlations. *Phys. Rev. Lett.*, 82:4745, 1999. [doi:10.1103/PhysRevLett.82.4745](https://doi.org/10.1103/PhysRevLett.82.4745).
- [135] R. Assaraf and M. Caffarel. Zero-variance zero-bias principle for observables in quantum Monte Carlo: Application to forces. *J. Chem. Phys.*, 119:10536, 2003. [doi:10.1063/1.1621615](https://doi.org/10.1063/1.1621615).
- [136] D. M. Ceperley and M. H. Kalos. Quantum many-body problems. In K. Binder, editor, *Monte Carlo Methods in Statistical Physics*, page 145. Springer-Verlag, Heidelberg, 1979.
- [137] R. Fantoni. Radial distribution function in a diffusion Monte Carlo simulation of a Fermion fluid between the ideal gas and the Jellium model. *Solid State Communications*, 159:106, 2013. [doi:10.1140/epjb/e2013-40204-3](https://doi.org/10.1140/epjb/e2013-40204-3).
- [138] R. Gaudoin and J. M. Pitarke. Hellman-Feynman Operator Sampling in Diffusion Monte Carlo Calculations. *Phys. Rev. Lett.*, 99:126406, 2007. [doi:10.1103/PhysRevLett.99.126406](https://doi.org/10.1103/PhysRevLett.99.126406).

---

## BIBLIOGRAPHY

---

- [139] A. Bijl. The lowest wave function of the symmetrical many particles system. *Physica*, 7:869, 1940. [doi:10.1016/0031-8914\(40\)90166-5](https://doi.org/10.1016/0031-8914(40)90166-5).
- [140] R. B. Dingle. LI. The zero-point energy of a system of particles. *Philos. Mag.*, 40:573, 1949. [doi:10.1080/14786444908521743](https://doi.org/10.1080/14786444908521743).
- [141] R. Jastrow. Many-Body Problem with Strong Forces. *Phys. Rev.*, 98:1479, 1955. [doi:10.1103/PhysRev.98.1479](https://doi.org/10.1103/PhysRev.98.1479).
- [142] T. Gaskell. The Collective Treatment of a Fermi Gas: II. *Proc. Phys. Soc.*, 77:1182, 1961. [doi:10.1088/0370-1328/77/6/312](https://doi.org/10.1088/0370-1328/77/6/312).
- [143] T. Gaskell. The Collective Treatment of Many-body Systems: III. *Proc. Phys. Soc.*, 80:1091, 1962. [doi:10.1088/0370-1328/80/5/307](https://doi.org/10.1088/0370-1328/80/5/307).
- [144] D. M. Ceperley. Introduction to quantum monte carlo methods applied to the electron gas. In G. F. Giuliani and G. Vignale, editors, *Proceedings of the International School of Physics Enrico Fermi*, pages 3–42, Amsterdam, 2004. IOS Press. Course CLVII.
- [145] D. M. Ceperley. Ground state of the fermion one-component plasma: A Monte Carlo study in two and three dimensions. *Phys. Rev. B*, 18:3126, 1978. [doi:10.1103/PhysRevB.18.3126](https://doi.org/10.1103/PhysRevB.18.3126).
- [146] Y. Kwon, D. M. Ceperley, and R. M. Martin. Effects of three-body and backflow correlations in the two-dimensional electron gas. *Phys. Rev. B*, 48:12037, 1993. [doi:10.1103/PhysRevB.48.12037](https://doi.org/10.1103/PhysRevB.48.12037).
- [147] R. P. Feynman and M. Cohen. Energy Spectrum of the Excitations in Liquid Helium. *Phys. Rev.*, 102:1189, 1956. [doi:10.1103/PhysRev.102.1189](https://doi.org/10.1103/PhysRev.102.1189).
- [148] R. M. Panoff and J. Carlson. Fermion Monte Carlo algorithms and liquid  ${}^3\text{He}$ . *Phys. Rev. Lett.*, 62:1130, 1989. [doi:10.1103/PhysRevLett.62.1130](https://doi.org/10.1103/PhysRevLett.62.1130).
- [149] T. L. Hill. *Statistical Mechanics. Principles and Selected Applications*. McGraw-Hill Book Company Inc, Toronto, 1956.
- [150] S. Paziani, S. Moroni, P. Gori-Giorgi, and G. B. Bachelet. Local-spin-density functional for multideterminant density functional theory. *Phys. Rev. B*, 73:155111, 2006. [doi:10.1103/PhysRevB.73.155111](https://doi.org/10.1103/PhysRevB.73.155111).
- [151] G. Ortiz and P. Ballone. Correlation energy, structure factor, radial distribution function, and momentum distribution of the spin-polarized uniform electron gas. *Phys. Rev. B*, 50:1391, 1994. [doi:10.1103/PhysRevB.50.1391](https://doi.org/10.1103/PhysRevB.50.1391).
- [152] R. P. Feynman. The  $\lambda$ -Transition in Liquid Helium. *Phys. Rev.*, 90:1116, 1953. [doi:10.1103/PhysRev.90.1116.2](https://doi.org/10.1103/PhysRev.90.1116.2).
- [153] R. P. Feynman. Atomic Theory of the  $\lambda$  Transition in Helium. *Phys. Rev.*, 91:1291, 1953. [doi:10.1103/PhysRev.91.1291](https://doi.org/10.1103/PhysRev.91.1291).
- [154] R. P. Feynman. Atomic Theory of Liquid Helium Near Absolute Zero. *Phys. Rev.*, 91:1301, 1953. [doi:10.1103/PhysRev.91.1301](https://doi.org/10.1103/PhysRev.91.1301).
- [155] D. M. Ceperley. Path integral monte carlo methods for fermions. In K. Binder and G. Ciccotti, editors, *Monte Carlo and Molecular Dynamics of Condensed Matter Systems*, Bologna, Italy, 1996. Editrice Compositori.

---

## BIBLIOGRAPHY

---

- [156] L. D. Landau and E. M. Lifshitz. *Statistical Physics*, volume 5 of *Course of Theoretical Physics*. Butterworth-Heinemann, Oxford, 1951.
  - [157] M. Boninsegni, N. Prokof'ev, and B. Svistunov. Worm Algorithm for Continuous-Space Path Integral Monte Carlo Simulations. *Phys. Rev. Lett.*, 96:070601, 2006. [doi:10.1103/PhysRevLett.96.070601](https://doi.org/10.1103/PhysRevLett.96.070601).
  - [158] N. Metropolis, A. W. Rosenbluth, M. N. Rosenbluth, A. M. Teller, and E. Teller. Equations of State Calculations by Fast Computing Machines. *J. Chem. Phys.*, 1087:21, 1953. [doi:10.1063/1.1699114](https://doi.org/10.1063/1.1699114).
  - [159] E. L. Pollock. Properties and computation of the Coulomb pair density matrix. *Computer Physics Communications*, 52:49, 1988. [doi:10.1016/0010-4655\(88\)90171-3](https://doi.org/10.1016/0010-4655(88)90171-3).
  - [160] P. Vieillefosse. Coulomb pair density matrix I. *J. Stat. Phys.*, 74:1195, 1994. [doi:10.1007/BF02188223](https://doi.org/10.1007/BF02188223).
  - [161] P. Vieillefosse. Coulomb pair density matrix. II. *J. Stat. Phys.*, 80:461, 1995. [doi:10.1007/BF02178368](https://doi.org/10.1007/BF02178368).
  - [162] J. P. Hansen. Statistical Mechanics of Dense Ionized Matter. I. Equilibrium Properties of the Classical One-Component Plasma. *Phys. Rev. A*, 8:3096, 1973. [doi:10.1103/PhysRevA.8.3096](https://doi.org/10.1103/PhysRevA.8.3096).
  - [163] J. P. Perdew and A. Zunger. Self-interaction correction to density-functional approximations for many-electron systems. *Phys. Rev. B*, 23:5048, 1981. [doi:10.1103/PhysRevB.23.5048](https://doi.org/10.1103/PhysRevB.23.5048).
  - [164] E. L. Pollock and J. P. Hansen. Statistical Mechanics of Dense Ionized Matter. II. Equilibrium Properties and Melting Transition of the Crystallized One-Component Plasma. *Phys. Rev. A*, 8:3110, 1973. [doi:10.1103/PhysRevA.8.3110](https://doi.org/10.1103/PhysRevA.8.3110).
  - [165] E. Brown, M. A. Morales, C. Pierleoni, and D. M. Ceperley. Quantum monte carlo techniques and applications for warm dense matter. In F. Graziani *et al.*, editor, *Frontiers and Challenges in Warm Dense Matter*, pages 123–149. Springer, 2014.
  - [166] J. P. Hansen and P. Vieillefosse. Quantum corrections in dense ionized matter. *Phys. Lett. A*, 53:187, 1975. [doi:10.1016/0375-9601\(75\)90523-X](https://doi.org/10.1016/0375-9601(75)90523-X).
  - [167] U. Gupta and A. K. Rajagopal. Exchange-correlation potential for inhomogeneous electron systems at finite temperatures. *Phys. Rev. A*, 22:2792, 1980. [doi:10.1103/PhysRevA.22.2792](https://doi.org/10.1103/PhysRevA.22.2792).
  - [168] F. Perrot and M. W. C. Dharma-wardana. Exchange and correlation potentials for electron-ion systems at finite temperatures. *Phys. Rev. A*, 30:2619, 1984. [doi:10.1103/PhysRevA.30.2619](https://doi.org/10.1103/PhysRevA.30.2619).
  - [169] S. Tanaka and S. Ichimaru. Thermodynamics and Correlational Properties of Finite-Temperature Electron Liquids in the Singwi-Tosi-Land-Sjölander Approximation. *Journal of the Physical Society of Japan*, 55:2278, 1986. [doi:10.1143/JPSJ.55.2278](https://doi.org/10.1143/JPSJ.55.2278).
  - [170] F. Perrot and M. W. C. Dharma-wardana. Spin-polarized electron liquid at arbitrary temperatures: Exchange-correlation energies, electron-distribution functions, and the static response functions. *Phys. Rev. B*, 62:16536, 2000. [doi:10.1103/PhysRevB.62.16536](https://doi.org/10.1103/PhysRevB.62.16536).
-

---

## BIBLIOGRAPHY

---

- [171] M. W. C. Dharma-wardana and F. Perrot. Simple Classical Mapping of the Spin-Polarized Quantum Electron Gas: Distribution Functions and Local-Field Corrections. *Phys. Rev. Lett.*, 84:959, 2000. [doi:10.1103/PhysRevLett.84.959](https://doi.org/10.1103/PhysRevLett.84.959).
- [172] S. Dutta and J. Dufty. Classical representation of a quantum system at equilibrium: Applications. *Phys. Rev. E*, 87:032102, 2013. [doi:10.1103/PhysRevE.87.032102](https://doi.org/10.1103/PhysRevE.87.032102).
- [173] B. Jancovici. *Physica (Amsterdam)*, 91A:152, 1978.
- [174] M. D. Jones and D. M. Ceperley. Crystallization of the One-Component Plasma at Finite Temperature. *Phys. Rev. Lett.*, 76:4572, 1996. [doi:10.1103/PhysRevLett.76.4572](https://doi.org/10.1103/PhysRevLett.76.4572).
- [175] C. C. Grimes and G. Adams. Evidence for a Liquid-to-Crystal Phase Transition in a Classical, Two-Dimensional Sheet of Electrons. *Phys. Rev. Lett.*, 42:795, 1979. [doi:10.1103/PhysRevLett.42.795](https://doi.org/10.1103/PhysRevLett.42.795).
- [176] B. Tanatar and D. M. Ceperley. Ground state of the two-dimensional electron gas. *Phys. Rev. B*, 39:5005, 1989. [doi:10.1103/PhysRevB.39.5005](https://doi.org/10.1103/PhysRevB.39.5005).
- [177] M. D. Knudson et al. Probing the Interiors of the Ice Giants: Shock Compression of Water to 700GPa and 3.8g/cm<sup>3</sup>. *Phys. Rev. Lett.*, 108:091102, 2012. [doi:10.1103/PhysRevLett.108.091102](https://doi.org/10.1103/PhysRevLett.108.091102).
- [178] R. Ernstorfer et al. The formation of warm dense matter: experimental evidence for electronic bond hardening in gold. *Science*, 323:5917, 2009. [doi:10.1126/science.1162697](https://doi.org/10.1126/science.1162697).
- [179] L. B. Fletcher et al. Observations of Continuum Depression in Warm Dense Matter with X-Ray Thomson Scattering. *Phys. Rev. Lett.*, 112:145004, 2014. [doi:10.1103/PhysRevLett.112.145004](https://doi.org/10.1103/PhysRevLett.112.145004).
- [180] G. Mazzola, S. Yunoki, and S. Sorella. Unexpectedly high pressure for molecular dissociation in liquid hydrogen by electronic simulation. *Nat. Commun.*, 5:3487, 2014. [doi:10.1038/ncomms4487](https://doi.org/10.1038/ncomms4487).
- [181] T. Dornheim, S. Groth, T. Sjostrom, F. D. Malone, W. M. C. Foulkes, and M. Bonitz. *Ab Initio* Quantum Monte Carlo Simulation of the Warm Dense Electron Gas in the Thermodynamic Limit. *Phys. Rev. Lett.*, 117:156403, 2016. [doi:10.1103/PhysRevLett.117.156403](https://doi.org/10.1103/PhysRevLett.117.156403).
- [182] M. Dewing and D. M. Ceperley. Methods for Coupled Electronic-Ionic Monte Carlo. In W. A. Lester, S. M. Rothstein, and S. Tanaka, editors, *Recent Advances in Quantum Monte Carlo Methods, II*. World Scientific, Singapore, 2002.
- [183] D. M. Ceperley, M. Dewing, and C. Pierleoni. The coupled electronic-ionic monte carlo simulation method. In *Bridging Time Scales: Molecular Simulations for the Next Decade*, pages 473–500. Springer-Verlag, 2002.
- [184] N. H. March and M. P. Tosi. *Introduction to Liquid State Physics*. World Scientific Publishing Co Pte Ltd, Singapore, 2002.
- [185] N. H. March. *Liquid Metals. Concepts and theory*. Cambridge University Press, Cambridge, 1990.
- [186] M. Kac. *Probability and Related Topics in Physical Sciences*. Interscience Publisher Inc, New York, 1959.

---

## BIBLIOGRAPHY

---

- [187] M. Kac. Proceedings of the second berkeley symposium on probability and statistics. Berkeley, 1951. University of California Press. Sec. 3.
- [188] L. van Hove. Correlations in Space and Time and Born Approximation Scattering in Systems of Interacting Particles. *Phys. Rev.*, 95:249, 1954. doi:[10.1103/PhysRev.95.249](https://doi.org/10.1103/PhysRev.95.249).
- [189] J. Lindhard. *Mat.-Fys. Medd.*, 28(8), 1954.
- [190] M. P. Tosi. Many-body effects in jellium. In N. H. March, editor, *Electron Correlation in the Solid State*, chapter 1, pages 1–42. Imperial College Press, London, 1999.
- [191] D. R. Hartree. The Wave Mechanics of an Atom with a Non-Coulomb Central Field. Part I. Theory and Methods. *Proc. Cambridge Phil. Soc.*, 24:89 and 111, 1928. doi:[10.1017/S0305004100011919](https://doi.org/10.1017/S0305004100011919).
- [192] V. Fock. Naherungsmethode zur Losung des quantenmechanischen Mehrkorperproblems. *Zs. Phys.*, 61:126, 1930. doi:[10.1007/BF01340294](https://doi.org/10.1007/BF01340294).
- [193] J. C. Slater. Note on Hartree’s Method. *Phys. Rev.*, 35:210, 1930. doi:[10.1103/PhysRev.35.210.2](https://doi.org/10.1103/PhysRev.35.210.2).
- [194] M. Gell-Mann and K. A. Bruckner. Correlation Energy of an Electron Gas at High Density. *Phys. Rev.*, 106:364, 1957. doi:[10.1103/PhysRev.106.364](https://doi.org/10.1103/PhysRev.106.364).
- [195] E. P. Wigner. Effects of the Electron Interaction on the Energy Levels of Electrons in Metals. *Trans. Faraday Soc.*, 34:678, 1938. doi:[10.1039/tf9383400678](https://doi.org/10.1039/tf9383400678).
- [196] J. C. Kimball. Short-Range Correlations and Electron-Gas Response Functions. *Phys. Rev. A*, 7:1648, 1973. doi:[10.1103/PhysRevA.7.1648](https://doi.org/10.1103/PhysRevA.7.1648).
- [197] A. K. Rajagopal, J. C. Kimball, and M. Banerjee. Short-ranged correlations and the ferromagnetic electron gas. *Phys. Rev. B*, 18:2339, 1978. doi:[10.1103/PhysRevB.18.2339](https://doi.org/10.1103/PhysRevB.18.2339).
- [198] M. Hoffmann-Ostenhof, T. Hofmann-Ostenhof, and H. Stremnitzer. Electronic wave functions near coalescence points. *Phys. Rev. Lett.*, 68:3857, 1992. doi:[10.1103/PhysRevLett.68.3857](https://doi.org/10.1103/PhysRevLett.68.3857).
- [199] A. Alastuey and Ph. A. Martin. Decay of correlations in classical fluids with long-range forces. *J. Stat. Phys.*, 39:405, 1985. doi:[10.1007/BF01018670](https://doi.org/10.1007/BF01018670).
- [200] M. J. Lighthill. *Introduction to Fourier Analysis and Generalized Functions*. Cambridge University Press, London, 1958. Theorem 19.
- [201] H. F. Trotter. On the Product of Semi-Groups of Operators. *Proc. Am. Math. Soc.*, 10:545, 1959. doi:[10.1090/S0002-9939-1959-0108732-6](https://doi.org/10.1090/S0002-9939-1959-0108732-6).
- [202] B. Simon. *Functional integration and quantum physics*. Academic, New York, 1979.
- [203] M. Abramowitz and I. A. Stegun. *Handbook of mathematical functions*. Dover, New York, 1970.
- [204] J. A. Barker. A quantum statistical Monte Carlo method; path integrals with boundary conditions. *J. Chem. Phys.*, 70:2914, 1979. doi:[10.1063/1.437829](https://doi.org/10.1063/1.437829).
- [205] D. Pines e Ph. Nozières. *The Teory of Quantum Liquids*. W. A. Benjamin, Inc., New York, 1966. Chapter 2.

---

## BIBLIOGRAPHY

---

- [206] R. Balian and J. P. Blaizot. Stars and statistical physics: A Teaching experience. *Am. J. Phys.*, 67:1189, 1999. [doi:10.1119/1.19105](https://doi.org/10.1119/1.19105).
- [207] R. Silbar and S. Reddy. Neutron stars for undergraduates. *Am. J. Phys.*, 72:892, 2004. [doi:10.1119/1.1703544](https://doi.org/10.1119/1.1703544).
- [208] C. B. Jackson, J. Taruna, S. L. Pouliot, B. W. Ellison, D. D. Lee, and J. Piekarewicz. Compact objects for everyone: I. White dwarf stars. *European J. Phys.*, 26:695, 2005. [doi:10.1088/0143-0807/26/5/003](https://doi.org/10.1088/0143-0807/26/5/003).
- [209] L. D. Landau. On the theory of stars. *Phys. Z. Sowjetunion*, 1:285, 1932. [doi:10.1016/B978-0-08-010586-4.50013-4](https://doi.org/10.1016/B978-0-08-010586-4.50013-4).
- [210] S. Chandrasekhar and E. A. Milne. The Highly Collapsed Configurations of a Stellar Mass. *Monthly Notices of the Royal Astronomical Society*, 91:456, 1931. [doi:10.1093/mnras/91.5.456](https://doi.org/10.1093/mnras/91.5.456).
- [211] S. Chandrasekhar. XLVIII. The density of white dwarf stars. *The London, Edinburgh, and Dublin Philosophical Magazine and Journal of Science*, 11:592, 1931. [doi:10.1080/14786443109461710](https://doi.org/10.1080/14786443109461710).
- [212] S. Chandrasekhar. The maximum mass of ideal white dwarfs. *Astrophys. J.*, 74:81, 1931. [doi:10.1086/143324](https://doi.org/10.1086/143324).
- [213] P. A. M. Dirac. On the Theory of Quantum Mechanics. *Proc. Roy. Soc. Lond. A*, 112:661, 1926. [doi:10.1098/rspa.1926.0133](https://doi.org/10.1098/rspa.1926.0133).
- [214] R. H. Fowler. On dense matter. *Mon. Not. Roy. Astron. Soc.*, 87:114, 1926.
- [215] W. S. Adams. *Pub. Astron. Soc. Pac.*, 27:236, 1915.
- [216] W. S. Adams. The Relativity Displacement of the Spectral Lines in the Companion of Sirius. *Proc. Natl. Acad. Sci. USA*, 11:382, 1925. Erratum: *Observatory* **49**, 88. [doi:10.1073/pnas.11.7.382](https://doi.org/10.1073/pnas.11.7.382).
- [217] S. Chandrasekhar. *An introduction to the study of stellar structure*. The University of Chicago Press, Chicago, Illinois, 1938.
- [218] S. Chandrasekhar. The Highly Collapsed Configurations of a Stellar Mass. (Second Paper.). *Monthly Notices of the Royal Astronomical Society*, 95:207, 1935. [doi:10.1093/mnras/95.3.207](https://doi.org/10.1093/mnras/95.3.207).
- [219] S. Chandrasekhar. On Stars, Their Evolution and Their Stability. *Nobel Prize lecture*, December 1983.
- [220] J. Bosse, K. N. Pathak, and G. S. Singh. Analytical pair correlations in ideal quantum gases: Temperature-dependent bunching and antibunching. *Phys. Rev. E*, 84:042101, 2011. [doi:10.1103/PhysRevE.84.042101](https://doi.org/10.1103/PhysRevE.84.042101).
- [221] R. Fantoni. Radial distribution function in a diffusion Monte Carlo simulation of a Fermion fluid between the ideal gas and the Jellium model. *Eur. Phys. J. B*, 86:286, 2013. [doi:10.1140/epjb/e2013-40204-3](https://doi.org/10.1140/epjb/e2013-40204-3).
- [222] B. Militzer, E. L Pollock, and D. M. Ceperley. Path integral Monte Carlo calculation of the momentum distribution of the homogeneous electron gas at finite temperature. *High Energy Density Physics*, 30:13, 2003. [doi:10.1016/j.hedp.2018.12.004](https://doi.org/10.1016/j.hedp.2018.12.004).

---

## BIBLIOGRAPHY

---

- [223] C. Rovelli. General relativistic statistical mechanics. *Phys. Rev. D*, 87:084055, 2013. [doi:10.1103/PhysRevD.87.084055](https://doi.org/10.1103/PhysRevD.87.084055).
- [224] Michael E. Fisher. Renormalization group theory: Its basis and formulation in statistical physics. *Rev. Mod. Phys.*, 70:653, 1998. [doi:10.1103/RevModPhys.70.653](https://doi.org/10.1103/RevModPhys.70.653).
- [225] N. Goldenfeld. *Lectures on Phase Transitions and the Renormalization Group*. Frontiers in Physics. Westview Press, University of Illinois at Urbana-Champaign, 1992.
- [226] L. D. Landau and E. M. Lifshitz. *Statistical Physics*, volume 5 of *Course of Theoretical Physics*. Pergamon, London, 1958.
- [227] V. L. Ginzburg and L. D. Landau. On the Theory of Superconductivity. *Zh. Eksp. Teor. Fiz.*, 20:1064, 1959.
- [228] V. L. Ginzburg. Superconductivity and Superfluidity (What was done and what was not). *Phys. Usp.*, 40:407, 1997. [doi:10.1070/PU1997v040n04ABEH000230](https://doi.org/10.1070/PU1997v040n04ABEH000230).
- [229] L. Onsager. Crystal Statistics I. A Two-dimensional Model with an Order-Disorder Transition. *Phys. Rev.*, 62:117, 1944. [doi:10.1103/PhysRev.65.117](https://doi.org/10.1103/PhysRev.65.117).
- [230] L. Onsager. Discussion remark following a paper by G. S. Rushbrooke at the International Conference on Statistical Mechanics in Florence. *Nuovo Cimento Suppl.*, 9:261, 1949.
- [231] B. Kaufman and L. Onsager. Crystal Statistics II. Short-Range Order in a Binary Lattice. *Phys. Rev.*, 76:1244, 1949. [doi:10.1103/PhysRev.76.1244](https://doi.org/10.1103/PhysRev.76.1244).
- [232] M. E. Fisher. The Nature of Critical Points. In *Lectures in Theoretical Physics*, page 1. University of Colorado Press, Boulder, 1965.
- [233] C. Domb. On the Theory of Cooperative Phenomena in Crystals. *Adv. Phys. (Philos. Mag. Suppl.)*, 9:149, 1960. [doi:10.1080/00018736000101189](https://doi.org/10.1080/00018736000101189).
- [234] C. Domb. *The Critical Point: A Historical Introduction to the Modern Theory of Critical Phenomena*. Taylor and Francis, London, 1996.
- [235] J. W. Essam and M. E. Fisher. Padé Approximant Studies of the Lattice Gas and Ising Ferromagnet below the Critical Point. *J. Chem. Phys.*, 38:802, 1963. [doi:10.1063/1.1733766](https://doi.org/10.1063/1.1733766).
- [236] B. Widom. Surface Tension and Molecular Correlations near the Critical Point. *J. Chem. Phys.*, 43:3892, 1965. [doi:10.1063/1.1696617](https://doi.org/10.1063/1.1696617).
- [237] B. Widom. Equation of State in the Neighborhood of the Critical Point. *J. Chem. Phys.*, 43:3898, 1965. [doi:10.1063/1.1696618](https://doi.org/10.1063/1.1696618).
- [238] C. Domb and D. L. Hunter. On the Critical Behavior of Ferromagnets. *Proc. Phys. Soc. (London)*, 86:1147, 1965. [doi:10.1088/0370-1328/86/5/127](https://doi.org/10.1088/0370-1328/86/5/127).
- [239] L. Kadanoff. Scaling Laws for Ising Models near  $T_c$ . *Physics*, 2:263, 1966. (Long Island City, NY). [doi:10.1103/PhysicsPhysiqueFizika.2.263](https://doi.org/10.1103/PhysicsPhysiqueFizika.2.263).
- [240] A. Z. Patashinskii and V. L. Pokrovskii. Behavior of ordering systems near the transition point. *Zh. Eksp. Teor. Fiz.*, 50:439, 1966.
-

---

## BIBLIOGRAPHY

---

- [241] K. G. Wilson. The Renormalization Group and Critical Phenomena. *Rev. Mod. Phys.*, 55:583, 1983. (1982, Nobel Prize Lecture). [doi:10.1103/RevModPhys.55.583](https://doi.org/10.1103/RevModPhys.55.583).
- [242] K. G. Wilson. Renormalization Group and Critical Phenomena I. Renormalization Group and Kadanoff Scaling Picture. *Phys. Rev. B*, 4:3174, 1971. [doi:10.1103/PhysRevB.4.3174](https://doi.org/10.1103/PhysRevB.4.3174).
- [243] K. G. Wilson. Renormalization Group and Critical Phenomena II. Phase-Space Cell Analysis of Critical Behavior. *Phys. Rev. B*, 4:3184, 1971. [doi:10.1103/PhysRevB.4.3184](https://doi.org/10.1103/PhysRevB.4.3184).
- [244] F. J. Wegner. Corrections to Scaling Laws. *Phys. Rev. B*, 5:4529, 1972. [doi:10.1103/PhysRevB.5.4529](https://doi.org/10.1103/PhysRevB.5.4529).
- [245] F. J. Wegner. Critical Exponents in Isotropic Spin Systems. *Phys. Rev. B*, 6:1891, 1972. [doi:10.1103/PhysRevB.6.1891](https://doi.org/10.1103/PhysRevB.6.1891).
- [246] L. P. Kadanoff and F. J. Wegner. Some Critical Properties of the Eight-Vertex Model. *Phys. Rev. B*, 4:3989, 1971. [doi:10.1103/PhysRevB.4.3989](https://doi.org/10.1103/PhysRevB.4.3989).
- [247] L. P. Kadanoff. Scaling, Universality and Operator Algebras. In C. Domb and M. S. Green, editors, *Phase Transitions and Critical Phenomena*, volume 5a, page 1. Academic, London, 1976.
- [248] F. J. Wegner. The Critical State, General Aspects. In C. Domb and M. S. Green, editors, *Phase Transitions and Critical Phenomena*, volume 6, page 6. Academic, London, 1976.
- [249] K. G. Wilson and M. E. Fisher. Critical Exponents in 3.99 Dimensions. *Phys. Rev. Lett.*, 28:240, 1972. [doi:10.1103/PhysRevLett.28.240](https://doi.org/10.1103/PhysRevLett.28.240).
- [250] M. E. Fisher. The Theory of Condensation and the Critical Point. *Physics*, 3:255, 1967. (Long Island City, NY). [doi:10.1103/PHYSICS.3.255](https://doi.org/10.1103/PHYSICS.3.255).
- [251] M. E. Fisher. The Theory of Equilibrium Critical Phenomena. *Rep. Prog. Phys.*, 30:615, 1967. [doi:10.1088/0034-4885/30/2/306](https://doi.org/10.1088/0034-4885/30/2/306).
- [252] L. P. Kadanoff et al. Static Phenomena near Critical Points: Theory and Experiment. *Rev. Mod. Phys.*, 39:395, 1967. [doi:10.1103/RevModPhys.39.395](https://doi.org/10.1103/RevModPhys.39.395).
- [253] H. E. Stanley. *Introduction to Phase Transitions and Critical Phenomena*. Oxford University, New York, 1971.
- [254] G. A. Baker Jr. *Quantitative Theory of Critical Phenomena*. Academic, San Diego, 1990.
- [255] R. J. Creswick, H. A. Farach, and C. P. Poole Jr. *Introduction to Renormalization Group Methods in Physics*. John Wiley & Sons, Inc., New York, 1992.
- [256] M. E. Fisher. Scaling, Universality and Renormalization Group Theory. In F. J. Hahne, editor, *Critical Phenomena*, volume 186, page 1. Springer, Berlin, 1983.
- [257] M. E. Fisher and R. J. Burford. Theory of Critical Point Scattering and Correlations. I. The Ising Model. *Phys. Rev.*, 156:583, 1967. [doi:10.1103/PhysRev.156.583](https://doi.org/10.1103/PhysRev.156.583).
- [258] H. K. Kim and M. H. W. Chan. Experimental Determination of a Two-Dimensional Liquid-Vapor Critical-Point Exponent. *Phys. Rev. Lett.*, 53:170, 1984. [doi:10.1103/PhysRevLett.53.170](https://doi.org/10.1103/PhysRevLett.53.170).

---

## BIBLIOGRAPHY

---

- [259] M. E. Fisher. The Renormalization Group in the Theory of Critical Phenomena. *Rev. Mod. Phys.*, 46:597, 1974. [doi:10.1103/RevModPhys.46.597](https://doi.org/10.1103/RevModPhys.46.597).
- [260] A. Aharony. Dependence of Universal Critical Behavior on Symmetry and Range of Interaction. In C. Domb and M. S. Green, editors, *Phase Transitions and Critical Phenomena*, page 357. Academic, London, 1976.
- [261] F. Leonard and B. Delamotte. Critical exponents can be different on the two sides of a transition. *Phys. Rev. Lett.*, 115:200601, 2015. [doi:10.1103/PhysRevLett.115.200601](https://doi.org/10.1103/PhysRevLett.115.200601).
- [262] K. G. Wilson and J. Kogut. The Renormalization Group and the  $\epsilon$  Expansion. *Phys. Rep.*, 12:75, 1974. [doi:10.1016/0370-1573\(74\)90023-4](https://doi.org/10.1016/0370-1573(74)90023-4).
- [263] M. E. Fisher. General Scaling Theory for Critical Points. In B. Lundqvist and S. Lundqvist, editors, *Proceedings of the Nobel Symp. XXIV, Aspensgården, Lerum, Sweden, June 1973, in Collective Properties of Physical Systems*, page 16. Academic, New York, 1974.
- [264] M. E. Fisher. The Susceptibility of the Plane Ising Model. *Physica (Amsterdam)*, 25:521, 1959. [doi:10.1016/S0031-8914\(59\)95411-4](https://doi.org/10.1016/S0031-8914(59)95411-4).
- [265] M. E. Fisher. On the Theory of Critical Point Density Fluctuations. *Physica (Amsterdam)*, 28:172, 1962. [doi:10.1016/0031-8914\(62\)90102-7](https://doi.org/10.1016/0031-8914(62)90102-7).
- [266] M. E. Fisher. Correlation Functions and the Critical Region of Simple Fluids. *J. Math. Phys.*, 5:944, 1964. [doi:10.1063/1.1704197](https://doi.org/10.1063/1.1704197).
- [267] Ph. A. Martin. Sum rules in charged fluids. *Rev. Mod. Phys.*, 60:1075, 1988. [doi:10.1103/RevModPhys.60.1075](https://doi.org/10.1103/RevModPhys.60.1075).
- [268] S. K. Das, Y. C. Kim, and M. E. Fisher. When Is a Conductor Not Perfect? Sum Rules Fail Under Critical Fluctuations. *Phys. Rev. Lett.*, 107:215701, 2011. [doi:10.1103/PhysRevLett.107.215701](https://doi.org/10.1103/PhysRevLett.107.215701).
- [269] R. J. Baxter. *Exactly Solved Models in Statistical Mechanics*. Academic, London, 1982.
- [270] S. MacLane and G. Birkhoff. *Algebra*. MacMillan, New York, 1967. Chap. II, Sec. 9 and Chap. III, Sec. 1.2.
- [271] E. Hille. *Functional Analysis and Semi-Groups*. American Mathematical Society, New York, 1948.
- [272] F. Riesz and B. Sz.-Nagy. *Functional Analysis*. F. Ungar, New York, 1955. Chap. X, Secs. 141 and 142.
- [273] M. E. Fisher and M. F. Sykes. Excluded Volume Problem and the Ising Model of Ferromagnetism. *Phys. Rev.*, 114:45, 1959. [doi:10.1103/PhysRev.114.45](https://doi.org/10.1103/PhysRev.114.45).
- [274] G. S. Rushbrooke and P. J. Wood. On the Curie Points and High-Temperature Susceptibilities of Heisenberg Model Ferromagnetics. *Mol. Phys.*, 1:257, 1958. [doi:10.1080/00268975800100321](https://doi.org/10.1080/00268975800100321).
- [275] C. Domb and M. F. Sykes. Effect of Change of Spin on the Critical Properties of the Ising and Heisenberg Models. *Phys. Rev.*, 128:168, 1962. [doi:10.1103/PhysRev.128.168](https://doi.org/10.1103/PhysRev.128.168).
- [276] J. S. Kouvel and M. E. Fisher. Detailed Magnetic Behavior of Nickel near its Curie Point. *Phys. Rev. A*, 136:1626, 1964. [doi:10.1103/PhysRevA.136.A1626](https://doi.org/10.1103/PhysRevA.136.A1626).
-

---

## BIBLIOGRAPHY

---

- [277] P. Heller and G. B. Benedek. Nuclear Magnetic Resonance in  $\text{MnF}_2$  near the Critical Point. *Phys. Rev. Lett.*, 8:428, 1962. [doi:10.1103/PhysRevLett.8.428](https://doi.org/10.1103/PhysRevLett.8.428).
- [278] E. A. Guggenheim. *Thermodynamics*. North Holland, Amsterdam, 1949. Fig. 4.9.
- [279] J. S. Rowlinson. *Liquids and Liquid Mixtures*. Butter-Worth Scientific, London, 1959.
- [280] B. Widom and O. K. Rice. Critical Isotherm and the Equation of State of Liquid-Vapor Systems. *J. Chem. Phys.*, 23:1250, 1955. [doi:10.1063/1.1742251](https://doi.org/10.1063/1.1742251).
- [281] J. D. Gunton and M. S. Green, editors. *Renormalization Group in Critical Phenomena and Quantum Field Theory: Proceedings of a Conference*, Chestnut Hill, Pennsylvania, 29-31 May 1973. Temple University, Philadelphia.
- [282] S.-Y. Zinn and M. E. Fisher. Universal Surface-Tension and Critical-Isotherm Amplitude Ratios in Three Dimensions. *Physica A*, 226:168, 1996. [doi:10.1016/0378-4371\(95\)00382-7](https://doi.org/10.1016/0378-4371(95)00382-7).
- [283] G. A. Ahlers, A. Kornblit, and H. J. Guggenheim. Logarithmic Corrections to the Landau Specific Heat near the Curie Temperature of the Dipolar Ising Ferromagnet  $\text{LiTbF}_4$ . *Phys. Rev. Lett.*, 34:1227, 1975. [doi:10.1103/PhysRevLett.34.1227](https://doi.org/10.1103/PhysRevLett.34.1227).
- [284] D. R. Nelson. Defect-mediated Phase Transitions. In C. Domb and M. S. Green, editors, *Phase Transitions and Critical Phenomena*, page 1. Academic, London, 1983.
- [285] M. Gell-Mann and F. E. Low. Quantum Electrodynamics at Small Distances. *Phys. Rev.*, 95:1300, 1954. [doi:10.1103/PhysRev.95.1300](https://doi.org/10.1103/PhysRev.95.1300).
- [286] K. G. Wilson. The Renormalization Group: Critical Phenomena and the Kondo Problem. *Rev. Mod. Phys.*, 47:773, 1975. [doi:10.1103/RevModPhys.47.773](https://doi.org/10.1103/RevModPhys.47.773).
- [287] E. Brézin, J. C. Le Guillou, and J. Zinn-Justin. Field Theoretical Approach to Critical Phenomena. In C. Domb and M. S. Green, editors, *Phase Transitions and Critical Phenomena*, page 125. Academic, London, 1976.
- [288] D. J. Amit. *Field Theory, the Renormalization Group and Critical Phenomena*. McGraw-Hill Inc., London, 1978. see also 1993, the expanded Revised 2nd Edition (World Scientific, Singapore).
- [289] D. Itzykson and J.-M. Drouffe. *Statistical Field Theory*. Cambridge University Press, Cambridge, 1989.
- [290] A. I. Larkin and D. E. Khmel'nitskii. Phase Transition in Uniaxial Ferroelectrics. *Zh. Exsp. Teor. Fiz.*, 56:2087, 1969.

*BIBLIOGRAPHY*

---

# Index

Follows the analytic index of some of the most significant terms.

## A

- antiparticle ..... 2, 23, 73, 76
- anyons ..... 120
- atom ..... 4, 5, 11, 109–112, 115, 116, 164

## B

- Bijl-Dingle-Jastrow ..... 127
- black hole ..... 188

## C

- Chandrasekhar limit ..... 186–188
- chemical reaction ..... 115
- correlation exponent ..... 206
- correlation function ..... 199, 200, 204, 205
- correlation length ..... 204, 206
- critical exponent ..... 197, 199, 200, 204, 209

## D

- density matrix ..... 136, 137, 139–142, 147, 169, 170, 173
- differential forms ..... 7
- diffusion Monte Carlo ..... 10, 123–125

## E

- Einstein Relativity ..... 34
- electromagnetic wave ..... 7
- electron ..... 1, 2, 5–11, 15, 89–92, 110–112, 115, 116, 119–121, 147–149, 152, 177, 179, 182, 184, 191, 195
- electron fluid ..... 148

- electron gas ..... 4, 11, 119, 121, 128, 145, 167, 190, 191, 195

- electron plasma ..... 2

- electronegativity ..... 115, 116

- element ..... 112, 115, 116

- exterior derivative ..... 7

## F

- fermions nodes ..... 141, 142, 160
- fermions sign problem ..... 136, 142
- fine-structure constant ..... 6
- fractional statistics ..... 120

## G

- Galilean relativity ..... 27
- Galileo group ..... 29, 38

## H

- Hartree potential ..... 161, 177
- Hartree-Fock ..... 142, 164, 165
- Hartree-Jastrow ..... 160
- Hodge star ..... 7
- Hyper-Netted-Chain ..... 119

## I

- internal energy ..... 10, 132, 137, 142, 164, 183, 185

- invariance ..... 23, 24, 27

## J

- Jastrow factor ..... 127–129, 159, 171
- jellium ..... 10, 11, 119–121, 123, 128, 132, 136, 137, 144–148, 164, 169

---

## INDEX

---

- L**
- Lie group ..... 80, 85  
Linear-Response-Theory ..... 161, 173  
locality ..... 2, 23, 53, 71, 73, 75  
localization ..... 102  
Lorentz group ..... 34–36, 38, 49, 53, 54, 57  
luminosity ..... 180
- M**
- Maxwell equations ..... 7  
Mean-Spherical-Approximation ..... 119  
Metropolis algorithm ..... 90, 94, 102, 141  
molecule ..... 4, 116, 119, 164
- N**
- neutron drip ..... 179, 188
- O**
- one component plasma ..... 119, 144, 146
- P**
- path integral ..... 10, 11, 119, 136, 137, 170  
Percus-Yevick ..... 119  
periodic table ..... 5, 111  
phase diagram ..... 146  
phase transition ..... 11, 89, 90, 98, 100, 102, 103, 116, 117, 149, 150, 198, 199, 205  
phonons ..... 89, 90, 102, 103  
Poincaré group ..... 37, 38, 50, 51, 53, 56, 60, 61, 63, 64, 69, 71, 72, 76  
polaron ..... 89–91, 93, 98, 100–102, 108  
positron ..... 2  
Poynting vector ..... 9
- pressure ..... 10, 12, 117, 118, 131, 137, 179, 181, 184, 195  
primitive approximation ..... 137, 169, 170  
primitive model ..... 119, 148
- R**
- radial distribution function ..... 130–133, 142, 144, 163, 164, 167, 188, 190, 191  
Random-Phase-Approximation ..... 121, 128, 129, 144, 146, 161, 167  
random-walk ..... 124, 141, 159, 171  
RedOx ..... 115  
renormalization group ..... 197, 200, 204, 207  
restricted path integral ..... 139, 141
- S**
- Slater determinant ..... 127, 128, 163, 164  
Slater-Jastrow ..... 124, 160  
spin-statistics theorem ..... 2, 23, 71, 73, 75  
structure factor ..... 128, 132, 134, 142, 143, 152, 153, 161–163, 188  
superconductivity ..... 10, 11, 121, 136, 137  
superfluidity ..... 136, 137  
superionic ..... 149, 150  
supernovae ..... 188
- T**
- two component plasma ..... 117, 119
- V**
- variational Monte Carlo ..... 10, 124
- W**
- white dwarf ..... 179, 180, 187, 190, 191

